



University  
of Glasgow

Huma, Zilli (2014) Spinoreticular tract neurons: the spinoreticular tract as a component of an ascending descending loop. PhD thesis.

<http://theses.gla.ac.uk/5628>

Copyright and moral rights for this thesis are retained by the author

A copy can be downloaded for personal non-commercial research or study, without prior permission or charge

This thesis cannot be reproduced or quoted extensively from without first obtaining permission in writing from the Author

The content must not be changed in any way or sold commercially in any format or medium without the formal permission of the Author

When referring to this work, full bibliographic details including the author, title, awarding institution and date of the thesis must be given.

# **SPINORETICULAR TRACT NEURONS:**

## **THE SPINORETICULAR TRACT AS A COMPONENT OF AN ASCENDING DESCENDING LOOP**

**Dr. Zilli Huma**

MBBS, FCPS in General surgery  
(College of Physicians and Surgeons, Pakistan)

Thesis submitted in fulfilment for the degree of Doctor of Philosophy

Institute of Neuroscience and Psychology

College of Medical, Veterinary and Life Sciences

University of Glasgow

Glasgow, Scotland



**October 2014**

**"In the name of Allah, most Gracious, most Compassionate"**

## **Dedication**

*In loving memory of my dear brother Syed Wasif Ali Shah and  
beloved father-in-law Syed Manzar Hussain*

## Summary

The lateral reticular nucleus (LRN) is a component of the indirect spino-reticulo-cerebellar pathway that conveys sensorimotor information to the cerebellum. Although extensive work has been done on this pathway using electrophysiological techniques in cat, little is known about its infrastructure or neurochemistry in both cat and rat. Thus defining the morphology of this spinoreticular pathway would provide a better understanding of its intricate connections and the role of various neurotransmitters involved, which in turn would provide insight into the process by which these neurons carry out, for example, reflex modulation. We thus became interested in finding out more about the role of the spinoreticular neurons (SRT) in this pathway, what and how these cells receive inputs, their role within the spinal circuitry and how they modulate sensorimotor output.

Thus, in view of these limitations, we formulated a hypothesis: 'That spinoreticular neurons form a component of a feedback loop which influences activity of medullary descending control systems'. To test this hypothesis we developed four main aims: (1) to find out the distribution pattern of spinoreticular tract (SRT) neurons and their axonal projections to the LRN; (2) to examine the origins of two bulbospinal pathways projecting to the rat lumbar spinal cord via the medial longitudinal fasciculus (MLF) and caudal ventrolateral medulla (CVLM); (3) to determine the origin of excitatory and inhibitory contacts on SRT neurons in rat and cat lumbar spinal cord; and (4) to analyse some of the neurochemical phenotypes of SRT neurons and their response to noxious stimulus.

In order to fulfil these aims, we combined tract tracing by retrograde and in some cases anterograde transport of the b subunit of cholera toxin (CTb) and retrograde transport of fluorogold (FG) along with immunohistochemistry in rats. In addition to this, SRT cells in cat were identified electrophysiologically and intracellularly labelled with Neurobiotin (NB), *in vivo* which were further investigated by using immunohistochemistry. As most of the electrophysiological data available to date is from cat studies so in this study we wanted to see how well this correlated to the anatomical results obtained from both cat and rat experiments.

Results from Aim 1 demonstrated that, although there was extensive bilateral labelling of spinoreticular neurons in rat on both sides of the lumbar spinal cord, ~ 70% were contralateral, to the LRN injection site, in the ventromedial Lamina V to VIII. There were also some SRT cells that project ipsilaterally (31-35%) in addition to ~8% projecting bilaterally to both lateral reticular nuclei. Further experiments showed that the majority of SRT axons ascending via the ventrolateral funiculus terminate within the ipsilateral LRN with fewer projections to the contralateral LRN (2.6:1 ratio). These projections are predominantly excitatory (~80% both vesicular glutamate transporter 1 and 2; VGLUT-1, VGLUT-2) in addition to a significant inhibitory component (~15%, vesicular GABA transporter; VGAT), that consists of three subtypes of axons containing GABA, glycine or a mixture of GABA and glycine. LRN pre-cerebellar neurons receive convergent connections from excitatory (~13%) and inhibitory (~2%), SRT axons.

Experiments undertaken to meet the second aim of this thesis revealed that, in rat, bulbar cells projecting via the MLF (medial longitudinal fasciculus) or the CVLM (caudal ventrolateral medulla) to the lumbar spinal cord have mostly overlapping spatial distributions. The vast majority of cells in both pathways are located in identical reticular areas of the brainstem. Furthermore, both pathways have a mixture of crossed and uncrossed axonal fibres, as double labelled cells were located both ipsi and contralateral to unilateral spinal injection sites. Bulbospinal (BS) cells that project via CVLM, form predominantly excitatory contacts with spinoreticular cells but there is also an inhibitory component targeting these cells; ~56% and ~45% of the BS contacts, respectively,

In investigating the third aim to provide insight into the inputs to spinoreticular cells in two species, rat and cat we observed that; in both species these cells receive predominantly inhibitory inputs (VGAT) in addition to excitatory glutamatergic contacts that are overwhelmingly VGLUT-2 positive (88% to 90%). Thus, it appears that most inputs to these cells are from putative interneuronal populations of cells, for example PV (parvalbumin) and ChAT cells (choline acetyl transferase). SRT neurons in the rat receive a significant proportion of contacts from proprioceptors (~17%) but in the cat these cells do not seem to

respond monosynaptically to inputs from somatic nerves. Furthermore, a significant proportion of contacts on rat SRT cells originate from myelinated cutaneous afferents (~68%).

Data from the final series of experiments demonstrate the heterogeneity of spinoreticular neurons in terms of immunolabelling by neurochemical markers as well as their varied responses to noxious stimulation. Many SRT neurons express NK-1 receptors (~27%, neurokinin 1) and approximately 20% of SRT neurons were immunoreactive for calcium binding proteins, CB, CR (calretinin) or both CB & CR and hardly any cells labelled for ChAT. While a smaller proportion immunolabelled for neuronal nitric oxide synthase (nNOS). Nine percent of SRT cells responded to mechanical noxious stimulation as demonstrated by phosphorylation of extracellular signal regulated kinase (ERK).

The present findings provide a new basis for understanding the organisation and functional connectivity of spinoreticular tract neurons which convey information from peripheral and spinal inputs to the LRN where it is integrated with information from the brain and conveyed to the cerebellum and their role in a spino-bulbo-spinal loop that is responsible for modulating activity of pre-motor networks to ensure co-ordinated motor output.

## Acknowledgement

I would like to begin by thanking Almighty Allah for helping me finish this project in time and for all the amenities He has provided to make it possible.

My sincere gratitude goes to my supervisor, Professor David J Maxwell for accepting me as a PhD student when all seemed lost and for his guidance and support throughout my research and write up, for always being there. A heartfelt thank you, to Dr Ingela Hammar from the Department of Physiology, University of Gothenburg, Sweden, for her continuous support, being my mentor and wonderful host.

Thank you to my advisors, Professor Andrew J Todd for his invaluable comments and observations and Professor Mhairi McRae for her expert advice especially in all matters statistical. There is a long list of people within the spinal cord group who have helped, advised or just been there for me throughout this PhD, in particular, Robert Kerr and Christine Watt for not only their expert technical assistance but also for all the tit bits of information about Scottish life. Special thanks to two wonderful friends and colleagues Sony and Anne for all your help and being a shoulder to cry on in dire times.

I am greatly indebted to my family for all their sacrifices and allowances on my behalf, my parents and brothers, in helping me fulfil a lifelong dream.

A special thank you to my loving husband Masud for without you this PhD would not have even been conceivable, for your belief, love and endless patience. Thank you to my awesome kids Hasan, Fatima and Haris for just being there and for putting up with my absences, even when I am physically present.

Last but not least I would like to thank my funding body, Higher Education Commission and Khyber Medical University, Pakistan, for providing me this unique opportunity of pursuing higher studies in this beautiful and friendly city, Glasgow.

## **Author's declaration**

All work in this thesis was carried out solely by me, apart from some of the surgical procedures and electrophysiology. Professor David Maxwell contributed to this work by performing surgical procedures on rats. Dr Ingela Hammar contributed by performing surgical procedures and electrophysiological recordings on cats. Students in my supervision, Christina Brown, Kirsty Ireland and Megan Tailford have participated in some parts of this study. This thesis has been composed by me and has not been previously submitted for examination leading to the award of a degree.

The copyright of this thesis belongs to the author under the terms of the United Kingdom Copyright Acts as qualified by University of Glasgow Regulations. Due acknowledgement must always be made of the use of any material contained in, or derived from, this thesis.

**Dr Zilli Huma**

**Signature:**

**Date:**

## Table of Contents

Summary	I
Acknowledgement	IV
Author's declaration	V
Table of contents	VI
List of Tables	X
List of Figures	XII
List of Abbreviations	XVI

## Chapter

<b>Chapter 1 Introduction</b>	<b>2</b>
1.1 The reticular formation (RF)	3
1.1.1 Subdivisions of the brain stem reticular formation	4
1.1.2 Spinoreticular tracts	7
1.1.3 Reticulospinal tracts	10
1.2 Lateral reticular nucleus (LRN)	14
1.2.1 Gross Morphology	14
1.2.2 Cytoarchitecture of the LRN	17
1.2.3 Afferents to the LRN	20
1.2.4 Spinal inputs	21
1.2.5 Somatotopic vs. topographic organisation of the LRN	25
1.2.6 Physiological response properties of the LRN neurons	26
1.2.7 Efferents of the LRN	27
1.2.8 Neurochemical properties of bulbospinal (BS) pathways	29
1.2.9 Functional aspects of the LRN	30
1.3 Cells of origin of the lateral Spinoreticular pathway	32
1.3.1 Anatomical distribution patterns of the SRT cells in the spinal cord	32
1.3.2 Neurochemical properties of the SRT cells	34
1.3.3 Neurochemical contacts to the spinoreticular neurons	35
1.3.4 Response properties of spinoreticular neurons	38
1.4 Spinal reflexes	43
1.4.1 Flexor reflex afferents vs. withdrawal reflex	43
1.4.2 Spinobulbar spinal reflex	44
1.5 Scope of this study	46
1.6 Aims and Objectives	47

<b>Chapter 2 General experimental procedures</b>	<b>49</b>
2.1 Surgical procedures	49
2.2 Identification of the injection site	51
2.3 Tissue processing and multiple immune-labelling for confocal microscopy	52
2.4 Confocal microscopy, reconstructions and analysis	53
2.5 Statistical analysis	54
<b>Chapter 3 The ascending pathway; the topography of the spinoreticular tract neurons to the lateral reticular nucleus (LRN)</b>	<b>56</b>
3.1 Introduction	56
3.2 Methods	59
3.2.1 The pattern of distribution of spinoreticular tract neurons in the rat lumbar spinal cord	59
3.2.2 The projection patterns of spinoreticular neurons to the LRN	60
3.2.3 Investigation of different phenotypes of spinoreticular projections to the LRN	62
3.2.4 Spinoreticular contacts onto pre-cerebellar neurons in the LRN	66
3.2.5 Statistical analysis	67
3.3 Results	69
3.3.1 Distribution of SRT neurons in rat lumbar cord	69
3.3.2 The projection patterns of spinoreticular neurons to the LRN	70
3.3.3 Investigation of transmitter phenotypes of spinoreticular projections to the LRN	72
3.3.4 Spinoreticular contacts on pre-cerebellar neurons in the LRN	76
3.4 Discussion	104
3.4.1 Technical considerations	104
3.4.2 Lumbar distribution of Spinobulbar neurons and collateralisation	106
3.4.3 Spinoreticular projections to the lateral reticular nucleus	107
3.4.4 Excitatory and inhibitory terminals in the LRN	108
3.4.5 Functional implications	110
<b>Chapter 4 The descending pathway; origin of bulbospinal neurons projecting via the caudal ventro-lateral medulla (CVLM) and medial longitudinal fasciculus (MLF) to the rat lumbar spinal cord</b>	<b>114</b>
4.1 Introduction	114
4.2 Materials and Methods	117
4.2.1 Surgical procedures	117

4.2.2	Immunocytochemistry, confocal microscopy and analysis	118
4.2.3	Statistical analysis	119
4.3	Results	123
4.3.1	Spinally projecting cells via CVLM and MLF	123
4.3.2	Bulbospinal contacts on spinoreticular cells	125
4.4	Discussion	146
4.4.1	Technical considerations	146
4.4.2	Comparison with other studies	147
4.4.3	Transmitter phenotypes of Bulbospinal pathway via the CVLM	149
4.4.4	Functional implications	150
<b>Chapter 5 Origins of excitatory and inhibitory contacts on spinoreticular tract neurons in rat and cat lumbar spinal cord</b>		<b>155</b>
5.1	Introduction	155
5.2	Methods	158
5.2.1	Aim Ia: Excitatory and inhibitory contacts onto spinoreticular neurons in the rat lumbar spinal cord	159
5.2.2	Aim Ib: Excitatory and inhibitory contacts on spinoreticular neurons in the cat lumbar spinal cord	162
5.2.3	Aim II: Myelinated primary afferent contacts on spinoreticular cells in rat	171
5.2.4	AIM III: ChAT and calbindin contacts on spinoreticular cells in rat lumbar cord	174
5.2.5	Statistical Analysis	176
5.3	Results	177
5.3.1	AIM I: What are the proportions of excitatory and inhibitory contacts associated with spinoreticular neurons in the lumbar spinal cord of the rat and cat?	177
5.3.2	AIM II What proportion of contacts on rat spinoreticular tract cells originate from myelinated primary afferents?	186
5.3.3	AIM IV: What proportion of contacts on spinoreticular tract cells is from ChAT, CB and PV terminals in the rat lumbar spinal cord?	189
5.4	Discussion	228
5.4.1	Technical considerations	228
5.4.2	Excitatory contacts on spinoreticular cells in the rat and cat lumbar spinal cord and primary afferent contacts	229
5.4.3	Inhibitory contacts to spinoreticular cells in the rat and cat lumbar spinal cord	231
5.4.4	Choline acetyltransferase, parvalbumin and calbindin contacts on SRT neurons	233
5.4.5	Functional considerations	236

<b>Chapter 6 Spinoreticular neurons; neurochemical phenotypes and response to noxious stimulus</b>	<b>240</b>
6.1 Introduction	240
6.2 Methods	243
6.2.1 Data analysis	244
6.3 Results	247
6.3.1 Aim I: To investigate the neurochemical phenotypes of spinoreticular neurons in the rat lumbar spinal cord	247
6.3.2 Aim II: Do some subtypes of SRT cells express pERK in response to acute mechanical noxious stimuli?	250
6.4 Discussion	270
6.4.1 Technical considerations	270
6.4.2 Neurochemical phenotypes of spinoreticular neurons	271
6.4.3 Response to noxious stimulus	274
6.4.4 Functional aspects	276
<b>Chapter 7 Concluding remarks</b>	<b>280</b>

References

Publication

## List of Tables

### Chapter 1

Table 1-1 General overview of various types of cutaneous and proprioceptive primary afferents.	40
--	----

### Chapter 2

Table 2-1 Excitation-emission wavelength of the fluorophore used	53
--	----

### Chapter 3

Table 3-1 Summary of primary and secondary antibody combinations and concentrations used in this experiment (n=4)	62
---	----

Table 3-2 Summary of primary and secondary antibody combinations and concentrations used in this experiment (n=3).	65
--	----

Table 3-3. Summary of primary and secondary antibody combinations and concentrations used in the present experiment (n=3)	68
---	----

Table 3-4. Percentages of excitatory (VG1&2) and inhibitory (VGAT, GAD, GLYT2) boutons in the ipsi and contralateral lateral reticular nuclei anterogradely labelled from spinal injections of CTb	75
--	----

Table 3-5 Excitatory (VGLUT-2, CTb+ VGLUT-2) and inhibitory (VGAT, CTb+VGAT) terminals and their contact densities onto pre-cerebellar cells in the LRN	77
---	----

### Chapter 4

Table 4-1 Summary of primary and secondary antibody combinations and concentrations in the analysis of spinally projecting cells via the CVLM and MLF (n=6)	121
---	-----

Table 4-2 Summary of the primary and secondary antibody concentrations and combinations used in the bulbospinal contacts to the spinoreticular cells (n=3)	122
--	-----

Table 4-3 Double labelled cells in the various areas of the brainstem following fluorogold injections into the right lumbar cord and injections of cholera toxin in the MLF or right CVLM	127
---	-----

Table 4-4 Bulbospinal contact densities (CTb) on fluorogold (FG) labelled SRT neurons for excitatory VGLUT2 (VG2) and inhibitory VGAT immunoreactive terminals (n=3)	129
--	-----

Table 4-5 Total Bulbospinal (BS), VGAT and VGLUT2 (VG2) contacts on retrogradely labelled spinoreticular cells (n=3)	130
--	-----

### Chapter 5

Table 5-1 Summary of primary and secondary antibody combinations and concentrations to label excitatory and inhibitory contacts on SRT cells in rat (n= 3)	161
--	-----

Table 5-2 Summary of primary and secondary antibody combinations and concentrations to label excitatory and inhibitory contacts to spinoreticular cells in cat (n= 6 cells)	170
---	-----

Table 5-3 Primary and secondary antibody combinations and concentrations to identify retrogradely labelled fluorogold (FG) spinoreticular cells in the rat lumbar cord with CTb contacts (primary afferent) n=3	173
Table 5-4 Primary and secondary antibody concentrations and combinations to label spinoreticular cells (CTb) for ChAT and CB contacts (n=3)	175
Table 5-5 The number and densities of VGLUT-1(VG-1) and VGLUT-2 (VG-2) axon terminals in apposition with cell bodies and dendrites of retrogradely labelled spinoreticular tract neurons in rats (n=3)	179
Table 5-6 The numbers and contact densities of VGLUT-1 & 2 (VG 1&2) and VGAT axon terminals in apposition to the soma and	181
Table 5-7 The number and densities of VGAT, VGLUT-1 and 2 (VG 1&2) axon terminals in apposition with the cell bodies and dendrites of intra intracellularly labelled Spinoreticular cat cells (n=6)	185
Table 5-8 Primary afferent (CTb), VGLUT-1(VG1) and Parvalbumin (PV) positive contact densities on retrogradely labelled SRT cells in the rat mid-lumbar spinal cord (n=3)	188
Table 5-9 Choline acetyltransferase (ChAT), calbindin (CB) and parvalbumin (PV) contact densities associated with spinoreticular cells (n=6)	191
<b>Chapter 6</b>	
Table 6-1 Primary and secondary antibody combinations and concentrations used to find out neurochemical phenotypes of SRT neurons	245
Table 6-2 Primary and secondary antibody combinations and concentrations used to investigate response to noxious stimulus by SRT neurons (n=7)	246
Table 6-3 Percentages of spinoreticular cells immunoreactive for calbindin (CB) and/or calretinin (CR) ipsi and contralateral to the LRN injection	249
Table 6-4 Percentages of SRT cells labelled by neurochemical markers; NK-1r, nNOS, CB, CR and ChAT	249
Table 6-5 Percentage of various subpopulations of retrogradely labelled spinoreticular cells (SRT/CTb) in response to noxious stimulation	252

## List of Figures

### Chapter 1

Figure 1-1 The reticular nuclei in the rat brain stem	6
Figure 1-2 The spinoreticular tracts; a simplified schematic diagram of the ascending reticular tracts	9
Figure 1-3 The reticulospinal tracts; a simplified schematic diagram of the descending reticular tracts not including the raphe nuclei	13
Figure 1-4 The lateral reticular nucleus, gross morphology and anatomical location in the brain stem	16
Figure 1-5 The cytoarchitecture of the lateral reticular nucleus (LRN)	19
Figure 1-6 Distribution pattern of excitatory neurotransmitters in rat and cat lumbar (L4) spinal cords	37

### Chapter 2

Figure 2-1 A schematic diagram for the surgical procedure of retrograde labelling of spinoreticular tract neurons in the rat lumbar spinal cord	50
---	----

### Chapter 3

Figure 3-1 Photomicrographs of representative sections of rat medulla with reconstructions illustrating the CTb injection sites	78
Figure 3-2 Soma locations of retrogradely labelled spinoreticular cells in animals 1 and 2 which correspond to the injection sites in figure 3-1	80
Figure 3-3 Soma locations of retrogradely labelled spinoreticular cells in animals 3 and 4 that correspond to the injection sites in Figure 3-1	82
Figure 3-4 Laminar distribution of spinoreticular cells in the lumbar spinal cord after unilateral injections of CTb tracer in the lateral reticular nucleus (LRN)	84
Figure 3-5 Bilateral lateral reticular nuclei (LRN) injections of b subunit of cholera toxin (CTb) and fluorogold (FG)	85
Figure 3-6 A tiled confocal scan of a lumbar section of the spinal cord illustrating the distribution of retrogradely labelled cells by both CTb and FG	87
Figure 3-7 Soma locations of spinobulbar cells retrogradely labelled by bilateral LRN injections	89
Figure 3-8 Bar graphs showing the distribution patterns of three types of spinoreticular projection neurons	91
Figure 3-9 Spinal injection of CTb in the lumbar segments with anterogradely labelled terminals in the LRN	93
Figure 3-10 Confocal scans of the lateral reticular nucleus (LRN) illustrating the immunocytochemical properties of spinoreticular terminals ipsilateral to the spinal injection	95
Figure 3-11 Confocal scans of the lateral reticular nucleus (LRN) illustrating the immunocytochemical properties of spinoreticular terminals contralateral to the spinal injection site	97
Figure 3-12 Fluorogold injection into the cerebellum to retrogradely label reticulo-cerebellar cells in the LRN with spinal injections of CTb in lumbar	

segments of the same animals to anterogradely label spinoreticular terminals in the LRN	99
Figure 3-13 A confocal scan of a reticulo-cerebellar cell with spinoreticular inputs in the LRN	101
Figure 3-14 Contact densities of excitatory and inhibitory spinoreticular terminals onto reticulo-cerebellar cells in the LRN	103
Figure 3-15 Summary of the ascending projections of spinoreticular neurons	112
<b>Chapter 4</b>	
Figure 4-1 CTb injections into the caudal ventrolateral medulla (CVLM, LRt) and fluorogold injections into the ipsilateral lumbar spinal cord of the same animals	131
Figure 4-2 CTb injection into the medial longitudinal fasciculus (MLF) and fluorogold injections into the lumbar spinal cord of the same animal	133
Figure 4-3 A maximum intensity projection confocal scan of a representative medullary coronal section showing the pattern of distribution of cells collateralised to both sites following a CVLM injection of CTb and spinal injection of FG	135
Figure 4-4 A confocal scan of a representative pontine coronal section of an animal with CTb injection in the MLF and FG injection in the lumbar spinal cord, illustrating the distribution pattern of double labelled cells (Bregma -8.76)	137
Figure 4-5 Distribution of labelled cells in the medulla of animals with CVLM and MLF injections	139
Figure 4-6 Distribution of cells in the pons and midbrain of animals injected in either the right CVLM or MLF	141
Figure 4-7 Anterogradely labelled excitatory and inhibitory bulbospinal terminals in contact with a retrogradely labelled spinoreticular cell	143
Figure 4-8 Excitatory and inhibitory bulbospinal inputs onto retrogradely labelled spinoreticular tract neurons	145
Figure 4-9 Summary of the descending bulbospinal pathways	153
<b>Chapter 5</b>	
Figure 5-1 A schematic diagram showing some of the surgical and recording procedures for spinoreticular neurons in the cat lumbar spinal cord	165
Figure 5-2 Electrophysiological identification of a spinoreticular neuron in the cat lumbar spinal cord with excitatory and inhibitory inputs from various sources	192
Figure 5-3 Soma locations of all intracellularly labelled SRT cells in the lumbar segment of the cat and representative sections of the medulla and cerebellum with locations of the stimulated sites	195
Figure 5-4 Fluorogold injection into the right lateral reticular nucleus and injection of the b subunit of cholera toxin into the left sciatic nerve in the hind limb of the rat with myelinated terminals labelled in the lumbar segments	196
Figure 5-5 CTb injection sites into the lateral reticular nucleus of the rat to retrogradely label SRT cells in the lumbar spinal cord	197

Figure 5-6 Confocal image of a representative, retrogradely labelled spinoreticular rat neuron (red) with VGLUT-1 (blue) and VGLUT-2 (green) contacts (Large panel)	198
Figure 5-7 Contact densities of excitatory and inhibitory inputs on spinoreticular tract neurons in rat (A-B) and cat (C) lumbar segments of the spinal cord	200
Figure 5-8 Sholl analysis showing the mean number of excitatory and inhibitory contacts on both retrogradely labelled rat SRT neurons (A) and intracellularly labelled cat spinoreticular neurons (B)	202
Figure 5-9 Confocal image of a representative, retrogradely labelled spinoreticular rat neuron (red) with excitatory inputs (VGLUT-1&2) and VGAT synapses	203
Figure 5-10 A neurobiotin-rhodamine filled cat spinoreticular cell with excitatory (VGLUT-1&2) and inhibitory (VGAT) contacts	205
Figure 5-11 Reconstructions of intracellularly labelled neurobiotin cat lumbar spinoreticular tract neurons illustrating the patterns of distribution of excitatory and inhibitory inputs	207
Figure 5-12 A neurobiotin-rhodamine filled spinoreticular cat cell with VGAT synapses and VGLUT-1 and VGLUT-2 positive terminals	212
Figure 5-13 Reconstructions of neurobiotin labelled cat spinoreticular tract neurons illustrating the patterns of distribution of excitatory inputs and inhibitory synapses	214
Figure 5-14 Spinoreticular cells (FG, green) with myelinated primary afferent inputs (CTb, red)	217
Figure 5-15 Mean contact densities of CTb inputs onto spinoreticular cells distributed in the rat lumbar spinal cord	219
Figure 5-16 Percentage of primary afferent CTb positive contacts on rat spinoreticular neurons	220
Figure 5-17 A single optical section of a retrogradely labelled spinoreticular cell in the rat lumbar spinal cord with calbindin (CB) and choline acetyltransferase (ChAT) inputs	221
Figure 5-18 Bar graphs showing choline acetyltransferase (ChAT) and calbindin (CB) contact densities onto two sub-populations of spinoreticular cells (SRT)	223
Figure 5-19 Bar graph showing a comparison of PV, ChAT and CB contact densities on Spinoreticular cells in rat lumbar spinal cord	225
Figure 5-20 Confocal scans of some retrogradely labelled rat spinoreticular cells positive for calbindin, with both calbindin (CB) and choline acetyltransferase (ChAT) inputs	226
Figure 5-21 Summary of excitatory and inhibitory inputs to spinoreticular cells	238
 <b>Chapter 6</b>	
Figure 6-1 Injection site of CTb into the lateral reticular nucleus of the rat retrogradely labelling SRT cells (red) and distribution of pERK stimulation (green)	253
Figure 6-2 Distribution of spinoreticular cells in the lumbar spinal cord immunoreactive for calcium binding proteins	255

Figure 6-3 Laminar distribution of SRT cells immunoreactive for calcium binding proteins	257
Figure 6-4 Neurochemical phenotypes of spinoreticular cells in the rat lumbar spinal cord	258
Figure 6-5 A. Percentage of spinoreticular cells immunoreactive to NK-1r, nNOS, CB, CR and ChAT; B. Laminar distribution of double labelled cells	260
Figure 6-6 Distribution of Spinoreticular cells (CTb, red) responding to noxious pinch in the rat lumbar spinal cord	261
Figure 6-7 Sub-groups of spinoreticular cells (CTb,red) that are responsive to noxious stimuli by the phosphorylation of ERK	263
Figure 6-8 Spinoreticular cells illustrating phosphorylation of extracellular signal regulated kinase and negative for nNOS	265
Figure 6-9 Percentages of spinoreticular cells expressing pERK, NK-1r, CB, CR and nNOS	267
Figure 6-10 A. Comparison of sub-groups of spinoreticular cells (SRT) that have pERK and are labelled by NK-1r, CB, CR or ChAT; B. Laminar distribution of the cells	268
Figure 6-11 A comparison of SRT cells that are pERK positive within the NK-1r, nNOS, CB, CR and ChAT immunoreactive sub-populations	269
Figure 6-12 Summary of the role of spinoreticular cells in the spinal circuitry of pain	278
<b>Chapter 7</b>	
Figure 7-1 Summary of the connectivity of spinoreticular cells as a component of an ascending descending loop	281

## Abbreviations

5-HT	5-hydroxy tryptamine
VSCT	ventral spinocerebellar tract
bVFRT	bilateral ventral flexor reflex tract
BS	bulbospinal
C3-C4 PN	C3-C4 propriospinal tract
CB, CR	calbindin,calretinin
CVLM	caudal ventrolateral medulla
CNS	central nervous system
ChAT	choline acetyltransferase
CTb	b subunit of cholera toxin
DAB	3, 3'-diaminobenzidine
DNIC	diffuse noxious inhibitory control
EPSPs	excitatory postsynaptic potentials
IPSPs	inhibitory postsynaptic potentials
FG	fluorogold
GABA	gamma amino butyric acid
GAD	glutamate decarboxylase
Gi, LPGi	gigantocellular reticular and lateral paragigantocellular
GLYT2	glycine transporter 2
HRP	horseradish peroxidase
HRP-WGA	HRP conjugated with wheat germ agglutinin
iFT	ipsilateral forelimb tract
lReST, mReST	lateral and medial reticulospinal tract
LRN	lateral reticular nucleus
LRt	lateral reticular nucleus
lSRT, mSRT	lateral and medial spinoreticular tracts

MdD, MdV	medullary reticular nucleus, dorsal and ventral part
MLF	medial longitudinal fasciculus
NK-1r	neurokinin-1 receptor
nNOS	neuronal nitric oxide synthase
PMn	paramedian reticular nucleus
PCRt	parvicellular reticular nucleus
PAG	periaqueductal grey
PB, PBS, PBST	phosphate buffer, PB saline, PBS with 0.3% Triton X-100
pERK	phosphorylation of extracellular signal regulated kinase
PV	parvalbumin
PN	propriospinal neuron
ReST	reticulospinal tract
RF	reticular formation
RS	rubrospinal tract
RSTi, RSTc	ipsi and contralateral reticulospinal tracts
RIP	raphe interpositus nucleus
RMg	raphe magnus nucleus
ROb	raphe nuclei obscuris nucleus
RPa	raphe pallidus nucleus
RtTg	pontine reticulotegmental nucleus
SBS	spinobulbar spinal reflex
SBC	spino-bulbar-cerebellar pathway
SD	standard deviation
SRT	spinoreticular tract
VST	vestibulospinal tract
VGLUT	vesicular glutamate transporter
VGAT	vesicular GABA transporter

# Chapter 1

# 1 Introduction

In addition to the classical spinocerebellar pathways, the cerebellum receives input from the spinal cord via the indirect spino-bulbar-cerebellar pathway (SBC), which projects via the medullary lateral reticular nucleus (LRN). However, the LRN is also involved in a multitude of diverse functions from nociception to not only modifying somatosensory but also special sensory inputs (Buttner-Ennever JA, 1992). Although extensive work has been done, both from the anatomical and physiological point of view, there are still many questions to be answered.

In this chapter, I have reviewed the literature available to date regarding the spinoreticular pathways with the main focus on LRN, projections to it and descending pathways from the brain stem reticular formation to the spinal cord. The study was performed in order to achieve a better understanding of the role of LRN in the control of transmission through spinoreticular pathways, along with afferent inputs to the spinoreticular neurons, their neurochemical properties and the major descending pathways that have modulatory actions on these neurons. Therefore, this chapter is divided into four major sections. The first section focuses on the elementary organisation and general characteristics of the reticular formation; the second section provides an account of the lateral reticular nucleus (LRN); the third section gives an outline of spinoreticular cells, including their distribution, neurochemical properties, and primary afferent contacts and the last section describes their role in spinal reflexes.

## 1.1 The reticular formation (RF)

The reticular formation (RF) is made up of a network of neurons intermingled with dendrites and axons that are involved in a variety of functions from consciousness, to regulation of breathing and from sending sensory information to the brain, to helping regulate muscular activity and posture (Corvaja N et al., 1977b).

This involvement in an extensive variety of functions may to some extent be explained by the morphology of the RF, which has a net-like structure of cells and fibres and extends as a central core of tissue from the spinal cord to the medulla, pons and midbrain. This reticular organisation has some distinct characteristics in that:

- the neurons lie in and receive input from a network of traversing fibres from multiple sources (Brodal A, 1949);
- most of the formation provides a scaffold for integration from multiple afferents without any part being structurally dominant in contrast to a nuclear or laminar organisation;
- most of the neurons have more generalised (isodendritic) rather than specialised (idiiodendritic) characteristics with long dendrites radiating out into different afferent fibre systems (Ramón-Moliner E and Nauta WJ, 1966); and
- the axons are branched and highly collateralised with long descending projections exacting a widespread influence on the spinal cord and brain (Valverde F, 1961a).

This cytoarchitecture is thus ideal for the role of a sensorimotor co-ordinator integrating massive inputs and outputs over vast and diverse areas of the nervous system. Although not very clearly demarcated in some places it serves to integrate sensory information not only from the spinal cord, but also from the supraspinal structures like the cerebral cortex, the cerebellum, the red nucleus and the vestibular apparatus (see review by (Alstermark B and Ekerot CF, 2013).

### 1.1.1 Subdivisions of the brain stem reticular formation

Despite all of these common features of the reticular neurons there are differences across the extent of the RF which forms distinct fields (Brodal P, 1975) or nuclei with overlapping dendrites and axons. In earlier studies the reticular formation was described as being poorly organised because its cell clusters lack distinct boundaries, but now it has been shown that it is highly organised with distinct populations serving specific functions. These populations can be differentiated by their cytoarchitecture within the reticular core using latest techniques of neurochemistry and immunocytochemical localisation by retrograde neuronal tracing and by microelectrode recordings and intracellular labelling not only in rats but also in humans (Allen AM et al., 1988, Huang X-F and Paxinos G, 1995).

In the spinal cord the reticular neurons in the lumbar segments, are mostly distributed in the intermediate laminae (Rexed laminae VI and VII, (Rexed B, 1952) extending ventrally along the base of the dorsal horn. This area extends into the medulla as the ventral (MdV) and dorsal medullary fields (MdD), respectively (Paxinos G and Watson C, 1986, Grant G et al., 2004, Paxinos G and Watson C, 2013).

In standard neuroanatomy text books, the RF in the brain stem has been subdivided into a median, paramedian, medial and lateral reticular zone depending on the mediolateral locations from the midline (Snell RR, 2006, Patestas et al., 2007). Various areas or nuclei within these zones extending rostrocaudally have been recognised according to their morphology and immunohistochemistry in rats as well as humans (Figure 1-1)(Paxinos G and Watson C, 2013). The intermediate reticular nucleus (IRt) extends radially from the floor of the fourth ventricle to the ventral edge of the medulla on a line that separates the alar and basal plate derivatives during development (Allen AM et al., 1988, Huang X-F and Paxinos G, 1995) and thus serves as an anatomical landmark; caudally dividing the medullary reticular nucleus into a ventral (MdV) and dorsal (MdD) part that rostrally merge into the gigantocellular (Gi) and parvocellular reticular nuclei (PCRt), respectively. The Gi and the MdV along with the pontine reticular nuclei constitute the medial zone of the pontomedullary

reticular formation. The PCRt and the MdD form the lateral zone. In the median zone are the raphe nuclei obscuris (ROb), pallidus (RPa), magnus (RMg) and interpositus (RIP), extending caudorostrally. The paramedian reticular nucleus (PMn) and pontine reticulotegmental nucleus (RtTg) are in the paramedian zone. The heterogeneity of the RF was further established by Newman et al in 1992 in rats. They described 13 groups of reticulospinal neurons in the medulla based on their dendritic geometry as revealed by tracer injections combined with Golgi and Nissl stains projecting to the spinal cord via the lateral funiculus with varying amounts of laterality (Newman DB, 1987). Functionally it has been postulated that the lateral zone of the reticular formation is more concerned with sensory aspects, the medial zone with locomotion and the central (median) mostly with autonomic functions (Wang D, 2009). But as we delve deeper into these areas it becomes clearer that there is considerable overlap; and although one function may be dominant there is a high level of integration and interdependence.

The RF extends throughout the spinal cord and continues into the brainstem. Thus there is a heavy spinal input to the bulbar reticular neurons. These are defined as spinoreticular pathways and, in turn, the RF modifies sensorimotor output via descending reticulospinal pathways as explained below.

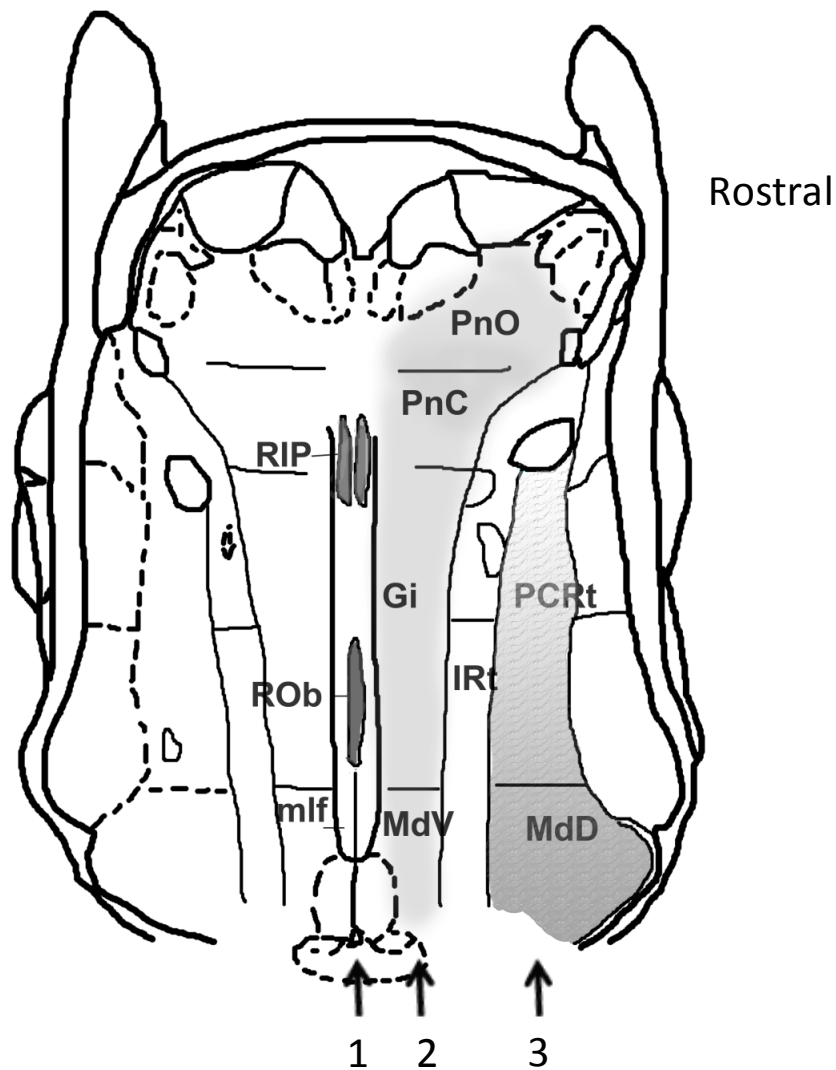


**Figure 1-1** The reticular nuclei in the rat brain stem

Reconstruction of a horizontal section of the rat brain illustrating three zones of the reticular nuclei:

**1) Median zone** (dark grey) showing the raphe nuclei obscurus (ROb) and interpositus (RIP);

**2) Medial zone** (light grey) showing the ventral medullary nucleus (MdV), the gigantocellular (Gi) and the caudal and oral pontine reticular nuclei (PnC, PnO), caudo-rostrally; and the

**3) Lateral zone** (grey textured) with the dorsal medullary nucleus (MdD) and parvocellular reticular nucleus (PCRt).

IRt (intermediate reticular nucleus), mlf (medial longitudinal fasciculus).

*The diagram has been modified and reproduced with permission from 'The rat brain in stereotaxic coordinates', Paxinos & Watson, 2013, Figure 183, interaural 0.9mm, Bregma -9.1mm.*

## 1.1.2 Spinoreticular tracts

Ascending tract cells are classified according to the type of information they process and the targets to which they ascend to (Poppele RE et al., 2002). Hence, there are three groups of spinoreticular pathways: those projecting mostly contralaterally via the ventrolateral funiculus which are subdivided into medial (mSRT) and lateral spinoreticular tracts (LSRT); and neurons innervating the dorsal reticular nucleus (MdD) projecting mostly ipsilaterally (Wang C-C et al., 1999). The medial spinoreticular tract (mSRT) projects to the more medial bulbopontine reticular formation and the lateral spinoreticular tract (LSRT) projects to the LRNs (Menetrey D et al., 1982, Chaouch A et al., 1983, Menetrey D et al., 1983, Villanueva L et al., 1991). Both of which have different cells of origin in the spinal cord as shown below.

### 1.1.2.1 Medial spinoreticular tract (mSRT)

Most of the cells projecting to the medial nuclei of the pontomedullary reticular formation, the Gi, LPGi (lateral paragigantocellular) and the caudal part of the PnC are located in contralateral lamina V and in medial areas of the intermediate and ventral horn equivalent to lamina VII and VIII in the cat (Menetrey D et al., 1982, Chaouch A et al., 1983), as shown in the schematic drawing in [Figure 1-2](#) in red. These projections ascend in the ventrolateral funiculus (Zemlan FP et al., 1978). They respond to high threshold cutaneous afferents and may be involved in chronic pain (Haber LH et al., 1982, Kevetter GA et al., 1982, Sahara Y et al., 1990, Pezet S et al., 1999).

### 1.1.2.2 Lateral spinoreticular tract (LSRT)

In a study on retrograde labelling of spinal neurons projecting to the LRN using HRP, labelled cells were found throughout the rostrocaudal extent of the spinal cord in the intermediate and ventral grey as well as in the lateral spinal nucleus (Corvaja N et al., 1977a, Menetrey D et al., 1983). These axons ascend in the ventrolateral funiculus terminating in a topographical manner in the caudal three quarters of the nucleus (Zemlan FP et al., 1978, Rajakumar N et al., 1992), as shown in [Figure 1-2](#) in blue. The LSRT is involved in motor control as

well as nociception, as explained in greater detail below in ‘Spinal inputs’ Section 1.2.4 (Menetrey D et al., 1983, Janss AJ and Gebhart GF, 1988 , Ness TJ et al., 1998).

### 1.1.2.3 Dorsal medullary reticular nucleus (MdD) tract

The cells of origin of this tract are located in ipsilateral laminae V, VI and VII at all levels of the spinal cord (Bing Z et al., 1990, Villanueva L et al., 1991, Villanueva L et al., 1994) with the superficial dorsal horn and lamina X providing only sparse projections to the nucleus (Raboisson P et al., 1996) as can be seen in [Figure 1-2](#) in green. By contrast Lima et al. labelled cells in lamina I and X and superficial dorsal horn with hardly any in the intermediate lamina (Lima D, 1990), possibly because their injection sites were located more dorsally into the cuneate and gracile nuclei. These fibres project to the dorsal reticular nucleus via the ventrolateral funiculus (Bing Z et al., 1990) and are involved in nociception with inputs from A $\delta$  and C fibres from mechanical and thermal nociceptors (Villanueva L et al., 1994) thus forming an important link in the transmission of signals to the thalamic nuclei as well as projections to several motor areas of the CNS (Villanueva L et al., 1994, Almeida A et al., 2002, Leite-Almeida H et al., 2006).

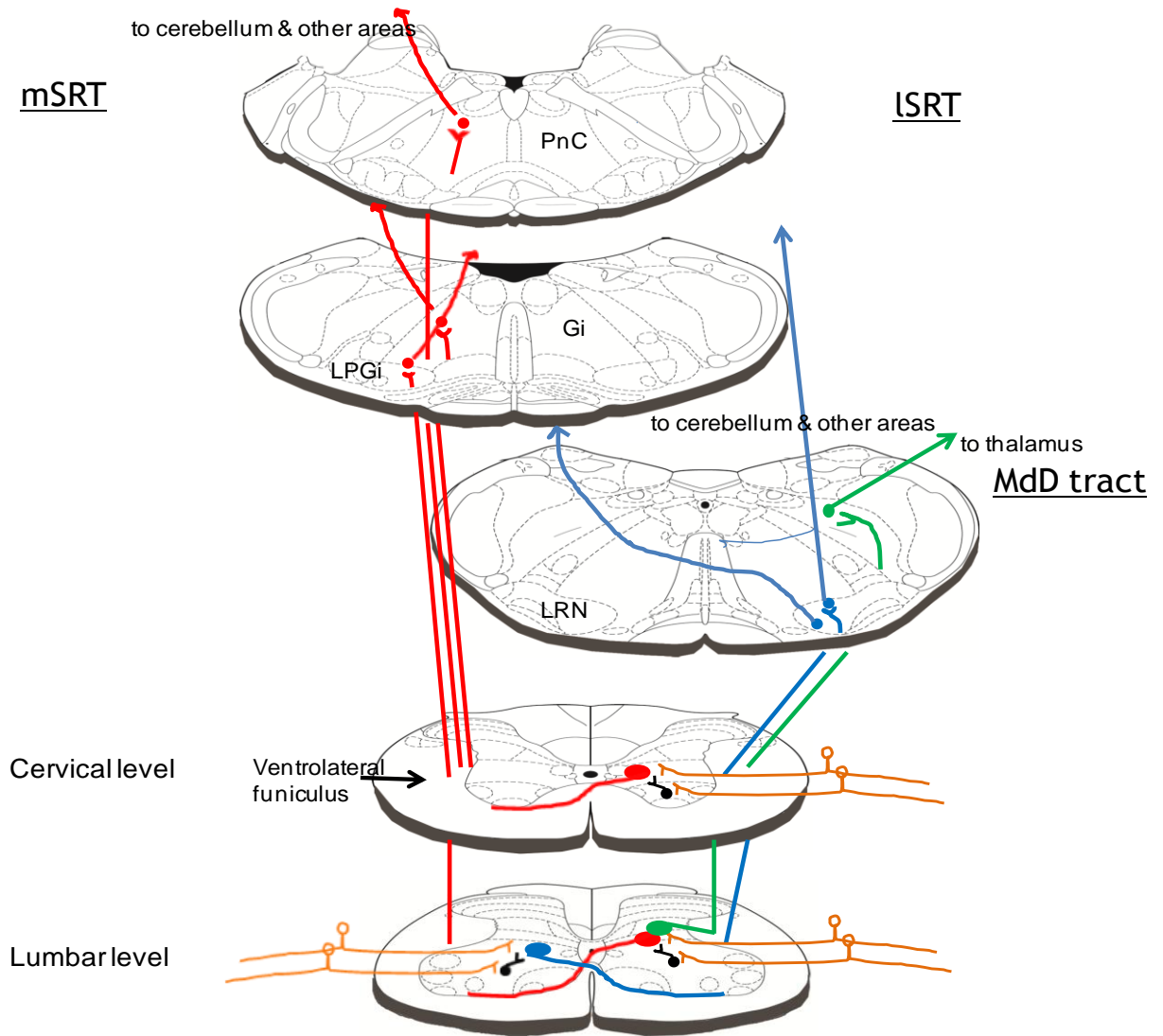


**Figure 1-2 The spinoreticular tracts; a simplified schematic diagram of the ascending reticular tracts**

On the left, the medial spinoreticular tract (mSRT, in red) projects to the lateral paragigantocellularis (LPGi), the gigantocellularis (Gi) and the pontine reticular nucleus (PnO).

On the right, the lateral spinoreticular tract (lSRT, in blue) projects via the ventrolateral funiculus to the lateral reticular nucleus (LRN) and the MdD tract (in green) projects ipsilaterally to the medullary dorsal nucleus (MdD).

*The maps have been modified and reproduced with permission from Paxinos & Watson, 2005.*

### 1.1.3 Reticulospinal tracts

Anatomical and subsequently, physiological studies in rats, cats, macaques and mice have established the presence of fibres descending to the spinal cord, from the medial pontomedullary reticular formation. Two major descending systems have been identified: the medial and the lateral reticulospinal tracts that provide rapidly conducting pathways to the spinal cord (Petras JM, 1967, Peterson BW et al., 1978, Peterson BW, 1979a, Peterson BW et al., 1979b, Jones BE and Yang TZ, 1985, Holstege G, 1991, Reed WR et al., 2008, Sakai ST et al., 2009, Liang H et al., 2011, Watson C and Harrison M, 2012) (Figure 1-3). These pathways are also sometimes referred to as the pontine and medullary reticulospinal tracts, respectively, and because of their role in motor functions are considered to be an extrapyramidal motor system (Peterson BW, 1979a). In addition to these pathways there are other descending fibres that originate from various reticular nuclei including the pedunculopontine and pontine reticular fibres (Martin GF et al., 1979, Martin GF et al., 1985). The raphe nuclei and the ventral part of Gi also have projections to the spinal cord where 5-hydroxy tryptamine (5-HT) is the major neurotransmitter (Bowker RM and Abbott LC, 1990). The RMg and the ventral Gi project via the dorsolateral funiculus and terminate mainly in the dorsal horn with sparse projections in the ventral horn (Bowker RM and Abbott LC, 1990), whereas the ROb and RPa project via the ventrolateral funiculus and end in the ventral horn (Hermann GE et al., 1998).

#### 1.1.3.1 Medial reticulospinal tract (mReST)

The mReST tract originates from neurons located in the medial PnC, PnO and the dorso-rostral part of the Gi and hence is called the pontine reticulospinal tract (Petras JM, 1967, Peterson BW et al., 1979b). Its principal projection is to ipsilateral motor neurons (Figure 1-3, in red). This more rostral pathway descends in the ventral funiculus along with other descending tracts but gradually acquires a more ventromedial position (Petras JM, 1967). Degeneration studies in the cat have shown that although most of the fibres from the pontomedullary region descend in the ipsilateral medial tegmentum (magnocellular), there are some fibres descending in the contralateral medial tegmentum as well as the MLF (medial longitudinal fasciculus) (Petras JM, 1967,

Jones BE and Yang TZ, 1985). Most of the mReST fibres terminate ventrally in medial lamina VIII and adjacent VII at different segmental levels but predominantly in the cervical and to a lesser extent in the lumbar enlargements (Petras JM, 1967). Stimulation of these neurons produce direct monosynaptic excitation of motor neurons predominantly to flexor neurons of limb musculature (Peterson BW et al., 1979b); thus they are a component of the spinobulbar spinal reflex (SBS)(Shimamura M and Kogure I, 1979).

#### 1.1.3.2 Lateral reticulospinal tract (lReST)

This tract as its name suggests descends in the lateral funiculus; originating more caudally from the MdV and the ventro-caudal part of the Gi (Peterson BW, 1979a, Peterson BW et al., 1979b, Watson C and Harvey AR, 2009b). As it descends it assumes a more dorsal position in the lateral funiculus lying in between the ascending tracts (Petras JM, 1967) and finally projecting onto cells in the intermediate lamina with sparser terminations in the dorsal horn (Figure 1-3). It is subdivided into ipsi and contralateral reticulospinal tracts (RSTi, RSTc) as illustrated in Figure 1-3 in green.

A component of the RSTi is restricted to the cervical region (neck cells), descending predominantly from the rostrocaudal aspect of the Gi, and may have a somatotopic distribution. Another part of the RSTi extends into the lumbar spinal cord from a more ventral region of the Gi with some contribution to direct reticulospinal excitation of limb motoneurons, possibly via slowly conducting reticulospinal neurons (Peterson BW, 1979a).

On the other hand Jankowska et al. (2003) described reticular-evoked excitation of hindlimb motoneurons after destruction of the medial reticulospinal tracts. Kuypers suggested that the crossed pathway (RSTc) may be involved in fine distal movements in the forelimbs (Brinkman J and Kuypers HGJM, 1973).

Thus the lSRT has bilaterally projecting fibres that are preferentially distributed to the axial motoneurons (Grillner S et al., 1968, Peterson BW et al., 1978, Sakai ST et al., 2009), with mostly indirect access to limb motoneurons as well as some involved in fine motor control in the forelimb (Peterson BW et al., 1979b).

In addition, it has an inhibitory component to the neck motor neurons from the MdV but limited direct inhibitory influence on motoneurons supplying the limb musculature (Engberg I et al., 1968, Peterson BW et al., 1978).

Although there are some topographical difference between the two tracts; the mReST and the lReST, because they produce different patterns of action on the spinal motor apparatus (Peterson BW et al., 1979b). There are some common elements: stimulation of both ipsilateral and contralateral sides in the PnC, the Gi and MdV evoke monosynaptic responses in lamina VII and VIII in the spinal cord (Maunz RA et al., 1978). Subpopulations of these tracts terminate in both the cervical and lumbar segments at multiple segmental levels (Peterson BW et al., 1979b, Martin GF et al., 1985, Shinoda Y et al., 1996). It has been suggested that these tracts in combination with the vestibulospinal tracts are involved in the bilateral control of locomotion and posture (Krutki P et al., 2003, Cabaj A et al., 2006, Jankowska E et al., 2006, Reed WR et al., 2008, Hammar I et al., 2011). In addition, there is some evidence that the reticulospinal neurons may also be involved in fine finger movements, as seen in monkeys, during an index flexion-extension task with simultaneous recordings from the pontomedullary reticular formation (Soteropoulos DS et al., 2012).

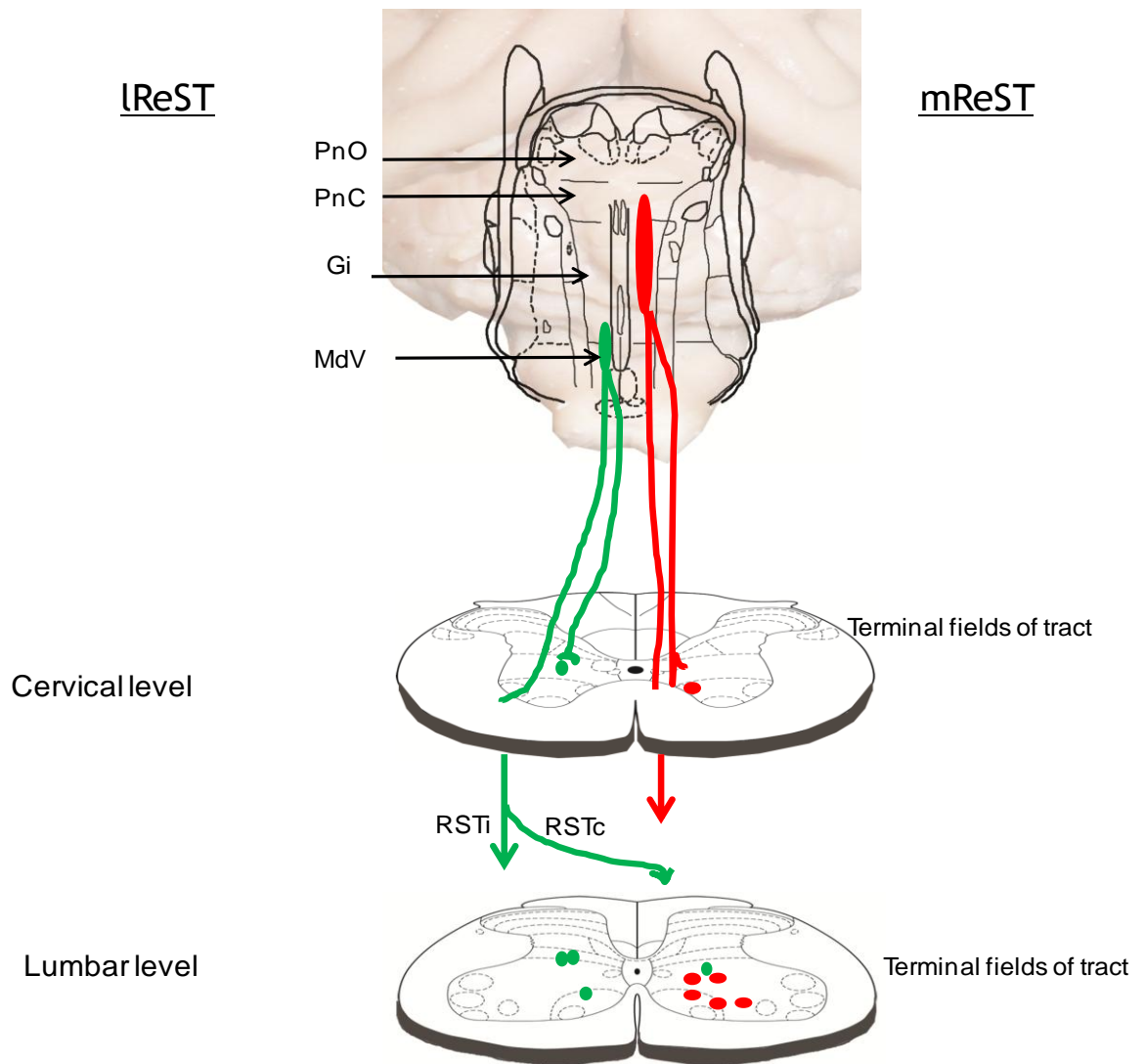


**Figure 1-3 The reticulospinal tracts; a simplified schematic diagram of the descending reticular tracts not including the raphe nuclei**

On the left, the lateral or medullary reticulospinal tract (lReST, in green) projects from the lateral bulbo-medullary area (caudal gigantocellularis, Gi; medullary ventral nucleus, MdV) via the ventrolateral funiculus with ipsilateral (RSTi) and contralateral (RSTc) components.

On the right, the medial or pontine reticulospinal tract (mReST, in red) projects ipsilaterally from the pontine reticular formation to the spinal cord (pontine reticular nuclei caudal and oral, PnC, PnO; rostral gigantocellularis, Gi).

*The maps have been modified and reproduced with permission from Paxinos & Watson, 2005 & 2013.*

## 1.2 Lateral reticular nucleus (LRN)

Most of the brainstem nuclei projecting to the cerebellum are part of the reticular formation including the Gi, MdV, PnO, PnC, IRt, PCRt, LRN and the reticulotegmental nucleus of the pons (RtTg) (Fu Y et al., 2011). The latter two nuclei; LRN and the RtTg are major pre-cerebellar nuclei while the rest are termed minor pre-cerebellar nuclei, classed on the basis of their inputs to the cerebellar cortex. The LRN is distinguished from the myriad of nuclei that make the reticular formation, since it has little in common with the rest of the areas, except for the reticulotegmental nucleus, in terms of functionality (Brodal A, 1949, Brodal P, 1975, Wang D, 2009).

The lateral reticular nucleus sends mossy fibre input to the cerebellar cortex as well as the cerebellar nuclei, fastigial and interpositus (Künzle H, 1975, Hrycyshyn AW et al., 1982, Ghazi H et al., 1987, Fu Y et al., 2011) and has a role in motor activity, including coordination of limb movements and fine reaching movements (Oscarsson O and Rosén I, 1966, Clendenin M et al., 1974 c, Illert M et al., 1977, Arshavsky YI et al., 1978 a, Arshavsky YI et al., 1986, Alstermark B et al., 1987, Alstermark B and Ekerot CF, 2013). In addition to this it plays an important role in the modulation of sensory information and nociception (Ness TJ et al., 1998).

### 1.2.1 Gross Morphology

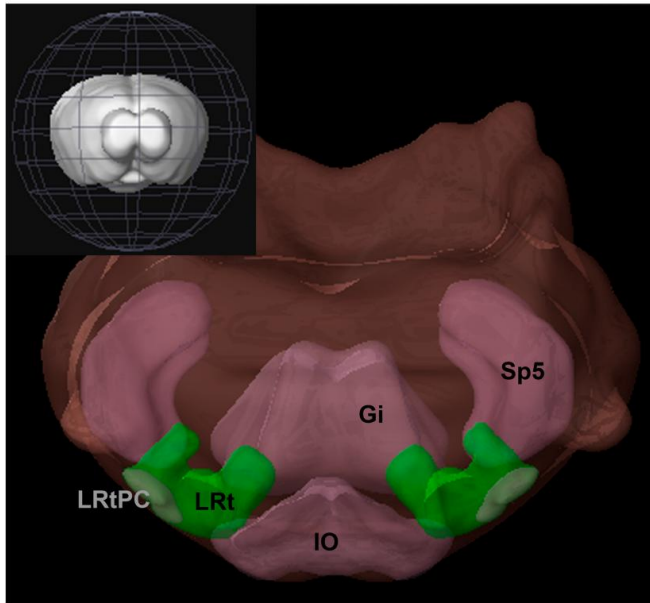
The LRN has a similar morphology in most mammals, as shown by Walberg (1952) in his comparative anatomical study of the LRN in cat, rat, mouse and rabbit. It first appears as a cluster of cells 200µm caudal to the inferior olivary complex and ends at approximately the rostral third of the complex in the rat (Kapogianis EM et al., 1982a, 1982b, Paxinos G and Watson C, 2013). It is situated laterally to the inferior olivary complex throughout its caudorostral extent with the spinal tract of the trigeminal nucleus caudally and the rubrospinal tract more rostrally, on its lateral side (see [Figure1-4A](#) for a three dimensional perspective). The LRN is clearly defined caudally as compared to its rostral extent. It is separated from the ventral surface of the medulla by the ascending ventral spinocerebellar tract (VSCT), with the reticular formation at its dorsal surface, caudally and the

nucleus ambiguus at its dorsal aspect more rostrally, where it eventually subdivides into its medial and lateral parts. Its greatest extent in the rat rostrocaudally is 2800 $\mu$ m, followed by 1400 $\mu$ m mediolaterally and 800 $\mu$ m dorsoventrally (Kaneko T et al., 1989, Newman DB and Ginsberg CY, 1992, Ruigrok TJ et al., 1995a). The LRN is quite varied in all its dimensions changing from one plane to another; it lies more laterally as it extends caudorostrally because of the increasing size of the inferior olive (Blakeslee GA et al., 1938, Kapogianis EM et al., 1982a) (Figure 1-4B).

The LRN in the rat is a distinct structure made up of compact groups of cells that are separated by bundles of fibres coursing in between them. These fibres subdivide the LRN into three parts based on cell sizes. Although each of the subdivisions has a mixture of all cell types there is a predominant cell size within each division, which are referred to as the magnocellular (large celled, 18-23 $\mu$ m), parvicellular (small celled, less than 13 $\mu$ m) and subtrigeminal parts (medium celled, 13-18 $\mu$ m) (Brodal A, 1949, Walberg F, 1952, Ramón-Moliner E and Nauta WJ, 1966, Kitai ST et al., 1967, Kitai ST et al., 1972, Hrycyshyn AW and Flumerfelt BA, 1981a, Hrycyshyn AW et al., 1982, Kapogianis EM et al., 1982b). The majority of the parvicellular cells are small; however there are cells of intermediate and very large diameters (23-33 $\mu$ m) interspersed within this part as opposed to the mostly large cells in the magnocellular portion with small and medium sized cells dispersed throughout. In the subtrigeminal part most of the cells are medium sized fusiform along with some large cells (Kapogianis EM et al., 1982b).

Caudally, after its first appearance as a cluster of cells the LRN rapidly differentiates into a principal dorsomedial magnocellular part and a ventrolateral parvicellular part. The parvicellular part appears as a thin strip that is fused laterally to the larger wedge shaped magnocellular part. More rostrally the nucleus gradually changes its shape and position and about halfway up is divided into a medial principal portion with a medial magnocellular part and a lateral parvicellular part. The subtrigeminal portion appears here and is an extension of the lateral extreme of the LRN. The greatest extents of the magno and parvicellular portions are about midway in the rostrocaudal axis of the LRN (Figure 1-4B) (Blakeslee GA et al., 1938, Brodal A, 1949, Walberg F, 1952).

**A.**



**B.**

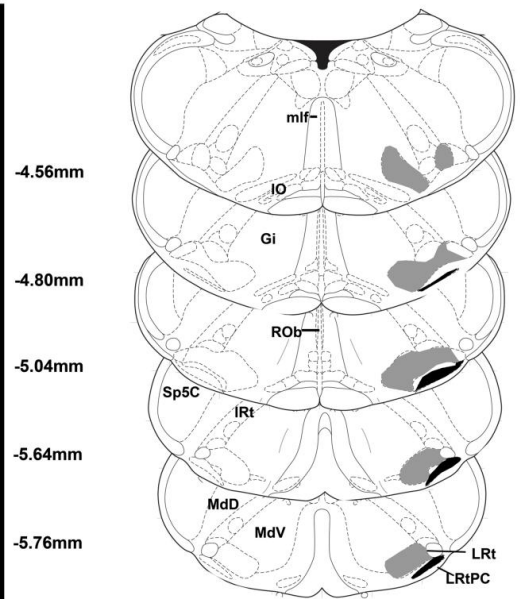


**Figure 1-4 The lateral reticular nucleus, gross morphology and anatomical location in the brain stem**

A. A 3-dimensional image of the lateral reticular nucleus (LRt/ LRN) in the mouse brain shown in green, bordered by; the inferior olivary complex (IO) medially, the spinal tract of the trigeminal nerve (Sp5) laterally and the gigantocellularis dorsomedially (Gi). The plane of view is coronal (image top left hand corner) looking at the structures rostrocaudally.

*Image modified and reproduced with permission from ‘Allen Institute for Brain Science, (Aibf, 2014)’.*

B. A 2-dimensional image of the lateral reticular nucleus (LRt/LRN) in the rat brain illustrating magnocellular (grey) and parvicellular parts (black, LRtPC) and the changes in form, rostrocaudally and mediolaterally.

*The maps are modified and reproduced with permission from ‘(Paxinos G and Watson C, 2005)’.*

## 1.2.2 Cytoarchitecture of the LRN

The somata of the neurons in each division of the LRN are a mixed variety of multipolar, piriform, triangular and fusiform shapes. The large cells are mostly multipolar with cell diameters of 18-23 $\mu$ m, the small ones round or ovoid (<13 $\mu$ m) and the medium sized triangular or piriform (13-18 $\mu$ m) with no interneurons present as no locally ramifying axons or axon collaterals are found. Most of the small neurons are postulated as sending a continuous stream of information to the cerebellum (Brodal A and Courville J, 1973, Brodal P, 1975, Andrezik JA and King JS, 1977) while the larger cells are involved in processing exteroceptive information (Kitai ST et al., 1972, Hrycyshyn AW and Flumerfelt BA, 1981b).

LRN neurons are arranged into unique clusters of cells of about five to ten cells as seen in Golgi preparations (Valverde F, 1961a, Kapogianis EM et al., 1982b), but it is now evident that many more cells make up these clusters as can be seen in the confocal image in [Figure 1-5](#). Most of the cells lie close together with their dendrites intertwined, forming dendritic plexuses. These plexuses receive contributions not only from adjoining clusters but also from far off cells, and in return send overlapping dendrites back to these clusters (Ramón-Moliner E and Nauta WJ, 1966, Kapogianis EM et al., 1982a, 1982b). The dendrites irrespective of soma morphology are polarized and travel to and from cell clusters winding around each other with major trunks bifurcating and passing close to the somata of other cells (Kapogianis EM et al., 1982b).

The RF is made up of two major types of neurons based upon their unique dendritic morphology; iso- and idiodendritic. The isodendritic neurons are named thus because their dendrites are more or less similar or uniform and make up most of the LRN with an overlap of dendritic fields extending from the spinal cord to the midbrain, hence their role in integration of signals from distant sources (Ramón-Moliner E and Nauta WJ, 1966, Andrezik JA and King JS, 1977, Martin GF et al., 1977, Hrycyshyn AW and Flumerfelt BA, 1981b, Hrycyshyn AW et al., 1982, Ghazi H et al., 1987). The soma is triangular or polygonal with primary dendritic trunks running rectilinearly a short distance, bifurcating into secondary branches that end in plexuses with some long dendrites extending

further away. In addition the LRN has allodendritic cells with several twisting irregular orders of dendrites as can be seen in [Figure 1-5](#). Most secondary branches are contorted with irregular calibres, bulbs and spines. These multipolar, fusiform and piriform cells have been reported as pre-cerebellar cells by Ramón-Moliner and Nauta in 1966 (Hrycyshyn AW and Flumerfelt BA, 1981a).

In addition cervical hemisections show that only 5% of the terminals in the LRN undergo degeneration mostly on the distal dendrites of LRN neurons (Hrycyshyn AW and Flumerfelt BA, 1981b, Flumerfelt BA et al., 1982). Hrycyshyn and Flumerfelt in 1981 reported both round and pleomorphic-vesicle terminals undergoing degeneration. This may well be an indication of the excitatory and inhibitory terminals of projection fibres reported by Ekerot et al. (1975).

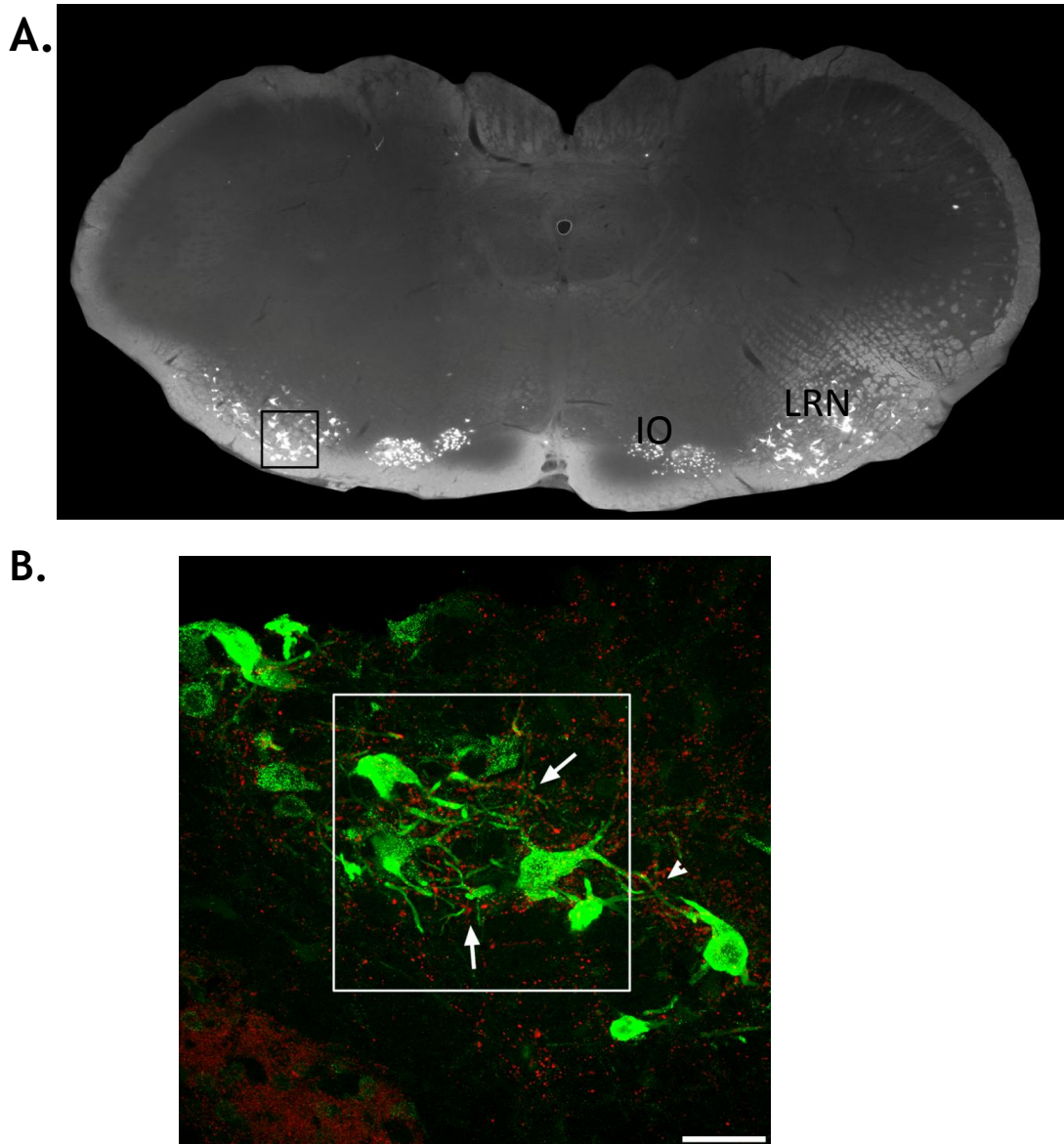


**Figure 1-5 The cytoarchitecture of the lateral reticular nucleus (LRN)**

**A.** Fluorescent photomicrograph of a transverse section of the medulla illustrating retrogradely labelled pre-cerebellar LRN neurons (white cells in black inset) and IO, (inferior olivary nucleus).

**B.** A magnified view of the inset in 'A' showing fluorogold labelled pre-cerebellar cells (in green) forming clusters (white box). Allodendritic cells with wavy dendrites inter-lacing within the cluster (white arrows) and some dendrites projecting to neighbouring clusters (arrow head). The spinoreticular terminals are anterogradely labelled (in red) from the lumbar spinal cord. Scale bar 50µm.

*The images are obtained from rat medullary tissue analysed in Chapter 3.*

### 1.2.3 Afferents to the LRN

Anatomical investigations using retrograde tracers, like horseradish peroxidase conjugated to wheat germ agglutinin (WGA-HRP), and induced degeneration have shown that the major contribution to the LRN is via bilaterally projecting fibres from the spinal cord (Brodal A, 1949, Rossi GF and Brodal A, 1956, 1957, Kitai ST et al., 1967, Künzle H, 1973, Clendenin M et al., 1974 b, Corvaja N et al., 1977a, Hrycyshyn AW and Flumerfelt BA, 1981a, 1981b, Flumerfelt BA et al., 1982, Menetrey D et al., 1983, Shokunbi MT et al., 1985). This projection is from a highly diverse spinal subpopulation of neurons that form a selective path to the LRN, as shown in studies using latest trans-synaptic viruses (Pivetta C et al., 2014). The caudal three fourths of the LRN receives a large topographical projection from the entire contralateral spinal cord (Rajakumar N et al., 1992). The lumbosacral fibres terminate mostly in the parvicellular part (lateral) and the cervical fibres end more medially in the magnocellular part (Brodal A, 1949, Künzle H, 1973).

In addition, the lateral half of the rostral LRN receives both ipsi and contralateral rubro-reticular afferents (Corvaja N et al., 1977a, Hrycyshyn AW and Flumerfelt BA, 1981b, Qvist H et al., 1984, Shokunbi MT et al., 1985, Alstermark B et al., 1992, Matsuyama K et al., 2004) and the medial half of the rostral LRN receives predominantly contralateral sensorimotor cortico-reticular afferents (Hrycyshyn AW and Flumerfelt BA, 1981b, Shokunbi MT et al., 1985). These tracts monosynaptically excite LRN neurons (Kitai ST et al., 1974a). Most of the projection fibres to the middle third of the LRN are from the contralateral fastigial nucleus (Corvaja N et al., 1977a, Hrycyshyn AW and Flumerfelt BA, 1981b), where fibres from the red nucleus and the spinal cord overlap substantially. The middle third of the LRN receives extensive overlapping contributions from the spinal cord, the red nucleus, the fastigial nucleus and the cerebral cortex and thus this region of the LRN integrates spinal and supraspinal inputs to the cerebellum (Corvaja N et al., 1977a, Rajakumar N et al., 1992). LRN neurons in addition receive input from the respiratory centres (Ezure K and Tanaka I, 1997), the vestibular system with inputs from the propriospinal afferents in the neck (Ladpli R and Brodal A, 1968, Kubin L et al., 1980), the contralateral superior colliculus (Kawamura S et al., 1974), the oculomotor

region (Qvist H, 1988) and the contralateral inferior olive (Corvaja N et al., 1977a).

Neurons receiving input from forelimb afferents via a pathway in the dorsal funiculus (DF) and from the face via the trigeminal afferents send a multimodal input to the magnocellular region of the LRN (Clendenin M et al., 1975). This DF-trigeminal pathway provides information regarding face and head movements and with a cervical input from the bVFRT (bilateral ventral flexor reflex tract) indicate an integration of these movements with the forelimb (Clendenin M et al., 1975).

#### **1.2.4 Spinal inputs**

The spinal input to the LRN via the lateral spinoreticular pathway (LSRT) has been identified as consisting of three very distinct physiological pathways: the bilateral ventral flexor reflex tract (bVFRT); the ipsilateral forelimb tract (iFT); and the C3-C4 propriospinal tract (C3-C4 PNs) (Holmqvist B, 1960, Lundberg A and Oscarsson O, 1962b, Rosén I and Scheid P, 1973a, Clendenin M et al., 1974 b, Illert M et al., 1978, Alstermark B et al., 1981, Ekerot CF, 1990a). These tracts ascend in the ventrolateral funiculus, with the bVFRT projecting contralaterally and the iFT and C3-C4 PNs projecting ipsilaterally (Lundberg A and Oscarsson O, 1962b, Alstermark B and Ekerot CF, 2013).

##### **1.2.4.1 bVFRT**

The bVFRT neurons are distributed throughout the ventromedial extent of the intermediate laminae of the spinal cord from the cervical to the lumbar segments (Oscarsson O and Rosén I, 1966, Clendenin M et al., 1974 b). They receive input from bilateral polymodal primary afferents (flexor reflex afferents) in the hind and forelimb nerves (Eccles RM and Lundberg A, 1959a, Lundberg A and Oscarsson O, 1962a, Rosén I and Scheid P, 1973a, Clendenin M et al., 1974 b, Ekerot CF, 1990c) and also a modulatory input from the descending lateral vestibulospinal tract (Grillner S et al., 1968, Rosén I and Scheid P, 1973a, Corvaja N et al., 1977a, Kubin L et al., 1980). Their axons cross segmentally and ascend in the ventrolateral funiculus and terminate in a more ventromedial part

of the LRN, overlapping extensively (Oscarsson O and Rosén I, 1966, Rosén I and Scheid P, 1973c, Alstermark B and Ekerot CF, 2013).

In addition although most bVFRT projections are contralateral there are some terminations in the ipsilateral LRN as well (Künzle H, 1973, Flumerfelt BA et al., 1982). Furthermore projections from the LRN to the cerebellar cortex are bilateral with collaterals to the cerebellar fastigial and interpositus nuclei (Clendenin M et al., 1974 a). This may have a bearing on their functional roles as physiological studies conducted in cats show that contralaterally projecting cells receive bilateral inputs from flexor reflex afferents (Rosén I and Scheid P, 1973a, Clendenin M et al., 1974 b, Ekerot CF, 1990c) with excitatory vestibulospinal inputs (Holmqvist B, 1960, Lundberg A and Oscarsson O, 1962b, Grant G et al., 1966, Grillner S et al., 1968, Rosén I and Scheid P, 1973b) whereas ipsilaterally projecting neurons have an ipsilateral receptive fields with no monosynaptic supraspinal control (Clendenin M et al., 1974 b, Ekerot CF, 1990b). The convergence effects seen in the LRN can be explained by bilateral, ipsilateral and contralateral convergence at the spinal segmental levels. Cervical and thoracic neurons receive input from both fore and hindlimbs while lumbar neurons have additional inputs from the forelimbs. Thus the bVFRT conveys information to the LRN regarding interneuronal circuitry involved in spinal reflexes (Sherrington CS, 1910, Rosén I and Scheid P, 1973b).

#### *Functional aspect*

The bVFRT consists of not only excitatory but also inhibitory neurons projecting to the LRN (Rosén I and Scheid P, 1973c, Ekerot CF, 1990b). Although both monosynaptic EPSPs and IPSPs are evoked in the ventrolateral part of the LRN from the ipsilateral ventrolateral funiculus, there is apparently no differentiation in the termination pattern of excitatory and inhibitory terminals (Ekerot CF, 1990a, 1990c). The neurons at the origin of the bVFRT path receive information regarding activity in local spinal circuits that are involved in motor functions like standing, locomotion and scratching (Clendenin 1974, (Ekerot CF, 1990c). Although it has previously been suggested that the bVFRT works in a complementary fashion with the direct ventral spinocerebellar tract (VSCT), one being active in the flexion stage and the other in the extension stage of movement, respectively (Arshavsky YI et al., 1978 a, 1978 b), it has now come to

light that the bVFRT neurons may in fact be involved also in the extension phase. This is true not only in the case of scratching but also in fictive locomotion (Ezure K and Tanaka I, 1997). So when thinking about the possible function of the bVFRT it should be taken into consideration that a) the neurons in the spinal cord receive excitatory and inhibitory input from both contra and ipsilateral nerves (Lundberg A and Oscarsson O, 1962b, Rosén I and Scheid P, 1973b) and b) they have very prominent vestibulospinal inputs at all segmental levels of the spinal cord (Holmqvist B et al., 1959, Grant G et al., 1966, Rosén I and Scheid P, 1973b). Hence, the bVFRT is involved in limb movements and their coordination, as well as in axial control and posture.

#### 1.2.4.2 i-FT

The ipsilateral forelimb tract originates from neurons in the dorsolateral part of the cervical segments innervating the forelimb musculature. They receive a multimodal input which is exclusively from the ipsilateral forelimb (Corvaja N et al., 1977a, Ekerot CF, 1990b, Alstermark B and Ekerot CF, 2013, Pivetta C et al., 2014) and some descending input via the rubro and corticospinal tracts (Ekerot CF, 1990a). Their axons ascend ipsilaterally in the ventrolateral funiculus and terminate in the dorsolateral magnocellular part of the LRN (Clendenin M et al., 1974 c, Ekerot CF, 1990b, Pivetta C et al., 2014) with projections to the ipsilateral cerebellum (Clendenin M et al., 1974 a, Hrycshyn AW and Flumerfelt BA, 1981b, Pivetta C et al., 2014).

#### *Functional aspect*

The function of the iFT is control of the ipsilateral forelimb (Ekerot CF, 1990b) in grasping movements of the digits in cats. Information about cervical spinal motor activity is carried to the magnocellular LRN via the iFT where input from the cortex and red nucleus modify output to lower motor centres via a descending path (Oscarsson O and Rosén I, 1966, Miller R, 1996), thus participating in the integration of all these ascending and descending systems (Alstermark B et al., 1984, Alstermark B and Ekerot CF, 2013).

In addition to the excitatory iF-tract there is an inhibitory tract from the ipsilateral forelimb receiving monosynaptic low threshold cutaneous input from the distal part of the forelimb and projecting to the same areas in the LRN

(Clendenin M et al., 1974 a, Ekerot CF, 1990b). Both the inhibitory and excitatory pathways are stimulated monosynaptically by the iDLF (ipsilateral dorsolateral funiculus). The iF-tract and the bVFRT converge on some LRN neurons with strong inhibitory as well as excitatory input from the ipsilateral forelimb (Ekerot CF, 1990b).

#### 1.2.4.3 C3-C4 propriospinal system

This pathway like the iFT has its origin from the cervical segments, more specifically C3 and C4 in the intermediate lamina VI, VII and VIII (Illert M et al., 1978, Alstermark B et al., 1981, Alstermark B et al., 1987, Alstermark B et al., 1990). The C3-C4 propriospinal neurons (PNs) have bifurcating axons; one ascending to the dorsocaudal LRN and the other descending to lower motor neurons (Illert M et al., 1978, Alstermark B et al., 1981). They act as interneurons that mediate descending tract information from the cortical, rubral, reticular and tectal spinal tracts and send short descending axons to the forelimb motor neurons in C6-Th1. In addition there are long rather weak descending projections to the thoracic and lumbar spinal cord similarly controlled by higher centres and forelimb afferents. These projections are ipsilateral and are located in the ventral part of the lateral funiculus. They receive low threshold cutaneous and Group I muscle afferents (Illert M et al., 1978).

##### *Functional aspect*

C3-C4 propriospinal neurons (PNs) receive disynaptic information from higher motor centres and form monosynaptic inputs, excitatory as well as inhibitory, with forelimb motor neurons (Illert M et al., 1978, Alstermark B et al., 1984). In addition to this they influence motor neurons indirectly via 1a inhibitory interneurons. Furthermore, forelimb afferents have strong inhibitory influences on these PNs in addition to some excitatory inputs. Thus these two paths coordinate in the final execution of forelimb activity: indirectly via 1a inhibitory neurons to both flexors and extensors providing reciprocal inhibition during limb movements; and the direct inhibitory input to forelimb motor neurons involved in more complex inhibitory actions, requiring inhibition of muscles in different combinations (Alstermark B et al., 1984 a, 1984 b).

Behavioural experiments by Alstermark have shown that these neurons send information to the descending systems to help in visually guided forelimb reaching in the cat as well as precision grip with thumb and index finger in monkeys (Alstermark B et al., 1981, Alstermark B et al., 1992, Alstermark B and Ekerot CF, 2013). Hence, along with the primary function of these PNs in ipsilateral forelimb control, input from the descending systems plays a subsidiary role in positioning of the body during forelimb movement. In addition it has been postulated that these PNs may play a role in inter-limb reflexes (Arshavsky YI et al., 1986).

### **1.2.5 Somatotopic vs. topographic organisation of the LRN**

The somatotopic organisation of the spinoreticular pathways in the LRN has been shown by retrograde tracers (Brodal A, 1949, Künzle H, 1973, Corvaja N et al., 1977a, Garifoli A et al., 2006) and physiological experiments in cats (Clendenin M et al., 1974 a, Ekerot CF, 1990a) and by induced degeneration in rats (Flumerfelt BA et al., 1982), cats (Künzle H, 1973) and monkeys (Mehler WR et al., 1960). To summarise, the hindlimb projections to the lateral part of the LRN project to cerebellar hindlimb areas of the anterior lobe and paramedian lobule. The medial part of the LRN receives cervical inputs and projects to the forelimb areas of the cerebellum. Thus there is a tendency for the lumbar cells to project to the parvicellular, the cervical cells to the magnocellular region (Künzle H, 1973) and the thoracic to the intermediate transition zone between the parvicellular and magnocellular regions. The pattern of distribution within these regions is actually a mediolateral lamellar arrangement of neurons projecting from the cervical areas and progressing caudally (Künzle H, 1973). However, there are some physiological studies that failed to show this somatotopic pattern (Grant G et al., 1966, Oscarsson O and Rosén I, 1966, Rosén I and Scheid P, 1973b). Künzle (1973) has argued that the LRN spinal afferents are more topographical rather than somatotopic. The explanation provided is that most bVFRT have large bilateral receptive fields with inputs from different areas of the body, for example lumbar neurons receive input not only from the hindlimbs but also from the forelimbs as demonstrated by Rosén and Scheid (1973). There is thus a convergence at the spinal level of monosynaptic and/or polysynaptic input via ascending and descending propriospinal pathways rather than within

the LRN itself (Rosén I and Scheid P, 1973c). The projection from the spinal segments would thus be topographically relayed to the LRN and onto the cerebellum (Künzle H, 1975). This sheds some light on the actual role of the LRN in not only relaying information but also in the integration of inputs.

### **1.2.6 Physiological response properties of the LRN neurons**

Approximately 48% of the neurons in the LRN can be stimulated by antidromic stimulation of the contralateral ventrolateral quadrant of the spinal cord with monosynaptic input onto bVFRT neurons (Clendenin M et al., 1974 b, Clendenin M et al., 1974 c). These LRN neurons were then classified by Clendenin et al. based on their physiological response properties:

a) The bVFRT-LRN neurons have disynaptic responses to activation of the contralateral ventral funiculus and the contralateral vestibulospinal tract. Most of the cells are activated by more than one limb afferent with more than half of them located in the parvicellular region. The reticulocerebellar fibres, from these neurons, then project to lobules IV-V bilaterally and ipsilaterally to the paramedian lobule. The bVFRT-LRN neurons have been further subdivided into four categories based upon the inputs they receive from various spinal segments: cervical, thoracic, lumbar and convergence. The first three groups respond to stimulation of the bVFRT at their respective segmental levels while the convergence group responds to stimulation from several different levels (Clendenin M et al., 1974 b). There is a considerable overlap in the location of these cells in the parvicellular and magnocellular LRN. The cervical and lumbar groups of LRN neurons project more to the intermediate cortex of the cerebellum and hence convey information regarding limb movements while the thoracic, because of their projections to the vermis, are involved in trunk movements (Clendenin M et al., 1974 b, Ekerot CF, 1990c). Most of the convergence from the fore and hindlimbs are onto thoracic cells in the LRN presumably because they are located at equidistance from both cervical and lumbar segments. The lumbar neurons receive both ipsi and contralateral inputs whilst the cervical receive mostly ipsilateral or contralateral convergence. This convergence may play a role in integrating the information from various parts of the body and then transmitting it to the cerebellum, thus producing better

coordination and fluidity of movement. This theory has been further advanced by Arshavsky et al. (1984) who demonstrated that the main spinal input to the SRT neurons as well as ventral spinocerebellar tract (VSCT) neurons, is a rhythmic generator in L3-4 spinal segments. These neurons then convey generalised information to the cerebellum via the LRN about limb movements. Hence the final information to the cerebellum concerns activity of spinal circuitry rather than the peripheral motor apparatus.

b) The iF-LRN neurons receive exclusive excitation from the ipsilateral forelimb nerves, located mostly (85%) in the magnocellular part of the LRN and project ipsilaterally to lobule V and the paramedian lobule (Clendenin M et al., 1974 c).

c) The X-LRN neurons are weakly activated by stimulation of the ventrolateral quadrant with more activation from ipsilateral forelimb afferents. They are distributed throughout the parvicellular and magnocellular regions with projections to the ipsilateral lobule V.

d) The Y-LRN neurons are only activated from the dorsal funiculus at C3 and hence may be involved in the dorso funicular trigeminal pathway (DF-trigeminal) (Clendenin M et al., 1975).

### **1.2.7 Efferents of the LRN**

The LRN is a major pre-cerebellar nucleus but in addition to this primary role it sends projections to other structures in the brainstem and the spinal cord. It has been suggested that these fibres are actually collaterals arising from mossy fibre inputs to the cerebellum (Ito J et al., 1982, Qvist H et al., 1984, Qvist H, 1988, 1989). These studies utilising retrograde HRP tracer injections in the cerebellum indicate a topographic organisation of afferent fibres to the LRN from the spinal cord, red nucleus and cerebral cortex; with this pattern being preserved in the projections from the LRN to the cerebellar cortex.

Mossy fibre projections arising in the LRN terminate bilaterally in the cerebellar cortex as well as the cerebellar nuclei, the interpositus and fastigial in cat (Künzle H, 1975, Hammar I et al., 2011) as well as in rats (Hryciyshyn AW et al.,

1982, Ghazi H et al., 1987). These fibres enter the cerebellum via the inferior cerebellar peduncle ending in the anterior lobe, vermis and paramedian lobule. They also send collaterals caudoventrally to the anterior and posterior interpositus nuclei, and the medial and lateral cerebellar nuclei in the cat (Qvist H, 1989). These reticulocerebellar fibres project topographically to the interpositus in a similar way to the cerebellar cortex, thus while the anterior part receives fibres from all the LRN, its rostral part receives input from the lateral LRN i.e. the parvicellular hindlimb part (Martin GF et al., 1977, Martin GF et al., 1988). The caudal interpositus receives input from the medial magnocellular forelimb part (Brodal P, 1975, Qvist H, 1989).

Some studies have revealed a direct ipsilateral projection from the LRN to the lateral vestibular nucleus (Ito J et al., 1982) whereas Ruigrook et al. (1995) reported a bilateral projection from the LRN to the lateral vestibular nucleus in rats but not as a direct reticulo-vestibular pathway. They describe a reticulo-cerebellar-vestibular pathway in which mossy projections send collaterals to the vestibular nuclei and may play a role in the control of descending vestibulospinal input to bVFRT neurons. That in turn would eventually affect the co-ordination of movement in maintaining body equilibrium.

The LRN also sends fibres to the ipsilateral cochlear nucleus as well as a minor projection to the contralateral nucleus which originates mainly from cells in the magnocellular portion (Ryugo D et al., 2003, Zhan X and Ryugo DK, 2007). The processing of sound is not only defined by the circuits traditionally viewed as auditory (pathways directly or indirectly associated with the cochlea) but also by non-auditory circuits like somatic proprioception (Haenggeli C-A et al., 2005, Shore SE, 2005) and head position via vestibular afferents (Ito J et al., 1982, Newlands SD et al., 2003, Zhan X and Ryugo DK, 2007). All these inputs could involve a state of arousal and proprioceptive effect that may involve the LRN as a possible seat of integration affecting acoustic processing (Jones BE and Yang TZ, 1985).

LRN neurons projecting to the spinal cord are located in the magnocellular division bilaterally with an ipsilateral predominance but hardly any cells are present in the parvicellular part as reported by Lee et al. (1999) with some of

these cells sending collaterals to the periaqueductal grey (PAG) influencing endogenous analgesic mechanisms in the CNS and thus may modulate pain circuitry in the spinal cord. The role of the LRN in the descending control of nociception and also in local spinal circuitry has been shown by many electrophysiological experiments (Fields HL et al., 1977, Jones SL and Gebhart GF, 1988, Janss AJ and Gebhart GF, 1988b). Hall et al. demonstrated descending inhibitory inputs from the LRN terminating bilaterally in the dorsolateral funiculi of the spinal cord (Hall JG et al., 1982). Reticulospinal tract neurons have powerful actions in the spinal cord and are important for adjusting both posture and a variety of reflex and centrally initiated movement (Peterson BW et al., 1978, Peterson BW et al., 1979b) and are considered to be particularly important for coordinated actions of the limbs and trunk. Pontomedullary reticular fibres descending via the MLF have a monosynaptic action on flexor motoneurons of the hindlimb and back (Grillner S et al., 1968, Galea MP et al., 2010). However the CVLM pathway has been hardly studied in this respect.

In addition the neurons in the rostro-medial medulla have a high level of collateralisation of their descending projections which suggests that they may ultimately act on widely distributed peripheral targets. This would signify that they play a generalised modulatory role across various functional modalities rather than having specific topographically limited roles.

### **1.2.8 Neurochemical properties of bulbospinal (BS) pathways**

The bulbospinal system is made up of fibres originating in the brainstem that project to the spinal cord via tracts in the medulla, including the MLF and axons from the caudal ventrolateral medulla (CVLM) including the LRN (Holstege JC, 1996a). The descending systems of the brain modify the sensorimotor processes within the spinal cord. Immunocytochemical evidence shows that some BS terminals contain inhibitory neurotransmitters, GABA/glycine, (Holstege JC, 1996a, Du Beau A et al., 2012, Huma Z et al., 2014) although the majority use the excitatory neurotransmitter, L-glutamate (Jankowska E and Stecina K, 2007, Hossaini M et al., 2012). Axons projecting via the MLF mainly terminate in the intermediate grey and ventral horn areas of the lumbar spinal cord while fibres passing through the CVLM terminate in the deep dorsal horn and intermediate

grey matter mostly on the ipsilateral side (Du Beau A et al., 2012, Huma Z et al., 2014). Although the majority of excitatory fibres are immunoreactive for VGLUT-2 (vesicular glutamate transporter 2), a significant proportion of these bulbospinal terminals are inhibitory and are immunoreactive for the vesicular GABAergic transporter (VGAT) (Du Beau A et al., 2012, Huma Z et al., 2014). On the other hand extensive electrophysiological data in the cat suggest that most descending systems have monosynaptic excitatory action on spinal target neurons and descending inhibitory mechanisms operate predominantly via interneurons. However, neurochemical properties of BS neurons suggest that descending inhibitory reticulospinal contacts (ReST) would directly influence target neurons in the spinal cord as suggested by Engberg et al. (1968). In addition many BS terminals also contain serotonin co-localised with a variety of peptides such as substance P, TRH (thyrotropin releasing hormone) and enkephalin (ENK) (Bowker RM and Abbott LC, 1990) which terminate predominantly in the ventral horn. These bulbospinal projections appear to mediate different types of behaviour, ranging from muscle atonia to running and walking. The balance of inhibitory and excitatory activity between GABA and glycine containing fibres on the one hand and glutamate and serotonin on the other hand will determine the level of muscular activity (Sqalli-Houssaini Y et al., 1993, Holstege JC, 1996a). This pathway is also part of the spinobulbar-spinal reflex (SBS) originating from the medial bulbar reticular formation and descending to the motor neurons (see below) (Shimamura M and Kogure I, 1979).

### **1.2.9 Functional aspects of the LRN**

The LRN due to its afferent and efferent projections serves to integrate and regulate various sensorimotor functions. Magnusson et al., in a series of electrophysiological experiments on neonatal rats, showed that there is a bilaterally projecting pathway from the lumbar enlargement to the locomotor specific nuclei in the brain stem because sectioning at this level abolished any locomotion via the ventrolateral funiculus (Magnuson DS et al., 1998). They then went ahead, using tract tracing techniques, to show that the origin of this tract was in the contralateral intermediate lamina with largest field potentials recorded in the caudal LRN (Antonino-Green DM et al., 2002).

As discussed above, the LRN receives input from spinal as well as supraspinal structures and the present evidence suggests, as proposed by Alstermark et al. (2013), that the LRN serves not only to relay but also to integrate information from all these structures before sending it to the cerebellum (Künzle H, 1973, Rosén I and Scheid P, 1973b, Clendenin M et al., 1974 c, Flumerfelt BA et al., 1982, Ekerot CF, 1990c). This counters the original theory that the LRN subserves purely as a relay station between the cerebellum, other supraspinal structures and the spinal cord (Flumerfelt BA et al., 1982). As mentioned previously because of the afferent and efferent connections of the ventrolateral LRN it may have a more global control of motor functions. Thus cerebellar output is likely to be fine tuned according to peripheral sensory input, for example, motor response to painful stimulus by withdrawal and posture adjustment via the LRN.

In addition, the LRN has been postulated to be involved not only in sensorimotor but also in nociceptive activity. Liu et al. (1990) showed four types of LRN neurons: Type 1, responsive only to non-noxious stimuli; Type 2, responsive to both noxious and innocuous stimuli; Type 3, responsive exclusively to noxious stimuli; and Type 4, not responsive to any type of cutaneous stimuli. All of these neurons had large bilateral receptive fields with the majority responding to noxious stimuli. Hall et al. (1982), by examining electrolytic lesions in various areas of the brainstem, found that tonic descending inhibition was reduced by bilateral lesions of the caudal ventrolateral medulla in the region of the LRN. Thus the LRN may have a functional role in the control of pain via anti-nociceptive inputs to the spinal cord (Hall JG et al., 1982, Jones SL and Gebhart GF, 1988, Rong-Huan L et al., 1990, Rong-Huan L et al., 1993).

Furthermore, LRN cells also respond to visceral noxious stimulation and are involved in autonomic control (Ness TJ et al., 1998). However, further projection of these nociceptive neurons to the cerebellum has not yet been clearly defined (Shokunbi MT et al., 1985, Lee HS and Mihailoff GA, 1999) as yet. The LRN is a site of integration of hypothalamic, cardiovascular and somatic afferent inputs where stimulation of the LRN elicits an increase in heart rate and arterial pressure in response to stimulation of somatic afferents. This phenomenon has been exhibited by bilateral lesions of the LRN where any such response was eliminated in response to stimulation of the carotid sinus,

posterior hypothalamus, sciatic nerve or even static contraction of the hindlimb muscles (Ciriello J and Calaresu FR, 1977, García-Larrea L et al., 1993).

Thus the LRN has a multifaceted role in not only the somatosensory but also the autonomic functions of the body integrating all these systems and modifying motor responses through the cerebellum.

### **1.3 Cells of origin of the lateral Spinoreticular pathway**

#### **1.3.1 Anatomical distribution patterns of the SRT cells in the spinal cord**

Most anatomical descriptions of the SRT have been based upon anterograde and retrograde tracer studies that identify the cells of origin in the spinal cord and terminations in the LRN. Generally, horseradish peroxidase (HRP) has been the tracer of choice. Corvaja et al. injected HRP in the LRN, which produced retrograde labelling throughout the cat spinal cord with greater numbers of cells labelled in the cervical segments when compared to the more distal lumbar segments (Corvaja N et al., 1977a). In the cervical region, the retrogradely labelled cells are located principally in the ipsilateral intermediate grey area with clusters in the lateral part of lamina V & VI and in lamina VII (Menetrey D et al., 1983). In the thoracic segments, the cells are localised around the central canal with ventral extensions, whereas in the lumbar segments most of the cells are found contralaterally in lamina VII, VIII and X (Oscarsson O and Rosén I, 1966, Fields HL et al., 1977, Hrycyszyn AW and Flumerfelt BA, 1981b, Kevetter GA et al., 1982) and in the neck of the dorsal horn on the contralateral side (Menetrey D et al., 1983). Furthermore, Menetrey et al. (1983) observed some common features within the spinal segments of rats; with neurons in the contralateral ventromedial parts of both intermediate zone (Rexed laminae VII, VIII), ventral horn (Rexed laminae VIII) and lamina X. In addition to these areas a further study showed that the reticular area of the neck of the dorsal horn, and the superficial layers of the dorsal horn project mainly to the lateral LRN (Garifoli A et al., 2006).

However in 1988, Shokunbi observed a variation in the distribution patterns of retrogradely labelled cells in rats, depending on whether the cells were labelled from the caudomedial or caudolateral LRN; no cells were labelled in the dorsal horn from the latter injection. In addition, using *Phaseolus vulgaris* leucoagglutinin (PHA-L) Wang et al. (1999) demonstrated a population of cells around the central canal in the lumbar segments projecting to the LRN. Conversely, Rajakumar et al. (1992), using WGA-HRP in rats, showed no ipsilateral SRT neurons in the lumbar spinal cord and no differences in the projection patterns to the LRN from dorsal or ventral horn lumbar injections. A reason given by Rajakumar et al. for this apparent discrepancy in their SRT projections to others is because free HRP may be taken up by axons of passage and thus the ipsilateral cells labelled in these studies may actually be false positives. But, a study by Blomqvist et al. (1992) using WGA-HRP demonstrated the same bilateral projections from the lumbar spinal cord in cats, as did other studies in rat using tracers like Fast Blue and Di-amidino yellow (Garifoli A et al., 2006).

Chaouch et al. (1983) injected HRP into various areas of the bulbopontine region of rats and retrogradely labelled cells in the spinal cord. They demonstrated that the medial SRT had a different distribution of cells with no projections from the superficial dorsal horn, unlike the spinomesencephalic tract. It also had no projections from the Clarke's column, unlike the spinocerebellar tract and none from the base of the dorsal horn neck in its medial part, unlike the lateral SRT projection to the LRN.

Hence, we see that there is a difference in the distribution pattern of the cervical and lumbar neurons, which may be indicative of equivalent anatomical pathways to the physiological bVFRT and i-FT of the cat. This hypothesis, however, is challenged by the fact that although these cells can project either ipsilaterally or contralaterally on an individual basis, they seldom project bilaterally suggesting that each side of the body receives a unique afferent input (Koekkoek SK and Ruigrok TJ, 1995). A study by Garfili et al. (2006), on the other hand, has shown that ~7% of these SRT cells, located in the deep dorsal (Rexed laminae V and VI) and intermediate laminae of both cervical and lumbar cord, project bilaterally. The difference between the two studies (Koekkoek and

Garifoli) may be due to the fact that the former used a non-fluorescent technique in light microscopy; while the later, using fluorescent dyes, had a better resolution of the images and the cells were easily distinguishable and hence, quantifiable.

### **1.3.2 Neurochemical properties of the SRT cells**

Few SRT neurons contain peptides and the majority of these types of cells are clustered into two distinct regions, the lateral spinal nucleus and lamina X around the central canal. In addition, there are few peptide-containing cells in lamina I or lateral lamina V (Leah J et al., 1988). Some cells of the lateral spinoreticular tract in lamina X, are immunoreactive to enkephalin (ENK) (Nahin RL and Micevych PE, 1986) with cholecystokinin (CCK) in the medial lamina VII, and substance-P and vasoactive intestinal polypeptide (VIP) cells in lamina V and the deeper grey matter (Nahin RL, 1987). These neuropeptides within long ascending systems, like the spinoreticular tract, would play a significant role in modifying brain activity, along with their involvement in local spinal circuit physiology.

Spinoreticular cells are also reactive to calbindin which is a calcium binding protein (Ren K and Ruda MA, 1994) and these calbindin positive ISRT cells are much more numerous than cells with various neuropeptides (Menetrey D et al., 1992). Calretinin (CR) positive cells are present in areas of projection neurons but no CR immunoreactive SRT cells have been reported as yet (Morona R et al., 2006). Similarly spinal neurons containing nNOS and ChAT are present in areas of SRT neurons such as the intermediate grey matter and deep dorsal horn as well as lamina X but it is not known if particular subgroups of SRT cells contain these substances (Morona R et al., 2006). However, they are valuable markers for classifying sub-populations of neurons for anatomical studies (Baimbridge KG et al., 1992, Ren K and Ruda MA, 1994).

The ISRT projects via the ventrolateral funiculus, carrying spinal information to the LRN, thus enabling precise communication between command and execution centres of movement. Using the latest mouse genetic and viral tools, Pivetta et al. showed that these projections to the LRN are both excitatory (by the

presence of VGLUT-2) and inhibitory (VGAT) and are mostly located on the ipsilateral side with a topographical input from cervical and lumbar segments (Pivetta C et al., 2014).

### 1.3.3 Neurochemical contacts to the spinoreticular neurons

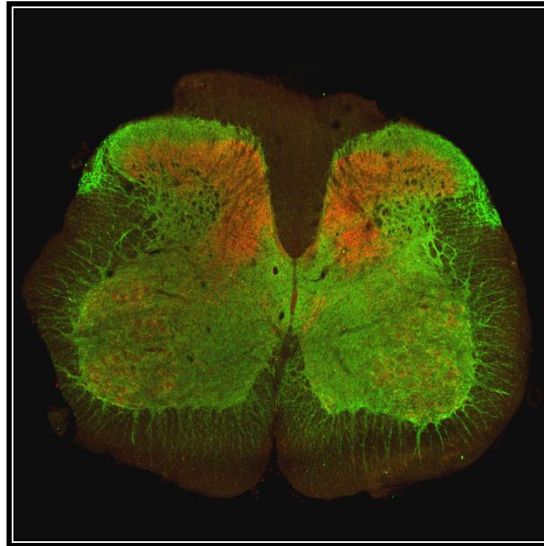
Although extensive work has been done on descending, primary afferent and spinal inputs to spinoreticular cells, most of our knowledge is based on electrophysiological experiments and hardly any studies have been done to determine the neurochemistry of these inputs (Fields HL et al., 1977, Maunz RA et al., 1978, Menetrey D et al., 1980, Haber LH et al., 1982, Foreman RD et al., 1984, Ammons WS, 1987, Cervero F et al., 1988). Glutamate is the principal excitatory neurotransmitter in the spinal cord. It is transported into synaptic vesicles by vesicular glutamate transporters (VGLUTs) and is present in cells and axons (Masson J et al., 1999, Fremeau RT et al., 2001, Reimer RJ et al., 2001, Oliveira AL et al., 2003). The discovery of VGLUT-1 and VGLUT-2 (Fremeau RT et al., 2001) and now VGLUT-3 (Liguz-Leczna M and Skangiel-Kramska J, 2007) and the production of specific antibodies against them for immunocytochemistry, has provided a reliable method for identifying axon terminals that use glutamate as a neurotransmitter (Todd AJ et al., 2003, Alvarez FJ et al., 2004). This method has been used to determine transmitter phenotypes associated with axons in the spinal cord. Most large myelinated primary afferents contain VGLUT-1, while spinal interneurons contain VGLUT-2. In descending systems, VGLUT-1 is found in corticospinal tract terminals and VGLUT-2 in vestibulospinal (VST), rubrospinal (RS) and reticulospinal (ReST) terminals (Du Beau A et al., 2012, Shrestha SS et al., 2012, Huma Z et al., 2014).

**Figure 1-6** illustrates the distribution of VGLUT-1 and VGLUT-2 terminals in both rat and cat lumbar spinal cord. VGLUT-1 localisation is consistent with an origin from cutaneous and muscle proprioceptors as it is most abundant in lamina II/IV, medial V, the intermediate grey matter and also to a lesser extent within lamina X (Celio MR, 1990, Olave MJ et al., 2002, Shehab SA and Hughes DI, 2011), whereas VGLUT-2 primarily of non-primary afferent origin, is distributed across all laminae of the spinal cord (Varoqui H et al., 2002, Todd AJ et al., 2003,

Alvarez FJ et al., 2004, Takamori S, 2006, Boulland J-L et al., 2009, El Mestikawy S et al., 2011, Brumovsky PR, 2013).

The introduction of antibodies for the identification of VGAT has, likewise, provided a reliable method for identifying inhibitory axon terminals as this transporter is found in both GABAergic and glycinergic boutons (Chaudhry FA et al., 1998). The known sources of VGAT terminals in the lumbar spinal cord are inhibitory interneurons (Bannatyne BA et al., 2003, Bannatyne BA et al., 2009) and descending ReST fibres (Du Beau A et al., 2012, Shrestha SS et al., 2012a). Utilising these vesicular transporters, we can, to a certain extent, identify the input sources to spinoreticular cells whether from descending systems, primary afferents or interneurons, because of the differential expression of VGLUT isoforms and VGAT in combination with tract tracing ([Figure 1-6](#)).

**A.**



**B.**

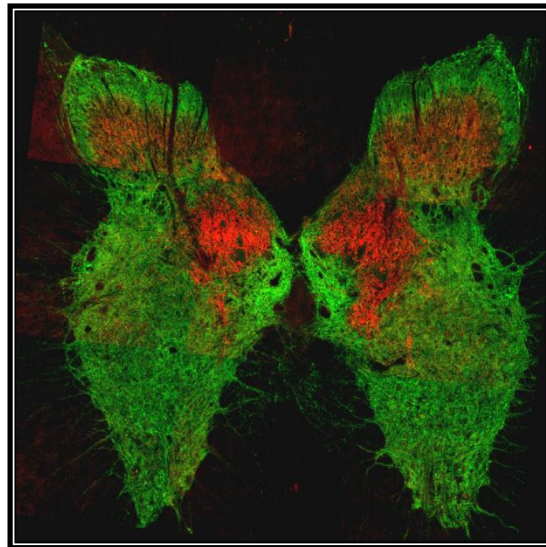


**Figure 1-6 Distribution pattern of excitatory neurotransmitters in rat and cat lumbar (L4) spinal cords**

**A.** A confocal image of a transverse section of rat lumbar spinal cord showing the distribution pattern of VGLUT-2 (in green) and VGLUT-1 (in red) throughout the entire section.

**B.** A confocal image of a transverse section of cat lumbar spinal cord showing the distribution pattern of VGLUT-2 (in green) and VGLUT-1 (in red) throughout the entire section.

*These images are taken from rat and cat tissue used for input analysis to spinoreticular rat as well as cat neurons in Chapter 5.*

## 1.3.4 Response properties of spinoreticular neurons

### 1.3.4.1 Background to input properties

Somatic afferents originate from receptors in the skin, muscles, ligaments, fascia and joints. These can be further differentiated into: exteroceptive, from the skin, mediating sensations like touch, pressure, warmth, cold and pain; and proprioceptive, from muscles and joints, i.e. deeper somatic structures, mediating sense of body position.

The cutaneous receptors are subdivided into mechanoreceptors, nociceptors, thermoreceptors and chemoreceptors, whilst the muscle and joint receptors are stretch receptors (Burgess PR and Perl ER, 1967, Cervero F and Wolstencroft JH, 1984, Cervero F et al., 1988). First order sensory neurons have cell bodies located in the dorsal root ganglia and give rise to split axons with a peripheral and central branch. These <sup>1</sup>primary afferents enter the spinal cord via the dorsal roots: 34 in rats (8 cervical, 13 thoracic, 6 lumbar, 4 sacral and 3 coccygeal); and 38 in cats, 8 cervical, 7 lumbar, 3 sacral and 7-8 coccygeal (Rexed B, 1952, Molander C et al., 1984, Watson C et al., 2009a). The central branch travels either in the dorsal columns or Lissauer's tract with some giving off collaterals that terminate in the dorsal horn.

To have a better understanding of how the spinal circuitry responds to information from the periphery via these afferents in terms of reflexes, movements and integration of various functions, these primary afferents have been further subdivided depending on various parameters. They can be classified according to receptors (cutaneous, muscular, joint, visceral), their conduction velocities, which depends on their size and myelination (myelinated A $\alpha$ B $\delta$ , unmyelinated C), their response in terms of sensory modality and intensity of stimulus (for example, low/high threshold cutaneous or mechanoreceptors) and also on their neurochemical properties (peptidergic, non-peptidergic). All these features are interrelated, thus a fibre may be defined as large myelinated cutaneous (AB) and also, a low-threshold mechanoreceptive, responding to touch. These fibres are distributed throughout the laminae of the spinal cord,

<sup>1</sup> Primary afferents in this thesis have been defined as all spinal afferents including cutaneous (A $\alpha$ B $\delta$ , C) and proprioceptive (Groups I, II, III and IV).

with the unmyelinated fibres terminating mostly in the superficial dorsal horn and myelinated ones extending more ventrally into the deeper dorsal and ventral horns. There is a somatotopic organisation as well, with fibres from the more distal part of the limbs ending most medially in the superficial dorsal horn and more proximal limb afferents ending more laterally (Molander C and Grant G, 1987, Todd AJ, 2010b). For an overview of the types of fibres that make up the primary afferents, see [Table 1-1](#).

The cutaneous primary afferent fibres are classified into:

- **Large myelinated fibres**, A $\alpha$  and AB have the highest conduction velocities, ~30-100m/s in cats, therefore allowing rapid signal conduction, with a low activation threshold and responsive to innocuous touch. These are mostly low threshold mechanoreceptors terminating more ventrally in lamina III to VI.
- **Thin myelinated A $\delta$  fibres** that conduct impulses pertaining to fast pain and temperature with a relatively intermediate conduction velocity of 5-30m/s. The high threshold (nociceptive) A $\delta$  fibres terminate in lamina I, lamina V and dorsal to the central canal. The low threshold A $\delta$  mechanoreceptors (innocuous stimulus) terminate mostly in lamina V some extending to lamina II. Thus, the superficial dorsal horn receives direct projections from cutaneous nociceptors, but not from cutaneous receptors responding to innocuous stimuli (Light A and Perl E, 1979a).
- **Small and un-myelinated C-fibres** conduct at a very slow velocity of 0.5-2 m/s and are related to modalities such as slow pain, temperature and itch. Thus polymodal nociception travels through C-fibres. The majority of these fibres terminate in lamina I and Lamina II (Todd AJ, 2010a).

**Table 1-1 General overview of various types of cutaneous and proprioceptive primary afferents.**

	Type	Conduction Velocity	Stimulus
<b>Cutaneous</b>			
myelinated	A $\alpha$	30-100 m/s	innocuous touch low threshold mechanoreceptors
	A $\beta$		innocuous touch & noxious low & high threshold mechanoreceptors
	A $\delta$	10-30 m/s	peptidergic, non-peptidergic noxious, polymodal low & high threshold mechanoreceptors
unmyelinated	C	<2.5 m/s	peptidergic non-peptidergic noxious , polymodal high threshold mechanoreceptors
<b>Proprioceptive</b>			
myelinated	Gp I	72-120 m/s	innocuous stretch
	Gp II	24-71 m/s	
	Gp III	6-23 m/s	nociception
Un-myelinated	Gp IV	<2.5 m/s	nociception

The proprioceptive afferents from muscles and joints are classified according to a different terminology:

- **Myelinated Group I and II** have the highest conduction velocities, ~72-120m/s conducting proprioceptive information from skeletal muscles. Group Ia fibres terminate in the intermediate region VI, VII and lamina IX (Brown AG and Fyffe RE, 1978) and are involved in posture and coordination of movements. Group Ib are mostly from joints and thus are involved in stepping. Group II muscle and joint afferents are active in general flexion reflex.
- **Myelinated Group III** have slower conduction velocities and respond to mechanical as well as nociceptive impulses (Mense S and Meyer H, 1985).
- **Un-myelinated Group IV** are slow conducting fibres responding to painful stimuli (Hunt CC and Kuffler SW, 1954).

#### 1.3.4.2 Physiological response properties of spinoreticular neurons

Extracellular recordings have shown that SRT neurons have large bilateral receptive fields with complex inhibitory and excitatory areas (Fields HL et al., 1977, Maunz RA et al., 1978, Haber LH et al., 1982, Cervero F and Wolstencroft JH, 1984, Foreman RD et al., 1984, Ammons WS, 1987, Cervero F et al., 1988). Although these neurons are believed to play an important role in nociception, not much work has been done on them compared to other ascending systems like the spinothalamic and spinomesencephalic tracts (Haber LH et al., 1982, Chaouch A et al., 1983, Willis WD, 1985). Based on electrophysiological experiments conducted on cats (Sahara Y et al., 1990), SRT neurons are classified into three types according to their response to primary afferents and location: deep inhibited, deep complex and intermediate.

- **The deep inhibited type** of neurons is located in the medial part of laminae VI, VII and VIII. Inhibitory postsynaptic potentials (IPSPs) are evoked in them by low threshold cutaneous afferents and also via high threshold cutaneous and muscle afferents oligosynaptically (via large AB

cutaneous fibres and A $\delta$  inputs). They have no excitatory receptive fields and are the most common type of SRT neurons.

- **The deep complex** type are located in the same laminae VI, VII and VIII, and both inhibitory (IPSPs) and excitatory (EPSPs) postsynaptic potentials can be evoked from low threshold cutaneous afferents as well as long-latency C-fibre-like EPSPs.
- **Intermediate** type neurons are located relatively superficially in lamina V and the lateral spinal grey matter. These neurons are wide dynamic range (WDR) neurons with large excitatory and inhibitory cutaneous receptive fields, which are stimulated by both low and high threshold cutaneous afferents producing mono or disynaptic EPSPs followed by IPSPs. High threshold muscle afferents evoke EPSPs.

In addition to these areas, there are projection cells around the central canal that respond to both innocuous and noxious stimuli in cats (Honda CN and Perl ER, 1985). In contrast, a study on rats has shown neurons in this area respond to purely noxious stimuli (Nahin RL et al., 1983). Some of these cells are spinobulbar neurons with some projecting to the LRN (Nahin RL et al., 1983). Intracellular records show SRT cells responding to low threshold mechanoreceptors (in deep dorsal horn), multiceptive neurons responding to both noxious and innocuous stimuli and a group stimulated by intense mechanical noxious stimuli in the ventral horn of the spinal grey (Fields HL et al., 1977). It is thus apparent that spinoreticular neurons have considerable functional heterogeneity.

## 1.4 Spinal reflexes

Spinal reflexes may be considered as changes in efferent outflow due to actions produced in the spinal cord by incoming impulses in afferent nerve fibres. Cutaneous receptors are responsible for a wide range of sensations. A cutaneomuscular response to an innocuous stimulus or a withdrawal reflex to a noxious stimulus is relayed through a path involving several key components: type of receptor, primary afferent fibre, ascending spinal pathway, central projection and descending control leading finally to the output or functional role. This role of the cutaneous afferents capable of modulating motor behaviour through various pathways is discussed below.

### 1.4.1 Flexor reflex afferents vs. withdrawal reflex

The motor response to a noxious stimulus is to withdraw it from the source of irritation, thus reducing chances of damage to the tissue. The classical view of this withdrawal reflex was presented by Sherrington in 1910, who found that in decerebrate cats, the response to an electric stimulus to the hind limb was to move it towards the body (flexion) and a concomitant relaxation (extension) on the opposite side irrespective of site of stimulus. Thus, flexor reflex afferents include Group II and III muscle and joint afferents as well as cutaneous afferents, both low and high threshold, and are grouped together because of their common action on motor neurons i.e. ipsilateral flexion and contralateral extension (classical flexion reflex and crossed extension reflex)(Sherrington CS, 1910, Eccles RM and Lundberg A, 1959a, Jankowska E et al., 1973). They have wide receptive fields, converge on common interneurons and activity in these pathways is facilitated by descending systems. The flexor reflex afferents are involved not only in segmental activity which may then influence cortical arousal via bVFRT, but also via the reticulocerebellar tract influence cerebellar excitation (Lundberg A and Oscarsson O, 1962b, Grant G et al., 1966, Ghazi H et al., 1987, Park IK et al., 2003).

However, this is not the only motor response elicited by noxious stimuli, as shown by Hagbarth, that extensor muscles can be activated by a noxious

stimulus applied to the overlying skin (Hagbarth KE, 1952). A modular organisation of a withdrawal reflex was put forward in which each muscle has a separate cutaneous receptive field corresponding to the area of noxious stimulus, nociceptors (high threshold A $\delta$ ) converge on interneurons under supraspinal control specific for these muscles (Schouenborg J, 2002). This is organised in a way to produce rapid movement away from the offending object. The long-loop pathways like the spinoreticular, ascending through the anterolateral quadrant, may modulate the spinal nociceptive reflex. As is seen in patients with ipsilateral anterolateral cordotomy (where the spinothalamic tract has been cut) who have a withdrawal reflex on the contralateral side dissociated from pain (García-Larrea L et al., 1993).

Spinoreticular fibres project onto different brainstem areas involved in nocifensive and motor controls (Hall JG et al., 1982, Jones SL and Gebhart GF, 1988, Degtyarenko AM and Kaufman MP, 2002, Heinricher MM et al., 2009). Neurons in these areas project back to exert both excitatory and inhibitory influences at all segmental levels on spinal cord units (Menetrey D and Basbaum AI, 1987, Basbaum AI and Braz JM, 2010). Indeed, it has been suggested that the spinoreticular tract may be involved in flexion reflex modulation both in animals (Villanueva L et al., 1986 a) and man (De Broucker T et al., 1990, García-Larrea L et al., 1993). This tract has been considered to contain the afferent branch of a diffuse noxious inhibitory control (DNIC) system (Villanueva L et al., 1986 b, Bouhassira D et al., 1993). The evolutionary value of sensitisation of withdrawal reflexes is that it enhances the protective functions of reflexes after tissue has been injured (Clarke RW and Harris J, 2004). This reflex comes from intact descending inhibitory systems like the reticulospinal fibres from the LRN in response to un-myelinated C fibre inputs (Hall JG et al., 1982).

#### **1.4.2 Spinobulbar spinal reflex**

This is a system in which impulses from mostly cutaneous afferents ascend to the bulbar reticular formation and then send recurrent descending impulses to the spinal motor neurons (Shimamura M and Aoki M, 1969). The ascending pathways are in the spinoreticular and spino-cervico-reticular tracts in the dorsolateral

funiculus (Shimamura M et al., 1976), while the descending pathways are via the reticulospinal tracts originating in the caudomedial bulbar formation (Gokin AP et al., 1977). Neurons at the origin of the spinoreticular tracts are in lamina V to VI and are activated monosynaptically by primary afferents and antidromically from the bulbar reticular formation (Shimamura M et al., 1976). The SBS reflex is involved in stepping, as seen in thalamic cats (pre-thalamic decerebration), with stimulation producing prolonged flexion (Shimamura M et al., 1982). It is also possible that the SBS reflex is involved in quadrapedal movements of the limbs and may involve integration within the bulbar reticular formation (Grillner S et al., 1968, Shimamura M et al., 1980, Leblond H et al., 2000). Spinoreticular neurons also play a role in the fictive scratch reflex in cats (Arshavsky YI et al., 1978 a, Arshavsky Yu I et al., 1984).

## 1.5 Scope of my study

In addition to the classical spinocerebellar pathways, the cerebellum receives input from the spinal cord via the indirect spino-bulbar-cerebellar pathway (SBC), which projects via the medullary lateral reticular nucleus (LRN). The bulbospinal pathways, on the other hand, originate from various regions of the brain stem reticular formation and influence spinal neurons via classical synaptic mechanisms. Various physiological and anatomical studies have elaborated on the complexity of the pathways connecting the LRN to the supraspinal structures like the cerebellum and to the spinal cord. Despite the importance of this pathway in influencing a variety of spinal networks, concerned not only with motor activity but also sensory input and autonomic function, little is as yet known about the organisation of the synaptic afferent input to the spinoreticular neurons and the mechanisms responsible for the control of afferent transmission through this pathway. Similarly little is known about the projection patterns to the LRN and the role of the LRN as an integrative as opposed to a relay nucleus. Therefore, I believe that by investigating the properties of the spinoreticular tract neurons and their role in an ascending-descending loop, the information gathered will provide a better understanding of the intricate circuitry of a crucial part of the reticular formation.

## 1.6 Aims and Objectives

The hypothesis to be tested in this project is that “spinoreticular neurons form a component of a feedback loop which influences activity of medullary descending control system”.

In order to have a better understanding of the organisation and function of the reticular formation especially the indirect spino-bulbo-cerebellar pathway (SBC) to the cerebellum I undertook a series of experiments to fulfil the following aims:

- To investigate the distribution patterns of spinoreticular tract neurons and their axonal projections to the lateral reticular nucleus; the ascending pathway.
- To compare the origins of two bulbospinal pathways projecting to the rat lumbar spinal cord via the MLF and CVLM; the descending pathway.
- To determine the organisation of SRT neurons and origin of excitatory and inhibitory contacts to these neurons in rat and cat lumbar spinal cord; and
- To investigate the neurochemical phenotypes of the SRT neurons and their response to noxious stimuli in rats.

## Chapter 2

## 2 General experimental procedures

This chapter provides a detailed overview of the experimental procedures performed on rats in this study. Any changes in these procedures or specific experiments carried out to fulfil certain aims are explained in greater detail at the beginning of each corresponding chapter.

Experiments were approved by the Ethical Review Process Applications Panel of the University of Glasgow and were performed in accordance with the UK Animals (Scientific Procedures) Act 1986.

### 2.1 Surgical procedures

At the beginning of this study, some of the adult male Sprague Dawley rats weighing between 250-300gm (Harlan, Bicester, UK) were anaesthetised with intra-peritoneal injections of Ketamine (0.1ml/100gm; 2:1) (Boehringer Ingelheim Vetmedica, Inc., USA) and Xylazine (Bayer Plc, UK). Towards the end of my PhD, all of the animals were induced and maintained under general anaesthesia with 2-4% Isoflurane in Oxygen (30%O<sub>2</sub>/70%N<sub>2</sub>O).

The rats were placed in a stereotaxic frame during the tracer injections. Using strict aseptic techniques, the scalp was incised in the midline and the skull exposed. A small burr hole was then made in the skull according to the respective inter-aural co-ordinates. Glass micropipettes (tip diameter of 20µm) were filled with tracers of either 0.2µl b subunit of cholera toxin (CTb, 1%; Sigma-Aldrich, Co., UK) or 50nl of 4% fluorogold (FG, Fluorochrome, LLC, USA) in distilled water as appropriate and lowered into the lateral reticular nucleus at inter-aural co-ordinates, -4.8mm (antero-posterior), ±1.8mm (medio-lateral) and at a dorso-ventral coordinate of -0.4mm (Paxinos and Watson, 1997), as illustrated in [Figure 2-1 A & B](#). The tracer was then injected using an air pressure device (10ms pulses at 20 psi; Pico-injector, World Precision instruments, USA). During surgery, heart rate and oxygen saturation were continuously monitored by a pulse oximeter applied to the hind foot (Surgivet, Pulse oximeter sensors, Harvard Apparatus, Holliston, USA).

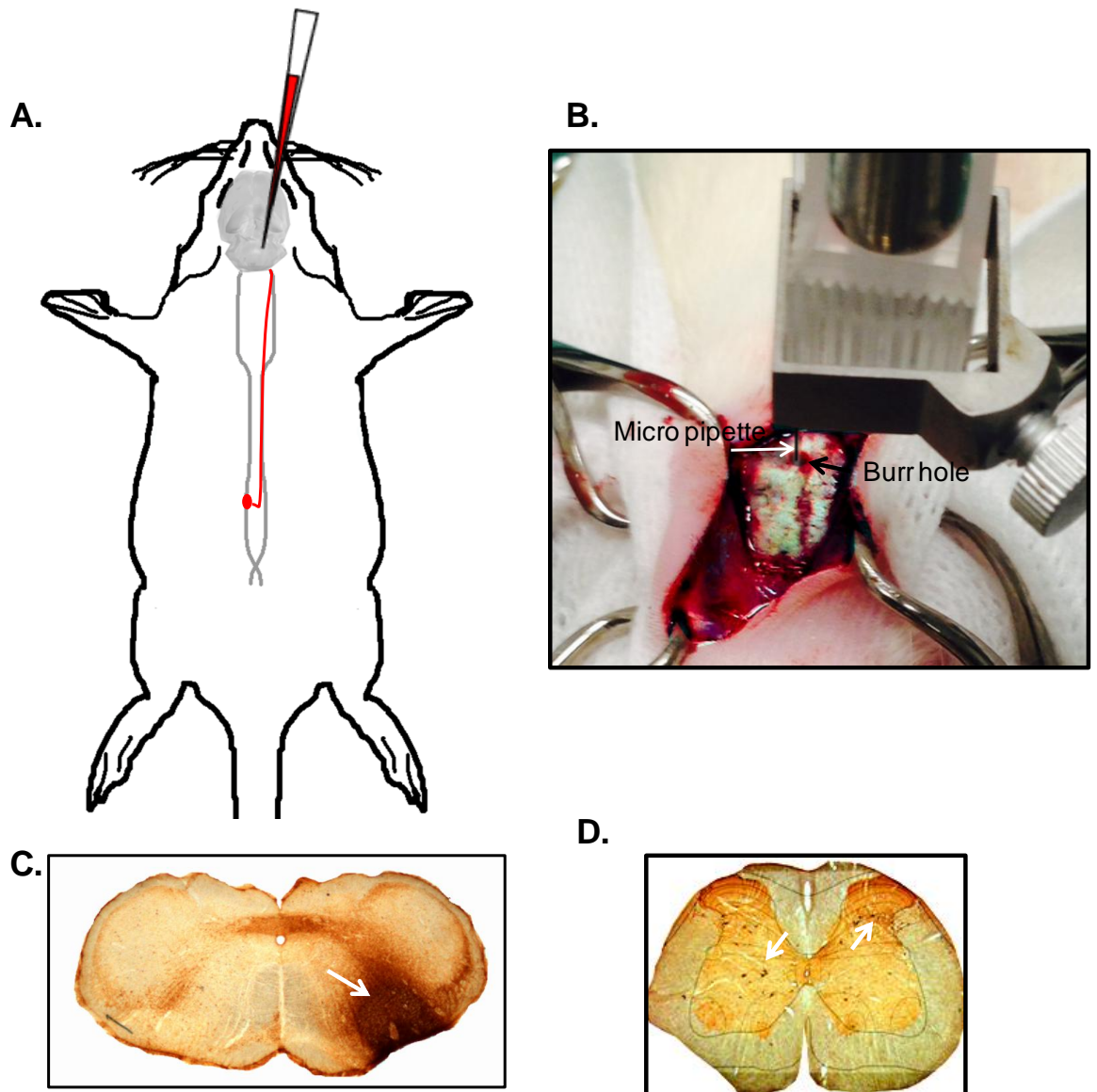


**Figure 2-1** A schematic diagram for the surgical procedure of retrograde labelling of spinoreticular tract neurons in the rat lumbar spinal cord

**A.** Spinoreticular tract neurons were labelled by retrograde transport of CTb following Stereotaxic injection in the LRN.

**B.** An image showing the pipette in the LRN through a burr hole in the skull of the rat.

**C.** A DAB photomicrograph of the injection site in the LRN (white arrow).

**D.** A DAB photomicrograph of a lumbar section showing the anatomical locations of the retrogradely labelled spinoreticular cells (white arrows).

After the injection, the micro-pipette was left in place for 5mins to prevent any backflow of the tracer. The scalp was sutured and the animals were placed in an incubator to aid recovery. Within a couple of hours, the animals recovered and started to drink and explore their environment.

Following a 6 day, post-injection survival period, the animals were re-anesthetised with Pentobarbitone (1ml at 200mg/ml i.p; Sigma-Aldrich, UK). They were then perfused trans-cardially with 25-50ml of mammalian ringer's solution followed by 1000ml of 4% freshly depolymerised formaldehyde (Sigma-Aldrich, Co., UK) in 0.1M phosphate buffer (PB, Sigma-Aldrich, Co., UK) via the left ventricle. The brain and mid-lumbar segments were dissected and post fixed overnight in the same fixative at 4°C. The brainstem was then rinsed in 0.1M PB sucrose and 100µm thick sections cut with a freezing microtome, collected in five separate bottles in PB for the histological examination of the injection site. Lumbar 3, 4 and 5 segments were identified on the basis of their dorsal roots, and were dissected and rinsed in 0.1M PB. Finally, 50µm thick sections were cut using a vibrating microtome (Leica VT1200, Leica Microsystems, UK). Both the brain and spinal cord sections were placed in an aqueous solution of 50% ethanol for 30 minutes to enhance antibody penetration.

## 2.2 Identification of the injection site

As seen in [Figure 2-1 C&D](#), the injection sites were visualised using 3, 3'-diaminobenzidine (DAB) as a chromogen. The brain medullary sections were first of all incubated in goat anti-CTb (1:50,000; List Quadrantech, USA) for two days at 4°C, then rinsed in PBS (phosphate buffer saline) and placed overnight in biotinylated anti-goat IgG (immunoglobulin, 1:5000; Jackson ImmunoResearch, USA) for 3 hours at room temperature. These sections were then rinsed again in PBS and incubated in avidin-horseradish peroxidase (AV-HRP; 1:1000; Sigma-Aldrich, UK) for 1 hour. Finally, hydrogen peroxide (H<sub>2</sub>O<sub>2</sub>) and DAB were applied for 15mins and a golden brown colour revealed the injection sites. This reaction was also done for randomly selected transverse spinal cord sections from each L3, L4 and L5 segments in order to examine the anatomical location of retrogradely labelled cells. These sections were then mounted onto gelatine coated slides and fixed with 4% formalin vapours overnight. After dehydration in

70%, 90% and 100% ethanol and clearing in histoclear (National Diagnostics, Hesse Hull, UK) the sections were cover-slipped with histomount and viewed with a transmission light microscope. Photographs were taken digitally with AxioCam (Carl Zeiss, Inc, Germany) using the AxioVision 4.8 software (Zeiss, Germany). The injection site was then confirmed by the stereotaxic rat brain atlas of Paxinos & Watson (2005). The laminar location of retrogradely labelled neurons in spinal cord sections were recorded using Adobe Photoshop by superimposing the photomicrographs onto the templates of L3, L4 and L5 spinal cord segments (Figure 2-1 C&D).

## **2.3 Tissue processing and multiple immune-labelling for confocal microscopy**

Spinal cord sections were processed for various markers using immunocytochemistry. Immunofluorescence allows for more than one antigen to be used in the same section of the spinal cord. This technique involves two principal steps (two step indirect method):

First, these sections were incubated for 48hrs at 4°C in primary antibodies raised in different species. Three to four antibodies against the target antigen were used depending upon the reaction set up.

In the second step, the sections were then incubated overnight in a species specific, secondary antibody conjugated to a fluorophore. In most experiments, the secondary antibody used was an immunoglobulin (IgG) raised in donkey and in turn raised against the IgG of the animal species in which the primary antibody has been raised. This coupling of the secondary to the primary antibody can then be readily detected by the fluorophore attached to it. Fluorescent antibodies were conjugated to Rhodamine Red (1:100), Dylight 649/Alexa 647 (1:500; both from Jackson Immunoresearch) or Alexa 488 (1:500; Molecular Probes). Secondary antibodies labelled with biotin (1:500) or horseradish peroxidase (HRP; 1:1000, both from Jackson Immunoresearch) were also used. The biotinylated antibodies were revealed with avidin-Pacific blue (1:1000; Molecular probes). All antibodies were diluted in PBS containing 0.3% Triton X-100.

Following three rinses in PBS, the sections were mounted with an anti-fade medium (Vectashield; Vector laboratories, Peterborough, UK) on glass slides and were then ready to be scanned with the confocal laser scanning microscope. The individual antigens could then be visualised due to the immunoreactivity of the corresponding fluorophore-coupled secondary antibody. In the same optical section, the images could be studied as either individual colours or as a merged image showing the spatial distribution of the respective antigens and their relationship to each other.

## 2.4 Confocal microscopy, reconstructions and analysis

Most of the sections were scanned through full thickness with a Radiance 2100 microscope (Bio-Rad, UK) and the Zeiss LSM 710 confocal microscope through dry (x10, x20) and oil (x40) immersion lenses at numerical apertures of 0.3, 0.5/0.8 and 1.3, respectively. The Zeiss microscope is equipped with Argon multi-line, 405 nm diode, 561 nm solid state and 633 nm HeNe lasers). The Radiance 2100 microscope is equipped with three lasers: blue diode (405nm) Argon multi-line, green Helium Neon (543), and red diode (637 nm). For all scans obtained with the 40x lens the pinhole was set to 1.0 Airy unit. [Table 2-1](#) shows the excitation-emission wavelengths of different fluorophores conjugated with various secondary antibodies used.

**Table 2-1 Excitation-emission wavelength of the fluorophore used**

<b>Fluorophore</b>	<b>Excitation(<math>\lambda</math>)</b>	<b>Emission(<math>\lambda</math>)</b>
Rhodamine-red (Rh Red)	543	591
Alexa-Fluor 488 (Alexa488)	488	517
Alexa 647/Dylight 649	652	670
Avidin Rhodamine (AV-Rh)	570	590
Avidin Pacific blue (AV-PB)	410	455

Retrogradely labelled rat SRT neurons were scanned at low magnification (x10 lens) to categorise them into different populations based on their anatomical location in the various laminae of the spinal cord grey matter and to determine their neurochemical properties. For cell counts, sections were randomly selected and scanned systematically to obtain a complete series of images in order to make a montage. The neurons were then scanned at a higher magnification (40X

lens, zoom factor 1.4/2 at a z-step of 0.5 $\mu$ m intervals). These scans were analysed with NeuroLucida for Confocal software (MicroBrightfield Inc., USA) and the cell bodies and dendritic trees of the neurons were drawn. Reconstruction of the cells was always started from the cell body, the dendritic processes added subsequently and contacts plotted simultaneously with appropriate markers until the dendritic tree was reconstructed throughout the z-steps. The extent of co-localisation was quantified by using NeuroLucida for confocal by placing a marker for each type of immunoreactivity and double or triple labelled profiles were then counted for each animal per 100 $\mu$ m<sup>2</sup> dendritic length  $\pm$  standard deviation (mean $\pm$ SD) and the final overall mean percentage value calculated for all animals. Only contacts in close apposition to the cell in the same focal plane and with no intervening black pixel spaces were counted.

Contact densities were calculated using data generated by NeuroLucida and expressed as numbers of contacts per unit area (100 $\mu$ m<sup>2</sup>). Sholl analysis was performed with NeuroLucida Explorer (9.14, MicroBrightfield Inc, USA) and contact densities calculated within a series of 25 $\mu$ m concentric spheres from the centre of the cell body (/100 $\mu$ m<sup>2</sup> of dendritic length). The surface area of the cell body was calculated by measuring the perimeter of a projected confocal image of each labelled cell body using image J software (1.4.3.67, National Institute of Health, USA) and calculating the surface area of an equivalent sphere. This was done so that all the cells can be compared irrespective of the various shapes we might encounter.

## 2.5 Statistical analysis

Data are expressed as mean  $\pm$  standard deviation (SD). Multi-group comparisons were done using analysis of variance (ANOVA) followed by a post hoc *Tukey's* analysis as appropriate and two variable comparisons among the same population was done by using Student's *t* test. A  $p < 0.05$  was considered to be statistically significant (Prism 6.00 for Windows, GraphPad Software, La Jolla California USA, [www.graphpad.com](http://www.graphpad.com)).

## Chapter 3

### **3 The ascending pathway; the topography of the spinoreticular tract neurons to the lateral reticular nucleus (LRN)**

#### **3.1 Introduction**

The first step in understanding the LRN, how it processes information and relays it to the cerebellum is to understand the architecture of its major input: the lateral spinoreticular tract. This tract, in contrast to the classical direct spinocerebellar tracts conveys information regarding motor activity to the cerebellum via the pre-cerebellar neurons in the LRN (Shimamura M et al., 1982, Alstermark B et al., 1984, Ekerot CF, 1990c) and also plays a vital role in the regulation of peripheral sensory input by influencing descending systems (Arshavsky Yu I et al., 1984, De Broucker T et al., 1990, Habaguchi T et al., 2002).

Tract tracing and degeneration studies have been used to define the anatomical locations of SRT cells in lamina VII, VIII and X that have terminations in the LRN (Hryciyshyn AW and Flumerfelt BA, 1981b, Flumerfelt BA et al., 1982, Menetrey D et al., 1983, Shokunbi MT et al., 1985, Rajakumar N et al., 1992). Both ipsilateral and contralateral projections to the LRN have been demonstrated but some authors have shown limited evidence for the possibility of bilateral projections (Koekkoek SK and Ruigrok TJ, 1995). In addition, electrophysiological experiments have defined projections from the lumbar spinal cord as arising from the lumbar bVFRT with neurons in the intermediate laminae that receive inputs from the flexor reflex afferents and relay sensorimotor information via the ventrolateral funiculus to the LRN (Holmqvist B et al., 1959, Lundberg A and Oscarsson O, 1962b, Grant G et al., 1966, Oscarsson O and Rosén I, 1966, Rosén I and Scheid P, 1973a, Clendenin M et al., 1974 a, 1974 b, Ekerot CF, 1990c). This suggests that the LRN plays an important role in co-ordinating motor activities and body posture by integrating information from all spinal levels, from both sides of the cord (Corvaja N et al., 1977a).

Neurons in the LRN receive information from the spinal cord, from the cerebral cortex and other brain stem nuclei in a topographical manner, with most lumbar spinal projections terminating in the parvicellular part and cervical projections in the magnocellular part (Künzle H, 1973, Garifoli A et al., 2006). This organised input is then preserved in the reticulo-cerebellar projections (Clendenin M et al., 1974 a, Künzle H, 1975). The inputs to the LRN neurons not only produce strong excitatory but also inhibitory responses with monosynaptic latencies (Rosén I and Scheid P, 1973b, 1973c, Clendenin M et al., 1974 a, Ekerot CF, 1990a). Recently, evidence of such long, ascending pathways was brought forward by Hossaini et al. (2012). Ekerot (1990c) has shown both excitatory and inhibitory effects from SRT neurons throughout the LRN but in an anatomical study using elaborate viral tracing techniques in genetically modified mice, Pivetta et al. (2014) noted almost exclusively, excitatory terminals with sparse inhibitory terminals at the periphery of the LRN.

This pattern of connectivity suggests that the LRN has a pivotal role in co-ordinating motor activity by integrating information from the spinal cord and projecting it to the cerebellum. The cerebellum receives this integrated information from the LRN via the spino-bulbar-cerebellar path and along with segregated information from the spinocerebellar pathways, fine tunes motor activities (Alstermark B and Ekerot CF, 2013).

The aims of the present study therefore were to find out;

- The distribution of the spinoreticular neurons in the rat lumbar spinal cord.
- How is this pathway organised?
- What are the transmitter phenotypes of the spinoreticular axons and their pattern of termination in the LRN?
- Finally, do excitatory and inhibitory SRT terminals converge onto individual pre-cerebellar neurons in the LRN?

In order to achieve these aims we used tract tracers, CTb and FG to label SRT cells retrogradely in the lumbar spinal cord and CTb injection in lumbar cord to label spinoreticular terminals anterogradely in the LRN. In addition, to label

excitatory and inhibitory terminals in the LRN we used antibodies for VGLUT-1/ VGLUT-2 and VGAT, respectively along with GAD (glutamate decarboxylase) and GLYT2 (glycine transporter 2 [Tables 1-2 to 1-4](#)) to further define the inhibitory terminals. Finally FG was used to retrogradely label pre-cerebellar cells in the LRN and CTb to anterogradely label SRT terminals onto these cells.

## 3.2 Methods

Fifteen adult male Sprague-Dawley rats (Harlan, Bicester, UK) weighing between 250-350gm were deeply anaesthetised and surgery was performed following the procedures outlined in the General experimental procedures (Chapter 2, Section 2.1). However, each set of experiments contained some variations that are explained in greater detail below. Experiments were approved by the Ethical Review Process Applications Panel of the University of Glasgow and were performed in accordance with the UK Animals (Scientific Procedures) Act 1986.

### 3.2.1 The pattern of distribution of spinoreticular tract neurons in the rat lumbar spinal cord

For this part of the experiment we mostly followed the procedures outlined in Chapter 2 regarding surgery, with injection of CTb in the LRN, identification of injection site and also immunohistochemistry. In four adult male Sprague Dawley rats (Harlan, Bicester, UK), the injection sites were visualised using 3, 3'-diaminobenzidine (DAB) as chromogen (Figure 3-1). Further analysis was carried out in animals 2, 3 and 4 with injection sites centred in the LRN. Animal 1 had an off target injection site and is used shown just as a comparison to the other sites.

Along with the brainstem sections, DAB reactions were prepared for every fifth 50µm transverse spinal cord section from L3, L4 and L5 segments. This was accomplished by sequentially collecting each spinal section into five bottles and then using one bottle for the DAB reactions. Three sections were then randomly selected from these spinal cord segments to plot the anatomical location of retrogradely labelled cells. Only those cells that had well labelled somata with visible proximal dendrites were chosen.

#### *Reconstruction and analysis*

The DAB sections were examined under a light microscope and photographed digitally with a x4 lens using AxioVision 4.8 software (Zeiss, Germany). These photomicrographs were then stitched in Microsoft ICE (Microsoft image composite editor v 1.4.4.0, Microsoft corporation) and exported to Adobe

Photoshop cs v8 (Adobe systems, USA) where they were superimposed on L3, L4 and L5 spinal cord templates (from Paxinos and Watson, 2005). The location of each CTb-labelled cell was recorded as a dot on the corresponding site (Figure 3-2 & 3-3). Separate cell counts were made for the following locations; Laminae I-II (superficial dorsal), laminae III, IV, V (deep dorsal), laminae VI, VII (intermediate), lamina VIII (ventral), lamina X and the LSN (lateral spinal nucleus).

### **3.2.2 The projection patterns of spinoreticular neurons to the LRN**

#### *Surgical procedures*

Two different retrograde tracers were injected into the left and right LRN of four adult male Sprague-Dawley rats. CTb (1%, 200nl) was pressure injected into the left LRN at inter-aural co-ordinates -4.8mm (antero-posterior), +1.8mm (medio-lateral) and at a dorso-ventral coordinate of -0.4mm (Paxinos G and Watson C, 2005). The micropipette was left in place for 5mins to prevent any backflow of the tracer and then emptied by ejecting the remaining CTb and cleaned by drawing distilled water and ejecting it several times. The outer surface of the tip was cleaned by giving a gentle swab with distilled water. Following this, another burr hole was made on the contralateral side at interaural co-ordinates -4.8mm (anteroposterior) and -1.8mm (mediolateral) (Paxinos G and Watson C, 2005). The pipette was then filled with 50nl of 4% FG in distilled water (Fluorochrome, LLC, USA) and pressure injected into the right LRN at a dorso-ventral coordinate of -0.4mm to find out the type of SRT projections to the LRN (ipsilateral, contralateral or bilateral). The pipette was again left in place for 5mins and then removed. The scalp was sutured; 6 days post-recovery the animals were perfused, the brain and spinal cord removed and placed in the same 4% fixative overnight. The brain stem was sectioned into 100µm coronal sections with a freezing microtome (Leica, UK) and the sections placed sequentially in five bottles. So at the end each bottle would have a representative number of sections from the entire medulla. Spinal cord L3-L5 segments were sectioned at 50µm on a Vibratome and sections collected (details in Chapter 2).

### *Identification of the injection sites*

The injection site for CTb was identified using DAB as a chromogen, as described in Chapter 2 and the FG injection site was visualised by directly mounting the sections using Vectashield and viewed with a fluorescence microscope. The CTb sites were imaged as described above (section 3.2.1) while the FG sections were photomicrographed using an ultraviolet filter and images of the same sections captured with dark field. Both injection sites were then traced onto their respective templates from the stereotaxic rat brain atlas of Paxinos and Watson (2005) (Figure 3-5). Of the four animals injected, only the three with the most similar injection sites were used for further analysis (i.e. animals 5, 6, 8). Animal 7 had a different injection site and so showed a variation in cell pattern.

### *Immunocytochemistry, confocal microscopy and analysis*

Spinal cord sections were tile scanned through the full thickness with two channels of a confocal microscope (LSM 710, Zeiss, Germany), at a low magnification of x10. By using only one channel each time, all CTb and then FG cells were counted using NeuroLucida software with different markers to minimise bias. Then both channels were turned on and all double labelled cells (CTb and FG) rechecked to see that they were in the same optical planes and had the same shapes. The double labelled spinoreticular tract neurons in each of the three segments, L3, L4 and L5, were identified by the presence of both CTb and FG (Figure 3-6). A summary of the primary and secondary antibodies used along with their concentrations is given in Table 1-1. The inclusion criteria used was all cells, with intact somas and well labelled proximal dendrites, through the section thickness, excluding the first two optical sections to minimise any counting errors due to the presence of parts of neuronal soma that have been cut off while counting all such somas in the deeper sections.

**Table 3-1 Summary of primary and secondary antibody combinations and concentrations used in this experiment (n=4)**

Primary antibody combination	Primary antibody concentration	Supplier	Secondary antibody combination	Secondary antibody concentration	Supplier
gt CTb	1:5000	List, Quadratech Campbell, USA	Rh. Red	1:100	Jackson Immunoresearch, West Grove, USA
gp FG	1:500	Protos, Biotech, New York, USA	Dylight 488	1:500	Jackson Immunoresearch, West Grove, USA

### **3.2.3 Investigation of different phenotypes of spinoreticular projections to the LRN**

#### *Surgical procedures*

Three adult male Sprague-Dawley rats (Harlan, Bicester, UK), weighing between 250-350gm were deeply anaesthetised with 2-4% Isoflurane in Oxygen (30%O<sub>2</sub>/70%N<sub>2</sub>O). The animals were then placed in a stereotaxic frame and the spinous process of the first lumbar vertebra was identified at the point of attachment of the lowest rib at thoracic 13 (Th13). A small dorsal midline incision was made extending from, Th10 to L3 vertebrae. Then using a blunt dissecting forceps to hold onto the spine of the Th13 vertebra, the back was lifted and immobilised into the frame with spinal fixators. The lamina of the first lumbar vertebra was exposed (on the right side) and a small burr hole made near the midline. Taking care not to go too near the dorsal spinal artery, a nick was made in the pia mater with a small needle to aid the entry of the pipette and prevent any dimpling of the spinal cord. A micropipette was then filled with 0.2µl 1% CTb (Sigma-Aldrich, Co., Poole, UK) in distilled water and pressure injected into the intermedio-ventral spinal cord at an angle of 15° and a depth of ~1.5mm. After waiting for 5min the pipette was removed and the wound closed. These rats were given analgesia in the form of Buprenorphine 0.1 mg/100gm (Reckitt Benkiser Healthcare, Dumfries, UK) and Carprofen 5mg/100gm (Pfizer, Dumfries, UK) subcutaneously to prevent oedema postoperatively. Following a 5-6 days survival period, the animals were perfused with 4% freshly depolymerised formaldehyde (Sigma-Aldrich, Co., UK) in 0.1 M PB (Sigma-Aldrich, Co., UK) via the left ventricle and the brain and spinal cord

dissected out and post fixed overnight in the same fixative as explained previously (Chapter 2, section 2.1).

#### *Identification of injection site*

Transverse sections (50µm) of both brain stem and lumbar spinal cord (L1 to L3, depending upon the injection site) were cut using a Vibratome (Leica VT1200, Leica Microsystems, UK). The injection site for CTb in the lumbar spinal cord was identified using DAB as a chromogen and later with reference to the stereotaxic rat brain atlas of Paxinos and Watson (2005) as explained in section 2.2, chapter 2 (Figure 3-9).

#### *Immunocytochemistry*

Brainstem sections were sequentially collected into five bottles and each bottle incubated in a different combination of primary antibodies (Groups A, B and C, Table 3-2). Due to the varying morphology of the LRN throughout the medulla, low power images of all the incubated sections were first taken to identify the exact location of the LRN. The photomicrographs were superimposed onto the relevant maps from the stereotaxic rat brain atlas of Paxinos & Watson (2005) using Adobe Photoshop. Three to four sections were then selected at various levels (0.24 to 0.48µm increments) of the LRN (between stereotaxic coordinates inter-aural -4.8mm and -13.8mm respectively, see Chapter 1, Figure 1-4) and were subsequently incubated in various cocktails of primary antibodies as shown below.

#### *Characterisation of spinoreticular terminals in the lateral reticular nucleus*

In Group A, immunohistochemical reactions using a primary antibody combination of goat anti-CTb, guinea pig anti-VGLUT-1&2 (combined) and rabbit anti-VGAT was performed for 48hrs at 4<sup>0</sup> C. Following several washes in PBS, the sections were incubated overnight in secondary antibodies coupled to Rhodamine red, Alexa 647 and 488, in order to identify axon terminals containing CTb, VGLUT-1&2 and VGAT, respectively (Table 3-2, Figure 3-10 A). VGLUT-1&2 label glutamatergic terminals (Varoqui H et al., 2002, Todd AJ et al., 2003, Alvarez FJ et al., 2004) whereas VGAT labels both GABA and glycinergic terminals (Burger PM et al., 1991, Chaudhry FA et al., 1998).

### *Investigation of the various types of glutamatergic SRT terminals*

The purpose of experiments in Group B was to determine what proportions of the terminals were immunoreactive to VGLUTs; a primary antibody combination of goat anti-CTb, guinea pig anti-VGLUT-1 and rabbit anti-VGLUT-2 was used, incubating sections for 48hrs at 4<sup>0</sup> C. Following several washes in PBS, the sections were incubated in secondary antibodies coupled to Rhodamine red, Alexa 647 and 488, respectively. They were then rinsed in PBS, mounted on glass slides and cover slipped with Vectashield. All antibody solutions were made in PBST (see [Table 3-2](#)).

### *Comparison of proportions of SRT inhibitory terminals that are either GABAergic or glycinergic in origin*

In Group C, to further investigate what proportion of inhibitory boutons were either GABAergic or glycinergic, some sections were incubated in a combination of guinea pig anti-GLYT2 and rabbit anti-GAD primary antibodies and then in secondary antibodies Rhodamine red, Alexa 488 and 647, respectively ([Table 3-2](#)).

### *Confocal microscopy and analysis*

All these sections were then scanned using a confocal microscope (LSM 710, Zeiss, Germany). SRT terminals were identified by the presence of CTb in them. Tile scans of 5x3 covering most of the LRN were taken (magnification 40X, at 20 z-steps of 0.5µm intervals). These scans were analysed with Neurolucida for Confocal software (Microbrightfield Inc, USA). A grid with a box size of 25 x 25µm was placed and for each region, the first CTb bouton through the 10µm thickness, nearest the lower right hand corner, was marked and then checked to see whether it was labelled by VGLUT-1&2, VGAT, GAD or GLYT2 to find out the proportions of these neurotransmitters.

**Table 3-2 Summary of primary and secondary antibody combinations and concentrations used in this experiment (n=3).**

Group	Primary antibody combination	Primary antibody concentration	Supplier	Secondary antibody combination	Secondary antibody concentration	Supplier
A	gt CTb	1:5000	List (Quadrtech), Campbell, USA.	Rh. Red	1:100	Jackson Immunoresearch, West Grove, USA
	gp VGLUT-1&2	1:5000	Chemicon, Harlow, UK	Alexa 647	1:500	Molecular probes, Eugene, USA
	rbt VGAT	1:5000	Synaptic systems, Göttingen, Germany	Alexa 488	1:500	Molecular probes, Eugene, USA
B	gt CTb	1:5000	List(Quadrtech)	Rh. Red	1:100	Jackson Immunoresearch, West Grove, USA
	gp VGLUT-1	1:5000	Chemicon, Harlow, UK	Alexa 647	1:500	Molecular probes, Eugene, USA
	rbt VGLUT-2	1:5000	Chemicon, Harlow, UK	Alexa 488	1:500	Molecular probes, Eugene, USA
C	gt CTb	1:5000	List(Quadrtech)	Rh. Red	1:100	Jackson Immunoresearch, West Grove, USA
	gp GLYT2	1:10000	Chemicon, Harlow, UK	Alexa 488	1:500	Molecular probes, Eugene, USA
	rbt GAD 65&67	1:1000	Sigma	Alexa 647	1:500	Molecular probes, Eugene, USA

All secondary antibodies were raised in donkey and conjugated to Rh. Red, Rhodamine Red; Alexa 647 &488, Alexa fluor 647&488; gt, goat; gp, guinea pig; rbt, rabbit; CTb, b subunit of cholera toxin; VGLUT, vesicular glutamate transporter; VGAT, vesicular GABA transporter; GLYT2, glycine; GAD, glutamic acid decarboxylase.

### 3.2.4 Spinoreticular contacts onto pre-cerebellar neurons in the LRN

#### *Surgical procedures*

Stereotaxic surgery was performed in two steps on three adult male Sprague-Dawley rats. On the first day, the rats were placed into a spinal fixation frame. The same protocol was then followed, as already explained in the previous section ([Section 3.2.3](#)), with an injection of 0.2µl 1%CTb (Sigma-Aldrich, Co., UK) into the lumbar spinal cord. 48hrs later, the animal was re-anesthetised and placed in the stereotaxic frame for a tracer injection of 50nl of 4% FG (Fluorochrome, LLC, USA) into the cerebellum. A mid sagittal incision was given in the scalp and a burr hole made according to the interaural co-ordinates, dorso-ventral +6mm, antero-posterior -1.6mm and mediolateral -0.5mm. A glass micropipette was then lowered into the cerebellum and the FG tracer, pressure injected into it. After the injection, the micro pipette was left in place for 5mins to prevent backtracking of the FG. The scalp was then sutured and the animals placed in an incubator to await recovery.

Following a 5 day post second injection survival period, the animals were re-anesthetised with a lethal dose of Pentobarbitone (1ml at 200mg/ml i.p; Sigma-Aldrich, UK) and perfused trans-cardially. The brain and mid lumbar segments were dissected and post-fixed overnight in the same fixative at 4°C ([see Chapter 2, Section 2-1](#)).

#### *Identification of Injection sites*

Transverse sections of the cerebellum (100µm thick) and spinal cord (50µm thick, L1 to L3 depending upon the injection site) were cut on a Vibratome (Leica VT1200, Leica Microsystems, UK). The FG injections in the cerebellar sections were visualised directly under a fluorescence microscope and photomicrographed using an ultraviolet filter. The injection site for CTb in the spinal cord was identified using DAB as a chromogen as described in chapter 2. Both injection sites were then identified with reference to the stereotaxic rat brain atlas of Paxinos and Watson (2005) ([Figure 3-13](#)).

### *Immunocytochemistry, confocal microscopy and analysis*

The medulla was sectioned at 50µm thickness and low power images taken of each section with Axiocam. The exact level of the LRN identified using the stereotaxic rat brain atlas of Paxinos & Watson (2005) as described previously. Clusters of cells in the LRN were identified using the ultraviolet filter.

Table 3-3 shows the combination of primary antibodies used to label the pre-cerebellar cells and the types of contacts on these cells. These sections after combination with primary antibodies, goat anti-CTb, rabbit anti-FG and guinea pig anti-VGLUT-2, were then reacted two days later with Rhodamine red, Alexa 488 and Alexa 647. A fourth primary antibody, mouse VGAT, was reacted a day later for 48hrs and then coupled with anti-mouse Biotin for 3 hours and finally with Avidin pacific blue (Av-PB) overnight. This reaction was done sequentially to avoid any cross reactions with other secondary antibodies. The sections were rinsed in PBS, mounted on glass slides and cover slipped with Vectashield.

Four channels of a confocal microscope were used to scan these sections. Initially the CTb terminals were plotted to pre-cerebellar LRN neurons. Then later, by switching between channels for VGLUT-2 and VGAT, all excitatory and inhibitory terminals were plotted onto the cells. The inhibitory SRT terminals were identified by the presence of CTb and VGAT, whereas the glutamatergic contacts were identified by the presence of VGLUT-2 over CTb (Figure 3-13). Reconstruction of the neurons were made following the procedure outlined in Chapter 2 (Section 2-4), contacts formed by CTb labelled SRT terminals with or without VGAT or VGLUT-2 were counted and the contact density calculated /100 µm<sup>2</sup> of the neuronal surface area.

### **3.2.5 Statistical analysis**

Data are expressed as mean ± standard deviation (SD). Multi-group comparisons undertaken by analysis of variance (ANOVA) followed by a post hoc *Tukey's* analysis, as appropriate (GraphPad Prism version 6.02, GraphPad Software, La Jolla California USA). A  $p < 0.05$  was considered to be statistically significant.

**Table 3-3. Summary of primary and secondary antibody combinations and concentrations used in the present experiment (n=3)**

Primary antibody combination	Primary antibody concentration	Supplier	Secondary antibody combination	Secondary antibody concentration	Supplier
gt CTb	1:5000	List(Quadrantech)	Rh. Red	1:100	Jackson Immunoresearch, West Grove, USA
rbt FG	1:5000	Chemicon/ Millipore, CA, USA	Alexa 488	1:500	Molecular probes, Eugene USA
gpig VGLUT-2	1:5000	Chemicon, Harlow, UK	Alexa 647	1:500	Molecular probes, Eugene USA
mo VGAT	1:1000	Synaptic systems, Göttingen, Germany	mo Biotin AV-PB	1:500 1:1000	Molecular probes, Eugene USA

All secondary antibodies were raised in donkey and conjugated to Rh. Red, Rhodamine Red; Alexa 647&488, Alexa -fluor 647&488; AV-PB, Avidin pacific blue; gp, guinea pig; rbt, rabbit; gt, goat; mo, mouse; CTb, b subunit of cholera toxin; FG, Fluorogold; VGLUT, vesicular glutamate transporter; VGAT, vesicular GABA transporter.

## 3.3 Results

### 3.3.1 Distribution of SRT neurons in rat lumbar cord

#### *Injection Sites*

CTb injection into the LRN yielded well defined unilateral injection sites with a penumbra of diffuse CTb staining (Figure 3-1). Three out of the four animals injected had slightly varying areas of the LRN labelled but the first rat had hardly any LRN labelling, which resulted in a different pattern of distribution of retrogradely labelled cells in the lumbar spinal cord (Figures 3-2 & 3-3). All these injections spared the Inferior olivary nuclei and in the case of animal 1 the ascending fibres ventral to the LRN were also spared.

#### *Distribution of cells of origin of SRT*

Each of the four injections resulted in extensive retrograde labelling on both sides of the spinal lumbar segments, as can be seen in Figures 3-2 & 3-3. Also shown is the overall distribution of retrogradely labelled neurons from three sections per segment for each animal, plotted onto an outline of the respective rat spinal cord segment from the atlas of Paxinos and Watson (1997) and also expressed as cell counts (Figure 3-4). In the rats with a central core of injection into the LRN (2, 3, 4), most of the cells at the origin of the spinoreticular tract were located ventromedially in the deep dorsal, intermediate and ventral areas of the spinal cord grey matter with larger concentrations in Lamina VII (Figures 3-2 & 3-3). In Animal 1, with a central core of injection in the dorsal part of the medullary reticular nucleus rather than in the LRN, the distribution pattern on both sides of the central canal was almost even, with more cells in the superficial dorsal horn and the lateral spinal nucleus and fewer scattered cells in the ventromedial areas (Figure 3-2). Whereas, for animals 2, 3 and 4, the largest population of cells were found on the contralateral side in the intermediate zone,  $41.2 \pm 13.5\%$  with peaks in lamina VII and V and a scattering of cells in lamina VI and X. The greatest number of cells seemed to be concentrated at the border of lamina X and VII. There were fewer cells in the deep dorsal laminae and in the grey matter around the central canal. Clusters of labelled cells were

also found in the superficial dorsal horn concentrated at the lateral edge and in the lateral spinal nucleus.

#### *Laterality of Projections*

Although SRT neurons were retrogradely labelled on both sides of the spinal cord, in all three segments analysed (L3, L4 and L5), contralateral labelling predominated ( $p < 0.01$ ). Of the total number of cells counted in each experiment, 70% ( $\pm 9.2$ , mean  $\pm$  SD) were found contralateral to the injection sites. This pattern was seen throughout the various laminae from the superficial dorsal horn to the ventral horn and lamina X. In comparing each of the laminae with the contralateral side, it was seen that only in contralateral lamina VII (part of the intermediate) were there significantly greater numbers of cells than in the corresponding lamina on the ipsilateral side (2 way ANOVA  $p < 0.01$ , [Figure 3-4](#)).

#### *Number of cells*

The total number of SRT cells counted for each animal ranged from 318 to 526. Animals 2, 3 and 4 had more or less the same number and pattern of distribution of cells (554, 427 and 526 cells, respectively), whereas animal 1 had the least number of cells with a more equal bilateral distribution patterns (318 cells).

### **3.3.2 The projection patterns of spinoreticular neurons to the LRN**

#### *Injection Sites*

CTb & FG injections into the LRN yielded bilateral well defined injection sites with a penumbra of diffuse CTb staining into the intermediate (IRt) and parvicellular (PCRt) reticular nuclei in all four animals. However, in animal 7 the FG injection extended into the spinal trigeminal nucleus (Sp5I, [Figure 3-5](#)). All these injections yielded retrogradely labelled cells but FG labelling produced more cells (63 % of all cells labelled).

### *Laterality of Projections*

In each of the three animals analysed, the injections resulted in extensive retrograde labelling on both sides of the spinal segments (Figures 3-6 & 3-7). Depending on the extent of labelling and the side of the spinal cord, three major groups of cells were identified (see Figures 3-7 and 3-8):

- those that project bilaterally and hence are double labelled; ~10% ( $\pm 4.7$  SD) and ~7% ( $\pm 2.87$  SD) on the right and left sides of the sections, respectively;
- SRT cells that project ipsilaterally, ~31% ( $\pm 9.11$ SD) of CTb labelled and ~35% ( $\pm 1.71$  SD) of FG labelled;
- by far the largest numbers of cells were labelled contralateral to their respective injection sites, 56% ( $\pm 6.38$  SD) of the CTb labelled cells and 61% ( $\pm 9.9$  SD) of the FG labelled cells (Figure 3-8A).

### *Distribution of cells of origin of SRT*

The pattern of distribution within the various laminae is the same as observed with the single CTb tracer injections (previous section), with more cells in the ventro-medial areas (lamina VI and VII, intermediate zone) of the spinal cord but with some clusters in the lateral half of the deep dorsal laminae and around the central canal in lamina X (Figures 3-7 & 3-8B).

Approximately 8% of all SRT labelled cells are double labelled ( $8.42 \pm 2.97\%$ ) mostly in the intermediate zone. Figure 3-7 shows the pattern of distribution of these bilateral projecting cells in the various zones examined (deep dorsal, intermediate and lamina X). The majority of cells projecting to the contralateral LRN have their somas located in the intermediate zone, in case of both markers (Figure 3-8B).

### *Number of cells*

The total number of SRT cells counted for each animal ranged from 656 to 796, nearly double the number seen with single LRN injections. Animals 5, 6 and 8 had more or less the same number and pattern of distribution of the cells (656,

796 and 760, respectively) whereas animal 7 had the least number of cells with more equal bilateral distributions (357 cells).

### **3.3.3 Investigation of transmitter phenotypes of spinoreticular projections to the LRN**

#### *Injection sites in the lumbar cord and distribution of terminals in the LRN*

Tracer injections of CTb into the lumbar spinal cord were well defined and concentrated unilaterally in the intermediate laminae, but with diffusion into the surrounding ventral areas (Figure 3-9). Animal 2 had the most extensive injection and this resulted in many more terminals labelled in the LRN compared to the other experiments. This may also be because the injection site for this animal was in L3, whilst in the other 2 animals the sites were centred more caudally in L4. Representative images of injection sites for the three animals are shown in Figure 3-9 (1).

A large number of anterogradely labelled axons were seen ipsilaterally in the LRN after CTb injection to the intermedio-ventral lumbar spinal cord (Figure 3-9, 2 b & c) with significantly less labelling seen on the contralateral side (Figure 3-9, 2 b' & c). The ratio of ipsilateral vs. contralateral terminals was 2.6 to 1.

The LRN extends from interaural co-ordinate -4.32 to -6.00mm but the largest dimensions are at -4.68 to -5.16mm (Figures 147 & 151 in Paxinos & Watson, 2005) and it is in these areas that the greatest densities of labelled terminals from the lumbar cord were found. Most of the terminals are present in the parvicellular parts of the LRN but in addition to this there was a heavy distribution of SRT terminals in the lateral magnocellular region, extending dorsoventrally. The density of these terminals progressively declines rostrally and caudally, more so in the magnocellular areas. Mediolaterally, the distribution seems to be more or less diffuse taking the various shapes of the LRN but with a denser distribution in the more medial intermediate areas (see Figure 3-9). Caudally, the terminals were concentrated in the ventral parvicellular regions of the LRN.

*What is the proportion of excitatory and inhibitory SRT axons terminating in the ipsilateral and contralateral lateral reticular nuclei of the medulla?*

Confocal microscope images of SRT axons in the ipsilateral and contralateral LRN, labelled according to the protocols shown in [Table 3-2](#), are shown in [Figures 3-10 & 3-11](#), respectively. Detailed data concerning these experiments are provided in [Table 3-4](#). In order to identify excitatory and inhibitory SRT terminals in the LRN, sections were reacted to reveal CTb, VGAT and a combination of VGLUT-1 & 2 as shown in [Table 3-2 Group A](#). In total 4038, CTb terminals were counted on the ipsilateral side (range of 1100-1500 for each experiment) and although most of the terminals were reactive for vesicular glutamate transporters ( $80.2 \pm 7.78\%$ , mean  $\pm$  SD%), there were a substantial number of VGAT spinoreticular axon terminals ( $15.4 \pm 8.98\%$ ). A post hoc *Tukey's* analysis showed a statistically significant difference of  $p < 0.001$  in case of excitatory and inhibitory terminals.

Although fewer terminals were present within the LRN contralateral to the injection site, the pattern of immunoreactivity was similar to the ipsilateral LRN ([Figure 3-11](#); [Table 3-4](#)). Approximately 72% ( $\pm 8.3$ , SD) of CTb terminals were positively labelled for the combined vesicular glutamate transporters, VGLUT-1 & 2, whereas ~17% ( $\pm 6.5$ ) were labelled for VGAT. A slightly higher percentage of CTb terminals (10.2% on the contralateral LRN as opposed to 3.9% for the ipsilateral LRN) were not immunoreactive for any of the excitatory and inhibitory antibodies tested ([Table 3-2](#)).

*What is the proportion of glutamatergic excitatory SRT axon terminals?*

In order to further clarify what types of vesicular glutamate transporters are present in the CTb boutons, another series of triple labelling experiments was conducted by incubating the sections in: CTb, VGLUT-1 and VGLUT-2 ([Table 3-2, Group B](#)). A total of 2594 terminals were counted on the ipsilateral side (range of 500-1500 per animal) in tile scans of the LRN. These scans revealed that more than three quarters of the terminals ( $79.6 \pm 2.98\%$ ) were positive for VGLUT-2, making it the primary excitatory glutamatergic transporter used by the SRT neurons. Additionally, there was a very small percentage ( $3 \pm 0.78\%$ ) of VGLUT-1 terminals ([Table 3-4](#)). A post hoc *Tukey's* analysis showed a statistically significant difference of  $p < 0.001$  between VGLUT-2 and VGLUT-1 terminals.

Although fewer contralateral projecting terminals were labelled for VGLUT-2 when compared with the ipsilateral side, 65% versus 81% (Table 3-4).

*What proportions of inhibitory terminals are GABAergic or glycinergic?*

A total of 8753 CTb terminals were counted on the ipsilateral side (ranging from 1500-4000 in each animal) (Table 3-2, Group C). An analysis of the confocal microscope images of all the CTb-labelled terminals (Figure 3-10, panel B) revealed that there was approximately an equal distribution of inhibitory VGAT terminals labelled by GAD, GLYT2 or with both GAD and GLYT2 ( $4.2 \pm 5.7\%$ ;  $5.7 \pm 2.2\%$ ;  $4.9 \pm 3.6\%$ , respectively, Table 3-4). Whereas, on the contralateral side (Figure 3-11, panel B), with fewer CTb labelled terminals (2092), GLYT2 and both GAD/GLYT2 terminals were  $\sim 8\%$  ( $\pm 2.86$  and  $\pm 1.21$ , respectively) while GAD only terminals were  $\sim 3\%$  ( $\pm 1.64$ ) of all CTb terminals.

Overall, in comparing the CTb labelled terminals for these excitatory and inhibitory neurotransmitters, with the exception of the difference in VGLUT-2 immunoreactivity ( $p < 0.001$ , Anova with post hoc *Tukey's*), none of these values were statistically different from the ipsilateral side.

Table 3-4. Percentages of excitatory (VG1&2) and inhibitory (VGAT, GAD, GLYT2) boutons in the ipsi and contralateral lateral reticular nuclei anterogradely labelled from spinal injections of CTb

Ipsilateral						Contralateral					
Animal	No. of terminals	Both VG1&2	VGAT	VGLUT1/2 & VGAT	CTb	Animal	No. of terminals	Both VG1&2	VGAT	VGLUT1/2 & VGAT	CTb
1	1128	84.1	10.5	0.4	5	1	147	64.6	19.0	0.7	15.6
2	1474	71.2	25.8	0.6	2.3	2	363	70.8	22.6	0.3	6.3
3	1436	85.2	10	0.3	4.5	3	321	81.0	10.0	0.3	8.7
	Mean%	<b>80.17</b>	<b>15.43</b>	<b>0.43</b>	<b>3.93</b>		Mean%	<b>72.1</b>	<b>17.2</b>	<b>0.4</b>	<b>10.2</b>
	±SD	7.78	8.98	0.15	1.44		±SD	8.27	6.51	0.22	4.84
		VGLUT1	VGLUT2	VGLUT-1&2	CTb			VGLUT1	VGLUT2	VGLUT1&2	CTb
1	517	1.93	84.14	1.35	12.57	1	119	1.7	61.3	0.8	36.1
2	641	1.25	76.44	0.94	21.37	2	205	2.0	59.5	2.0	36.6
3	1436	3.27	81.69	0.56	14.48	3	230	2.6	74.3	3.0	20.0
	Mean%	<b>2.15</b>	<b>80.76</b>	<b>0.95</b>	<b>16.14</b>		Mean%	<b>2.1</b>	<b>65.1</b>	<b>1.9</b>	<b>30.9</b>
	±SD	1.03	3.93	0.40	4.63		±SD	0.48	8.09	1.10	9.45
		GAD	GLYT2	GAD&GLYT2	CTb			GAD	GLYT2	GAD&GLYT2	CTb
1	1530	1.24	4.97	1.70	92.09	1	253	2.8	10.3	8.7	78.3
2	4017	10.80	8.12	8.79	72.29	2	1350	5.2	8.6	8.0	78.2
3	3026	0.66	3.99	4.12	91.24	3	489	2.0	4.7	6.3	86.9
	Mean%	<b>4.23</b>	<b>5.69</b>	<b>4.87</b>	<b>85.21</b>		Mean%	<b>3.3</b>	<b>7.9</b>	<b>7.7</b>	<b>81.1</b>
	±SD	5.70	2.15	3.60	11.19		±SD	1.64	2.86	1.21	5.01

### 3.3.4 Spinoreticular contacts on pre-cerebellar neurons in the LRN

Fluorogold injections were made into the anterior lobe of the cerebellum (focused on lobules III, IV, V) and injections of CTb were made into the right side of lumbar spinal segments (Figure 3-12). Injections of FG in the cerebellum resulted in extensive labelling of pre-cerebellar neurons in the medulla that were confined to the LRN and inferior olivary complex (Figure 3-13, also see Chapter 1, Figure 1-5A).

Diameters of neurons labelled within the LRN ranged from 18-33  $\mu\text{m}$ . Relationships between ipsilateral SRT terminals and pre-cerebellar neurons in the LRN were assessed using four channel confocal imaging, looking at the ratio of various excitatory and inhibitory contacts onto these cells. From the previous experiment it was seen that most of the SRT terminals were VGLUT-2 positive and very few were VGLUT-1. So taking this into consideration, the sections were processed to reveal VGLUT-2 and VGAT, along with CTb and FG (Table 3-3). The confocal scans (Figure 3-13) of these pre-cerebellar cells showed that, of all the terminals contacting these cells, ~53% were VGAT immunoreactive whereas ~47% contained VGLUT-2. Thus, it is interesting to note that although these cells had a predominantly inhibitory input; only ~2% ( $\pm 2.12$ ) were spinoreticular VGAT positive and ~13% ( $\pm 2.78$ ) were spinoreticular VGLUT-2 positive. Approximately 16% ( $\pm 5.5$ ) of all contacts on LRN pre-cerebellar cells originate from lumbar spinoreticular cells; most of which are VGLUT-2 positive (84.6% of CTb contacts) whereas only a small minority were VGAT-immunoreactive (10.7% of CTb terminals). Results of Sholl analysis can be seen in Table 3-5, with contact densities of 0.45/100 $\mu\text{m}^2$  of CTb positive VGLUT-2 terminals, as compared to 0.07/100  $\mu\text{m}^2$  VGAT positive (Figure 3-14).

Table 3-5 Excitatory (VGLUT-2, CTb+ VGLUT-2) and inhibitory (VGAT, CTb+VGAT) terminals and their contact densities onto pre-cerebellar cells in the LRN

Animals	No. of cells (n)	Contacts (total number both soma and dendrites)					Total Surface area ( $\mu\text{m}^2$ )	Average contact densities (n/ $100\mu\text{m}^2$ )				
		VGLUT2	CTb	VGAT	CTb+VGLUT2	CTb+VGAT		VGLUT2	CTb	VGAT	CTb+VGLUT2	CTb+VGAT
1	10	729	6	850	176	0	56546.30	1.29	0.01	1.50	0.31	0.00
2	11	571	30	860	282	77	66518.70	0.86	0.05	1.29	0.42	0.12
3	11	682	13	1347	326	47	49644.05	1.37	0.03	2.71	0.66	0.09
<b>Mean</b>		<b>660.67</b>	<b>16.33</b>	<b>1019.00</b>	<b>261.33</b>	<b>41.33</b>	<b>57569.68</b>	<b>1.15</b>	<b>0.03</b>	<b>1.77</b>	<b>0.45</b>	<b>0.07</b>

**Figure 3-1 Photomicrographs of representative sections of rat medulla with reconstructions illustrating the CTb injection sites**

**1a-4a** DAB images of coronal sections of the medulla illustrating the b subunit of cholera toxin (CTb) injection sites (black arrow) representing each animal.

**1b-4b** Corresponding reconstructions for all four experiments drawn on coronal brain maps from Paxinos & Watson (1997). The dark grey/black shaded area shows the primary injection site and the light grey shade illustrates the maximum spread of CTb

a, Lateral reticular nucleus; b, ventral medullary reticular nucleus; c, intermediate reticular nucleus; d, dorsal medullary reticular nucleus.

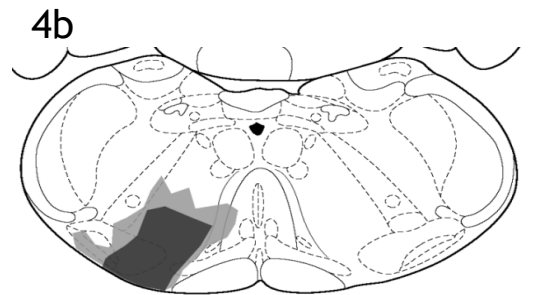
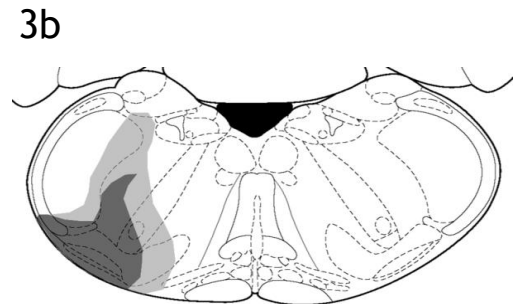
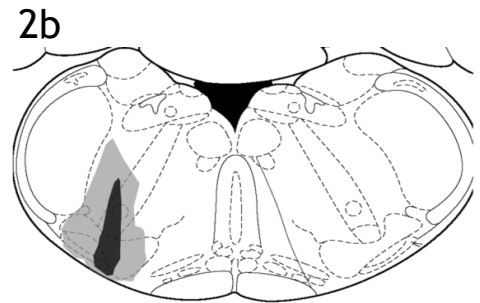
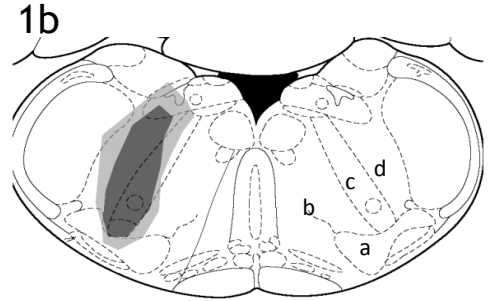
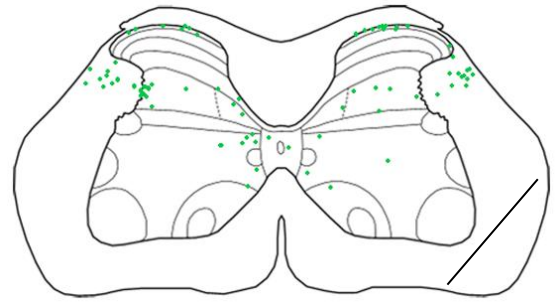
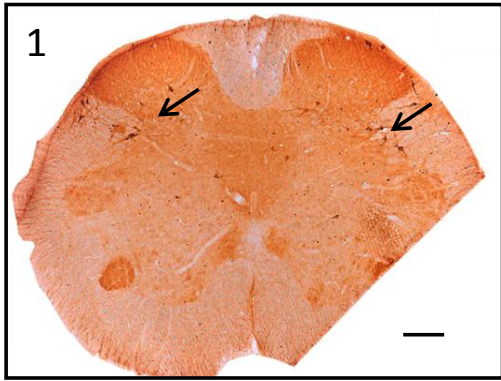


**Figure 3-2 Soma locations of retrogradely labelled spinoreticular cells in animals 1 and 2 which correspond to the injection sites in figure 3-1**

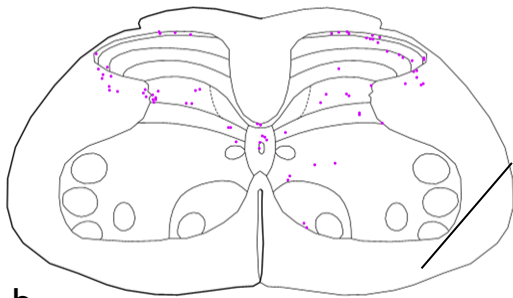
**1&2** DAB photomicrographs of representative L5 transverse sections of the rat spinal cord, illustrating spinoreticular neurons labelled by retrograde transport of CTb (black arrow)

**a, b, c and a', b', c'** Schematic drawings with plots of spinoreticular cells represented by coloured dots illustrating the laminar distribution of these cells onto maps of the L3 (a, a', green dots), L4 (b, b', magenta dots) and L5 (c, c', blue dots) transverse rat spinal cord. Each map is representative of a total of three sections per segment and each dot represents a retrogradely labelled cell from the lateral reticular nucleus. The right side i.e. notched side is contralateral to the brain injection site.

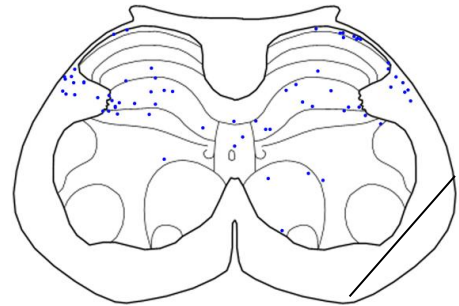
*Maps are from Paxinos & Watson, 1997 (Scale bar 200  $\mu$ m).*



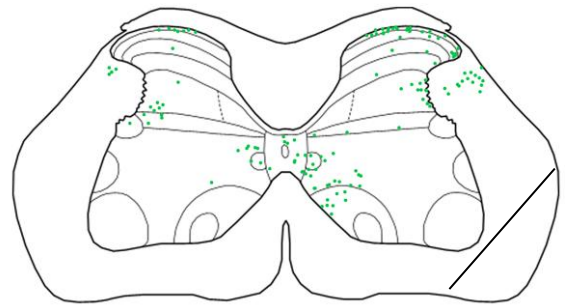
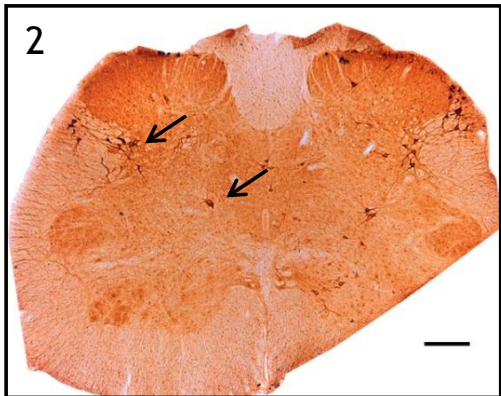
a



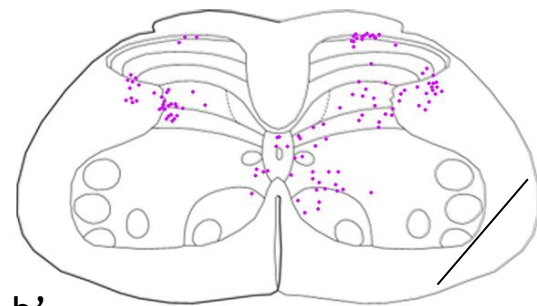
b



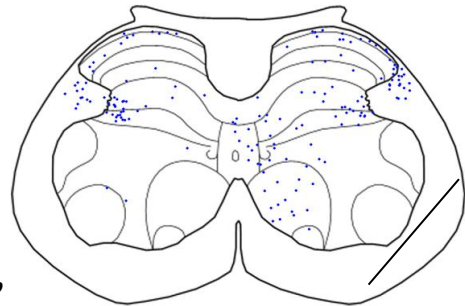
c



a'



b'



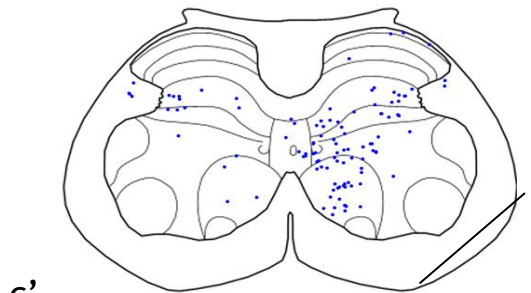
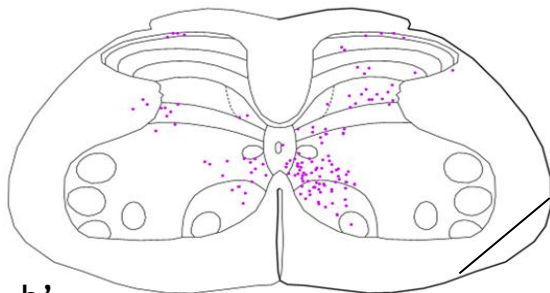
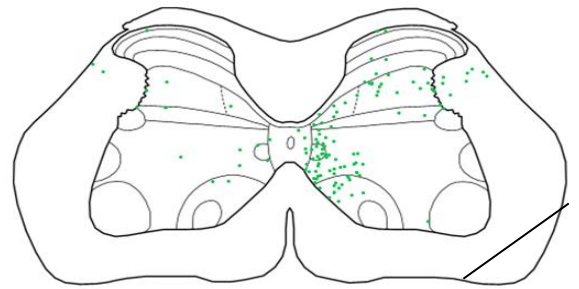
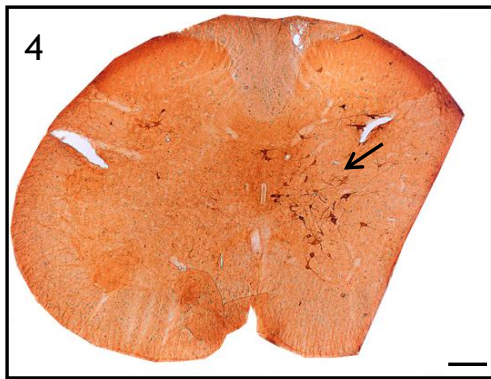
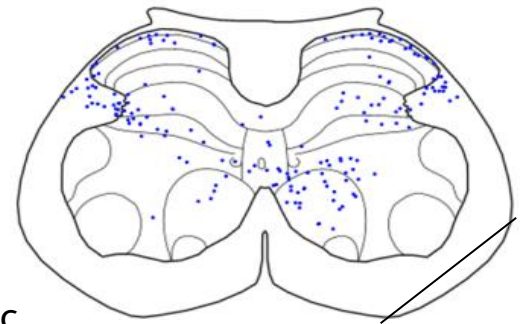
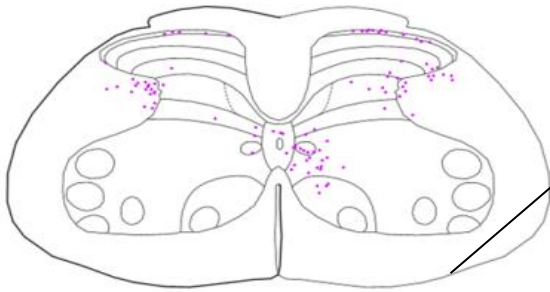
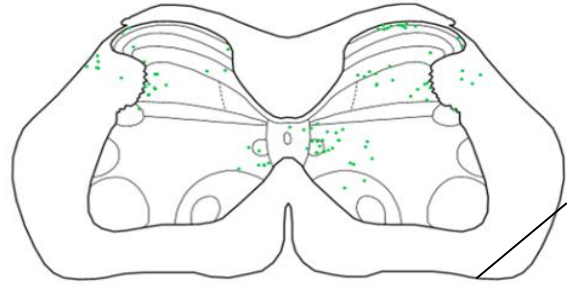
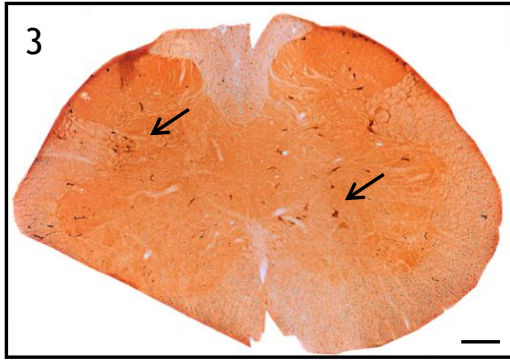
c'

**Figure 3-3** Soma locations of retrogradely labelled spinoreticular cells in animals 3 and 4 that correspond to the injection sites in Figure 3-1

**3&4** DAB photomicrographs of representative L5 transverse sections of the rat spinal cord illustrating spinoreticular neurons labelled by retrograde transport of CTb (black arrow)

**a, b, c and a', b', c'** Schematic drawings with plots of spinoreticular cells represented by coloured dots illustrating the laminar distribution of these cells onto maps of the L3 (a, a', green dots), L4 (b, b', magenta dots) and L5 (c, c', blue dots) transverse rat spinal cord. Each map is representative of a total of three sections per segment and each dot represents a retrogradely labelled cell from the lateral reticular nucleus. In animal (3), the right side, i.e. un-notched in this case is contralateral to the injection site and in animal (4), the notched right is contralateral to the brain injection site.

*Maps are from Paxinos & Watson, 1997 (Scale bar 200 µm).*



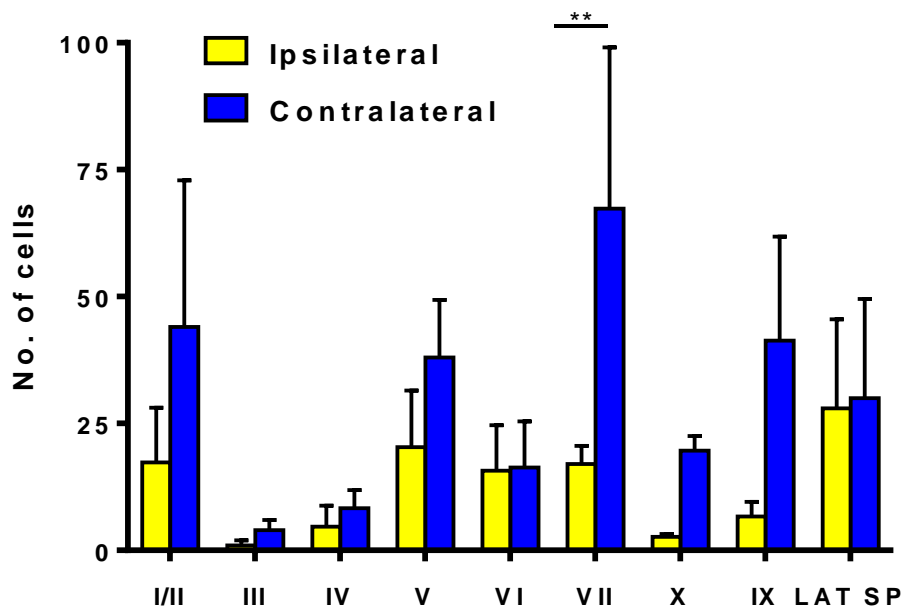


**Figure 3-4 Laminar distribution of spinoreticular cells in the lumbar spinal cord after unilateral injections of CTb tracer in the lateral reticular nucleus (LRN)**

This graph shows the total number of cells/3 sections in each lamina of the lumbar spinal cord, both ipsilateral and contralateral to the injection site in the brain. The number of cells in the contralateral lamina VII is significantly more than those on the ipsilateral side,  $**p < 0.01$  post hoc *Tukey's*.  $n = 3$  (animals 2, 3 & 4).  $T = SD$ .

**Figure 3-5 Bilateral lateral reticular nuclei (LRN) injections of b subunit of cholera toxin (CTb) and fluorogold (FG)**

**A.** Photomicrograph of a representative DAB section of the medulla with the CTb injection site (black arrow, left LRN).

**B.** Photomicrograph of a representative fluorescent over a dark field section of the medulla from the same animal illustrating the FG injection site (white arrow, right LRN).

**(5-8)** Reconstructions of the injection sites on brain maps from Paxinos & Watson, 2005, illustrating the injection sites for each of the four animals used in these experiments. The dark grey/black shaded area shows the primary injection site of CTb and the yellow represents FG injection, whereas the light grey shaded area represents the spread of the two tracers: .a, Lateral reticular nucleus (LRN); b, ventral reticular nucleus (MdV); c, intermediate reticular nucleus (IRt); d, dorsal reticular nucleus (MdD).

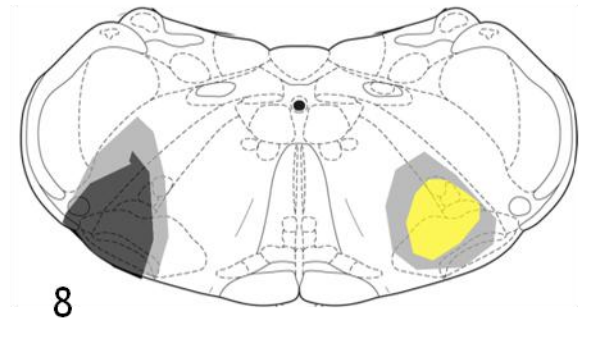
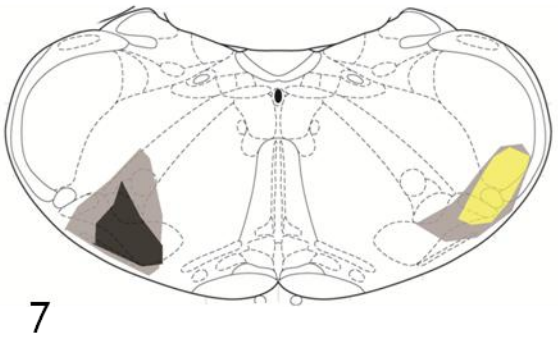
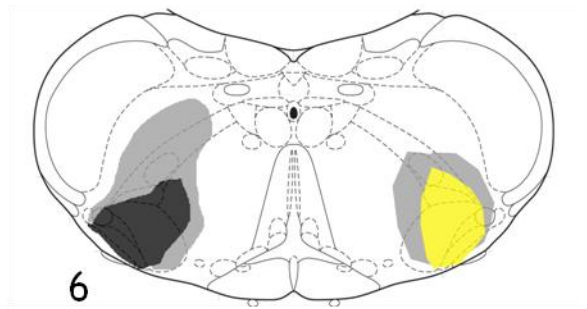
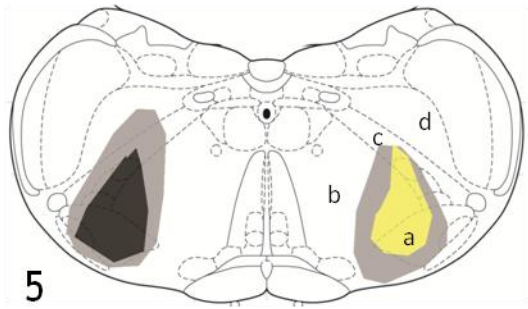
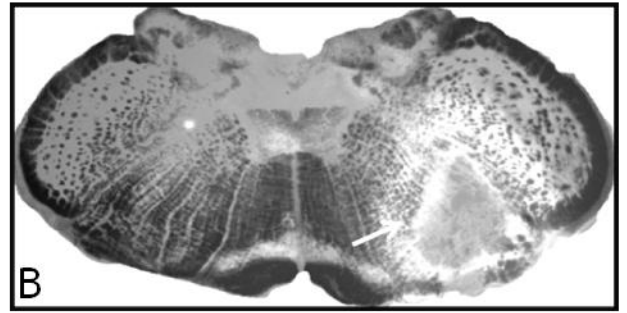
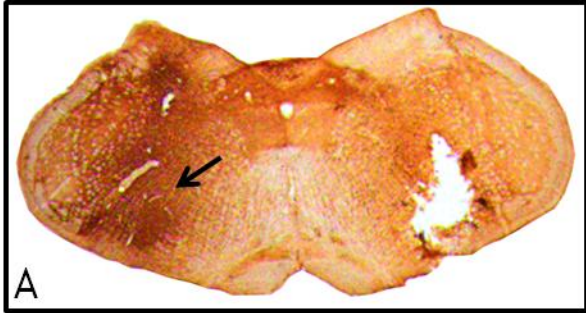


**Figure 3-6 A tiled confocal scan of a lumbar section of the spinal cord illustrating the distribution of retrogradely labelled cells by both CTb and FG**

**Top large panel** with white arrows at double labelled spinoreticular (SRT) neurons (CTb and FG, yellow, inset 1 &2); yellow arrow pointing towards a FG labelled spinoreticular neuron (green) and bigger arrow head at CTb labelled SRT neuron (red).

1. The inset shows a representative double labelled SRT neuron in lamina V contralateral to the CTb injection site in the LRN. A magnified view of the cell is shown in the lower panel, from Left to right 1a; CTb (red, Rhodamine), 1b; FG (green, Alexa 488) and 1c; merged image.

2. This inset shows a double labelled SRT cell in Lamina VII ipsilateral to the CTb injection in the LRN. A magnified view of the same cell in panel 2a; Red, CTb; 2b; Green, FG and 2c; yellow, double labeled SRT neurons (white arrows).

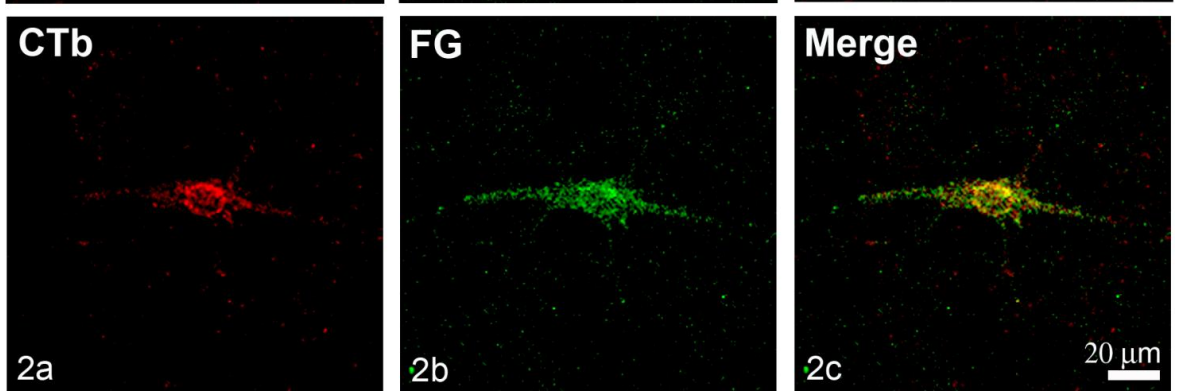
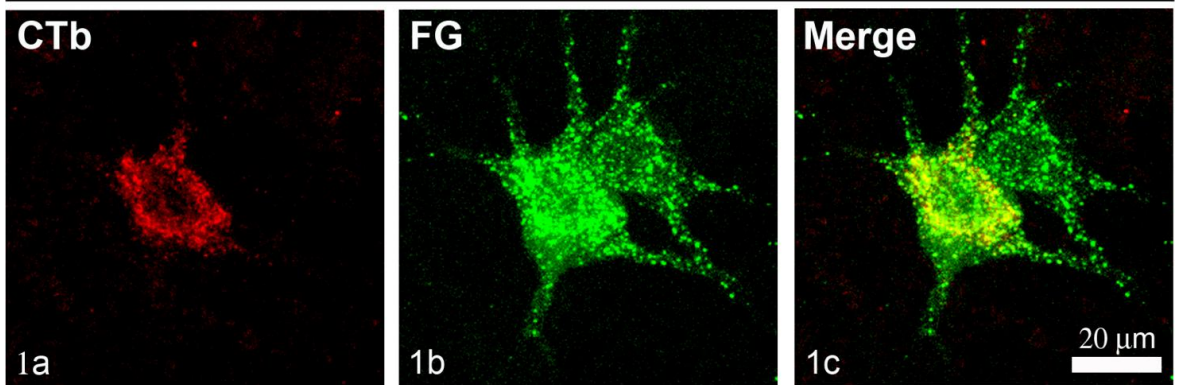
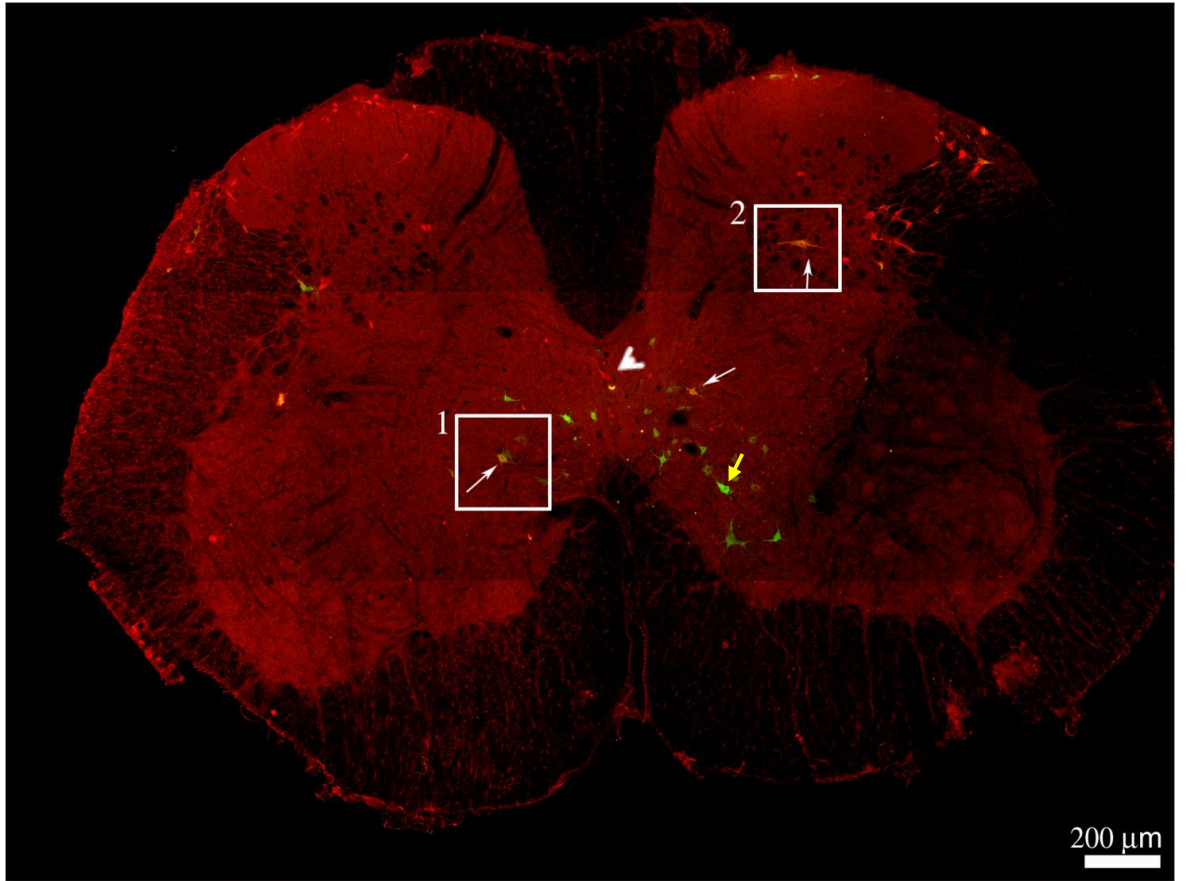


**Figure 3-7 Soma locations of spinobulbar cells retrogradely labelled by bilateral LRN injections**

These are representative drawings of the three types of retrogradely labelled SRT cells on maps of lumbar segments L3, L4 and L5 from each of the four animals (5,6,7,8) Each dot represents a single cell illustrated as;

**Red circles**, the laminar distribution of cells retrogradely labelled by CTb injection into the left LRN;

**Green dots**, spinoreticular neurons labelled by FG injection into the right LRN

**Black dots**, neurons projecting to both LRN (both CTb and FG labelled). The ipsilateral and contralateral indication is in respect to the CTb injection in the brain. The lumbar spinal maps are from Paxinos & Watson, 2005.

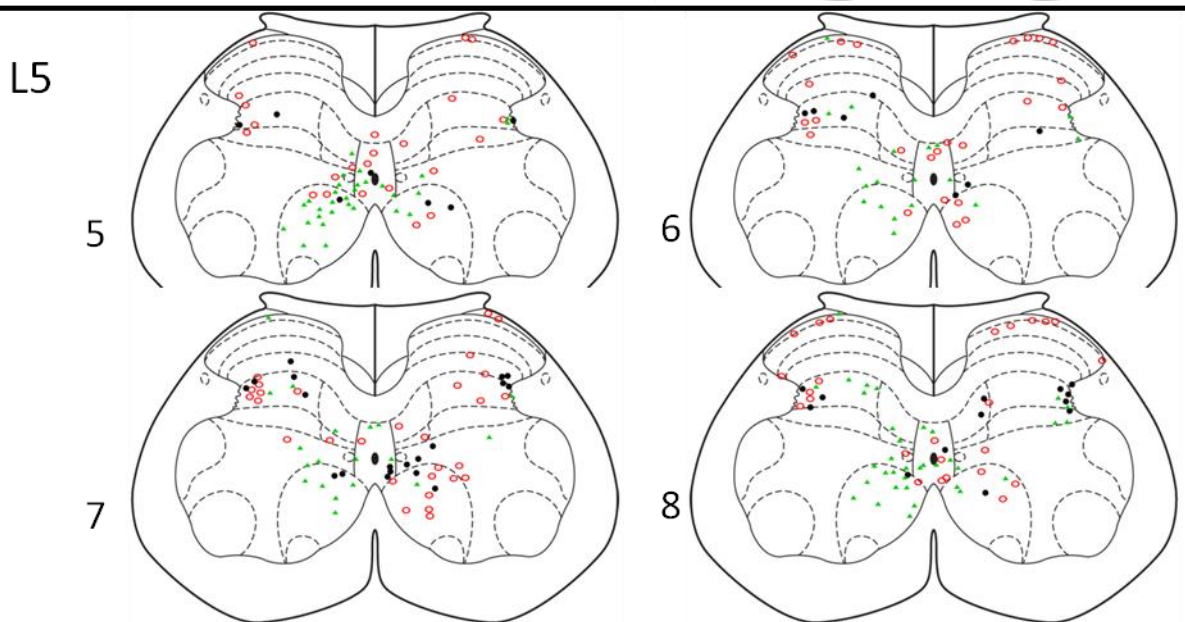
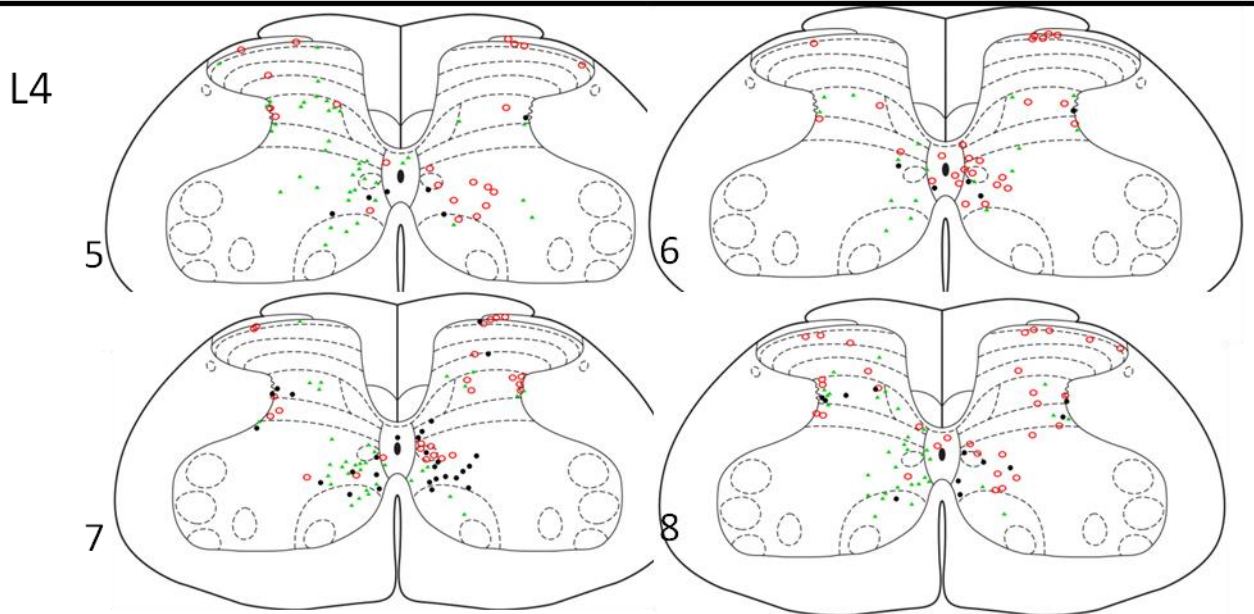
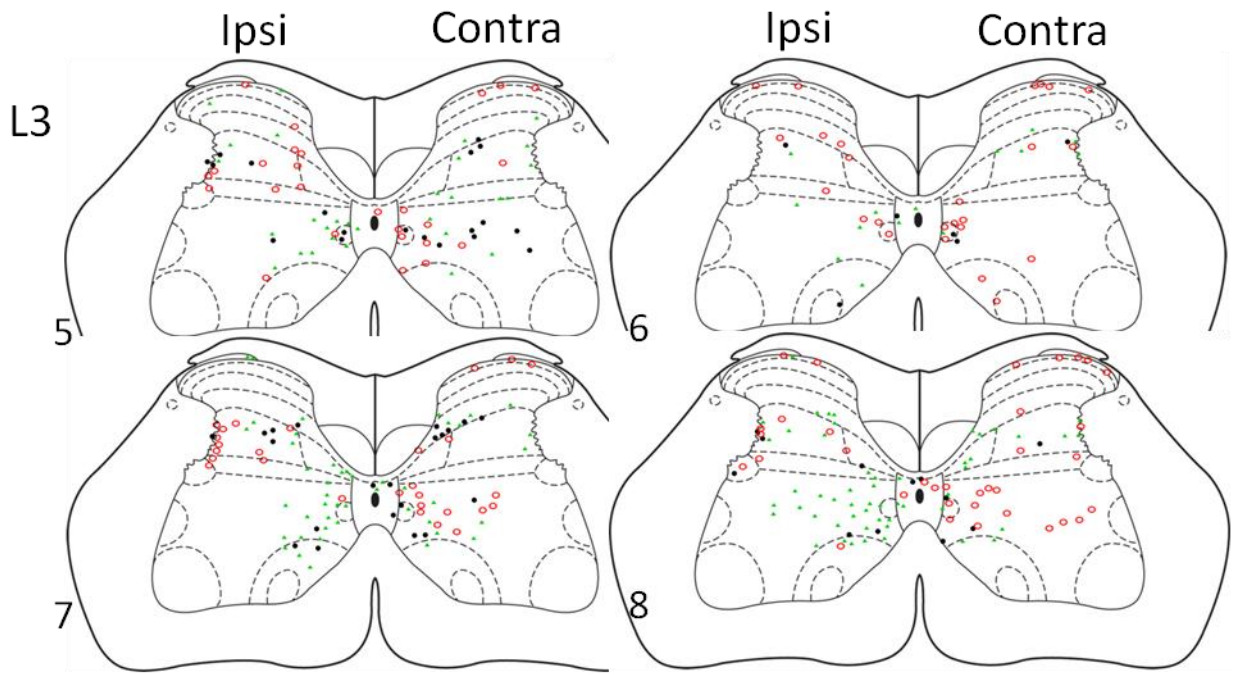


**Figure 3-8 Bar graphs showing the distribution patterns of three types of spinoreticular projection neurons**

**A. Comparison of the contra and ipsilateral distribution of the various subpopulations of SRT cells after bilateral LRN tracer injections.**

The laterality is defined according to the respective injection sites of both tracers and the laterality for the double labelled cells is defined according to the CTb injection site. There is a significant difference in the distribution pattern of the CTb labelled cells that project ipsilaterally and contralaterally (post hoc *Tukey's* \*\*\* $p < 0.001$ ).  $n=3$ , T= SD

In the contralateral group comparisons, there is a significant difference between CTb and FG, CTb and double labelled cells, and between FG and double labelled cells seen with a post hoc *Tukey's* analysis of \* $p < 0.05$ , \*\*\*  $p < 0.001$  and \*\*\* $p < 0.001$ , respectively. On the ipsilateral side there is a significant difference between CTb and FG cells, and double labelled and FG cells of \*\* $p < 0.01$  and \*\*\* $p < 0.001$ , respectively (post hoc *Tukey's*).

**B. The laminar distribution of subpopulations of SRT labelled cells in the lumbar spinal cord.**

There is a significant difference within the intermediate laminae (VI/VII) between, CTb+FG labelled cells and FG cells \*\*\* $p < 0.001$ , as well as between CTb +FG and CTb labelled cells, \* $p < 0.05$  respectively (post hoc *Tukey's*).  $n= 3$ , animals. T= SD.

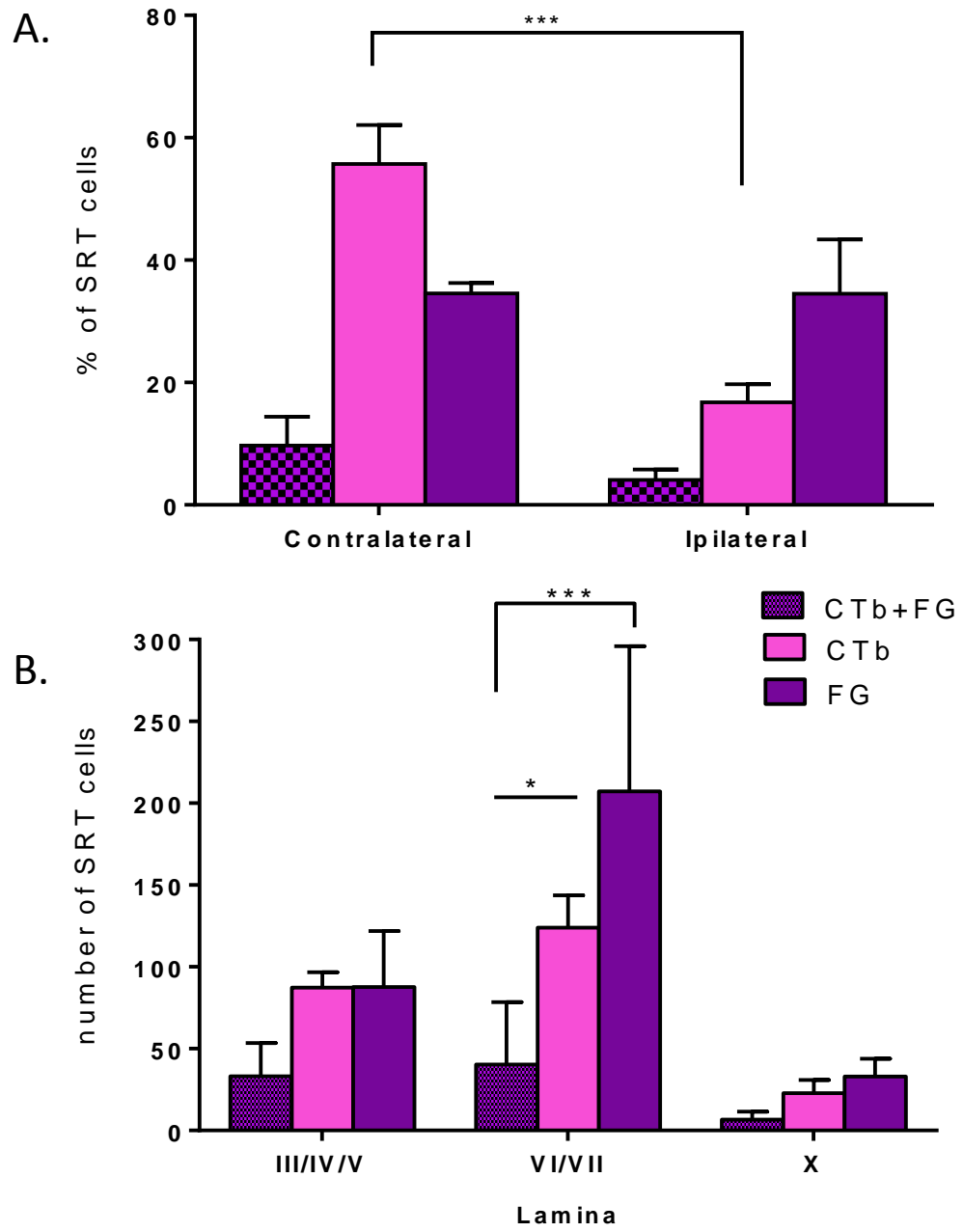


**Figure 3-9 Spinal injection of CTb in the lumbar segments with anterogradely labelled terminals in the LRN**

1. An image of a representative DAB section of the lumbar spinal cord with the CTb injection site (white arrow) and a-c, the injection sites of all the animals on a template of the L3 transverse section from Paxinos & Watson, 2005. The dark grey is the injection site with a light grey penumbra of tracer spread.

2 a Photomicrograph of a representative DAB section of the medulla illustrating the pattern of distribution of SRT terminals in the LRN (scale bar 100µm)

b and b' are magnified views of the insets in A with CTb terminals in the contralateral and ipsilateral LRN, respectively (scale bar 100µm). C. Corresponding brain map drawing of the SRT terminals plotted in both LRN (black dots, Paxinos & Watson, 2005).

Lrt, Lateral reticular nucleus; LRtPC, lateral reticular nucleus parvicellular part; MdV, medullary ventral reticular nucleus.

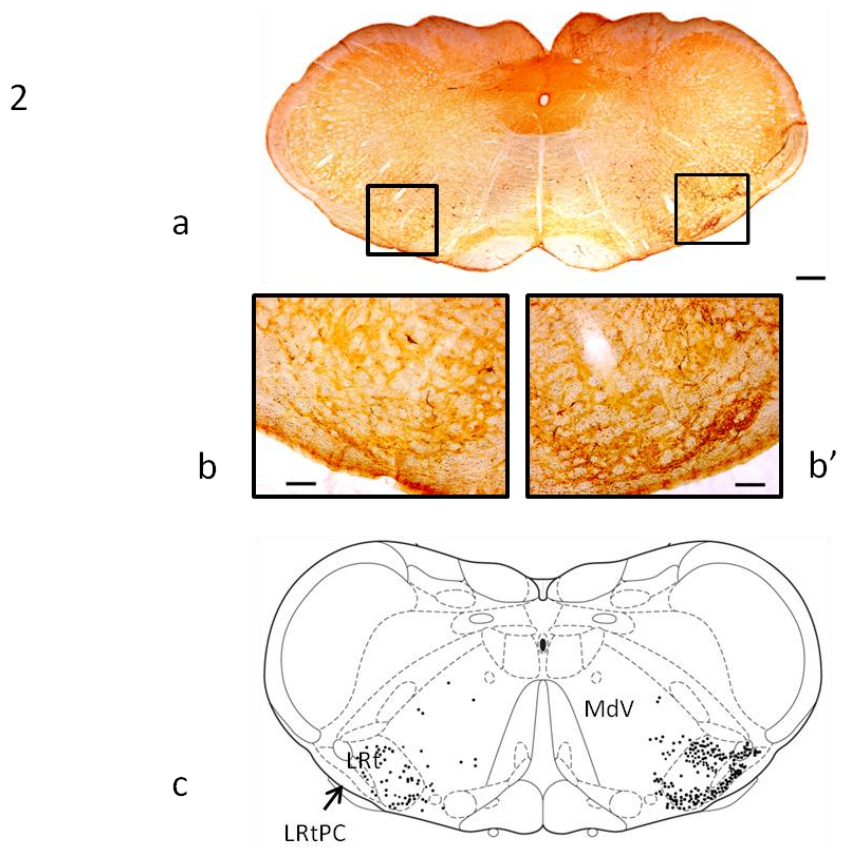
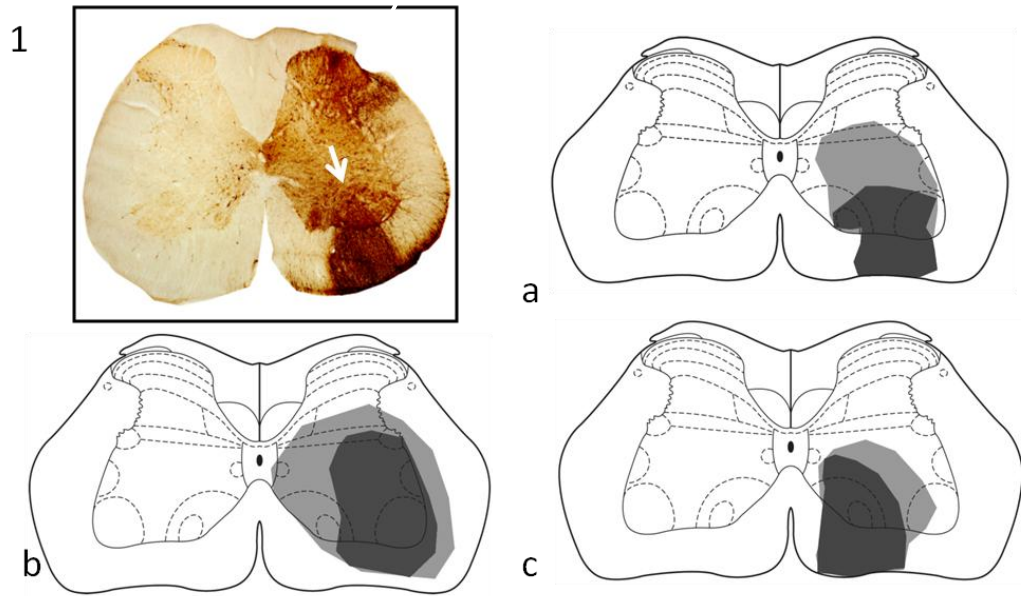


**Figure 3-10 Confocal scans of the lateral reticular nucleus (LRN) illustrating the immunocytochemical properties of spinoreticular terminals ipsilateral to the spinal injection**

**A. (1, large panel)** An overview of terminals within the LRN labelled for CTb (red), VGLUT-1&2 (blue) and VGAT (green). The area demarcated by the box is shown in series 2 and 3 (a, b &c). The inset shows a representative area with CTb and VGAT positive boutons (white arrow), and CTb and VGLUT-1&2 (arrow head).

The right panel from top to bottom illustrates a magnified view of the inset; CTb labelled terminals (2a, red); co-localised with VGAT (2b, green); and merged image (2c, yellow).

The lower panel shows CTb labelled terminals (3a, red) that are VGLUT-1&2 positive (3b, blue), and a merged image (3c, magenta). A merged image from both sides shows CTb, VGAT and VGLUT-1&2 positive terminals (4, red arrow, white).

**B. Spinoreticular terminals (CTb, red) and inhibitory neurotransmitters (GLYT2, green) and (GAD, blue)**

1. The first panel shows CTb terminals labelled by both GAD and GLYT2 (arrow heads).

2. The second panel shows CTb terminals labelled by GLYT2 only (white arrows).

3. The third panel shows CTb terminals labelled by GAD only (red arrows): CTb, (Red, Rhodamine); GLYT2 (Green, Alexa 488); and GAD 65/67 (Blue, Alexa 647).

Scale bars for panel 2 & 3 = 5µm.

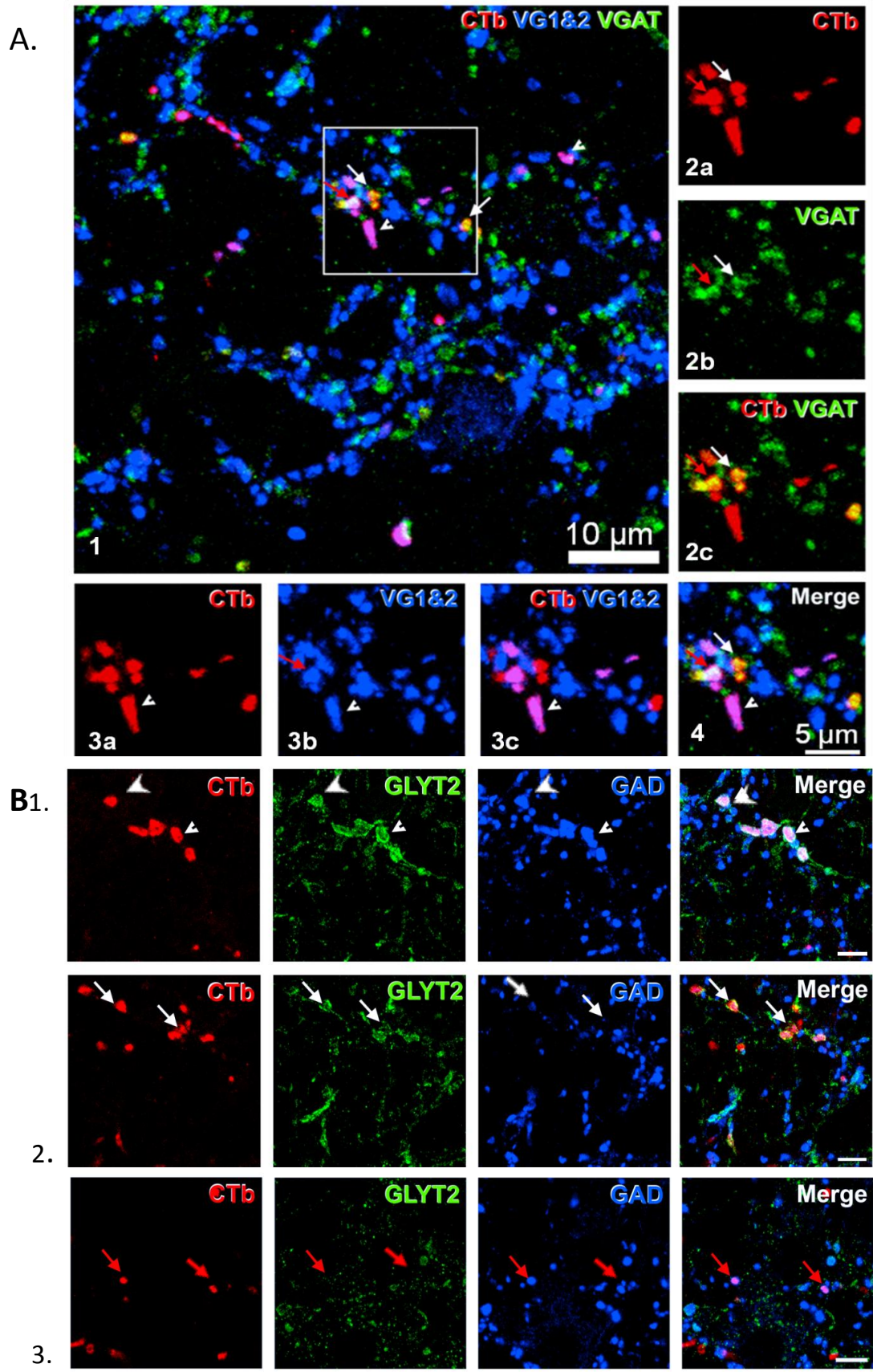


**Figure 3-11 Confocal scans of the lateral reticular nucleus (LRN) illustrating the immunocytochemical properties of spinoreticular terminals contralateral to the spinal injection site**

These single optical sections illustrate the immunocytochemical properties of the terminals co-localised with excitatory and inhibitory neurotransmitters.

**A. (1, large panel)** An overview of terminals within the LRN labelled for CTb (red), VGLUT-1&2 (blue) and VGAT (green). The area demarcated by the box is shown in series 2 and 3 (a, b & c). The inset shows a representative area with CTb and VGAT positive boutons (white arrow), and CTb and VGLUT-1&2 (arrow head).

The right panel from top to bottom illustrates a magnified view of the inset: CTb labelled terminals (2a, red); co-localised with VGAT (2b, green); and merged image (2c, yellow).

The lower panel shows CTb labelled terminals (3a, red) that are VGLUT-1&2 positive (3b, blue), and a merged image (3c, magenta). A merged magnified view of the inset image shows CTb VGAT and CTb VGLUT-1&2 positive terminals.

**B. Spinoreticular terminals (CTb, red) and inhibitory neurotransmitters (GLYT2, green) and (GAD, blue)**

1. The first panel shows CTb terminals labelled by both GAD and GLYT2 (arrow heads).

2. The second panel shows CTb terminals labelled by GLYT2 only (white arrows).

3. The third panel shows CTb terminals labelled by GAD only (red arrows): CTb, (Red, Rhodamine); GLYT2, (Green, Alexa 488); and GAD 65/67 (Blue, Alexa 647).

Scale bars for panels 1, 2 & 3 = 5µm.

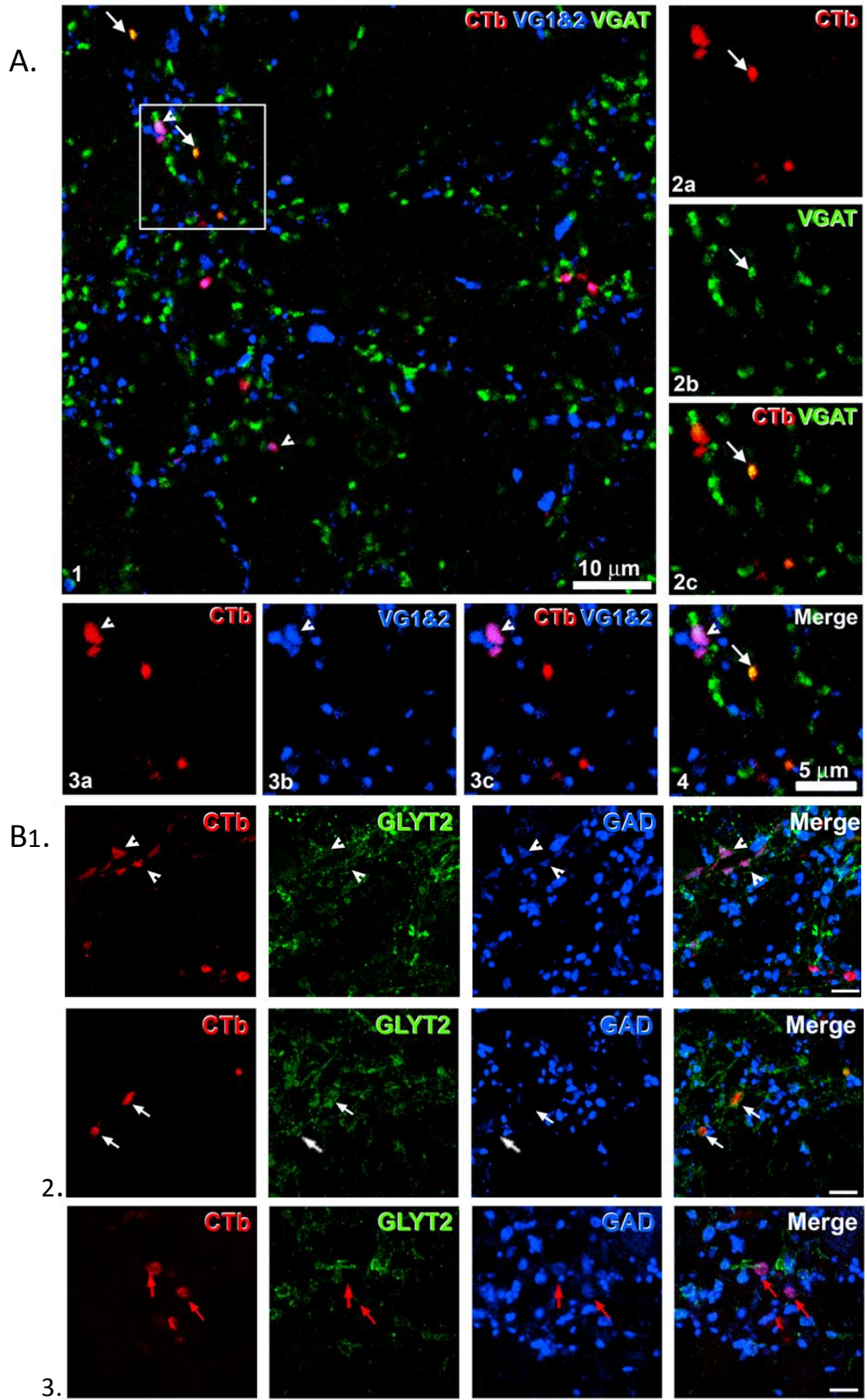


**Figure 3-12 Fluorogold injection into the cerebellum to retrogradely label reticulo-cerebellar cells in the LRN with spinal injections of CTb in lumbar segments of the same animals to anterogradely label spinoreticular terminals in the LRN**

1. A fluorescence micrograph (of animal a) showing fluorogold injection site within a coronal section of the anterior cerebellum (white arrow).

(a, b,c). Drawings of the core (black) and spread (grey) of fluorogold within lobules 3, 4 and 5 of the cerebellum for each animal (based on Paxinos & Watson, 2005).

2. A DAB image of a representative section of the lumbar spinal cord with the CTb injection site (black arrow).

(a, b, c). Schematic drawings of the CTb injections on templates of the thoracolumbar transverse sections from Paxinos & Watson, 2005, illustrating the injection site (black) with a penumbra (light grey) of tracer spread within the grey and white matter of the cord.

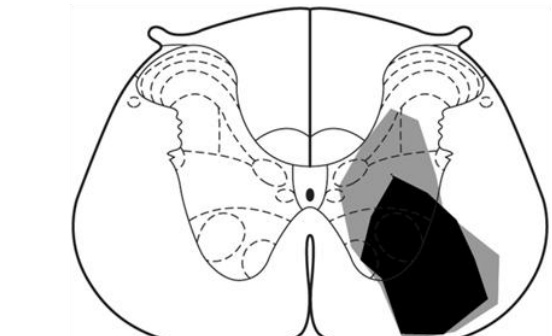
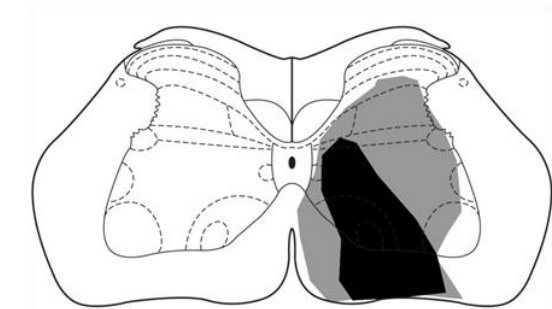
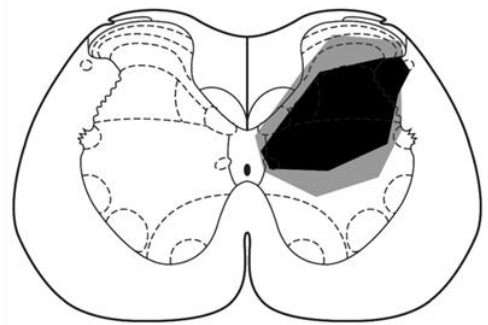
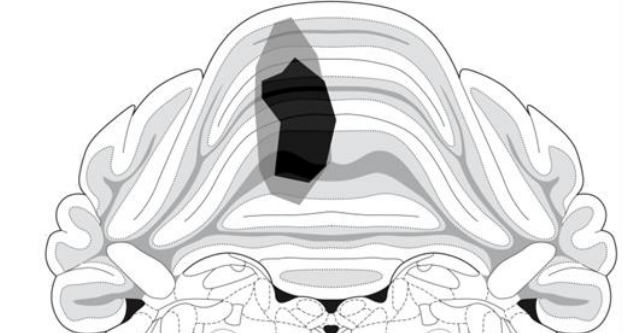
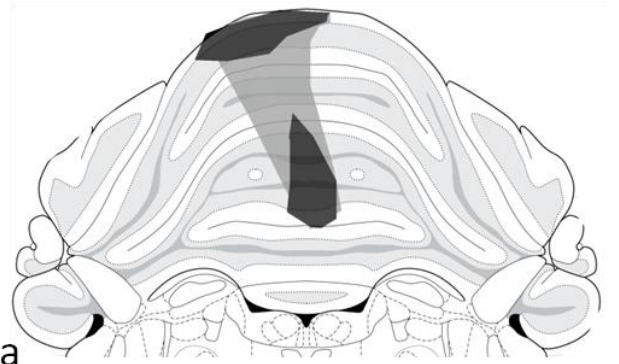
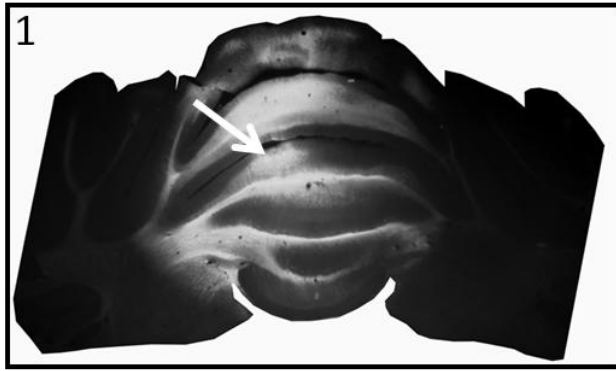
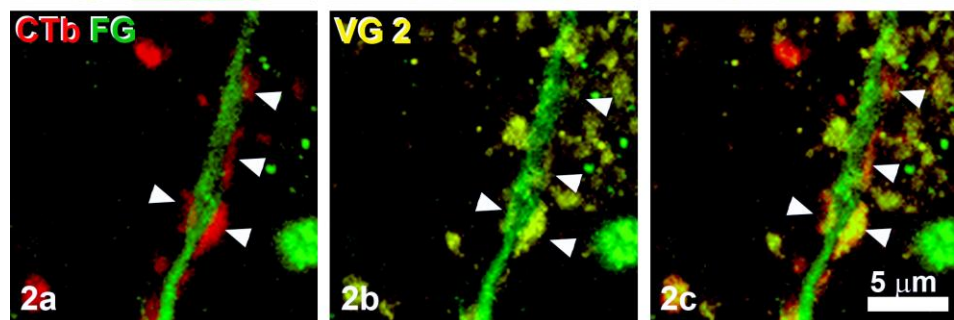
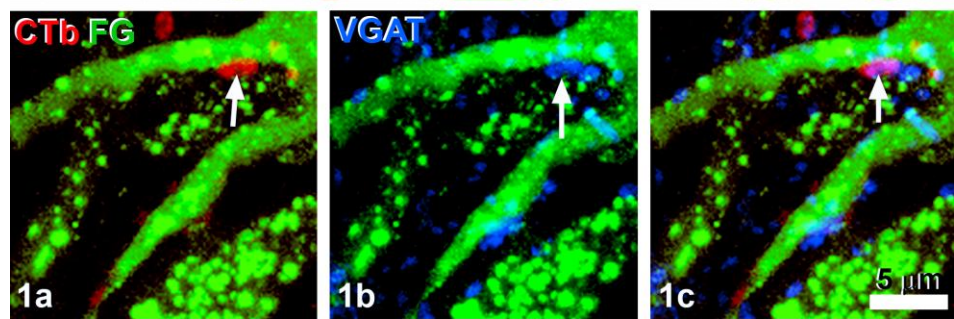
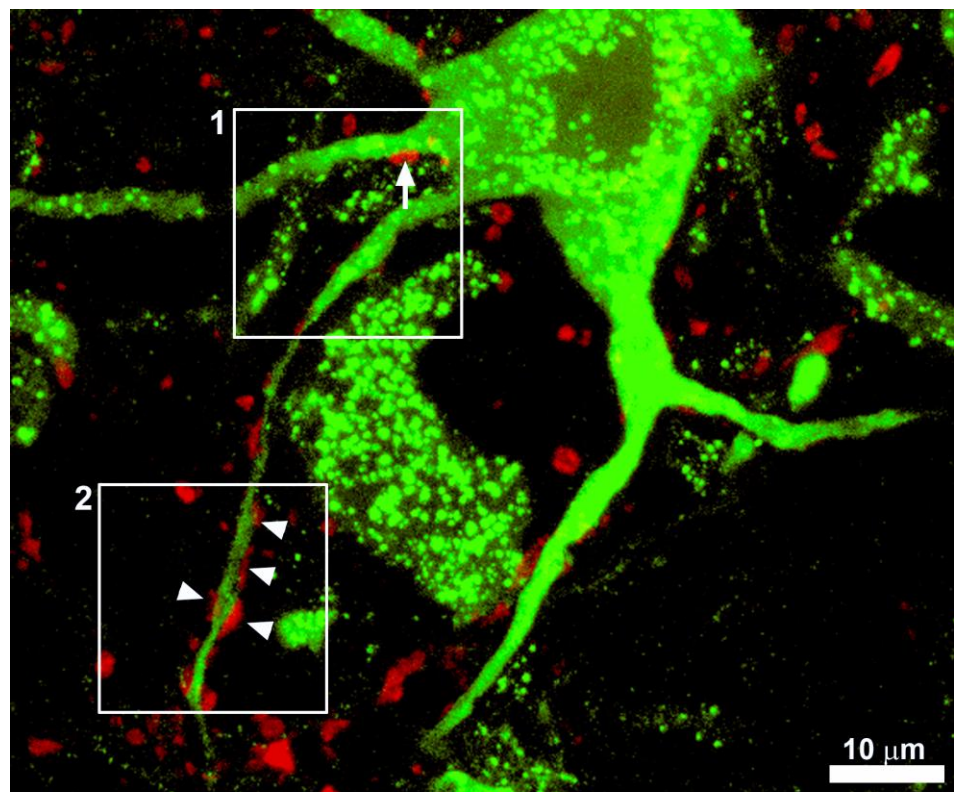


**Figure 3-13 A confocal scan of a reticulo-cerebellar cell with spinoreticular inputs in the LRN**

**Large panel,** FG (green; Alexa 488) filled dendrites of a cell with CTb labelled terminals (red; Rhodamine). The small lower panels show a magnified view of Inset 1 and 2.

**1a-c,** left to right, CTb labelled terminals (red; Rhodamine), onto a FG (green; Alexa 488) filled dendrite of the cell, co-localised with VGAT (blue; Av-Pacific blue, white arrow).

**2a-c,** left to right, CTb labelled terminals (red; Rhodamine), onto FG (green; Alexa 488) filled dendrite of the cell, co-localised with VGLUT-2 (shown in yellow; Dylight 647, white arrow heads).



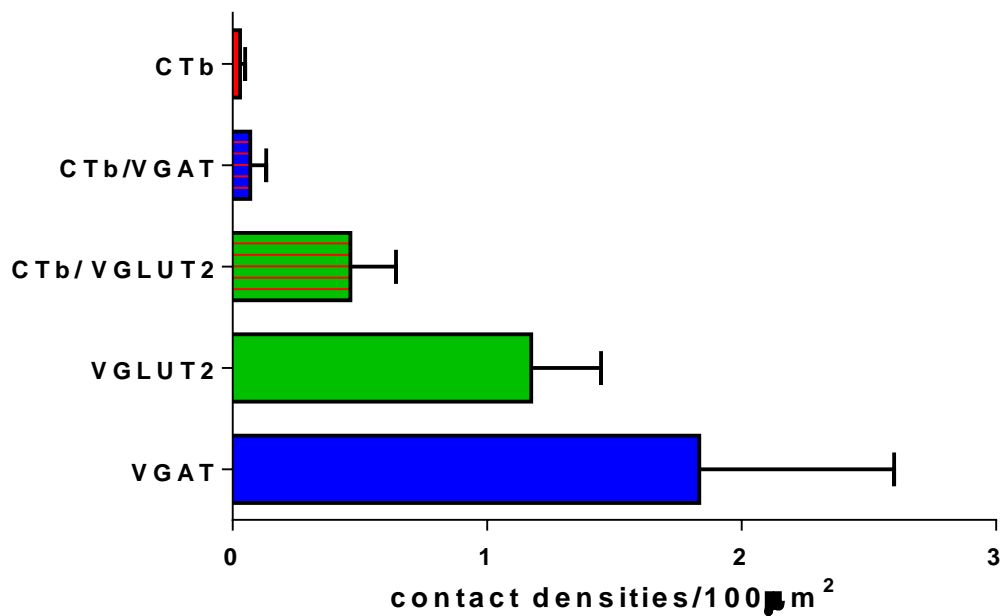


**Figure 3-14 Contact densities of excitatory and inhibitory spinoreticular terminals onto reticulo-cerebellar cells in the LRN**

There is a significant difference between the CTb/VGAT (inhibitory SRT terminals) and the VGAT (all other inhibitory) contact densities,  $p < 0.01$  (post hoc *Tukey's*). Within the SRT terminals (CTb positive), there is a significant difference between CTb/VGLUT-2 and CTb/VGAT,  $p < 0.05$  and CTb/VGLUT-2 and CTb contact densities,  $p < 0.001$  (post hoc *Tukey's*).  $n=3$ ,  $T=SD$ .

### 3.4 Discussion

In this study it was found that, although there was extensive bilateral labelling of SRT neurons on both sides of the lumbar spinal cord, most of the cells (~70%) were located contralateral to the injection site in ventromedial lamina V to VIII. Although many of the cells were concentrated in lamina VII, there were some in lamina X and the deep dorsal horn. In addition to these contralateral projections, there were some cells that project not only ipsilaterally, but also bilaterally to both left and right LRNs (~8%). Hence the majority of the SRT terminals, ascending via the ventrolateral funiculus, are to the ipsilateral LRN with relatively fewer projections to the contralateral LRN. These projections are predominantly excitatory but there is a significant inhibitory component that consists of three subtypes of axons containing GABA, glycine or a mixture of GABA and glycine. The only major difference between ipsilateral and contralateral projections was that fewer terminals in the contralateral nucleus expressed immunoreactivity for VGLUT-2. The overwhelming majority of ipsilateral SRT terminals (~85%) form excitatory contacts with LRN pre-cerebellar neurons but a smaller number of inhibitory contacts were also formed (~10%) with many cells receiving convergent connections from excitatory and inhibitory axons. These results are summarised in a simplified diagram in [Figure 3-15](#).

#### 3.4.1 Technical considerations

We used CTb both as a retrograde tracer to label spinoreticular neurons in the lumbar spinal cord (Ericson H and Blomqvist A, 1988, Luppi P-H et al., 1990) and as an anterograde tracer to label spinal axons projecting to the LRN (Angelucci A et al., 1996). It is a sensitive neuronal tracer with unique features; it binds to the GM1 ganglioside on the surface of neurons thus providing good retrograde labelling of the dendritic tree to about the second order dendrites (Hellenbrand DJ et al., 2013), and because it is added extraneously, is a highly sensitive marker in very minute amounts, yielding significant labelling. It also has an added advantage of being able to be used with immunocytochemical staining without suppressing the antigenicity of neuronal antigens, unlike HRP (Ericson H and Blomqvist A, 1988). However, despite all these advantages, some potential pitfalls in the use of CTb for tracing in the central nervous system have to be

considered; CTb is taken up not only from grey matter but also by fibres of passage especially if they are damaged (Ericson H and Blomqvist A, 1988, Chen S and Aston-Jones G, 1995). Our spinal injections extended from the intermediate grey matter and ventral horn into the ventromedial/ventrolateral funiculi, thus labelling axons of passage from more caudally situated cell bodies. The axons of the spinoreticular tracts ascend in the ventrolateral funiculus (Zemlan FP et al., 1978, Rajakumar N et al., 1992) and within these are the fibres of the bVFRT that cross at segmental levels (Holmqvist B et al., 1959, Lundberg A and Oscarsson O, 1962b, Rosén I and Scheid P, 1973c, Clendenin M et al., 1974 b, Ekerot CF, 1990c). Thus a possible explanation of why spinal-LRN projections were found to be predominantly ipsilateral in our study is because injections were focused on the white matter rather than the grey matter. Various studies of retrogradely labelled spinal cells, following injections of tracer substances into the LRN, are in agreement that neurons in laminae VII, VIII and X project predominantly to the contralateral LRN (Corvaja N et al., 1977a, Hrycyszyn AW and Flumerfelt BA, 1981b, Menetrey D et al., 1983, Shokunbi MT et al., 1985, Koekkoek SK and Ruigrok TJ, 1995, Lee HS and Mihailoff GA, 1999). As the spread of CTb tracer encompassed these regions, cells projecting contralaterally would have transported the tracer. In spite of this, the labelling of SRT terminals in the LRN is quite consistent with other studies involving other techniques, like axonal degeneration (Hrycyszyn AW and Flumerfelt BA, 1981b).

We also used FG to retrogradely label cells from the LRN and also the cerebellum to the spinal cord and LRN, respectively. When calculating the contact densities of neurotransmitters onto the pre-cerebellar cells, there is a chance that we may have underestimated the contacts because FG is stored as vesicles within the neuron; hence making it difficult to plot boutons onto the cells. Due to the unequal efficiency of the tracers (CTb and FG), in the animals with bilateral tracer injections in the LRN, more cells were labelled by FG in the lumbar cord, as compared to CTb (Schmued LC and Fallon JH, 1986, Naumann T et al., 2000). Although this might affect the spinobulbar population of individual tracers it does not distort the degree of collateralisation estimated from the prevalence of retrogradely labelled neurons marked by both tracers (Lefler YA et al., 2008).

In LRN injections, other ascending tract neurons could have been retrogradely labelled because of the ventral spread of the tracer, such as the spinocerebellar tract or the spinothalamic tract. Although it is difficult to exclude this possibility it is likely that the vast majority of CTb labelled neurons are SRT cells as the pattern of distribution for spinocerebellar cells is more ventrolateral (Shrestha SS et al., 2012a) and for spinothalamic more dorsolateral (Burstein R et al., 1990).

### **3.4.2 Lumbar distribution of Spinobulbar neurons and collateralisation**

Following CTb injection into the LRN, labelled cells are predominantly in the ventromedial area of the lumbar spinal cord, with clusters in lamina VII and the reticular portion of lamina V. This pattern fits in well with previous tracer studies in the rat (Chaouch A et al., 1983, Menetrey D et al., 1983, Todd AJ, 2010a) and the cat (Huber J et al., 1999). This labelling occurs, mainly if not exclusively, from the central core of injection because, despite the halo of diffusion to the adjacent structures the results for each LRN injection are quite consistent (Menetrey D et al., 1983). In support of this conclusion it is demonstrated that in animal 1, an injection more dorsal to the LRN yielded a more bilateral distribution of cells, more so in the superficial and deep dorsal horns than ventrally (Figures 3-1, 3-2) (Lima D et al., 1991, Cobos A et al., 2003). In contrast to observations made by Shokunbi et al. (1988), we observed cells labelled in the dorsal horn from injections placed more laterally in the LRN (see also, (Chaouch A et al., 1983, Menetrey D et al., 1983, Lima D et al., 1991). Electrophysiological studies have shown the existence of diffuse noxious inhibitory control (DNIC) pathways that are considered part of the spinoreticular tracts projecting to this area of the LRN (Schmued LC and Fallon JH, 1986, Villanueva L et al., 1986 a, Menetrey D and Basbaum AI, 1987, Janss AJ and Gebhart GF, 1988 ). Furthermore, the lateral part of the LRN is also involved in a descending nocifensive pathway to the superficial dorsal horn that suppresses nociceptive inputs mediated by primary C afferents (Hall JG et al., 1982, Heinricher MM et al., 2009). Our observations that the majority of the retrogradely labelled cells are in the contralateral ventromedial lumbar area, fit well with findings from other tracer studies (Kevetter GA et al., 1982, Chaouch A

et al., 1983, Menetrey D et al., 1983, Garifoli A et al., 2006) as well as with electrophysiological experiments (Grant G et al., 1966, Oscarsson O and Rosén I, 1966, Rosén I and Scheid P, 1973a, Rosén I and Scheid P, 1973b, Clendenin M et al., 1974 b, Alstermark B and Ekerot CF, 2013). In contrast Lima et al (1991) reported a distribution that was predominantly ipsilateral; this difference may be explained by the fact that they considered the cervical and lumbar segments together as cervical segments have more ipsilaterally labelled cells (Menetrey D et al., 1983).

Concerning the existence of spinoreticular neurons collateralizing, to both LRN; Koekkoek and Ruigrok (1995), using non-fluorescent double retrograde tracing techniques, concluded that hardly any spinal neurons project to the LRN bilaterally (~2%) and attributed this minute number to fibres of passage to other reticular nuclei. In contrast, in the present study we found a definite subgroup of SRT cells double labelled from both LRN (~8%). To some extent these findings are confirmed by another fluorescent study by Garifoli et al. (2006), who found that ~7% lumbar SRT cells collateralised to both LRNs as opposed to ~13% in the cervical cord. Even though some of these double labelled cells may be attributed to tracer spread. Although these double labelled cells are found in deep dorsal horn, where neurons projecting to the ventrolateral reticular formation are located, a significant majority is present in the intermediate laminae (Rexed laminae VI, VII) (Lima D et al., 1991, Almeida A et al., 2002). Moreover, more double labelled cells were visualised when the injection site involved more of the parvicellular part of the LRN.

### **3.4.3 Spinoreticular projections to the lateral reticular nucleus**

As shown by our results and data available from studies conducted in various mammals, there are both ipsi- and contralateral projections to the LRN (Rao GS et al., 1969, Clendenin M et al., 1974 b, Hrycyshyn AW and Flumerfelt BA, 1981b, Flumerfelt BA et al., 1982, Blomqvist A and Berkley KJ, 1992, Antonino-Green DM et al., 2002). Not only tract tracing but also degeneration studies, have confirmed the topographical arrangement of these projections and shown that it is dependent on the segments and laminae involved (Flumerfelt BA et al., 1982, Garifoli A et al., 2006). Hence, our findings of lumbar projections predominantly to the contralateral ventrolateral parvicellular part of the LRN

are in agreement with these studies. On the other hand, some of our results are at variance with those obtained by Rajakumar et al. (1992), who did not find any ipsilateral projection from the lumbar grey matter and also none in the caudal LRN. Whereas we observed CTb labelled terminals in the caudal, ~1.21mm of the LRN (the lower three quarters), even though our injections were not as extensive as those of Rajakumar et al. The results of these anterograde experiments, to some extent confirm data described by Garifoli et al. (2006), although we didn't find any significant variation in the terminations of injections centred in either the ventral or dorsal horn. However, we did find that the lumbar projections extended into the most ventromedial edge of the magnocellular LRN (Rajakumar N et al., 1992)(Figure 3-9, 2c). Conversely, electrophysiological experiments have shown monosynaptic responses in LRN neurons distributed throughout the LRN, not only in parvicellular but also magnocellular nuclei (Clendenin M et al., 1974 b). Antonino-Green et al. (2002) demonstrated a locomotor related tract originating bilaterally in the lumbar cord and ending in the ipsilateral LRN by antidromically activating lamina VII SRT neurons on both sides of the lumbar cord via the ventrolateral funiculus (Clendenin M et al., 1974 b, Ekerot CF, 1990c). The LRN neurons respond to specific segmental stimulation as well as convergence neurons from many segments, activated by cervical and lumbar afferents and thus make it harder to interpret the topographical arrangement of these terminals in the LRN in physiological experiments (Rosén I and Scheid P, 1973a, Rosén I and Scheid P, 1973b, Clendenin M et al., 1974 b).

#### **3.4.4 Excitatory and inhibitory terminals in the LRN**

Spinal axons within the LRN predominantly contain markers for glutamate (~80%) but there are a substantial number of terminals (~15%) that contain inhibitory neurotransmitters. In addition, there is no obvious segregation of their termination sites within the LRN. In contrast, Pivetta et al. (2014) using intraspinal viral injections on transgenic mice, found lumbar spinal VGLUT-2 terminals highly restricted to the ventral LRN both ipsi and contralaterally while the inhibitory terminals were confined even further ventromedially, with hardly any overlap. This finding may be as a consequence of the different methodological approaches used or may represent a species difference between

rats and mice. Moreover, there is a more or less equal distribution of inhibitory GAD, GLYT-2 and GAD/GLYT-2 terminals in both ipsi and contralateral LRN.

Ekerot (1990b) provided evidence that electrical stimulation of the ventrolateral quadrant evoked monosynaptic EPSPs and IPSPs in LRN cells and responses indicated that excitatory and inhibitory SRT neurons terminated in overlapping areas. However, Ekerot (1990c) concluded that the bVFRT, which is believed to be the principal pathway projecting from the lumbar cord to the LRN, consisted of roughly equal groups of excitatory and inhibitory neurons.

Inhibitory and excitatory SRT axons form contacts with pre-cerebellar LRN neurons projecting to the anterior lobe of the cerebellum. Looking at the contacts to pre-cerebellar cells we saw that excitatory SRT contacts form a significant proportion (13%) of all excitatory contacts, whereas inhibitory SRT axons constitute only 2% of inhibitory contacts onto these cells. These convergent excitatory and inhibitory contacts on LRN cells are in agreement with Ekerot et al (1990c) but in contrast to Ekerot et al. although we did not observe any cells with purely inhibitory lumbar spinal inputs, we did observe purely excitatory lumbar spinal contacts on LRN cells both ipsi and contralaterally. Although this was observed in just one animal, that may on one hand, represent a biological aberration but on the other hand, it poses an interesting question about the location of inhibitory SRT cells and maybe therefore be a study for possible future works.

It is established that neurons derived from different progenitor domains exhibit distinct intraspinal functions (Alaynick WA et al., 2011, Arber S, 2012, Pivetta C et al., 2014). Subpopulations of projection neurons with distinct intraspinal functions transmit these differences, in synaptic input and output patterns, to the brainstem in a highly organised manner. Our study indicates that there may be three distinct groups of inhibitory systems projecting to the LRN from the spinal cord; an exclusively glycinergic one, a GABAergic one and one that contains a mixture of both transmitters. Pharmacological information on the LRN is apparently very limited but ligand binding, in-situ hybridisation and immunocytochemical studies show that cells of the LRN express GABA and glycine receptors (Araki T et al., 1988, Sato K et al., 1991). However, it is not known how these receptors are organised and whether they are expressed by all LRN neurons or only by a subpopulation of cells. Nevertheless, it is probable that

these subgroups of inhibitory cells exert subtly different effects on their LRN target neurons. In addition to terminals originating from the lumbar spinal cord, pre-cerebellar neurons in the ventral and lateral regions of the LRN have an abundance of excitatory and inhibitory contacts on them. The majority of these are likely to originate from sources outside the nucleus as it is thought that the LRN contains no interneurons (Kapogianis EM et al., 1982a, 1982b).

### **3.4.5 Functional implications**

The spino-bulbar-reticular pathway provides the cerebellum with information that is different and distinct from classical spinocerebellar pathways because, as opposed to the classical pathway, it conveys not only motor but sensory as well as autonomic information. Although it is difficult to show functional aspects of anatomically defined neuronal circuits without any corroborating electrophysiological data, it can safely be said that the present investigation has demonstrated the existence of a substantial projection from the lumbar spinal cord to the LRN in the rat. This spinal projection arises largely from segments concerned with limb innervations and consist of a crossed projection which has been physiologically characterised (Menetrey D et al., 1984). Pre-cerebellar LRN neurons, identified by antidromic stimulation from the cerebellum, are activated by the bilateral ventral flexor reflex tract, bVFRT (Clendenin M et al., 1974 b). This pathway, in the ventral funiculus of the spinal cord, is felt to be equivalent to the anatomically demonstrated spinal projection to the LRN (Lundberg A and Oscarsson O, 1962b).

The bVFRT, in turn, is activated by cutaneous and Gp I, II muscle afferents that participate in limb flexor reflexes, for example withdrawal and SBS, (Eccles JC, 1959a, Hultborn H, 2006). The location of the SRT cells, in the intermediate zone adjacent to the base of the dorsal and ventral horns, places them amongst interneurons that provide connections with flexor reflex afferents as well as neurons in other segments. There is a phenomenon of convergence of inputs at the spinal level; a central pattern generator mechanism, which is seen in the spinal cat that can still step and rhythmically withdraw (Lundberg A and Oscarsson O, 1962b, Menetrey D et al., 1984) and the unique placement of the SRT neurons within this area gives an indication to their possible role in integration at the segmental level. The bVFRT originates from all spinal levels

and has cells of origin that characteristically have large bilateral receptive fields with additional input from the vestibulospinal system (Lundberg A and Oscarsson O, 1962b, Clendenin M et al., 1974 b, Ekerot CF, 1990c, Hultborn H, 2006). For this reason it has been suggested that this pathway is principally involved in the maintenance of posture.

The LRN has been referred to as a 'relay nucleus' but this description is now probably outdated, while the extensive topographical arrangement seen in the LRN, especially of inhibitory contacts, suggests a divergence of inputs there is also a convergence of inputs to the LRN cells. This topographical projection is conserved in the cerebellum (Alstermark B and Ekerot CF, 2013). In addition, the LRN is a complex structure that receives a myriad of inputs from different spinal and supraspinal brain areas. So, why else would the LRN receive such an extensive convergence of inputs, if only to act purely as a relay station? In answer to this, although some LRN cells appear to be components of parallel processing circuits, others receive convergent inputs (Kitai ST et al., 1974a, Kitai ST et al., 1974b) and therefore the LRN also has an integrative function. In the present study only 2% of inhibitory contacts on LRN cells originate from the lumbar spinal cord, and therefore the vast majority of inhibitory contacts would originate from cervical spinal regions or from the brain.

Thus the cerebellum may compare information provided by the classical 'pure lines i.e. the spinocerebellar tracts' from the spinal cord, with information provided via the indirect spino-reticulo-cerebellar pathway with more filtered amalgamated information from the LRN, for it to make more efficient and precise motor adjustments to maintain normal posture during locomotion and for the adjustment of motor programmes to compensate for injury and pain.

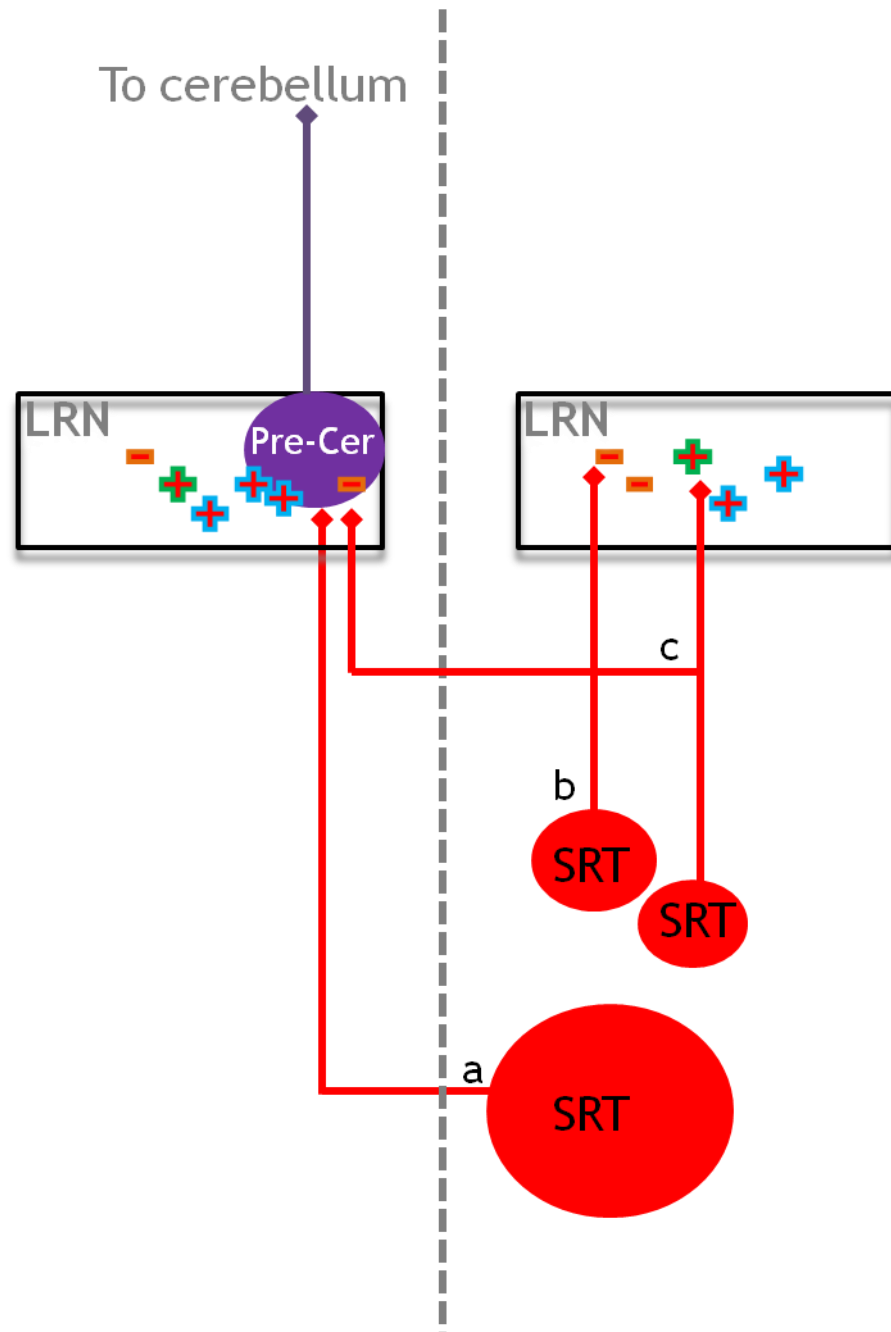


**Figure 3-15 Summary of the ascending projections of spinothalamic neurons**

Red circles represent spinothalamic cells (SRT) in the contralateral spinal cord (dotted grey line represents the midline) that project to the LRN: a) contralaterally (larger red circle); b) ipsilaterally; and c) bilaterally (red lines and diamonds). The purple circle represents pre-cerebellar cells (Pre-Cer) in the lateral reticular nucleus (LRN). The red positive signs, outlined in blue, indicate the percentage of VGLUT-2 SRT terminals in the LRN and the orange hyphens indicate the percentage of inhibitory SRT terminals. The positive signs, outlined in green, indicate the percentage of VGLUT-1 SRT terminals.

# Chapter 4

## **4 The descending pathway; origin of bulbospinal neurons projecting via the caudal ventro-lateral medulla (CVLM) and medial longitudinal fasciculus (MLF) to the rat lumbar spinal cord.**

### **4.1 Introduction**

Classical anatomical studies using degeneration techniques have demonstrated fibres passing from the reticular formation of the brainstem to the spinal cord and classified them according to their termination pattern within the spinal cord as medial (mReST) and lateral reticulospinal (lReST) systems (Kuypers HGJM et al., 1962, Nyberg-Hansen R, 1965). According to these studies there are two maximal areas of origin for these tracts: the pontine nuclei for the mReST; and the medullary part of the gigantocellular reticular nucleus (Gi) plus the ventral medullary reticular nucleus (MdV) for the lReST. Advances in autoradiographic tract tracing and particularly retrograde neuronal double labelling techniques have shown that other areas of the brainstem reticular formation also project to the spinal cord, for example the raphe nuclei and adjacent ventromedial medulla (Basbaum AI et al., 1978, Peterson BW et al., 1978, Peterson BW, 1979a, Peterson BW et al., 1979b, Holstege JC, 1996a, Reed WR et al., 2008, Liang H et al., 2011) as well as the LRN (Janss AJ and Gebhart GF, 1988, Rong-Huan L et al., 1990). It thus becomes more complicated to group all these descending bulbospinal pathways either as medial or lateral ReST. In addition, many axons in the central nervous system give off axon collaterals along their trajectory through the brain (Carlton SM et al., 1985).

Hence, the bulbospinal system is defined as a series of heterogeneous pathways originating from various areas of the brainstem and projecting to the spinal cord via tracts in the medulla; the MLF and CVLM including the LRN (Holstege JC, 1996a). These pathways influence a variety of spinal networks including those involved in motor control, sensory inputs (noxious and innocuous) and autonomic function. Anatomically, not only do their terminal distributions determine their functional capacities but their origin in the brainstem also plays a role in co-

ordinating the activity of spinal networks involved in these processes (Holstege JC, 1996a, Tavares I and Lima D, 2002). The MLF contains axons principally involved in motor control (Jankowska E and Stecina K, 2007) whereas axonal systems in the CVLM play a role in sensory and autonomic control along with motor activity (Tavares I and Lima D, 2002). In addition, bulbospinal neurons are influenced by higher motor cortical centres via the mesencephalic locomotor system (Prentice Sd DT, 2001, Matsuyama K et al., 2004, Jordan LM et al., 2008) and have complex effects on posture and reaching (Prentice Sd DT, 2001, Riddle CN et al., 2009). Individual axons from these neurons give off collaterals that terminate at different segmental levels thus influencing wide areas of the spinal grey matter, while integrating common neuronal elements in order to produce a variety of co-ordinated motor patterns (Peterson BW et al., 1978, Takakusaki K et al., 2001, Jordan LM et al., 2008).

Although a number of studies have documented the origin of BS cells within structures of the rat brainstem, the exact locations of the cells that project via the MLF or the CVLM are largely unknown (Hossaini M et al., 2012). Moreover, these bulbospinal trajectories to spinal neurons are predominantly excitatory (Janss AJ and Gebhart GF, 1988, Hossaini M et al., 2012) but there is an element of inhibition, as shown by electrophysiological (Takakusaki K et al., 2001, Matsuyama K et al., 2004) as well as anatomical evidence (Holstege JC, 1996a, Du Beau A et al., 2012, Hossaini M et al., 2012, Huma Z et al., 2014). Studies have shown that these BS terminals in the spinal cord not only contain excitatory (glutamate) and inhibitory (GABA/glycine) neurotransmitters but also contain monoamines as well as peptides (Bowker RM and Abbott LC, 1990, Du Beau A et al., 2012, Huma Z et al., 2014). Previous work in our lab has shown both excitatory and inhibitory components of bulbospinal paths projecting specifically via the MLF and CVLM (Du Beau A et al., 2012, Huma Z et al., 2014). The termination pattern of these BS neurons on specific target populations would help to define the functional aspect of these tracts. As spinoreticular neurons are distributed within the same areas as BS terminals in the medial intermediate grey matter, we hypothesise that these SRT cells would receive monosynaptic contacts from the BS system. The descending input to SRT cells, by facilitating or depressing specific actions, would modify behaviour in the form of readjustments to posture and bulbospinal reflexes.

Thus, the aims of the present study were twofold:

- Our primary aim was to determine the locations of the neurons that give rise to BS pathways via the LRN and the CVLM; and
- The secondary aim was to determine the neurotransmitter phenotypes of the bulbospinal projections via the CVLM that form contacts with spinoreticular cells in the lumbar spinal cord.

In order to fulfil the first aim we used a retrograde double labelling technique by exploiting the propensity of CTb to be taken up by axons of passage; in order to label cells in the brainstem structures, we injected CTb into MLF or CVLM and FG into the intermediate grey of the lumbar spinal cord. To fulfil the second aim, double labelling was again used but on this occasion FG was injected into the CVLM (targeting the LRN) retrogradely labelling spinoreticular cells, and CTb into the opposite CVLM to anterogradely label bulbospinal terminals in the lumbar spinal cord. In addition, immunohistochemistry was used to label excitatory and inhibitory BS terminals ([Tables 4-1 & 4-2](#)).

## 4.2 Materials and Methods

This part of the study investigates descending bulbospinal pathways, specifically pathways projecting via the CVLM and the MLF and the neurotransmitter phenotypes contained within CVLM axons contacting spinoreticular cells in the lumbar spinal cord. Nine adult male Sprague-Dawley rats (Harlan, Bicester, UK), weighing between 250-350gm, were deeply anaesthetised with Isoflurane and underwent surgery, following the procedures outlined in detail in General Experimental Procedures ([Chapter 2, Section 2.1](#)). There was some variation in the techniques applied and these are explained in detail below. Experiments were approved by the Ethical Review Process Applications Panel of the University of Glasgow and were performed in accordance with the UK Animals (Scientific Procedures) Act 1986.

### 4.2.1 Surgical procedures

#### *Spinally projecting cells via CVLM and MLF*

In the first group of three animals (n=3), 1% CTb (200nl) was pressure injected with a Pico injector (10 ms pulses at 20 psi; World Precision Instruments, Sarasota, USA) into the right CVLM (LRN), following the procedures explained in [Chapters 2 and 3](#). The stereotaxic coordinates for the injection were antero-posterior -4.8mm, medio-lateral -1.8mm and dorso-ventral -0.4mm. In the second group of animals (n=3) CTb was injected into the MLF at co-ordinates; antero-posterior -3.8mm, medio-lateral -0.1mm and +0.8mm dorso-ventral. The animals recovered and after a gap of two days were re-anaesthetised and placed in a stereotaxic frame for spinal fixation. 50nl of 4 % fluorogold (50nl, Fluorochrome, LLC, USA) a retrograde tracer primarily taken up by axon terminals, was injected into the lumbar spinal cord on the right side, to retrogradely label cells in the brain (for further details see [Chapter 3, Section 3.2.3](#)). The images in [Figures 4-1 and 4-2](#) show CVLM and MLF injection sites visualised by DAB immunoreactivity and fluorescent images of FG injection sites in the lumbar spinal cords of the same animals.

### *Transmitter phenotypes of bulbospinal contacts on spinoreticular cells*

In this set of experiments two tracers CTb and FG were injected into the left and right LRN, respectively, of three adult male Sprague-Dawley rats, to retrogradely label SRT neurons in the lumbar spinal cord (FG) and also to anterogradely label the bulbospinal contacts (CTb) on these cells. The details of the surgical procedures, dissection of the brain and spinal cord and identification of the injection sites using DAB as chromogen and ultraviolet light to detect the presence of fluorogold is explained in [Chapters 2 and 3, section 3.2.2](#) and illustrated in [Figure 3-5, Chapter 3](#).

## **4.2.2 Immunocytochemistry, confocal microscopy and analysis**

### *Spinally projecting cells via CVLM and MLF*

To examine spinally projecting cells via the CVLM and MLF, the brainstem was divided into the medulla, pons and midbrain at the medullary-pontine junction and at a level just inferior to the inferior colliculi, in the coronal plane. Sections of 50µm thickness from these areas were sequentially collected into five bottles, and one bottle each from these areas was chosen randomly. These sections were then reacted with solutions of primary antibodies for 48 hours to identify CTb and FG (See [Table 4-1](#) for details). Subsequently, they were incubated in secondary antibodies coupled to fluorophores for 3 hours and mounted on glass slides with anti-fade medium. Transmitted light images of all incubated sections were taken, using a x1 lens (AxioVision 4.8 software Carl Zeiss, Inc, Germany), to identify the various levels of the brainstem in relation to the stereotaxic rat brain atlas of Paxinos & Watson (2005). These were then superimposed onto relevant brain maps using Adobe Photoshop. This formed the basis for plotting double labelled CTb and FG cells throughout the brainstem. Sections were then scanned with a confocal microscope (LSM 710, Zeiss, Germany). Reticulospinal cells were identified by the presence of FG whereas cells with axons passing through the MLF or CVLM were identified by the presence of CTb and cells containing both FG and CTb were identified as bulbospinal cells with axons passing through CVLM or MLF (magnification x20, at z-steps of 1µm intervals). These scans were analysed with Neurolucida for Confocal software (Microbrightfield Inc, USA) in order to estimate numbers of cells contained within brainstem structures. A counting grid with box size of 100 x 100µm was

placed and the labelled neuron (CTb, FG or both CTb/ FG labelled) nearest the lower right hand corner of the box was marked, for the two groups of animals.

The tracings, together with the images, were then exported into Adobe Photoshop and plotted onto brain maps (Paxinos G and Watson C, 2005) to give the exact location of double labelled cells that have connections to both LRN and lumbar spinal cord. The cell counts are shown as an average number of double labelled cells per structure, both ipsilateral and contralateral, to the spinal injection for the animals in each group. An exception was made for cells in midline structures, such as the raphe nuclei and MLF, where data from both sides were pooled.

#### *Transmitter phenotypes of bulbospinal contacts on spinoreticular cells*

Three sections from lumbar segments L3, 4 and 5 were incubated in primary antibodies. FG was used to reveal the spinoreticular cells and CTb to visualise ReST terminals. In addition to this, to identify the proportion of excitatory and inhibitory contacts to these cells, sections were incubated in antibodies for VGLUT-2 and VGAT. Five fluorogold labelled cells each, in the deep dorsal laminae; the intermediate laminae and lamina X were randomly selected for each animal (~fifteen cells per animal). After the immunoreactions (Table 4-2) they were scanned with four channels of a confocal microscope (LSM 710, Zeiss, Germany) at a magnification of x40. ReST terminals were identified by the presence of CTb in them and labelled as inhibitory by the presence of VGAT (Av-Pacific blue) or excitatory by the presence of VGLUT-2 (Dylight 649). A summary of the primary and secondary antibodies used along with their concentrations is given in Table 4-2. Somata and dendrites were reconstructed and CTb contacts were indicated by markers. Subsequently contacts were examined for VGLUT-2 and VGAT immunoreactivity to determine which of the ReST contacts were excitatory or inhibitory. Contact density/ $100\mu\text{m}^2$  was then calculated.

#### **4.2.3 Statistical analysis**

Cell counts for the spinally projecting cells via the CVLM and MLF injections are presented as averaged percentages of double labelled cells per structure for the three animals in each group (mean%±SD). This was done for cells contralateral and ipsilateral to spinal injections with the exception of cells within midline

structures, such as raphe nuclei or the MLF, where data on both sides were pooled. In case of the bulbospinal terminals projecting to spinoreticular cells data are expressed as mean  $\pm$  standard deviation (SD). Multi-group comparisons were made by analysis of variance (ANOVA) followed by a post hoc *Tukey's* analysis as appropriate (GraphPad Prism version 6.02, GraphPad Software, La Jolla California USA). A  $p < 0.05$  was considered to be statistically significant.

**Table 4-1 Summary of primary and secondary antibody combinations and concentrations in the analysis of spinally projecting cells via the CVLM and MLF (n=6)**

Primary antibody combination	Primary antibody concentration	Supplier	Secondary antibody combination	Secondary antibody concentration	Supplier
gt CTb	1:5000	List(Quadrantech) Campbell, USA	Rh. Red	1:100	Jackson Immunoresearch, West Grove, USA
gp FG	1:500	Protos, Biotech, New York, USA	Alexa 488	1:500	Jackson Immunoresearch, West Grove, USA
<sup>2</sup> rbt FG	1:5000	Chemicon/ Millipore, CA, USA	Alexa 488	1:500	Jackson Immunoresearch, West Grove, USA

All secondary antibodies were raised in donkey and conjugated to Rh. Red, Rhodamine Red; Alexa 488, Alexa-fluor 488; gp, guinea pig; rbt, rabbit; gt, goat; CTb, b- subunit of cholera toxin; FG, fluorogold.

<sup>2</sup> Initially gp FG was used, however subsequently, rbt FG was used because it was noticed that rbt FG had the same immunostaining as gp FG and could therefore be used at a lower concentration.

**Table 4-2 Summary of the primary and secondary antibody concentrations and combinations used in the bulbospinal contacts to the spinoreticular cells (n=3)**

Primary antibody combination	Primary antibody concentration	Supplier	Secondary antibody combination	Secondary antibody concentration	Supplier
gt CTb	1:5000	List, Quadratech, Campbell, USA	Rh. Red	1:100	Jackson Immunoresearch, West Grove, USA
gp FG	1:500	Protos, Biotech, New York, USA	Alexa 488	1:500	Jackson Immunoresearch
rbt VGLUT-2	1:5000	Synaptic systems, Göttingen, Germany	Dylight 649	1:500	Jackson Immunoresearch
mo VGAT	1:1000	Synaptic Systems, Göttingen, Germany	IgG Biotin Av-pacific blue	1:500 1:1000	Jackson Immunoresearch Molecular probes, Eugene, USA

All secondary antibodies were raised in donkey and conjugated to Rh. Red, Rhodamine Red; Alexa 488, Alexa-fluor 488; gp, guinea pig; rbt, rabbit; gt, goat; mo, mouse; CTb, b- subunit of cholera toxin; FG, fluorogold; VGLUT-2, vesicular glutamate transporter; VGAT, vesicular GABA transporter.

## 4.3 Results

### 4.3.1 Spinally projecting cells via CVLM and MLF

#### *Injection sites*

The CTb injection into the CVLM was targeted on the LRN but there was spread into the surrounding reticular tissue, the gigantocellular reticular, the ventral medullary, parvicellular and the intermediate reticular nuclei. The rostro-caudal spread was  $\pm 0.65\text{mm}$  on average from the injection site (Figure 4-1A). The MLF injections as seen in Figure 4-2A, were directed to the right side but there was spread to the left side as well because the MLF is a midline structure. There was some spread into the raphe obscurus and the tectospinal tract with a rostro-caudal extent of  $\pm 1.38\text{mm}$ .

Fluorogold injections into the lumbar spinal cord were more or less confined to L1 and L2, with the injection centred in the intermediate grey area and spread confined to the right side of the cord with no spread to the opposite side (Figures 4-1B & 4-2 B). The rostro-caudal spread was  $\pm 0.27\text{mm}$  on each side of the lumbar spinal injection.

#### *Distribution of cells in the brainstem*

Double labelled cells were found throughout the brainstem for both CVLM and MLF injections (Figures 4-3 & 4-4). For CVLM injections ~80% of all double labelled cells were found within the medulla whereas in case of MLF injections ~66% of the double-labelled cells were found within medulla; the pons having relatively higher numbers of double labelled cells as compared to the CVLM injections (Figures 4-5 & 4-6). Small numbers of additional cells were found in the midbrain (Figure 4-6, 35 out of a total of 1103 double labelled cells) in CVLM and even fewer for MLF injections (26 out of 743). For CVLM injections the average percentage ( $\pm\text{SD}$ ) of double labelled cells in the medulla out of all labelled spinal projecting cells for the three animals was  $40.1\pm 4.04\%$  (1037 out of 2523 in total for all 3 animals) and the equivalent value for MLF injections was  $37.3\pm 6.2\%$  (489 out of 1370 cells in total ). In each experiment there were some variations in the distribution or number of cells because of inevitable differences in brainstem and spinal injections but there was a consistency in the cellular

distribution across animals in each experimental group. [Table 4-3](#) shows a full list of structures in the medulla, pons and midbrain that contained double labelled cells. These numbers are the mean percentages for the three animals per structure.

### *Medulla*

[Figure 4-5](#) shows some representative plots of cells at various levels in the medulla for CVLM and MLF injections. In CVLM injections, the majority of double labelled cells were found ipsilateral to the spinal injection ( $44.6 \pm 5.7\%$ ) as compared to  $33.32 \pm 2.07\%$  on the contralateral side. Double-labelled cells following MLF injections were also found predominantly ipsilateral to spinal injections ( $48.7 \pm 8.5$  ipsilateral to  $16.9 \pm 8.14$  contralateral). The greatest number of cells in both experiments, in descending order was found in the gigantocellular reticular nucleus (Gi), the inferior olivary complex (IO), the lateral paragigantocellular reticular nucleus (LPGi), dorsal medullary reticular nucleus (MdD) and the medial longitudinal fasciculus (MLF) on both the ipsilateral and contralateral sides. In addition the raphe pallidus (RPa) and the raphe magnus and obscurus (RMg, ROb) had double labelled cells following CVLM as well as MLF injections. Smaller numbers of cells were noted in a variety of other structures, including the nucleus of the solitary tract (sol), the lateral periaqueductal grey (LPAG) and the medial vestibular nucleus (MVe) ([Table 4-3](#)). Double labelled cells following CVLM injections were present in many of the same structures observed for the MLF except that many more cells were located within the LPGi and the RPa than were found for MLF injections, with additional cells in sol and MVe along with the facial nucleus (7n), the trigeminal nucleus (5n) and the lateral reticular nucleus (LRt).

### *Pons*

Pontine cell distributions are shown in [Figures 4-4 & 4-6](#). The majority of double-labelled cells in CVLM injections were found contralateral to spinal injections ( $40.9 \pm 14.4\%$  versus  $53.3 \pm 3.7\%$ ) in contrast with MLF injections where most of the double labelled cells were ipsilateral ( $44.6 \pm 14\%$  vs.  $33.8 \pm 14.8\%$  contralateral). Most of the cells in both groups were in both the oral and caudal regions of the pontine reticular nucleus, (PnO and PnC). For MLF injections cells were also observed in the deep mesencephalic nucleus (DpMe), the reticulotegmental

nucleus (RtTg) and the pedunculopontine tegmental nucleus (PPTg) and for CVLM injections cells were found in the dorsal subcoeruleus (subCD). Full details of other structures containing double labelled cells are given in [Table 4-3](#).

### *Midbrain*

Small numbers of double-labelled cells were found in the midbrain ([Figure 4-5](#)). For CVLM injections (35 out of 1103), they were concentrated in two areas: the parabrachial nucleus (PaR) and parabrachial pigmented nucleus of the ventral tegmental area (PbP). The only midbrain region containing cells, following MLF injections was the ventrolateral periaqueductal grey (VLPAG) with even fewer cells (26 out of 743). Although there were so few spinally projecting cells, most of them were double labelled (~97% in CVLM injections and ~71% in MLF injections).

## **4.3.2 Bulbospinal contacts on spinoreticular cells**

### *Injection sites*

[Figure 3-5](#) in Chapter 3 shows that the injection sites in the CVLM are mainly targeted at the LRN. Reconstructions of the injection site for CTb and FG are shown in [Figure 3-5 \(5, 6 & 8\)](#). There is diffusion of both CTb and FG into the adjacent reticular structures including the gigantocellular reticular nucleus (Gi), the intermediate reticular (IRt) and the ventral part of the medullary reticular nucleus (MdV).

In order to establish contacts to spinoreticular cells via the CVLM, a combination of tract tracing was used; to label spinoreticular cells and bulbospinal terminals and immunohistochemistry, utilizing VGAT and VGLUT-2, to find out whether these contacts were inhibitory or excitatory. A total of 46, retrogradely labelled cells in three animals, ([Table 4-4 & 4-5](#)) were analysed for contacts from the BS tract with ~5cells per area (deep dorsal, intermediate and Lamina X). As the confocal image in [Figure 4-7](#) illustrates there is sparse input from the bulbospinal pathway via the CVLM onto these cells.

Quantitative analysis revealed that 2-3% of all excitatory and inhibitory contacts to the SRT cells are from descending fibres from the CVLM ([Table 4-5; Figure 4-](#)

7). However, no inhibitory reticulospinal terminals contacting the soma of spinoreticular neurons were observed in the intermediate laminae (Table 4-4).

Average contact densities of excitatory and inhibitory bulbospinal terminals to retrogradely labelled SRT cells were  $0.08 \pm 0.07$  and  $0.03 \pm 0.04$  (mean  $\pm$  SD/100  $\mu\text{m}^2$ , Sholl analysis), respectively (Table 4-4). Most of the BS terminals are excitatory (VGLUT-2) ~56%, as compared to ~17% inhibitory (VGAT) but with ~27% neither VGLUT-2 nor VGAT immunoreactive (Table 4-4, Figure 4-8).

Table 4-5 illustrates all CTb contacts i.e. BS in comparison with VGAT and VGLUT-2 contacts from other sources. The contact densities of the CTb terminals are significantly lower than from the other sources,  $0.16 \pm 0.14$  (mean  $\pm$  SD, Anova,  $**p < 0.01$ , post hoc *Tukey's*) as compared to VGAT,  $3.11 \pm 0.77$  and; VGLUT2,  $2.93 \pm 0.74$  contact densities/100  $\mu\text{m}^2$ .

**Table 4-3 Double labelled cells in the various areas of the brainstem following fluorogold injections into the right lumbar cord and injections of cholera toxin in the MLF or right CVLM**

The values show averaged counts per structure for each of the three animals in MLF and CVLM experiments. Ipsilateral and contralateral sides are in respect to the spinal injection sites.

5n, trigeminal nucleus; 7n, facial nucleus; CIC, central nucleus of the inferior colliculus; Cu, cuneate nucleus; DpMe, deep mesencephalic nucleus; Gi, gigantocellular reticular nucleus; IO, inferior olive; IRt, intermediate reticular nucleus,; LDTg, latero-dorsal tegmental nucleus; LPAG, lateral periaqueductal grey; LPGi, lateral paragigantocellular nucleus; LRt, lateral reticular nucleus; MdV, medullary reticular nucleus; Mlf, medial longitudinal fasciculus; MVe, medial vestibular nucleus, MVPO, medio-ventral periolivary nucleus; PaR, parabrachial nucleus; PBP, parabrachial pigmented nucleus of the VTA; PCRt, parvicellular reticular nucleus; PnC, pontine reticular nucleus, caudal part; PnO, pontine reticular nucleus, oral part; PPTg, pedunculo-pontine tegmental nucleus; PPy, parapyramidal nucleus; RMg, raphe magnus nucleus; ROb, raphe obscurus nucleus, RPa, raphe pallidus nucleus; RR, retrorubral nucleus; RtTg, reticulotegmental nucleus; Sol, nucleus of the solitary tract; SPO, superior paraolivary nucleus; SPTg, subpeduncular tegmental nucleus; subCD, subcoeruleus nucleus; tz, trapezoid body; VLPAG, ventrolateral periaqueductal grey.

	MLF		CVLM	
	Ipsilateral	Contralateral	Ipsilateral	Contralateral
<b>MEDULLA</b>				
Gi	69.7	6.7	52.7	41.7
IO	7.7	18.3	37.7	20.0
LPGi	0.0	1.0	24.7	12.7
MdD	7.3	0.0	22.0	8.3
mlf	17.0		16.3	
5n	0.3	0.0	4.3	4.3
7n	0.0	0.0	6.0	2.7
RMg	14.3		13.3	
RoB	3.3		14.3	
Rpa	0.0		20.0	
RR	2.7	0.0	0.0	0.0
Cu	0.0	0.0	0.0	0.7
LPAG	0.0	0.0	0.3	0.0
LRt	0.0	0.0	5.3	0.0
MVe	9.3	0.0	3.0	5.0
PPy	0.0	0.0	1.3	1.3
Sol	0.0	6.3	0.7	4.7
SPO	0.0	0.0	3.0	1.0
<b>PONS</b>				
PnO	16.0	13.0	13.3	6.3
PnC	13.0	2.0	4.0	7.5
subCD	0.0	0.0	5.7	7.3
DpMe	2.7	10.7	0.0	0.0
IRt	0.0	1.3	5.3	0.0
MVPO	0.0	0.0	1.3	0.3
PCRt	0.0	0.0	0.7	2.3
LDTg	2.0	0.0	0.0	0.0
RtTg	6.0	0.0	0.0	0.0
SPTg	2.0	1.0	0.0	0.0
PPTg	6.0	0.3	6.0	2.7
tz	0.0	0.0	1.0	1.7
<b>MIDBRAIN</b>				
PaR	0.0	0.0	1.3	0.3
PBP	0.0	0.0	8.5	0.0
CIC	0.0	0.0	0.0	4.3
VLPAG	1.3	7.3	0.0	0.0

Table 4-4 Bulbospinal contact densities (CTb) on fluorogold (FG) labelled SRT neurons for excitatory VGLUT2 (VG2) and inhibitory VGAT immunoreactive terminals (n=3)

Animal	No. of cells	Soma									Dendrite								
		Total contacts			Contacts			Surface area ( $\mu\text{m}^2$ )	Density			Contacts			Surface area ( $\mu\text{m}^2$ )	Density			
		soma and dendrites			(n)				(n/ 100 $\mu\text{m}^2$ )			(n)				(n/ 100 $\mu\text{m}^2$ )			
		CTb/VGAT	CTb	CTb/VG2	CTb/VGAT	CTb	CTb/VG2	CTb/VGAT	CTb	CTb/VG2	CTb/VGAT	CTb	CTb/VG2	CTb/VGAT	CTb	CTb/VG2	CTb/VGAT	CTb	CTb/VG2
<b>Lamina X</b>	1	4	0	4	4	0	3	0	5594.99	0.00	0.05	0.00	0	1	4	7223.30	0.00	0.01	0.06
	2	5	5	25	41	7	7	15	5524.69	0.13	0.13	0.27	1	19	28	12399.36	0.01	0.15	0.00
	3	5	2	4	12	1	1	0	6654.23	0.02	0.02	0.00	1	3	13	13317.19	0.01	0.02	0.10
<b>Mean</b>										<b>0.05</b>	<b>0.07</b>	<b>0.09</b>					<b>0.01</b>	<b>0.06</b>	<b>0.01</b>
<b>SD</b>										<b>0.07</b>	<b>0.06</b>	<b>0.16</b>					<b>0.00</b>	<b>0.08</b>	<b>0.00</b>
<b>Intermediate</b>																			
<b>Laminae</b>	1	5	1	1	19	0	0	0	6283.10	0.00	0.00	0.00	1	1	17	13806.82	0.01	0.01	0.12
	2	5	10	10	41	0	3	7	8281.86	0.00	0.04	0.08	9	7	37	19045.35	0.05	0.04	0.19
	3	5	2	6	7	0	3	1	14054.41	0.00	0.02	0.01	2	3	12	28068.90	0.01	0.01	0.04
<b>Mean</b>										<b>0.00</b>	<b>0.02</b>	<b>0.03</b>					<b>0.02</b>	<b>0.02</b>	<b>0.12</b>
<b>SD</b>											<b>0.02</b>	<b>0.05</b>					<b>0.02</b>	<b>0.02</b>	<b>0.06</b>
<b>Deep Dorsal</b>																			
<b>Laminae</b>	1	5	6	12	26	3	1	6	10969.94	0.03	0.01	0.05	3	11	20	24763.38	0.01	0.04	0.08
	2	6	67	58	71	12	15	16	9968.83	0.12	0.15	0.16	49	40	60	41468.17	0.12	0.10	0.14
	3	6	2	7	2	2	2	0	7689.56	0.03	0.03	0.00	0	6	2	20967.78	0.00	0.03	0.01
<b>Mean</b>										<b>0.06</b>	<b>0.06</b>	<b>0.07</b>					<b>0.04</b>	<b>0.06</b>	<b>0.08</b>
<b>SD</b>										<b>0.05</b>	<b>0.08</b>	<b>0.08</b>					<b>0.07</b>	<b>0.04</b>	<b>0.07</b>

Table 4-5 Total Bulbosspinal (BS), VGAT and VGLUT2 (VG2) contacts on retrogradely labelled spinoreticular cells (n=3)

Animal	No. of cells	Soma									Dendrite								
		Total contacts			Contacts			Surface area ( $\mu\text{m}^2$ )	Density			Contacts			Surface area ( $\mu\text{m}^2$ )	Density			
		VGAT	VG2	BS	VGAT	VG2	BS		(n/ 100 $\mu\text{m}^2$ )	VGAT	VG2	BS	VGAT	VG2		BS	VGAT	VG2	BS
<b>Lamina X</b>																			
1	4	393	400	8	127	157	3	5594.99	2.27	2.81	0.05	266	243	5	7223.30	3.68	3.36	0.07	
2	5	697	689	71	195	195	29	5524.69	3.53	3.53	0.52	505	509	48	12399.36	4.07	4.11	0.39	
3	5	505	705	18	139	190	2	6654.23	2.09	2.86	0.03	393	551	17	13317.19	2.95	4.14	0.13	
<b>Mean</b>									<b>2.63</b>	<b>3.06</b>	<b>0.20</b>					<b>3.57</b>	<b>3.87</b>	<b>0.19</b>	
<b>SD</b>									<b>0.78</b>	<b>0.40</b>	<b>0.28</b>					<b>0.57</b>	<b>0.44</b>	<b>0.17</b>	
<b>Intermediate</b>																			
<b>Laminae</b>																			
1	5	515	459	21	126	119	0	6283.10	2.01	1.89	0.00	389	338	19	13806.82	2.82	2.45	0.14	
2	5	1155	896	61	251	201	10	8281.86	3.03	2.43	0.12	927	731	53	19045.35	4.87	3.84	0.28	
3	5	1051	738	15	402	189	4	14054.41	2.86	1.34	0.03	649	549	17	28068.90	2.31	1.96	0.06	
<b>Mean</b>									<b>2.63</b>	<b>1.89</b>	<b>0.05</b>					<b>3.33</b>	<b>2.75</b>	<b>0.16</b>	
<b>SD</b>									<b>0.55</b>	<b>0.54</b>	<b>0.06</b>					<b>1.35</b>	<b>0.98</b>	<b>0.11</b>	
<b>Deep Dorsal</b>																			
<b>Laminae</b>																			
1	5	781	902	44	188	182	10	10969.94	1.71	1.66	0.09	593	720	34	24763.38	2.39	2.91	0.14	
2	6	2109	1928	196	358	384	43	9968.83	3.59	3.85	0.43	1678	1547	149	41468.17	4.05	3.73	0.36	
3	6	832	662	11	302	234	4	7689.56	3.93	3.04	0.05	699	583	8	20967.78	3.33	2.78	0.04	
<b>Mean</b>									<b>3.08</b>	<b>2.85</b>	<b>0.19</b>					<b>3.26</b>	<b>3.14</b>	<b>0.18</b>	
<b>SD</b>									<b>1.19</b>	<b>1.11</b>	<b>0.21</b>					<b>0.83</b>	<b>0.52</b>	<b>0.16</b>	

**Figure 4-1 CTb injections into the caudal ventrolateral medulla (CVLM, LRt) and fluorogold injections into the ipsilateral lumbar spinal cord of the same animals**

**A.** A representative DAB reacted medullary section showing the CTb injection site in the LRN which extends into other CVLM structures (black arrow).

**1, 2, 3** These are drawings of the injection sites (dark grey) with spread (light grey) for each experimental animal on representative maps of the medulla (Paxinos & Watson, 2005).

**B.** A fluorescent/dark field micrograph showing a fluorogold injection site within a transverse section of the lumbar spinal cord (white arrow).

**1, 2, 3** Drawings of the core (black) and spread (grey) of fluorogold within the intermediate laminae on the ipsilateral side (based on Paxinos & Watson, 2005) for each animal. Gi, gigantocellular reticular nucleus; LRt, lateral reticular nucleus; MdV, ventral medullary reticular nucleus; IRt, intermediate reticular nucleus; PCRt, parvicellular reticular nucleus.

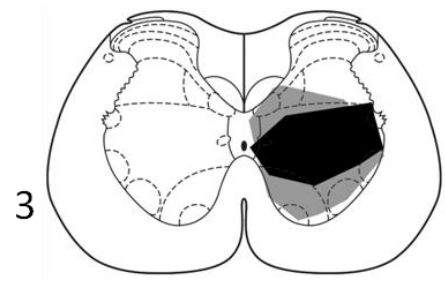
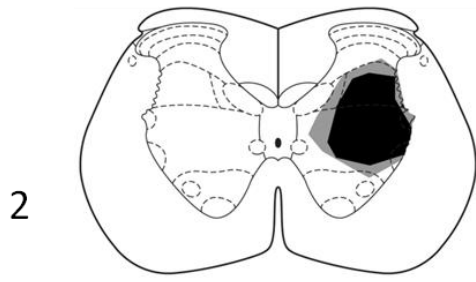
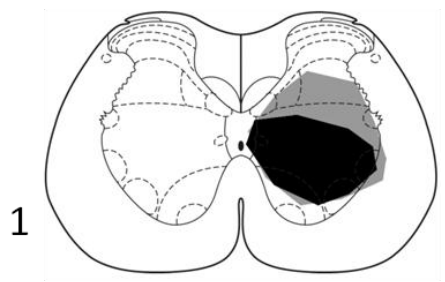
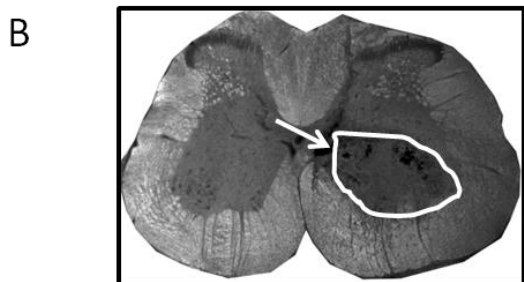
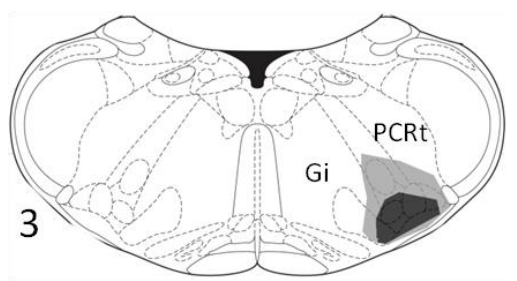
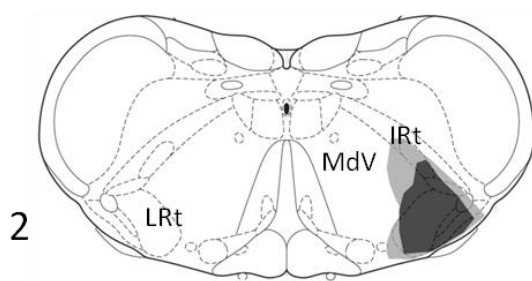
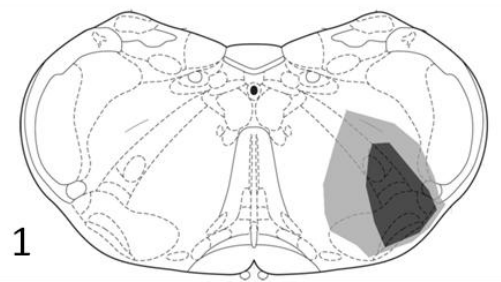


**Figure 4-2 CTb injection into the medial longitudinal fasciculus (MLF) and fluorogold injections into the lumbar spinal cord of the same animal**

**A.** A representative DAB reacted medullary section showing the CTb injection site in the MLF along with diffusion into the raphe obscuris and gigantocellularis (black arrow).

**(1, 2, 3)** Drawings of the core of the injection site (dark grey) with spread (light grey) onto maps of the medulla (Paxinos & Watson, 2005) for each animal.

**B.** A fluorescence micrograph showing a fluorogold injection site within a transverse section of the lumbar spinal cord (white arrow).

**(1, 2, 3)** Drawings of the core (black) and spread (grey) of fluorogold within the intermediate laminae (based on Paxinos & Watson, 2005) for each animal.

ROb, raphe obscurus; mlf, medial longitudinal fasciculus.

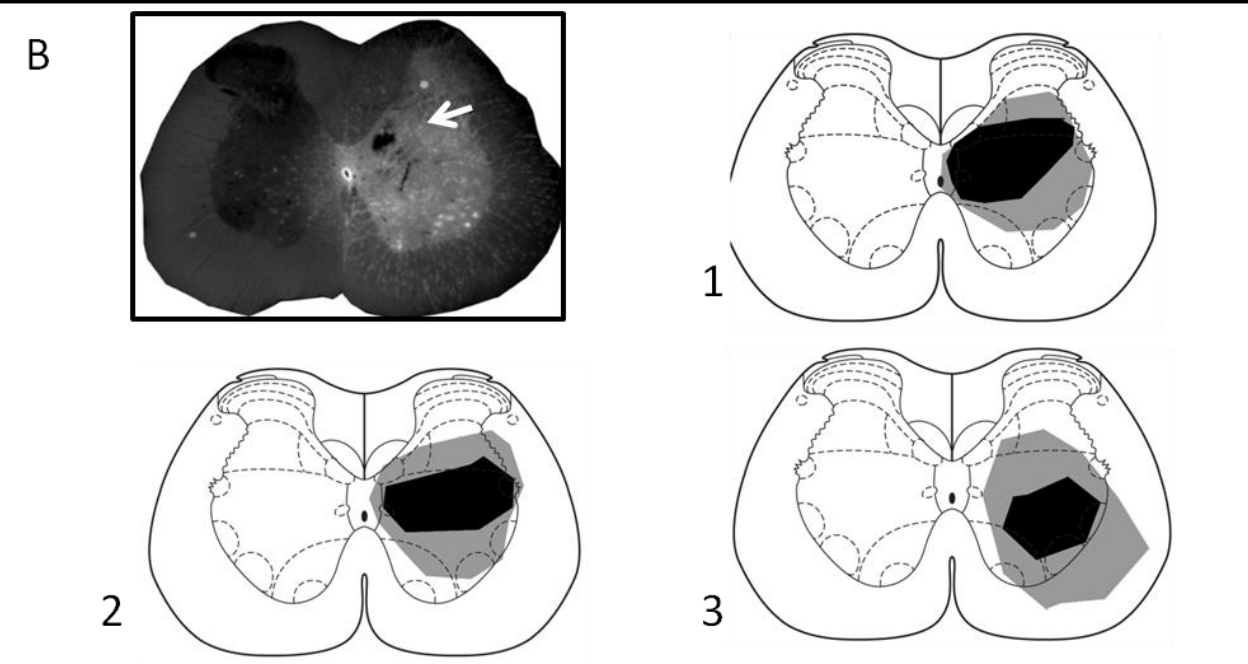
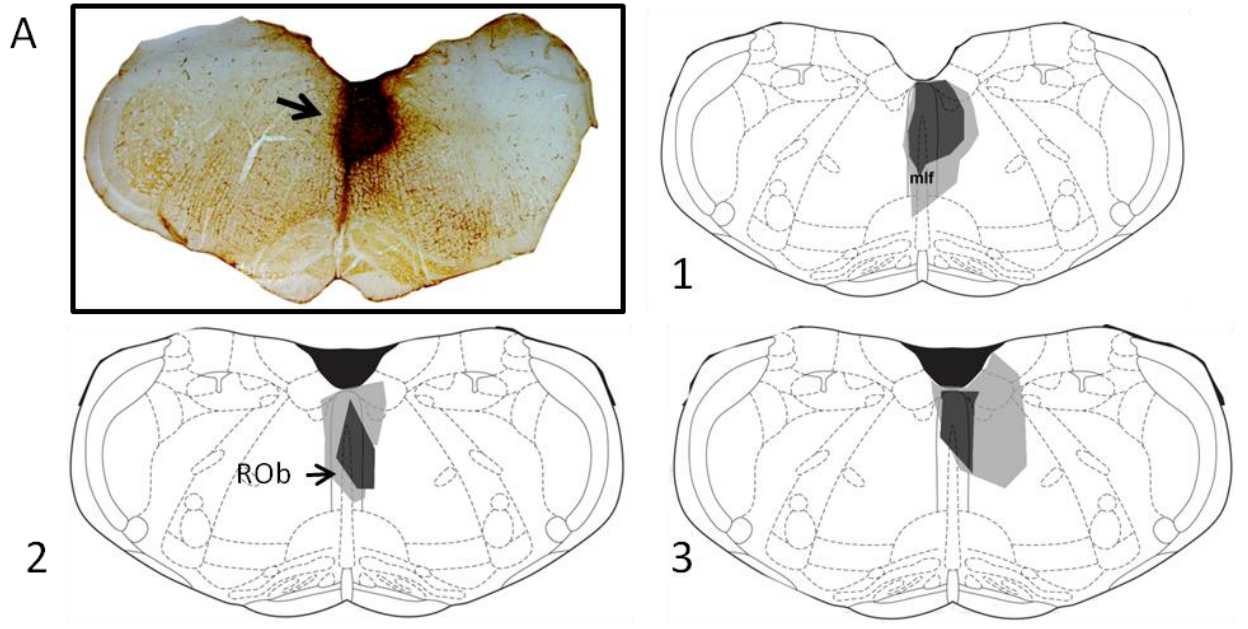


**Figure 4-3** A maximum intensity projection confocal scan of a representative medullary coronal section showing the pattern of distribution of cells collateralised to both sites following a CVLM injection of CTb and spinal injection of FG

**1 Lower panel**, a magnified view of the same medullary section (inset 1, Bregma 12.00mm) showing double labelled cells (white arrows) in the gigantocellular reticular nucleus (Gi) its ventral part (GiV) as well as the lateral paragigantocellularis (LPGi).

**2 a, b, c Right panel** from top to bottom, magnified view of CTb labelled cells (red, rhodamine), FG labelled cells (green, Alexa 488) and a merged image with double labelled cells (yellow, white arrows).

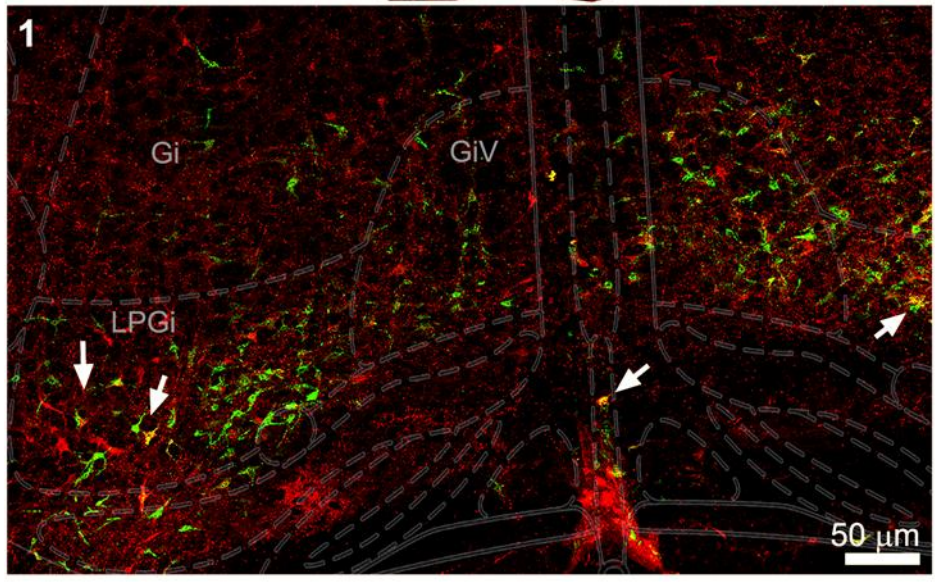
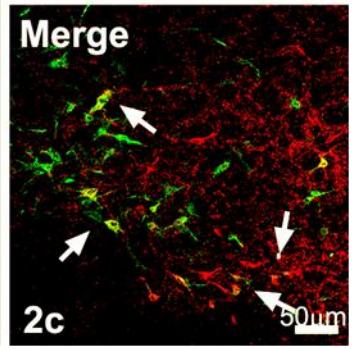
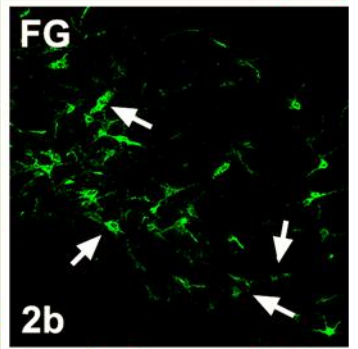
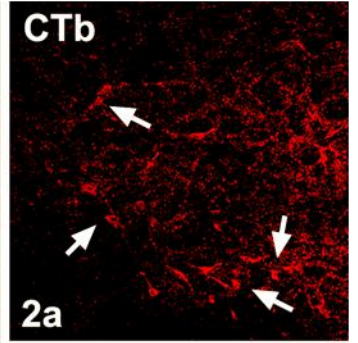
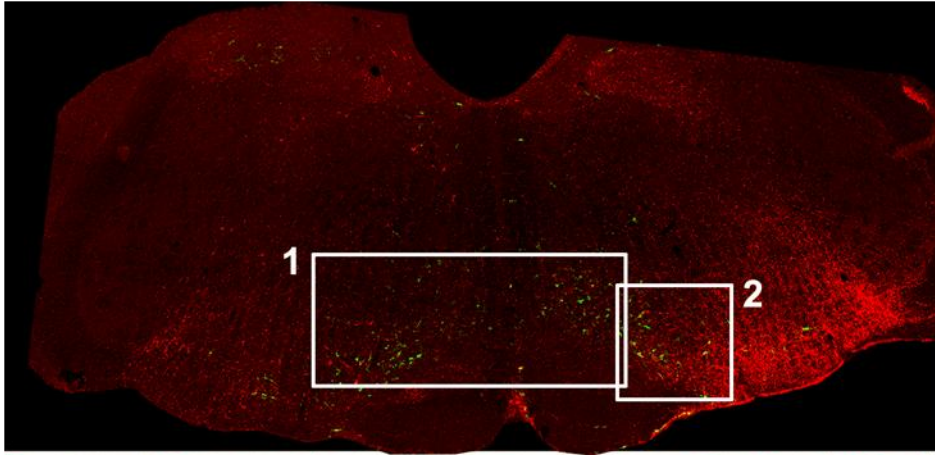


**Figure 4-4 A confocal scan of a representative pontine coronal section of an animal with CTb injection in the MLF and FG injection in the lumbar spinal cord, illustrating the distribution pattern of double labelled cells (Bregma - 8.76)**

**1 a, b, c** A magnified view of inset 1 from a site contralateral to the spinal injection. From left to right are CTb labelled cells (red, rhodamine), FG labelled cells (green, Alexa 488) and a merged image with double labelled cells (yellow, white arrows).

**2 a, b, c** A magnified view of inset 2 (ipsilateral to the spinal injection), left to right CTb labelled cells (red, rhodamine), FG labelled cells (green, Alexa 488) and a merged image with double labelled cells (yellow, arrow heads).

**3 a, b, c** A magnified view of a representative pontine area from an animal with CTb injection in the CVLM and FG injection in the ipsilateral lumbar spinal cord. From left to right, CTb labelled cells (red, rhodamine), FG labelled cells (green, Alexa 488) and a merged image with double labelled cells (yellow, yellow arrows).

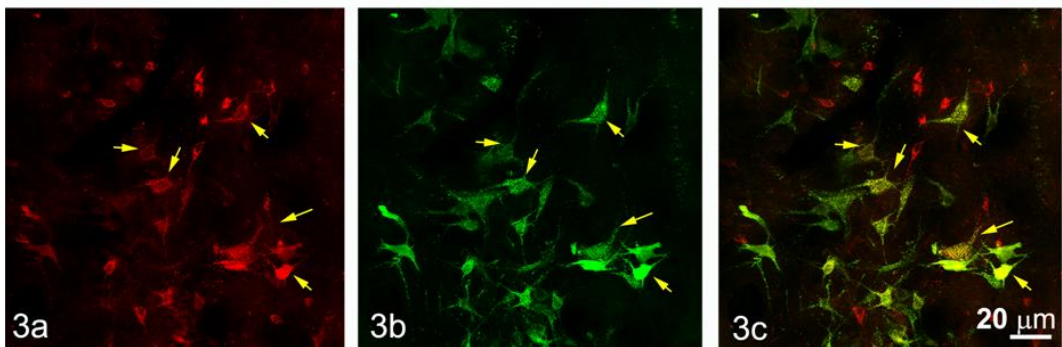
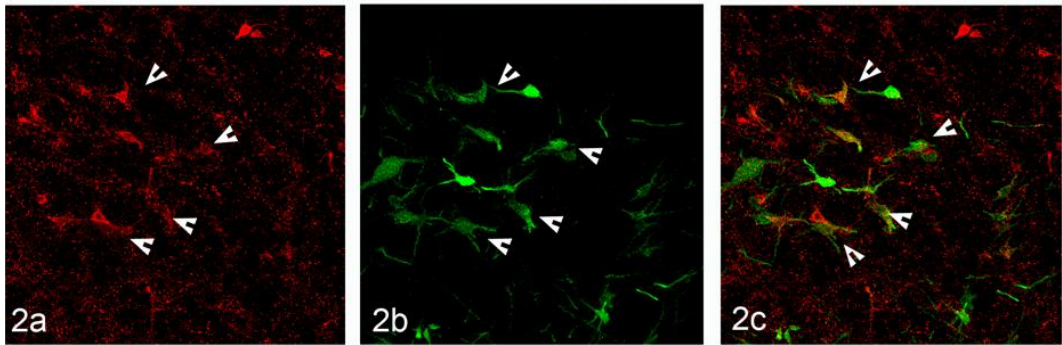
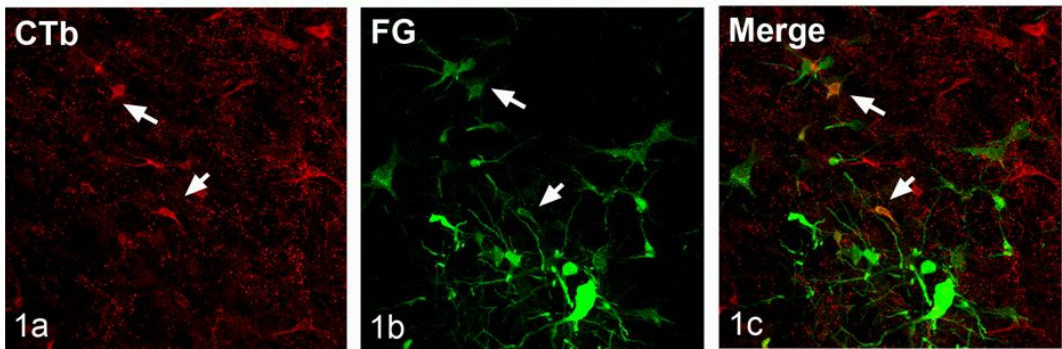
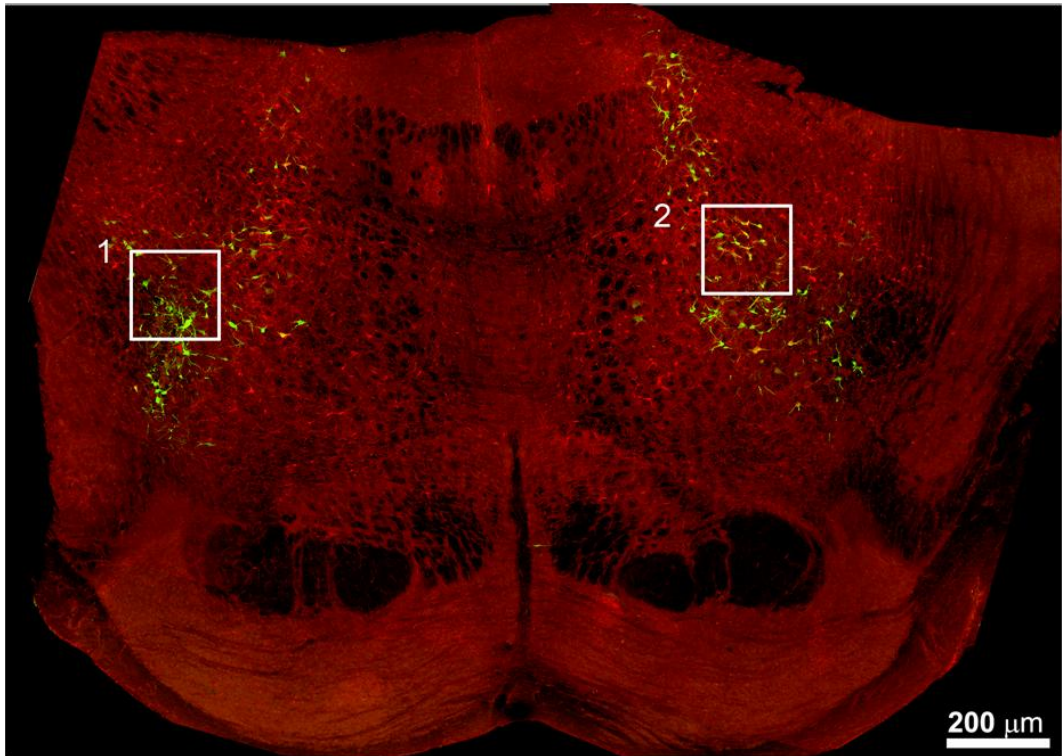


**Figure 4-5 Distribution of labelled cells in the medulla of animals with CVLM and MLF injections**

Outline diagrams of coronal sections in animals 1, 2 & 3, through the medulla at three levels (anterior-posterior coordinates according to Bregma) showing the locations of cells following spinal injections in the right intermediate grey matter and injections within the MLF or right CVLM. Black dots represent double labelled cells; green dots represent spinally-projecting cells; and red dots represent cells labelled from MLF or CVLM. Gi, gigantocellular reticular nucleus; LPGi, lateral paragigantocellular nucleus; MdV, ventral medullary reticular nucleus

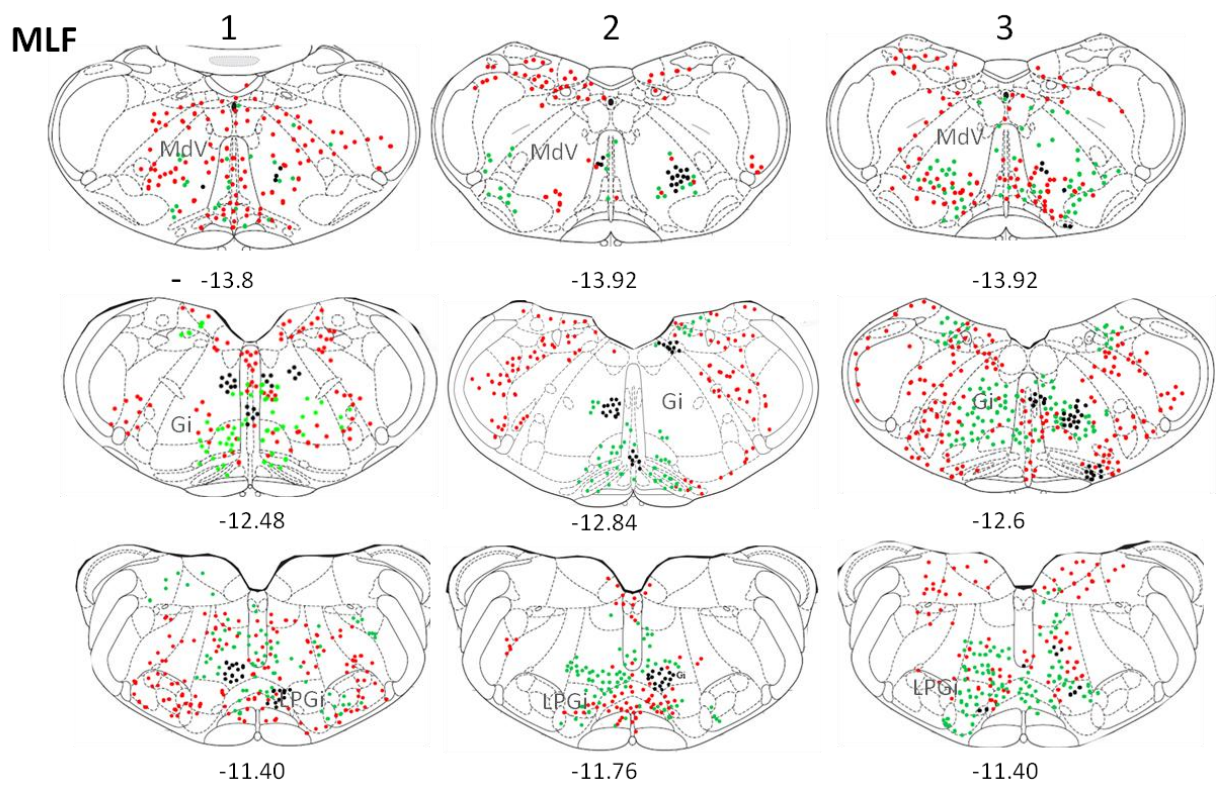
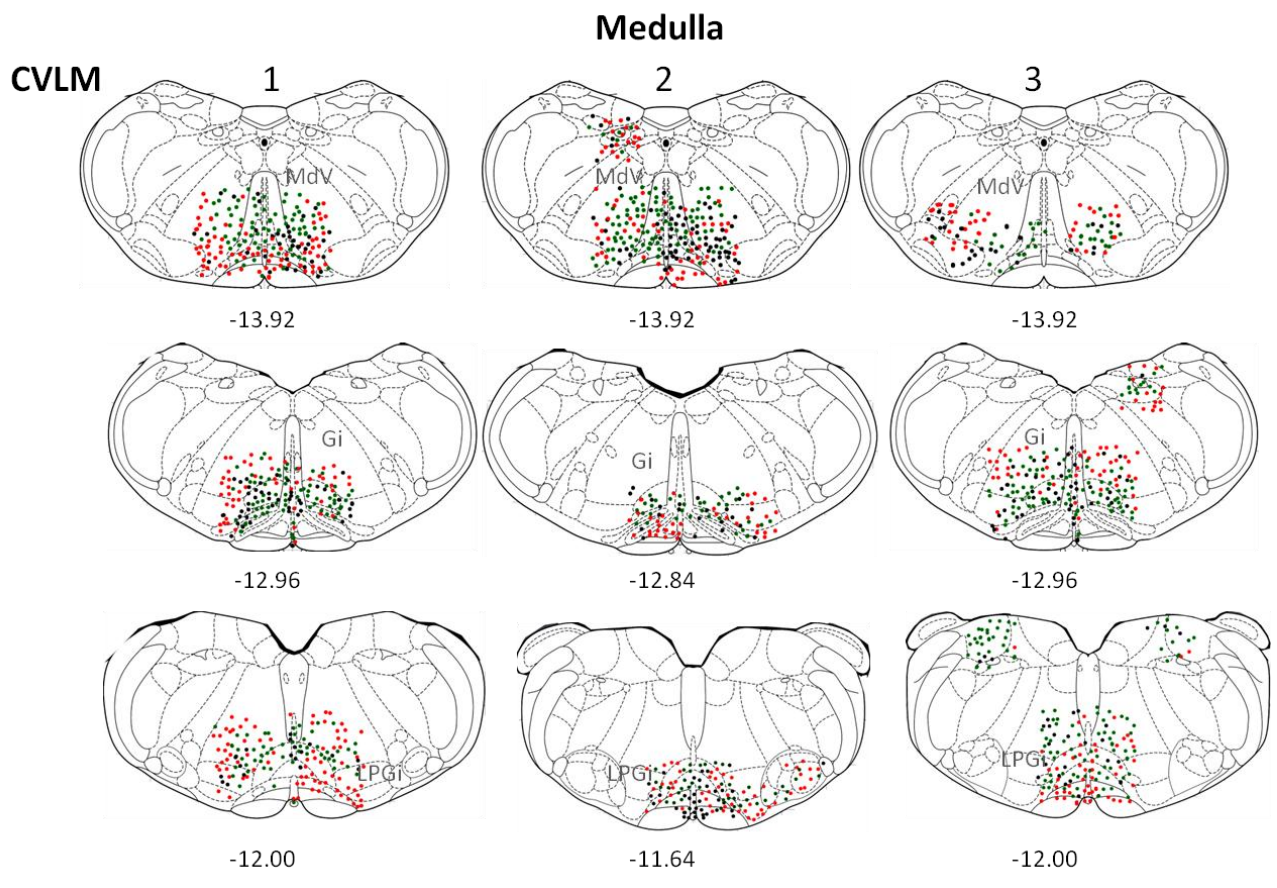


**Figure 4-6 Distribution of cells in the pons and midbrain of animals injected in either the right CVLM or MLF**

Outline diagrams of coronal sections from animals 1, 2 & 3 through the pons at two levels (anterior-posterior coordinates according to Bregma) showing the locations of cells, following spinal injections in the right intermediate grey matter and injections within the MLF or right CVLM.

The last panel shows the distribution of cells in the midbrain in animals 1, 2 & 3 at various levels after CTb injection in the CVLM and FG spinal injections.

Black dots represent double-labelled cells; green dots represent spinally-projecting cells; and red dots represent cells labelled from MLF or CVLM.

PnC, pontine reticular nucleus, caudal part; PnO, pontine reticular nucleus, oral part; PaR, parabrachial nucleus; PBP, parabrachial pigmented nucleus of the ventral tegmental area.

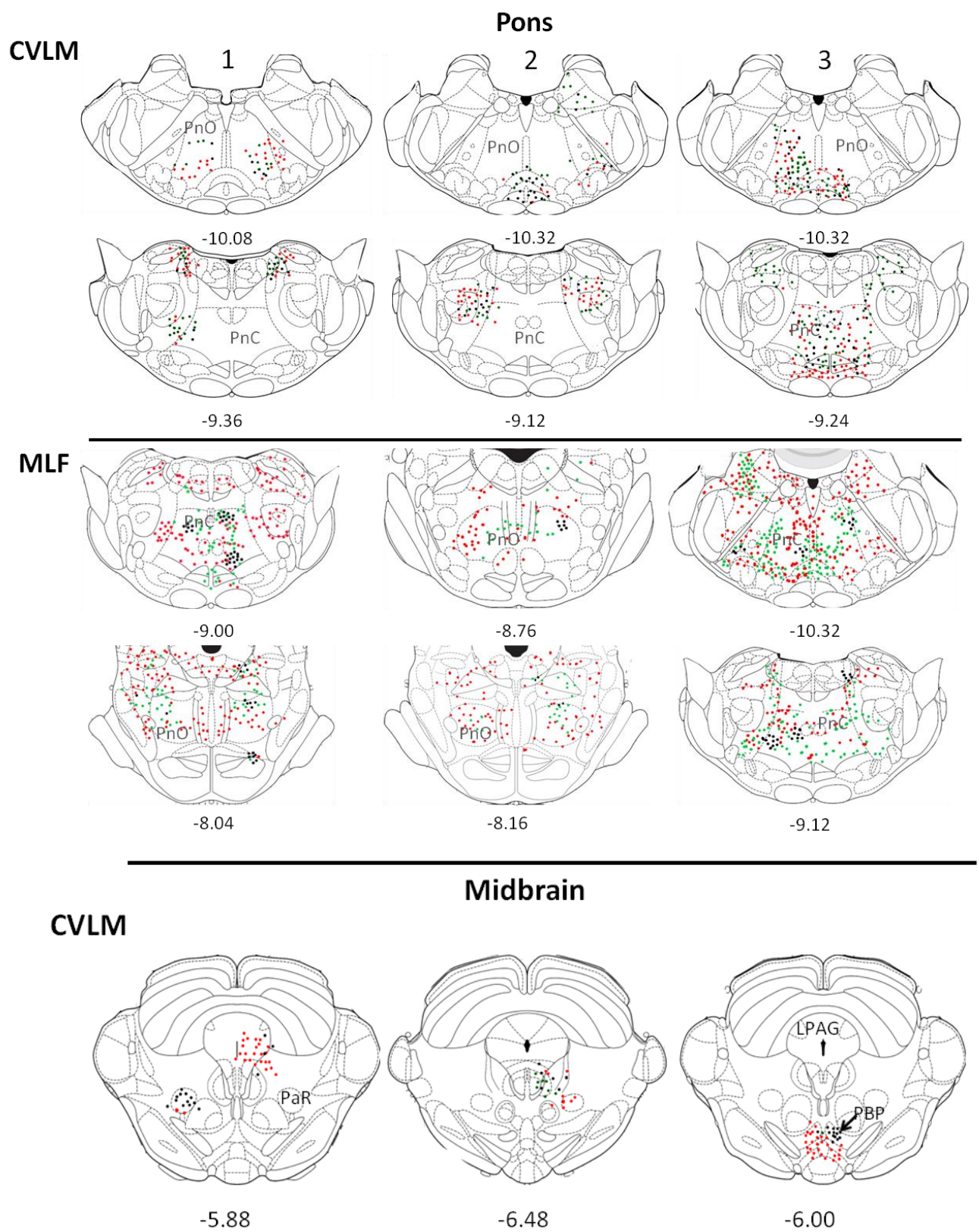
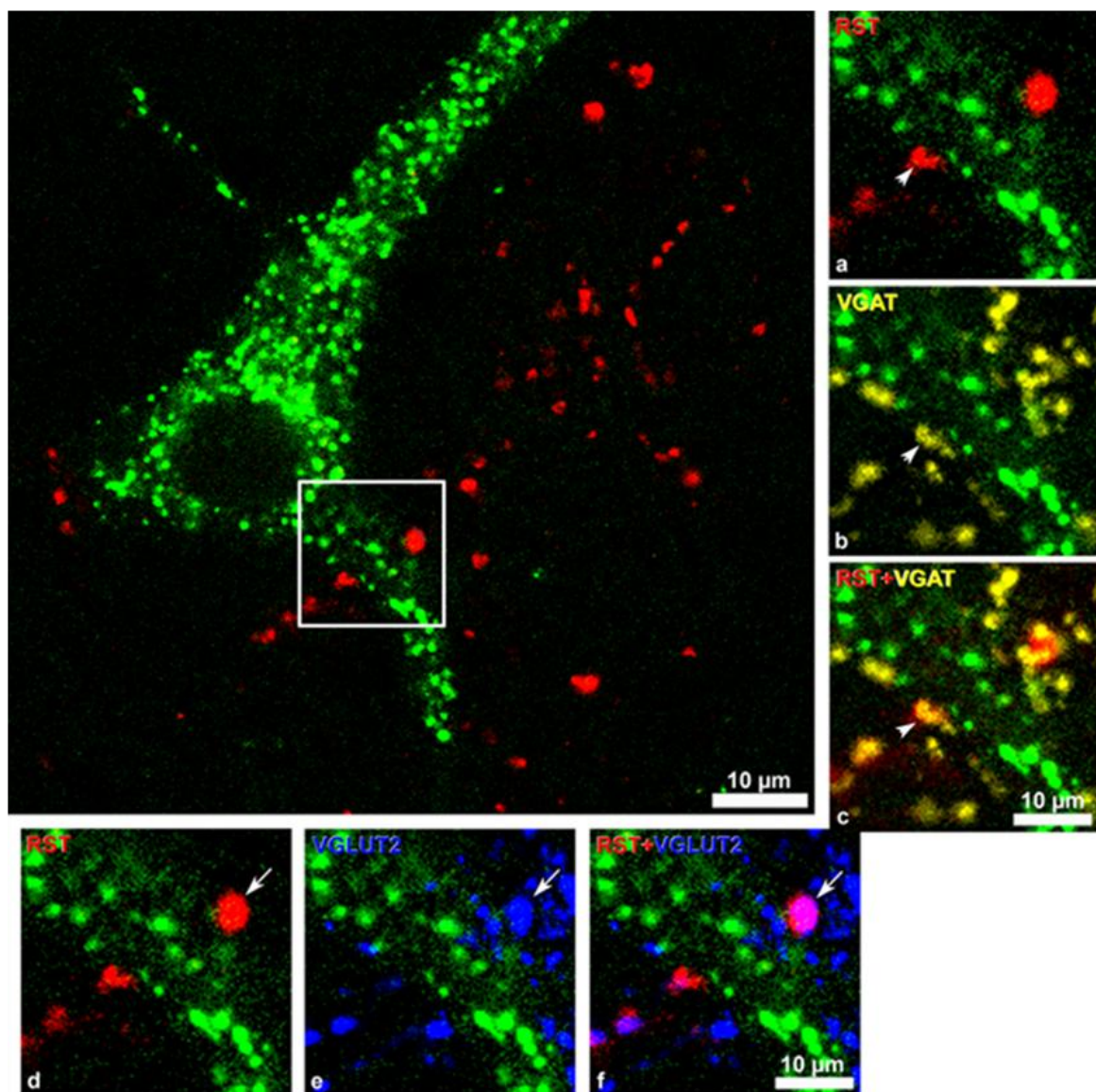


**Figure 4-7 Anterogradely labelled excitatory and inhibitory bulbospinal terminals in contact with a retrogradely labelled spinoreticular cell**

**Large panel**, on the left shows a fluorogold labelled SRT cell (green) with RST (reticulospinal, ReST) terminals (red, CTb) in contact with a dendrite.

**a-c Right panel**, top to bottom, a magnified view of a single optical section of the inset in the large panel, showing RST (CTb in red) with VGAT (yellow) indicated by arrow heads.

**d-f lower panel**, shows a magnified view of a single optical section of the same inset with ReST contact (CTb in red) with VGLUT-2 (blue) indicated by arrows.



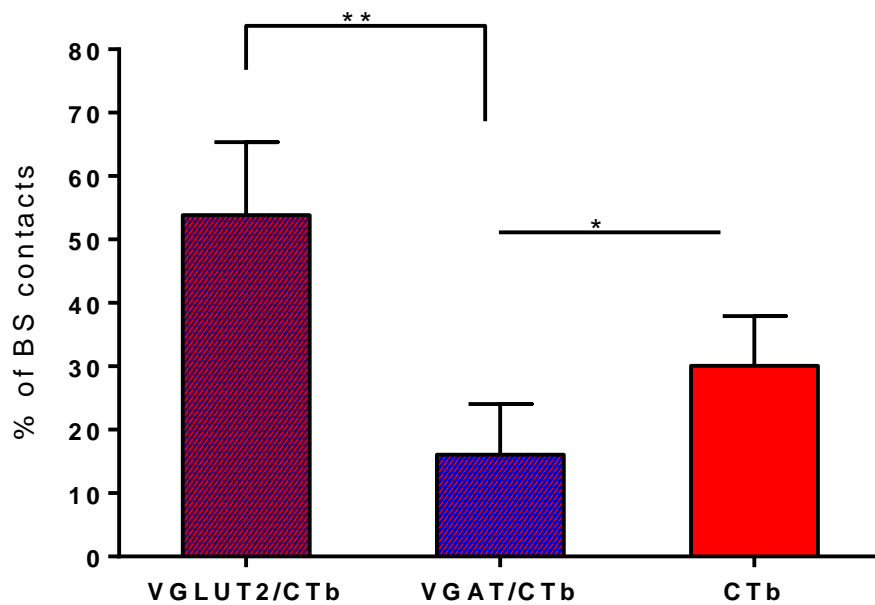


**Figure 4-8 Excitatory and inhibitory bulbospinal inputs onto retrogradely labelled spinoreticular tract neurons**

The percentage of excitatory bulbospinal (BS) contacts (VGLUT-2/CTb) is significantly more than inhibitory contacts (VGAT/CTb), as well as VGAT and VGLUT-2 negative BS terminals (CTb), \*\* $p < 0.01$  and \* $p < 0.05$ , respectively (Anova, post hoc *Tukey's*). Data is expressed as mean%±SD (T)  $n = 3$  animals.

## 4.4 Discussion

This study shows that cells projecting via the MLF or the CVLM to the lumbar spinal cord have mostly overlapping spatial distributions. The vast majority of cells in both pathways are located in identical reticular areas of the brainstem, such as Gi, LPGi, MLF, and MdD in the medulla and the PnO and PnC in the pons (Table 4-3). In addition both pathways contain raphe-spinal and olivo-spinal projecting cells. Furthermore, both pathways have a mixture of crossed and uncrossed axonal fibres, as double labelled cells were located both ipsi and contralateral to the spinal injection site. The differences between the two paths are subtle, with more double labelled cells in the LPGi, RPa and the midbrain areas in CVLM pathways compared with the MLF path (Figures 4-5 & 4-6). BS contacts on spinoreticular cells via the CVLM are predominantly excitatory but there is also an inhibitory element targeting these cells. Figure 4-9 summarises these findings in a simplified diagram.

### 4.4.1 Technical considerations

The b subunit of cholera toxin is both a retrograde as well as anterograde tracer and is also taken up by undamaged axons of passage in the CNS (Ericson H and Blomqvist A, 1988, Chen S and Aston-Jones G, 1995, Angelucci A et al., 1996). We thus utilised this characteristic of CTb to retrogradely label cells, with axons passing through the MLF and the CVLM, in order to determine the origin of bulbar spinally-projecting cells. For further merits and demerits of FG use in retrograde labelling of cells, see Chapter 3, Section 3.5. The CVLM injection sites are defined in this study as the reticular area adjoining and including the LRN dorso-laterally (Hardy SG et al., 1998, Iigaya K et al., 2007) as opposed to a small area sandwiched between the LRN and the spinal trigeminal nucleus as defined by Tavares et al. (2002) (see Figure 4-1). Furthermore, by targeting the LRN we kept away from the more ventromedial area defined by Holstege (1996); an area overlapping the inferior olivary complex and the raphe obscurus and pallidus so as not to overlap with the MLF path. CVLM injection sites are purely unilateral and label cells with axons passing through the right CVLM only; whereas, it is virtually impossible to label only one side of the MLF as a consequence of the inevitable spread of tracer across the midline (see Figure 4-

2). Thus, our sample of spinally-projecting MLF cells is likely to be composed of cells with axons that travel through either the left, or right side of the MLF.

To compensate for any variation between injection sites we attempted to identify consistent patterns of cell distribution for the three animals within each group quantitatively by averaging the numbers of double-labelled cells found within each structure and thus extracted the principal structures associated with spinally-projecting cells. Borders of many brainstem structures are not well-defined and therefore some cells may have been wrongly allocated by the mapping procedure we used which depended upon superimposing stylised diagrams upon coronal sections at various levels of the brainstem (Paxinos G and Watson C, 2005). For example, cells attributed to the MLF may have belonged to ROb or Gi. Another complication was that as we were injecting CTb into the brainstem itself, the area in the immediate vicinity of the injection site could not be used to identify double-labelled cells. This is possibly why no cells could be identified within RPa following MLF injections.

We also used the CTb tracing technique to label axon terminals in lumbar segments that originate or pass through the CVLM. In addition to anterograde labelling of descending axons, CTb injections in the CVLM also label spinomedullary neurons retrogradely; hence some of the terminals we observed could have arisen from collateral axons of these cells. However by looking at spinoreticular cells, retrogradely labelled from the contralateral LRN, with anterogradely labelled ReST terminals any inputs from collateral axons of ascending neurons was minimised.

#### **4.4.2 Comparison with other studies**

Cells in the reticular core share many common projections within the brain stem, as well as ascending (cortical) and descending (bulbospinal) projections which differ to a large extent in degree rather than in kind. Degenerative as well as tract tracing and electrophysiological studies have defined, to an extent some of these intricate projections, while identifying the anatomical locations of bulbospinal neurons in a variety of species from rats (Leong SK et al., 1984, Zemlan FP et al., 1984, Jones BE and Yang TZ, 1985, Reed WR et al., 2008), cats

(Kuypers HGJM et al., 1962, Basbaum AI and Fields HL, 1979, Mitani A et al., 1988), mice (Liang H et al., 2011) to opossums ((Martin GF et al., 1979) and even monkeys (Sakai ST et al., 2009). In this study we used two retrograde tracers to clarify anatomically, possible quantitative differences in neurons at the origin of the rat BS pathways via the MLF and CVLM. The major structure in both these pathways is the Gi with mostly ipsilateral projections to the spinal cord in both pathways. This agrees with a study in cat that showed mostly ipsilateral projections from the Gi via the MLF (Mitani A et al., 1988). The overall pattern of distribution of bulbospinal neurons irrespective of either the MLF or CVLM pathway in the reticular areas (Gi, LPGi) and the raphe nuclei (magnus, obscurus) is similar to findings in mice (Liang H et al., 2011), cats (Basbaum AI et al., 1978, Basbaum AI and Fields HL, 1979) and rats (Jones BE and Yang TZ, 1985). An unexpected finding in our study was the presence of double labelled cells in the inferior olivary complex (IO), in both MLF and CVLM injections (Figure 4-5, Bregma -13.92). The existence of an olivo-spinal pathway, although cited in older literature (Brodal A et al., 1950, Voneida TJ, 1967) has since been debated. Nevertheless, other studies have also reported spinally projecting cells within the IO (Leong SK et al., 1984, Zemlan FP et al., 1984). As to whether such a pathway exists is a matter of contention. A possible explanation as to our finding may be attributed to the difficulty in defining the exact borders of the brainstem nuclei, hence a misattribution of neurons from nearby structures to the IO.

In the pontine region, the majority of bulbospinal neurons were located in the ipsilateral PnO in both groups. However most of the caudal pontine (PnC) reticulospinal neurons in MLF injections were located ipsilaterally as opposed to the CVLM injections, where most cells were contralateral to the lumbar injections. Mitani et al. (1988) described a similar ipsilateral projection from the pontine Gi. Reed et al., on the other hand described ipsilateral BS projections from the Gi to both lumbar and cervical regions (Reed WR et al., 2008).

In addition to the reticulospinal projections mentioned above, another major component of these pathways originates from the raphe nuclei, especially the RMg which coincides with findings from other studies in cat (Basbaum AI et al., 1978) as well as rat (Huisman AM et al., 1981, Bowker RM and Abbott LC, 1990).

Another difference in our study is that, as we did not identify any double labelled cells in the red nucleus, the rubrospinal tract was not labelled for either group of animals in contrast to Huisman et al. (1981). However we did observe clusters of cells in the parabrachial area in CVLM injections (Figure 4-6, Bregma -5.88). These cells produce monosynaptic inhibition of rubrospinal neurons and are also influenced by cortical projections (Liu C-L et al., 2002). A small number of cells were also noted in the nucleus of the solitary tract (Loewy AD and Burton H, 1978), the medial vestibular nucleus (Bankoul S and Neuhuber WL, 1992), the subcoeruleus which is a source of noradrenergic fibres (Kuypers HGJM et al., 1962, Vanderhorst VG and Ulfhake B, 2006), the parabrachial pigmented nucleus of the ventral tegmental area which is likely to be a source of dopaminergic fibres (Huisman AM et al., 1981, Vanderhorst VG and Ulfhake B, 2006), and also the cranial nerve nuclei (facial, 7n; trigeminal; 5n)(Jones BE and Yang TZ, 1985).

Hence, it can be concluded that the major elements of the MLF and CVLM pathways originate principally from similar brainstem structures. The MLF begins to form its medial and lateral components at roughly -5.7mm anterior-posterior to the interaural zero point. As our CVLM injections were made at -4.8mm, it is unlikely that lateral components of the MLF pathway were labelled; therefore axons passing through the CVLM presumably form an additional pathway (Paxinos G and Watson C, 2005). As other studies have shown, these pathways may be highly ordered because components of the BS pathways are found in the ventromedial, dorsolateral and ventrolateral white matter of the spinal cord and they originate from distinct areas in the brain stem (Nyberg-Hansen R, 1965, Basbaum AI et al., 1978, Jones BE and Yang TZ, 1985, Martin GF et al., 1985, Mitani A et al., 1988, Vanderhorst VG and Ulfhake B, 2006). However, the possibility that some of the double-labelled cells we observed gave rise to bifurcating axons, which pass through both structures, cannot be excluded.

#### **4.4.3 Transmitter phenotypes of Bulbospinal pathway via the CVLM**

Both MLF and CVLM pathways have similar proportions of excitatory and inhibitory components (Du Beau A et al., 2012, Huma Z et al., 2014). The

majority of axon terminals in both pathways contain VGLUT-2 and thus are mostly excitatory (58% and 62%; MLF and CVLM respectively), but there is also a significant inhibitory component in both pathways that consists of purely GABAergic terminals (7 % and 9%), purely glycinergic terminals (9% and 13%) and a small group that are both GABAergic and glycinergic (3% and 3%). In addition to these studies, electrophysiological studies in cat (Peterson BW, 1979a, Peterson BW et al., 1979b) and monkey (Riddle CN et al., 2009) have also shown an inhibitory component of bulbospinal projections onto spinal target cells. Electrophysiological data shows polysynaptic inputs from the BS path to the SRT cells (Hammar I et al., 2011). This variation may be because of a difference in species (cat and rat) or it may also be because of the very low contact densities of these monosynaptic inputs to the SRT cells seen anatomically. The next chapter deals with this aspect in more detail. The pattern of connectivity of CVLM bulbospinal projections onto spinobulbar cells in the lumbar spinal cord reveals mostly excitatory VGLUT-2 terminals in addition to a minority that are inhibitory. This may provide a basis for a bulbospinal-spinobulbar loop involved in the facilitation of motor activities.

#### **4.4.4 Functional implications**

Bulbospinal pathways are known to have monosynaptic actions on motor neurons and pre-motor interneurons and are therefore components of a network involved in locomotor control, postural and gait adjustment (Grillner S et al., 1968, Leblond H et al., 2000, Prentice Sd DT, 2001, Bannatyne BA et al., 2003, Krutki P et al., 2003, Schepens B and Drew T, 2006, Riddle CN et al., 2009). In addition, they have profound influences on sensory systems (especially nociceptive pathways), respiration and autonomic activity (Basbaum AI and Fields HL, 1979, Stocker SD et al., 1997, Hardy SG et al., 1998, Tavares I and Lima D, 2002, Iigaya K et al., 2007). These pathways form extensive termination patterns within the spinal grey matter with individual BS cells having axons that innervate several segmental levels (Huisman AM et al., 1981, Matsuyama K et al., 2004, Reed WR et al., 2008). They provide input to extensive areas of the grey matter, with some axon collaterals projecting to both sides of the cord (Nyberg-Hansen R, 1965, Peterson BW et al., 1979b, Martin GF et al., 1985, Holstege JC, 1996a, Matsuyama K et al., 2004). Therefore these systems appear to be ideally suited

to coordinate activity of diverse neuronal networks on both sides of the cord located at different segmental levels. They also contain a multiplicity of neurotransmitters and neuromodulators, including inhibitory and excitatory amino acids, monoamines and peptides (Grillner S et al., 1968, Holstege JC, 1996a, Vanderhorst VG and Ulfhake B, 2006, Jordan LM et al., 2008). Thus BS neurons have the capacity to facilitate or depress network activity via direct inhibitory and excitatory synaptic actions on spinal neurons along with modulatory effects, for example on segmental interneurons involved with contralateral extensor FRAs (Leblond H et al., 2000).

The moot question is: what is the function of the CVLM pathway given its apparent similarities to the MLF pathway? A clue to the function of this pathway is provided by its anatomical organisation; it generally innervates a more circumscribed region of the mid-lumbar spinal grey matter than the MLF pathway and, unlike the MLF pathway, does not have many terminations within motor nuclei and lamina VIII (Huma Z et al., 2014). Furthermore, very few axons passing through the CVLM cross to form terminals in the contralateral grey matter and therefore the influence of this lateral pathway appears to be more restricted than the MLF pathway. In a study of CVLM terminations in the thoracic spinal cord, Hardy et al., (1998) reported that in addition to the ipsilateral pathway, which terminates principally on sympathetic pre-ganglionic neurons, there is a contralateral component that specifically targets phrenic motor neurons. These authors suggested that a possible function of the CVLM pathway is to coordinate respiratory and autonomic functions. In mid-lumbar segments, CVLM axons terminate predominantly in the deep dorsal horn and intermediate grey matter and are ideally located to influence pre-motor interneurons that are also found in this region (Tripodi M and Arber S, 2012). Thus the function of the CVLM pathway may be to harmonise motor activity with respiratory and autonomic activity to produce the co-ordinated output of these systems required for physical exercise.

Both reticulospinal and vestibulospinal neurons coordinate the activity of ipsilateral and contralateral limb muscles via pre-motor neurons (Bannatyne BA et al., 2003, Jankowska E et al., 2003, Krutki P et al., 2003, Jankowska E et al., 2006). It has been postulated that reticulospinal fibres from the MLF have not

only excitatory, but also disynaptic, inhibitory effects on ascending neurons in the spinal cord and thus may modulate the activity of interneurons mediating the flexion reflex (Grillner S et al., 1968). Since the monosynaptic excitatory effects originate from more than one descending system (VST & BS) there may be a reciprocal augmentation of these contacts and it is further conceivable that these pathways could be engaged in different stages of hindlimb movement (Clendenin M et al., 1974 b, Ekerot CF, 1990c). The spinoreticular neurons play a pivotal role in this by further relaying said information to the cerebellum via the spino-reticulo-cerebellar pathway, which by feed-forward excitation as well as inhibition alters or moderates posture and movement (Grillner S et al., 1968b). It may well be postulated that these SRT neurons form part of the spino-bulbar-spinal reflex, the descending component of which is made up of reticulospinal projections from the medulla (Shimamura M and Kogure I, 1979, Shimamura M et al., 1980).

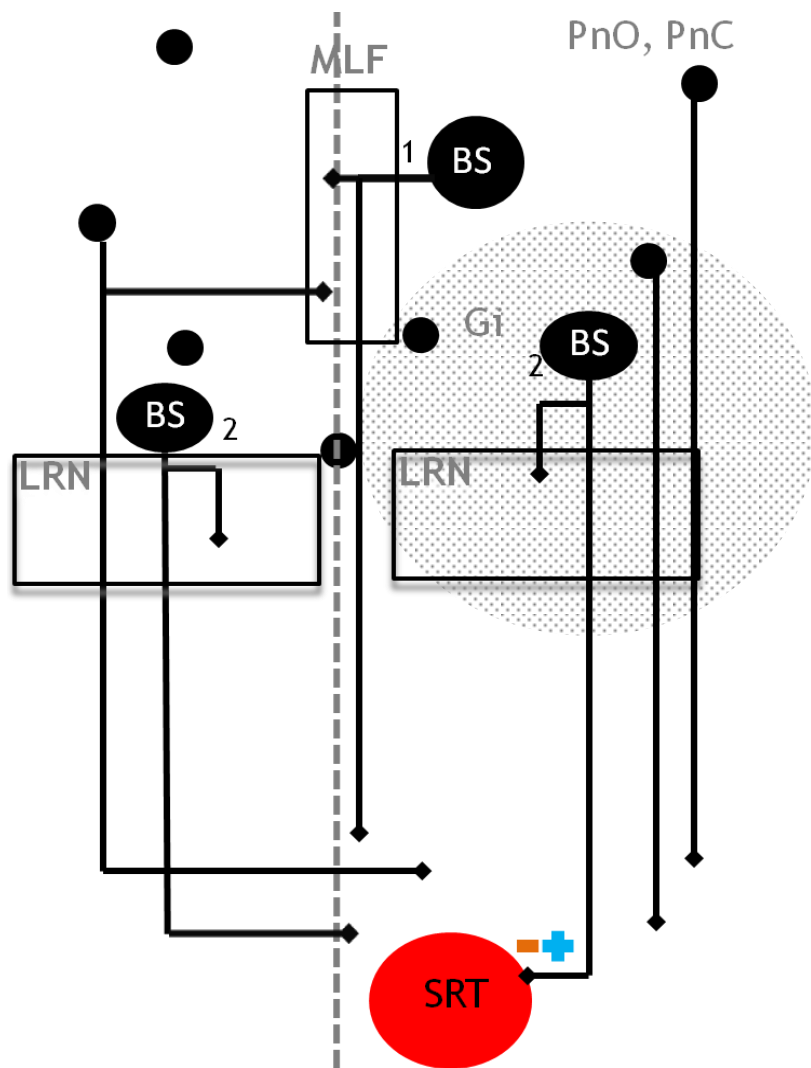


**Figure 4-9 Summary of the descending bulbospinal pathways**

Bulbospinal neurons (BS, big black circles and lines) projecting via the 1) MLF and 2) CVLM.

Small black circles and lines represent other BS pathways to the lumbar spinal cord. Red circle represents a spinoreticular cell (SRT) with excitatory (blue, VGLUT-2) and inhibitory (orange, VGAT) reticulospinal contacts.

LRN, lateral reticular nucleus, Gi, gigantocellular nucleus, PnO, PnC pontine reticular nuclei.

# Chapter 5

## 5 Origins of excitatory and inhibitory contacts on spinoreticular tract neurons in rat and cat lumbar spinal cord

### 5.1 Introduction

In order to achieve a better understanding about the role of neurons at the origin of the spinoreticular tract it is essential to understand not only the nature of synaptic contacts but also the potential sources of inputs to these cells. The origin of these contacts, be they proprioceptive, exteroceptive, from intrinsic spinal neurons or descending systems conveying signals from higher centres, would determine not only the type of information that the cerebellum receives via spinobulbar pathways. In addition these SRT neurons would modify the final sensorimotor output, for example, in the form of posture adjustment to painful stimuli.

Extensive work has been done on inputs to SRT cells using electrophysiological techniques in cat with some of these SRT cells classified as cells of origin of the bilateral ventral flexor reflex pathway (bVFRT)(Holmqvist B, 1960, Lundberg A and Oscarsson O, 1962b, Rosén I and Scheid P, 1973a, Clendenin M et al., 1974 b, Illert M et al., 1978, Alstermark B et al., 1981, Ekerot CF, 1990c). These bVFRT neurons are activated by flexor reflex afferents (FRA) that are composed of cutaneous as well as muscular Group I & II and high threshold joint afferents (Oscarsson O and Rosén I, 1966). In addition, they have a modulatory input from the descending lateral vestibulospinal tract (Grillner S et al., 1968, Rosén I and Scheid P, 1973c, Kubin L et al., 1980). Furthermore, they receive excitatory and inhibitory inputs from ipsilateral and contralateral hindlimb nerves (Lundberg A and Oscarsson O, 1962b, Rosén I and Scheid P, 1973a). Thus, these neurons are involved in not only limb movements and their co-ordination but also in axial control and posture. Extracellular recordings have shown that these SRT neurons have large bilateral receptive fields (Fields HL et al., 1977, Maunz RA et al., 1978, Menetrey D et al., 1980, Foreman RD et al., 1984, Ammons WS, 1987), which evoke both inhibitory and excitatory inputs via large A $\beta$  as well as some A $\delta$  cutaneous afferents (Sahara Y et al., 1990). Some of these spinobulbar

neurons projecting to the LRN respond to noxious stimuli as well as innocuous touch (Nahin RL et al., 1983, Cervero F and Wolstencroft JH, 1984, Cervero F et al., 1988).

Advances in immunocytochemistry, utilising various antibodies to specifically target neurons and their terminals, has enabled us to characterise various neurochemical subpopulations. The discovery of vesicular glutamate transporters (VGLUTs) has provided us with reliable markers for glutamatergic synapses (Aihara Y et al., 2000, Fremeau RT et al., 2001, Varoqui H et al., 2002, Alvarez FJ et al., 2004). Taking advantage of differences in the immunocytochemistry of glutamatergic terminals of peripheral afferents and of central neurons (with VGLUT-1 and VGLUT-2, respectively), I investigated the various sources of excitatory contacts on SRT neurons in the lumbar cords of both rats and cats. There is a complementary pattern of distribution of VGLUT-1 and VGLUT-2 in the rat as well as in the cat lumbar cord as can be seen in [Figure 1-6](#). Although this distribution of neurotransmitters was originally investigated in rat spinal cord, the pattern is quite similar in both rat and cat (Varoqui H et al., 2002, Todd AJ et al., 2003). Furthermore, all cat excitatory interneurons previously studied exclusively expressed VGLUT-2 (Bannatyne BA et al., 2009).

It is widely accepted that all myelinated <sup>3</sup>primary afferents are glutamatergic with VGLUT-1 being preferentially expressed in most of their axon terminals (Varoqui H et al., 2002, Oliveira AL et al., 2003, Todd AJ et al., 2003, Alvarez FJ et al., 2004). In addition parvalbumin is preferentially expressed by muscle proprioceptors and therefore terminals immunoreactive for both transmitters are likely to be of proprioceptive origin (Celio MR, 1990, Zhang JH et al., 1990, Clowry GJ et al., 1997).

In addition, many nerve endings in the spinal cord co-localise GABA and Glycine and share a vesicular uptake mechanism (VGAT) (Todd AJ and Sullivan AC, 1990, Todd AJ et al., 1996, Ornung G et al., 1998, Todd AJ et al., 2000). VGAT is used as a marker for the presence of both GABA and Glycine inhibitory neurotransmitters in axon terminals producing pre-synaptic inhibition of primary afferents and post synaptic inhibition of spinal neurons (Fields HL et al., 1977, Chaudhry FA et al., 1998).

<sup>3</sup> Primary afferents in this thesis include all cutaneous and proprioceptive afferents.

Distinct neuronal populations can also be identified using CB and ChAT (Barber RP et al., 1984, Celio MR, 1990, Zhang JH et al., 1990). Combinations of these markers can thus be used to visualise particular terminals to characterise excitatory and inhibitory interneurons to spinoreticular cells.

All the evidence supports the fact that the degree of peripheral, spinal and supraspinal control of SRT neurons is of paramount importance in the final sensorimotor outcome in terms of movement, posture and also spinal withdrawal reflexes. However despite indications of the existence of these complex neuronal networks and the key role of SRT neurons in decoding diverse signals and forwarding information to higher brain centres, the morphological basis and functional connectivity of these cells is poorly understood. Thus, based on the fact that historically most of the electrophysiological data is from cat studies, we wanted to further explore the similarities and/or differences between the cat and rat SRT neurons in terms of the origin of inputs. We compared the anatomical data from the rat, with both anatomical and electrophysiological results from cat.

Hence, to achieve a better understanding of the sensorimotor function of these spinoreticular tract neurons the aims of this part of the study were: a) to investigate excitatory and inhibitory contacts to SRT cells in the rat and cat lumbar spinal cord, b) to determine the origin of these contacts whether from the intra-spinal circuitry or c) from primary afferents.

In order to achieve these aims, the first part of the study was conducted using retrogradely labelled SRT neurons in rat lumbar segment and electrophysiologically characterised SRT neurons in cat utilizing immunocytochemistry to label excitatory and inhibitory synaptic boutons. In addition, the sciatic nerve, being a major nerve of the hindlimb with both sensory and motor components and its ease of access, made it an ideal nerve to study myelinated afferents to the lumbar spinal cord and hence their relationship with projection neurons like the SRT. In rats, PV, CB and ChAT were used as markers to further determine the sources of these contacts from spinal neurons, using immunohistochemistry.

## 5.2 Methods

In this part of the study, experiments were conducted on rats as well as on cats to investigate the excitatory and inhibitory contacts on spinoreticular neurons in the lumbar spinal cord. The procedures on six young cats were carried out in accordance to the EU guidelines of animal care as well as the Swedish Animal Protection Act and Animal Protection Ordinance approved by the Ethics Committee for Animal Research at the University of Gothenburg (Göteborgs Djurförsöksetiska Nämnd). While experiments on the nine adult male Sprague-Dawley rats (Harlan, Bicester, UK) weighing between 250-350gm were performed in accordance with the UK Animals (Scientific Procedures) Act 1986 approved by the Ethical Review Process Applications Panel of the University of Glasgow. Thus, to find out about the various types of contacts to the SRT neurons in the lumbar spinal cord of cat and their sources in the rat, this part of my thesis is subdivided into three parts under Aims I to III below:

- to investigate excitatory and inhibitory contacts on SRT cells both in, (a) rat and (b) cat (Aim I);
- to investigate primary afferent contacts on SRT cells in rat (Aim II); and
- to investigate contacts from intra-spinal neurons (Calbindin, ChAT and parvalbumin, Aim III).

Most of the surgical procedures, perfusion and dissection are already outlined in the General experimental procedures ([Chapter 2, Section 2.1](#)). However, each set of experiments contained some variations in the methodology, as explained in greater detail below.

## 5.2.1 Aim 1a: Excitatory and inhibitory contacts onto spinoreticular neurons in the rat lumbar spinal cord

### *Surgical procedure*

[Chapter 2, Section 2.1](#) (General experimental procedures) provides the outline of the procedures carried out on rats. In summary, the first step was to label SRT neurons in the lumbar spinal cord and to accomplish this, we injected 0.2  $\mu$ l of 1% CTb into the LRN of three adult male Sprague-Dawley rats at stereotaxic coordinates, antero-posterior -4.8 mm, -1.8 mm (medio-lateral) and at a dorso-ventral co-ordinate of -0.4 mm (Paxinos G and Watson C, 1997). The injection sites were identified by using DAB as a chromogen and the exact location plotted onto the corresponding brain map from Paxinos & Watson (1997) as shown in [Figure 3-1, Chapter 3](#).

### *Immunohistochemistry, confocal microscopy, reconstructions and analysis*

Transverse sections (50 $\mu$ m) from L3-L5 segments were processed following the procedure described in [Chapter 2 \(section 2.3\)](#). [Table 5-1](#) shows the combinations and concentrations of various antibodies used. Three colour immunofluorescence was performed on selected sections from each lumbar segment by incubating them in primary antisera; CTb, VGLUT-1 and VGLUT-2 for Group A ([Table 5-1](#)). This was done to differentiate between excitatory terminals of primary afferent or corticospinal origin (VGLUT-1), spinal origin via the interneurons (VGLUT-2) and most descending contacts (VGLUT-2) other than the corticospinal tract (Varoqui H et al., 2002, Todd AJ et al., 2003, Alvarez FJ et al., 2004, Du Beau A et al., 2012). In Group B, along with excitatory contacts, I also looked at the inhibitory contacts (VGAT) by incubating selected sections in a combination of primary antisera (CTb, VGLUT-1/2 and VGAT) which were subsequently immunoreacted with corresponding secondary antibodies as shown in [Table 5-1](#).

Retrogradely labelled SRT cells with contacts from glutamatergic and/or GABAergic nerve terminals were scanned using three channels of a confocal laser scanning microscope (Bio-Rad Radiance 2100, Hemmel Hempstead, UK and LSM 710, Zeiss, Germany). Three sections were randomly selected from lumbar segments L3 to L5 and CTb labelled cells selected from three zones of the

transverse lumbar spinal sections: deep dorsal consisting of lamina IV and V cells; intermediate consisting of lamina VI and VII cells; and Lamina X. At least five cells from each zone/section were then selected to be analysed with NeuroLucida for confocal software (Microbrightfield Inc, USA). Reconstruction was started with the cell body and the dendrites added along with the respective markers until the dendritic tree was fully reconstructed.

In a further experiment, an antibody for the post synaptic membrane scaffolding protein at inhibitory synapses, gephyrin was incubated along with the other antibodies in Group B. These sections were scanned with four channels of a Zeiss LSM 710 confocal microscope. Reconstructions were carried out and the markers; VGLUT-1/2, VGAT and gephyrin mapped onto the cells. Further analysis was performed as already described under the General methods, Chapter 2.

**Table 5-1 Summary of primary and secondary antibody combinations and concentrations to label excitatory and inhibitory contacts on SRT cells in rat (n= 3)**

Group	Primary antibody combination	Primary antibody concentration	Supplier	Secondary antibody combination	Secondary antibody concentration	Supplier
<b>A</b>	gt CTb	1:5000	List (Quadragech), Campbell, USA	Rh. Red	1:100	Jackson Immunoresearch, West Grove, USA
	gp VGLUT1	1:5000	Chemicon/Millipore, Harlow, UK	Dylt 649	1:500	Molecular probes, Eugene, USA
	rbt VGLUT2	1:5000	Chemicon/Millipore, Harlow, UK	Alexa 488	1:500	Molecular probes, Eugene, USA
<b>B</b>	gt CTb	1:5000	List(Quadragech), Campbell, USA	Rh. Red	1:100	Jackson Immunoresearch, West Grove, USA
	gp VGLUT1&2	1:5000	Chemicon/Millipore, Harlow, UK	Dylt 649	1:500	Molecular probes, Eugene, USA
	rbt VGAT	1:5000	Synaptic systems, Göttingen, Germany	Alexa 488	1:500	Molecular probes, Eugene, USA
	mo Gephyrin	1:500	Synaptic Systems, Göttingen, Germany	Biotin AV-PB	1:500 1:1000	Jackson Immunoresearch, West Grove, USA Molecular probes, Eugene USA

All secondary antibodies were raised in donkey and conjugated to Rh. Red, Rhodamine Red; Dylt 649, Dylight 649; Alexa 488, Alexa-fluor 488; AV-PB, Avidin pacific blue; gt, goat; gp, guinea pig; rbt, rabbit; mo, mouse; CTb, B- subunit of cholera toxin; VGLUT, vesicular glutamate transporter; VGAT, vesicular GABA transporter.

## 5.2.2 Aim Ib: Excitatory and inhibitory contacts on spinoreticular neurons in the cat lumbar spinal cord

Procedures on cats were approved by the Ethics Committee for Animal Research at the University of Gothenburg (Göteborgs Djurförsöksetiska Nämnd). The animals were housed under veterinary supervision at the laboratory of Experimental Biomedicine at Sahlgrenska Academy where the electrophysiological experiments were carried out. EU guidelines for animal care as well as the Swedish Animal Protection Act and Animal Protection Ordinance were followed. This study was carried out on a sample of 16 neurons labelled in 6 young adult cats weighing, 2.5-3.8 kg of both sexes usually aged 6-9 months.

### *Surgical procedure*

General anaesthesia was induced with sodium pentobarbital (Apoteksbolaget, Sweden; 40-44 mg/kg, i.p.) and maintained with intermittent doses of  $\alpha$ -chloralose (Rhône-Poulenc Santé, France; 5 mg/kg i.v, administered every 1-2 hours up to 30 mg/kg and every 2-3 hours up to 55 mg/kg, thereafter). Alpha chloralose has minimal side effects on the autonomic and cardiovascular systems. It binds to a different site on the GABA<sub>A</sub> complex as compared to benzodiazepines, neurosteroids and barbiturates (Garrett KM and Gan J, 1998). The depth of anaesthesia was assessed throughout the experiment by the absence of a withdrawal reflex and later by the size of the pupils and any changes in heart rate and blood pressure, with additional doses of  $\alpha$ -chloralose administered to counter these effects. Atropine (0.05-0.2 mg/kg i.m, Mylan AB, Sweden) was also administered to reduce any tracheal secretions. Neuromuscular inhibition using Pancuronium bromide (Pavulon, Organon, Sweden; about 0.4 mg/kg/hr i.v supplemented with 0.2mg i.v every 2-3 hrs) along with artificial ventilation was used to ensure the cats were totally paralysed during recordings. In addition, to increase the effectiveness of synaptic transmission, 4-AP was administered (0.1-0.2 mg/kg, i.v, 4-aminopyridine, Sigma, USA). Mean blood pressure was measured via an intra-arterial catheter, maintained at 100-140 mm Hg and an end-tidal concentration of CO<sub>2</sub> at about 3.9-4.3% by adjusting the parameters of artificial ventilation and continuous infusion of a bicarbonate buffer solution (5gm glucose and 0.84gm NaHCO<sub>3</sub>, in 100ml distilled water) at a rate of 1-2 ml/kg/hr. Urine was collected

by an indwelling catheter and the core body temperature (rectal thermometer) was kept at about 37.5° C by servo-controlled infrared lamps.

An initial dissection was carried out for; tracheostomy (for artificial respiration and continuous monitoring of end-tidal CO<sub>2</sub>), the femoral artery (for continuous monitoring of blood pressure) and left and right cephalic veins (for intravenous injection of anaesthetics and other fluids). A number of peripheral left and right hind limb nerves were identified in situ, dissected, transected, and mounted on pairs of silver wire stimulating electrodes in the form of subcutaneous cuff electrodes for: the ipsilateral Saphenous nerve (Saph) and another for both the ipsilateral Quadriceps (Q) and Sartorius (Sart) together; and on the contralateral side, Quadriceps (coQ) and Saph nerves separately. In addition silver ball electrodes were used for Tibialis (Tib) and Superficial Peroneal nerves (SP) (see [Figure 5-1C](#)).

A laminectomy ([Figure 5-1B](#)) was performed to reveal the lower thoracic cord (T11-T12) and another laminectomy at lumbar (L3-L6) segments. A small additional laminectomy was done at C2-C3 for pyramidal tract stimulation. The dura mater remained intact except for small holes (about 1mm<sup>2</sup>) over the dorsal columns through which recording electrodes were inserted. The animal was then transferred to a stereotaxic frame and put on an artificial respirator after paralysis and induction of bilateral pneumothorax was undertaken. A paraffin pool was constructed using the skin flaps surrounding the spinal cord and the peripheral nerves i.e. Tib and SP.

The caudal part of the cerebellum was exposed with a craniotomy to allow insertion of four tungsten electrodes (60-300 kOhms) placed into the; ipsilateral and contralateral LRN, the interpositus nuclei of the cerebellum (ipsilateral and contralateral) as shown in [Figure 5-1A](#). In some of the animals, an electrode was placed into the MLF and in others the contralateral pyramidal tract (coPT) was stimulated as well but then only the contralateral LRN was used as we could use no more than four electrodes at the same time. These electrodes were inserted at an angle of 25°, with the tip directed rostrally. The initial target for the lateral reticular nucleus (LRN) was at Horsley-Clarke coordinates AP 10, L 3.5-4 and H 9.5 to activate the axons of spinoreticular tract neurons antidromically,

for the interpositus (IP) it was AP 7.5-8, L 4 and H 0 and for the MLF at AP 10, L 0.5 and H 6 to stimulate ReST axons running in the MLF. The final positions were adjusted in each animal on the basis of records of descending volleys recorded at the dorsal surface of thoraco-lumbar cord and the cervical levels for the pyramidal tract. These were evoked by single stimulus intensity ( $\leq 50\mu\text{A}$ ) through each tungsten electrode at lumbar latencies of 3.2-3.5ms, 2.7-3.2ms and 2.8-2.9 for interpositus, LRN and MLF, respectively. Also from the contralateral pyramidal tract (coPT, co-ordinates AP 7, L 1.3 and H 10) at a latency of 0.8-1.15ms at the cervical level.

At the end of the experiments these sites were marked by passing a 0.4 mA constant current for 10s. The locations of stimulation sites were subsequently verified on 100- $\mu\text{m}$  thick coronal sections of the brain stem, cut in the plane of insertion of the electrodes using Vibratome (Leica VT1200, Leica Microsystems, UK) and counterstained with Cresyl Violet ([Figure 5-3C & D](#)).

#### *Stimulation and recording*

Reticulospinal tract fibers were stimulated in the MLF using constant-current stimuli (0.2ms, 50-150 $\mu\text{A}$ ) delivered via a 0.5mm thin tungsten wire electrode, insulated except for its tip and used as a cathode with a wire inserted into a neck muscle as an anode (Jankowska E et al., 2003). Either single or 2-3 stimuli, 2.5ms apart were applied at 3.3Hz.

Peripheral nerves were stimulated with constant voltage stimuli for 0.1ms: intensities were expressed in multiples of the threshold (T) for the activation of the most excitable fibres. Afferent volleys following these stimuli (recorded from the cord dorsum at the L5 segmental level) were used to determine the central latencies of postsynaptic potentials (PSPs).

Antidromic activation of intra-reticular (LRN) axonal branches of tract neurons and surface recording at either thoracic or lumbar levels for volleys was carried out by using 0.2ms long constant current pulses at intensities  $\leq 100\mu\text{A}$ .

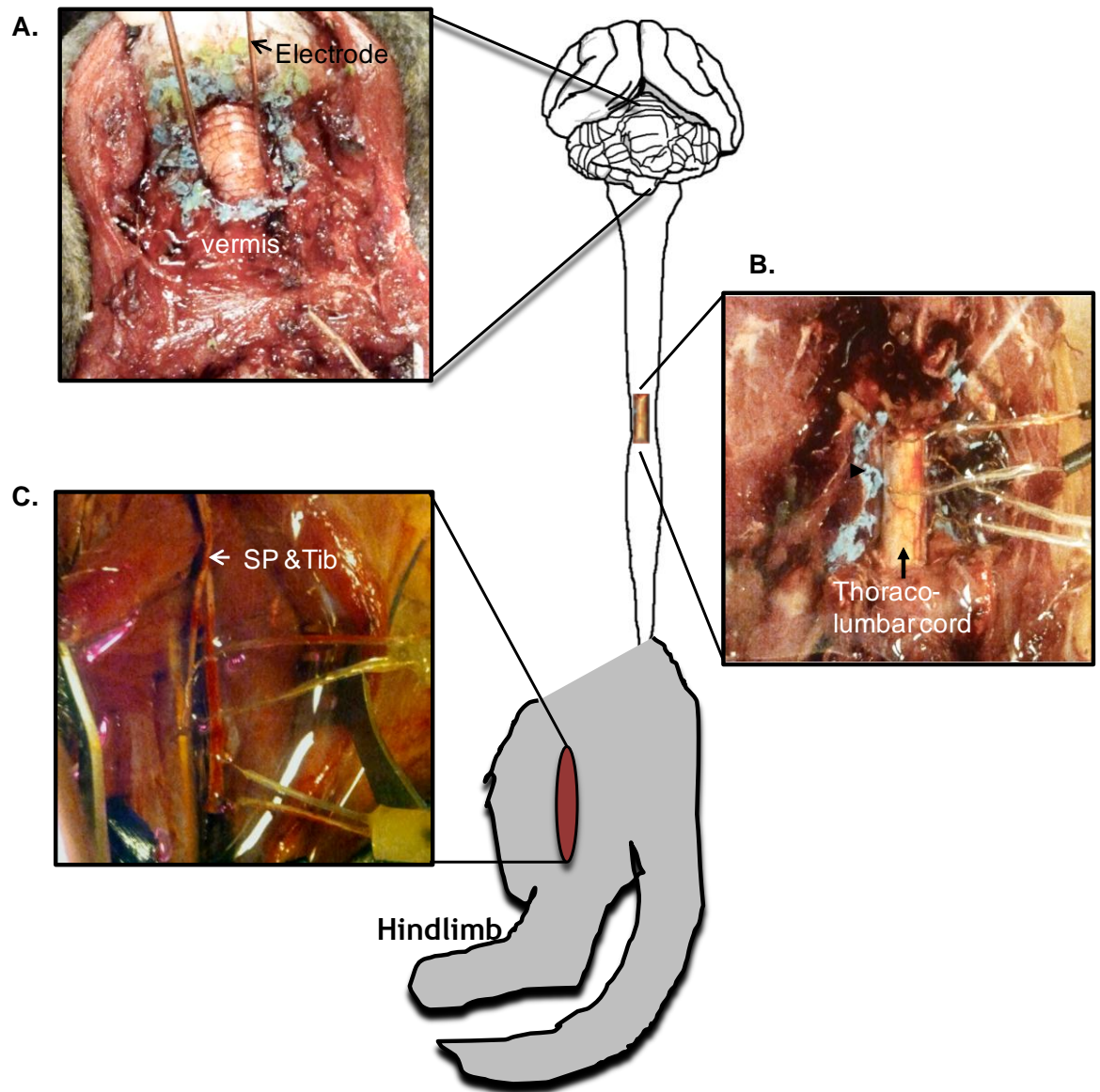


**Figure 5-1** A schematic diagram showing some of the surgical and recording procedures for spinothalamic neurons in the cat lumbar spinal cord

**A.** This image shows the vermis of the cerebellum exposed by a craniectomy with the tungsten electrodes in the left and right interpositus nuclei of the cerebellum (black arrow).

**B.** This is a laminectomy at T11-T12 (black arrow) with silver ball electrodes on the ipsi and contralateral side of the lateral funiculi.

**C.** A dissection of the Tibial (Tib) and Superficial Peroneal (SP) nerves in the hindlimb of the cat (white arrow) with electrodes in place.

In addition to this, to avoid the direct spinocerebellar neurons antidromic activation in the interpositus and recording from the surface of the thoracolumbar cord and vice versa, were done.

The stimulators (designed by E. Eide, D. Magnusson and N. Pihlgren, University of Gothenburg) allowed the use of square constant voltage or constant current pulses via inbuilt isolation units, setting the constant voltage stimuli in multiples of the threshold for activation of nerve fibres.

#### *Criteria for identification of spinoreticular tract neurons and labelling*

The SRT neurons were identified using a number of different criteria. These criteria included LRN stimulation, the location of the neuron and axonal projection.

1. The spinoreticular tract neurons were identified on the basis of antidromic activation from the contralateral LRN.
2. The neurons reported in this thesis are located in lumbar segments L4-L5 at the medial border of the dorsal horn at depths of 2.5-3.5mm from the surface of the dorsal columns corresponding to Rexed laminae VI-VII, [Figure 5-3](#). The recordings from these antidromically activated neurons were made by glass micropipettes, pulled and broken to a tip diameter of 1.5-2.5  $\mu\text{m}$ , filled with KCl (resistance 2-4 M $\Omega$ ). The distance from the surface of the spinal cord and the shape of the field potentials recorded as the pipette advanced helped identify these neurons.
3. The axons of these neurons within the contralateral funiculus, at the Th11-Th12 level were stimulated extradurally, with two silver ball electrodes in contact with the surface of ipsi and contralateral half of the spinal cord over the lateral funiculus (iTh, coTh), using constant current pulses of 100-150  $\mu\text{A}$  for 0.2ms duration to track neurons in the spinal cord. Any neurons antidromically activated were hence taken to be ascending tract neurons. When the neurons were recorded extracellularly prior to penetration a collision test was performed to ensure that the shortest latency spike potentials were indeed evoked antidromically and not synaptically by colliding the antidromic spike evoked by the LRN with the Th stimulus. Intracellular spikes at a constant latency, usually

approximately coinciding with the descending volleys induced by the LRN and Th stimuli, lack of preceding EPSPs and the appearance of these spikes in an all-or-none fashion were used as criteria for antidromic activation.

#### 4. Lack of antidromic activation to the SRT from the interpositus.

Monopolar records of incoming afferent and descending volleys, associated with the PSPs or spike potentials of the SRT neurons were taken from the surface of the spinal cord with a silver ball electrode in contact with the dorsal columns close to the dorsal root entry zone or the lateral funiculus on the side of location of the SRT, usually within 5-10mm of the microelectrode recording site. The reference electrode was inserted into the muscles surrounding the cord. Both the original records and averages of 10 or 20 single-sweep records were stored (using software designed by E. Eide, N. Pihlgren, and T. Holmström, Department of Physiology, Göteborg University). The measurements of amplitudes and latencies of PSPs evoked from the LRN were made from the averaged records. A paired Student's t test was used for the statistical analysis. The reproduction of the records was made using CorelDraw 15 system (Figure 5-2).

#### *Labelling and perfusion*

For the labelling experiments, once the area and the right angle for the cells were identified they were tracked with a rhodamine-containing electrode. After identification, the neurons were penetrated with micropipettes ("sharp", with tips broken to about 1.5-2.5 $\mu$ m, impedance of 7-20M $\Omega$ ). The neurons selected for morphological analysis were then labelled ionophoretically, with equal proportions of 5% tetramethylrhodamine-dextran (Molecular probes, Inc., Eugene, OR, USA) and 5% Neurobiotin (Vector, UK) in saline (Merck, Sweden, pH 6.5). This was achieved by passing a constant positive current of 1-10nA through the micropipette for up to 10mins, while continuous recordings verified that the electrode remained intracellular. A minimum space of 800 $\mu$ m was allowed between labelled neurons.

At the end, experiments were terminated by a lethal dose of Pentobarbital (Sigma-Aldrich, UK; 1ml at 200mg/ml i.p), the descending aorta was cannulated for perfusion of 2000ml of 4% freshly depolymerised formaldehyde (Sigma-Aldrich, Co, UK) in 0.1 M PB (Sigma-Aldrich, Co., UK).

Blocks of lumbar spinal cord (5-6 mm in length) containing labelled cells were removed and placed in the same fixative at 4°C for 8hrs. The remaining bits of dura and pia mater were cleaned off the blocks and with the rostral ends marked the spinal blocks were placed in PB for transportation.

#### *Revealing Neurobiotin and Rhodamine labelled cells*

At the University of Glasgow the spinal cord blocks were rinsed in 0.1 M PB, three times for 10 minutes each, and flat-embedded in 3% agar in distilled water. The tissue blocks (L3-L6 segments) were then cut into 50 µm thick transverse sections with a Vibratome (Leica VT1200, Leica Microsystems, UK). Serial sections were collected and placed in 0.1 M PB and then into 50% ethanol for 30 minutes to enhance antibody penetration. Thereafter the sections were washed three times with 0.1M phosphate buffered saline that contained 0.3 M sodium chloride (Sigma-Aldrich, UK; NaCl) in PBS, 10 minutes each and mounted in serial order with anti-fade medium, Vectashield (Vector Laboratories, UK) on glass slides. The sections were examined for labelled spinoreticular tract neurons with a fluorescence microscope and sectioned. The labelled neurons were then incubated in Avidin-Rhodamine (1:1000, Jackson Immunoresearch, UK) for three hours to reveal the detailed processes of the intracellularly Neurobiotin labelled neurons. Following three 10 minute washes in PBS, these sections were mounted serially on glass slides and cover slipped with Vectashield. Further processing for immunohistochemistry of the cells was performed on well labelled cells seen with the fluorescence microscope (see [Figure 5-3](#)).

#### *Processing for confocal microscopy*

Serial sections containing entire cell bodies and dendrites of intracellularly labelled cat neurons were scanned, using four channels of a confocal laser scanning microscope (LSM 710, Zeiss, Germany), and images were collected from each section. To examine contacts on these cells they were reacted in a cocktail of primary antibodies for two days; VGLUT-1, VGLUT-2 and VGAT in Group A. In the second group (Group B), gephyrin was added to reveal inhibitory post synaptic densities, ([Table 5-2](#)) along with VGLUT-1/2 & VGAT and subsequently immunoreacted in secondary fluorophores overnight.

### *Confocal microscopy analysis*

Although sixteen neurons were labelled, six were selected for detailed confocal analysis on the basis of the quality of labelling. These were scanned (x40, at a z-step of 0.5 $\mu$ m intervals) and analysed with NeuroLucida for Confocal software (MicroBrightfield Inc, Colchester, VT, USA). In reconstruction of cells, soma was drawn, the dendritic processes added and contacts plotted simultaneously with markers until the dendritic tree was fully reconstructed. The contact profiles were then counted for each animal and the final overall mean percentage contact densities  $\pm$  standard deviation (mean $\pm$ SD %) was calculated. Putative contacts were examined closely and only defined as appositions if the two labelled profiles were immediately adjacent with no intervening black pixels.

The contact densities were calculated using data generated by NeuroLucida and expressed as the number of contacts per unit area (100 $\mu$ m<sup>2</sup>) within a series of 25 $\mu$ m concentric spheres from the centre of the cell body using Sholl analysis with NeuroLucida Explorer (9.14, MicroBrightfield Inc, USA). The surface area of the cell body was calculated by measuring the perimeter of a projected confocal image of each labelled cell body using image J software (1.4.3.67, National Institute of Health, USA) and calculating the surface area of an equivalent sphere.

**Table 5-2 Summary of primary and secondary antibody combinations and concentrations to label excitatory and inhibitory contacts to spinoreticular cells in cat (n= 6 cells)**

	<b>Primary antibody combination</b>	<b>Primary antibody concentration</b>	<b>Supplier</b>	<b>Secondary antibody combination</b>	<b>Secondary antibody concentration</b>	<b>Supplier</b>
<b>A</b>	<b>gp VGLUT-1</b>	1:5000	Chemicon/Millipore, Harlow, UK	Alexa 488	1:500	Jackson Immunoresearch, West Grove, USA
	<b>rbt VGLUT-2</b>	1:5000	Synaptic systems, Göttingen, Germany	Pac-Blue	1:200	Jackson Immunoresearch
	<b>mo VGAT</b>	1:1000	Synaptic Systems, Göttingen, Germany	Alexa 647	1:500	Jackson Immunoresearch
<b>B</b>	<b>gpVGLUT-1/2</b>	1:5000	Chemicon/Millipore, Harlow, UK	Pac-Blue	1:200	Jackson Immunoresearch
	<b>rbt VGAT</b>	1:5000	Synaptic systems, Göttingen, Germany	Alexa 488	1:500	Jackson Immunoresearch
	<b>mo Gephyrin(7A)</b>	1:500	Synaptic systems, Göttingen, Germany	Alexa 647	1:500	Jackson Immunoresearch

All secondary antibodies were raised in donkey and conjugated to Rh. Red, Rhodamine Red; Alexa 647, Alexa-fluor647; Alexa 488, Alexa-fluor488; Pac-Blue, pacific blue; gp, guinea pig; rbt, rabbit; mo, mouse; VGLUT, vesicular glutamate transporter; VGAT, vesicular GABA transporter.

### 5.2.3 Aim II: Myelinated primary afferent contacts on spinoreticular cells in rat

#### *Surgical procedures*

Surgery was performed on three adult male Sprague-Dawley rats in two steps. In the first step, the rats were anaesthetised and placed in a stereotaxic frame for injection of 50nl 4% FG into the right LRN at inter-aural co-ordinates; anteroposterior -4.8mm, -1.8mm (medio-lateral) and at a dorso-ventral co-ordinate of -0.4mm to retrogradely label the SRT neurons in the lumbar spinal cord. The details of the surgery have already been described in Chapters 2 & 3. After recovery and a gap of about 48hrs, they were re-anaesthetised for the sciatic nerve injection.

The animals were placed prone on the table while the left sciatic nerve was exposed by making a 2cm curved incision approximately 1cm lateral to the spine extending down to the thigh. The trifurcation of the sciatic nerve, into the Posterior cutaneous nerve of the thigh, the Tibial and Common Peroneal nerves were identified and a small retractor placed distally under the sciatic nerve to stabilise it. A glass micro-pipette was then filled with a mixture of 4µl of 1% CTb and Fast-green dye. The tip was slid proximally at an angle of 45°, a centimetre into the perineurium of the sciatic nerve and the tracer pressure injected along the length just central to the trifurcation. It was then withdrawn slowly while injecting the tracer, which was visualised spreading around and along the length of the sciatic nerve. Care was taken while inserting the tip so as not to make another puncture through the perineurium and prevent extravasation of the tracer into the surrounding tissues. Once all the CTb/Dye was injected, the pipette was left in place for a minute to allow for diffusion and then gently withdrawn. The wound was then approximated, the skin sutured with 4.0 vicryl and the animal placed in an incubator to await recovery.

Following a five day post-sciatic nerve injection the animals were euthanised with Pentobarbitone and perfused with 4% formalin fixative trans-cardially. After dissecting out the brain and spinal cord, the medulla was sectioned at 100µm and the L3, L4 and L5 segments sectioned at 50µm ([Chapter 2, Section 2.1](#)).

### *Identification of the injection site*

The injection site in the brain was identified by mounting the medullary cut sections onto glass slides and was visualised with a fluorescence microscope as described previously in Chapter 3. The sections were photomicrographed using an ultraviolet filter and in dark field. The injection sites were then traced onto their respective templates from the stereotaxic rat brain atlas of Paxinos & Watson (2005) as shown in [Figure 5-4A, 1 to 3](#).

Some sections from the L3 to L5 segments were selected to determine if the CTb sciatic nerve injection was successful by using anti-CTb and DAB histochemistry ([Figure 5-4B](#)) as described in Chapter 2.

### *Immunocytochemistry, confocal microscopy and analysis*

Mid lumbar sections (L4-L5) were incubated in primary antibodies; FG to reveal the SRT cells and CTb to show the primary afferent contacts from the sciatic nerve. In addition to this, to determine if CTb originated from proprioceptors, they were reacted with parvalbumin (PV) and VGLUT-1.

Five fluorogold labelled cells from the deep dorsal, the intermediate laminae and lamina X were randomly selected for each animal (15 cells per animal). These cells were scanned with four channels of a confocal microscope (LSM 710, Zeiss, Germany) at x40 magnification. Reconstruction of the neurons was carried out following the procedure outlined in Chapter 2. CTb terminals (Rhodamine red) were identified and then checked for immunoreactivity to VGLUT1 (Av-Pacific blue) or PV (Alexa 647). A summary of the primary and secondary antibodies used along with their concentrations is given in [Table 5.3](#). The terminals were counted and contact densities/100 $\mu\text{m}^2$  calculated.

**Table 5-3 Primary and secondary antibody combinations and concentrations to identify retrogradely labelled fluorogold (FG) spinoreticular cells in the rat lumbar cord with CTb contacts (primary afferent) n=3**

Primary antibody combination	Primary antibody concentration	Supplier	Secondary antibody combination	Secondary antibody concentration	Supplier
mo CTb	1:5000	Abcam, Cambridge, UK	Rh. Red	1:100	Jackson ImmunoResearch, West Grove, USA
rbt FG	1:5000	Chemicon/Protos Biochem, CA, USA	Alexa 488	1:500	Jackson ImmunoResearch
gt PV	1:1000	Swant, Switzerland	Alexa 647	1:500	Jackson ImmunoResearch
gp VGLUT-1	1:5000	Chemicon/Millipore, Harlow, UK	IgG Biotin Av-pacific blue	1:500 1:1000	Jackson ImmunoResearch Molecular probes, Eugene, USA

All secondary antibodies were raised in donkey and conjugated to Rh. Red, Rhodamine Red; Alexa 647, Alexa fluor 647; Alexa 488, Alexa-fluor 488; Av-pacific blue, Avidin pacific blue; gt, goat; gp, guinea pig; rbt, rabbit; mo, mouse; CTb, B- subunit of cholera toxin; VGLUT, vesicular glutamate transporter; PV, parvalbumin; FG, fluorogold.

#### 5.2.4 AIM III: ChAT and calbindin contacts on spinoreticular cells in rat lumbar cord

To further investigate the types of contacts received by SRT cells from interneurons, experimental procedures were carried out on three rats as described in [Section 5.2.1](#) of this chapter and in [Chapter 2 Section 2.1](#) (General experimental procedures).

The first step, to label the SRT neurons in the lumbar spinal cord was accomplished by injecting 0.2 µl of 1% CTb into the left LRN of three adult male Sprague-Dawley rats with the injection sites identified by using DAB as a chromogen as seen in [Figure 5-5](#) (details in [Chapter 2, Section 2.2](#)).

##### *Immunohistochemistry, confocal microscopy, reconstructions and analysis*

Transverse sections from L3 to L5 of 50µm thickness were prepared following the procedure described in [Chapter 2 \(Section 2.3\)](#). Retrogradely labelled SRT cells were identified by the presence of CTb and additionally, ChAT and CB nerve terminals in contact with these neurons were analysed immunohistochemically. Three colour immunofluorescence was performed on selected sections from each lumbar segment by incubating them in primary anti-sera; CTb, ChAT and CB ([Table 5-4](#)).

CTb labelled cells were selected from each of the three zones of the transverse lumbar spinal sections, i.e. deep dorsal horn consisting of lamina IV and V cells, intermediate consisting of lamina VI and VII cells and lamina X cells. These cells were scanned using three channels of a confocal laser scanning microscope (Bio-Rad Radiance 2100, Hemmel Hempstead, Uk and LSM 710, Zeiss, Germany) and subsequently analysed using Neurolucida for Confocal software (Microbrightfield Inc, USA). The reconstruction was started with the cell body and the dendrites added on with the respective markers (ChAT and CB) simultaneously until the dendritic tree was fully reconstructed.

**Table 5-4 Primary and secondary antibody concentrations and combinations to label spinoreticular cells (CTb) for ChAT and CB contacts (n=3)**

Primary antibody combination	Primary antibody concentration	Supplier	Secondary antibody combination	Secondary antibody concentration	Supplier
mo *CTb	1:250	Annika Wilkstrom, Göteborg, Sweden	Rh. Red	1:100	Jackson Immunoresearch, West Grove, USA
gt ChAT	1:100	Chemicon/ Millipore, CA, USA	Dylight 649	1:500	Jackson Immunoresearch
rbt CB	1:1000	Swant, Switzerland	Alexa 488	1:500	Jackson Immunoresearch

All secondary antibodies were raised in donkey and conjugated to Rh. Red, Rhodamine Red; Alexa 488, Alexa-fluor 488; gt, goat; rbt, rabbit; mo, mouse; \*CTb, b subunit of cholera toxin (a gift from Annika Wilkstrom); ChAT, choline acetyl-transferase; CB, calbindin.

### 5.2.5 Statistical Analysis

Data are expressed as mean  $\pm$  standard deviation (SD). Multi-group comparisons were made using analysis of variance (ANOVA), followed by a post hoc *Tukey's* analysis as appropriate (GraphPad Prism version 6.02, GraphPad Software, La Jolla California USA). A  $p < 0.05$  was considered to be statistically significant.

## 5.3 Results

### 5.3.1 AIM I: What are the proportions of excitatory and inhibitory contacts associated with spinoreticular neurons in the lumbar spinal cord of the rat and cat?

#### 5.3.1.1 Contacts to SRT cells in rat

A total of 231 cells that were retrogradely labelled by CTb tracer injections into the LRN were analysed for contacts. The first criterion for choosing the cells to be analysed was that they had well labelled somata and dendrites of up to 50µm distance from the soma centre. The second criterion took into consideration the fact that we were looking at cells in three different zones, the deep dorsal laminae (Lamina IV and V), the intermediate laminae (VI and VII) and lamina X. The first subgroup was analysed for glutamatergic contacts from, both VGLUT-1 and VGLUT-2 containing axons as a first step to determine the possible sources of input to these cells. VGLUT-1 is found in most myelinated primary afferent terminals and some descending systems, such as the corticospinal tract, whereas any VGLUT 2 terminals would indicate an intraspinal origin or perhaps a descending tract (Varoqui H et al., 2002, Oliveira AL et al., 2003, Todd AJ et al., 2003, Alvarez FJ et al., 2004).

In the second subgroup, I looked at inhibitory contacts in the form of VGAT terminals which would define both GABAergic and glycinergic terminals as it is well established that both GABA and glycine are co-localised in most inhibitory boutons in the spinal cord (Todd AJ and Sullivan AC, 1990, Chaudhry FA et al., 1998, Du Beau A et al., 2012, Shrestha SS et al., 2012a, Huma Z et al., 2014). Gephyrin was added to find out whether these inhibitory terminals made synapses with SRT cells.

#### *Excitatory contacts on the spinoreticular cells in the rat*

In total, 116 cells in Group A (Table 5.1) were analysed. The confocal microscope images for these SRT cells, shown in Figure 5-6, illustrate that there are more VGLUT-2 contacts compared to VGLUT-1 immunoreactive contacts. Approximately 90% of the excitatory contacts on SRT cells are VGLUT-2 positive.

Furthermore, a quantitative comparison of VGLUT-1 and VGLUT-2 contact densities on SRT neurons reveal a significantly higher density of VGLUT-2 contacts in comparison to VGLUT-1, that is  $1.97 \pm 0.53$  and  $0.16 \pm 0.09$  contact densities/ $100\mu\text{m}^2$ , respectively (Anova,  $p < 0.01$ ; [Table 5-5](#), [Figure 5-7A](#)).

Cells in lamina X have contact densities of  $0.27 \pm 0.07$  and  $2.28 \pm 2.35/100\mu\text{m}^2$ , of VGLUT-1 and VGLUT-2, respectively, while cells from two other areas, the intermediate and deep dorsal laminae, have contact densities of,  $0.12 \pm 0.14$  &  $0.1 \pm 0.17$  contact densities/ $100\mu\text{m}^2$ , respectively, for VGLUT-1; and  $1.75 \pm 2.19$  &  $1.63 \pm 2.05$  contact densities/ $100\mu\text{m}^2$ , respectively for VGLUT-2.

[Table 5-5](#) provides a measure of differences in contact densities on the soma and dendrites seen in [Figure 5-6](#) and [Figure 5-7A](#). These show that there is significantly higher VGLUT-2 contact density on the dendrites when compared with the soma,  $1.34 \pm 0.44$  and  $0.25 \pm 2.42$  contact densities/ $100\mu\text{m}^2$  respectively ( $p < 0.01$ , 2 way Anova, post hoc *Tukey's*). There is a 3:1 ratio of VGLUT-1 contact densities between dendrites and soma. The Sholl analysis in [Figure 5-8A](#) illustrates that, along the length of the dendrites there is a decrease in VGLUT-2 contact density from the more proximal to distal dendrites whereas the VGLUT-1 terminals are more or less evenly spread out. This difference is statistically significant at each successive increment ( $p < 0.001$ , 2 way Anova, post hoc *Tukey's*).

**Table 5-5 The number and densities of VGLUT-1(VG-1) and VGLUT-2 (VG-2) axon terminals in apposition with cell bodies and dendrites of retrogradely labelled spinoreticular tract neurons in rats (n=3)**

Spinoreticular neurons	Animal	No. of cells	Total number of contacts soma and dendrites		Soma					Dendrite					
					Contacts (n)		Surface area ( $\mu\text{m}^2$ )	Density (n/ 100 $\mu\text{m}^2$ )		Contacts (n)		Total dendritic length ( $\mu\text{m}$ )	Surface area ( $\mu\text{m}^2$ )	Density (n/ 100 $\mu\text{m}^2$ )	
					VG-1	VG-2		VG-1	VG-2	VG-1	VG-2			VG-1	VG-2
					VG-1	VG-2	VG-1	VG-2	VG-1	VG-2	VG-1	VG-2	VG-1	VG-2	
<b>Lamina X</b>	1	11	189	1583	43	599	25865.71	0.17	2.32	145	1110	2580.5	27415.41	0.53	4.05
	2	9	72	502	20	234	18672.16	0.11	1.25	56	268	1071.3	14002.45	0.40	1.91
	3	18	108	1553	25	381	38463.29	0.06	0.99	86	1212	3474.5	44894.75	0.19	2.70
<b>Mean</b>							<b>0.11</b>	<b>1.52</b>					<b>0.37</b>	<b>2.89</b>	
<b>SDEV</b>							<b>0.05</b>	<b>0.70</b>					<b>0.17</b>	<b>1.08</b>	
<b>Intermediate laminae</b>	1	11	75	1604	19	419	33154.46	0.06	1.26	56	1193	3261.6	52151.68	0.11	2.29
	2	17	134	2005	15	669	46391.77	0.03	1.44	104	1326	3578.3	50078.40	0.21	2.65
	3	22	141	2229	29	608	55090.65	0.05	1.10	114	1635	6340.4	82930.20	0.14	1.97
<b>Mean</b>							<b>0.05</b>	<b>1.27</b>					<b>0.15</b>	<b>2.30</b>	
<b>SDEV</b>							<b>0.01</b>	<b>0.17</b>					<b>0.05</b>	<b>0.34</b>	
<b>Deep dorsal laminae</b>	1	5	70	779	15	159	13818.57	0.11	1.15	67	618	1676.6	17163.26	0.39	3.60
	2	12	65	989	33	411	24670.83	0.13	1.67	44	689	2309.4	27242.26	0.16	2.53
	3	11	119	2046	30	475	56213.21	0.05	0.84	89	1562	5693.3	73684.45	0.12	0.12
<b>Mean</b>							<b>0.10</b>	<b>1.22</b>					<b>0.22</b>	<b>2.08</b>	
<b>SDEV</b>							<b>0.04</b>	<b>0.41</b>					<b>0.15</b>	<b>1.78</b>	

### *Inhibitory synapses on the spinoreticular cells in rat*

In total, 115 cells were analysed in Group B (Table 5-1). Immunoreactivity for VGAT was used to reveal axonal inhibitory terminals containing GABA and/or glycine and a combination of antibodies against VGLUT-1 and VGLUT-2 was used to reveal excitatory contacts irrespective of their sources of origin. The confocal image in Figure 5-9 illustrates the distribution of these excitatory contacts and inhibitory synapses which are evenly distributed on the somata and dendrites of the cells. Gephyrin was used to confirm that the inhibitory contacts (VGAT) are synapses; the majority, if not all, of the VGAT terminals are associated with post synaptic gephyrin puncta.

The average contact density of VGAT terminals per  $100\mu\text{m}^2$  to VGLUT-1/2 contacts is  $2.45\pm 0.47$  and  $1.95\pm 0.59$  contact densities/ $100\mu\text{m}^2$ , respectively (mean $\pm$ SD, Table 5-6, Figure 5-7B). The overall distribution pattern along the dendrites is more or less consistent, with both the excitatory and inhibitory terminals spread out evenly as can be seen in the Sholl analysis in Figure 5-8A. The contact densities of VGAT terminals on both soma and dendrites are more or less the same throughout the various laminae (Table 5-6).

**Table 5-6 The numbers and contact densities of VGLUT-1 & 2 (VG 1&2) and VGAT axon terminals in apposition to the soma and dendrites of retrogradely labelled spinoreticular tract neurons in rats (n=3)**

Spinoreticular neurons	Animal	No. of cells	Total number of contacts soma and dendrites		Soma					Dendrite					
					Contacts (n)		Surface area ( $\mu\text{m}^2$ )	Density (n/ 100 $\mu\text{m}^2$ )		Contacts (n)		Total dendritic length ( $\mu\text{m}$ )	Surface area ( $\mu\text{m}^2$ )	Density (n/ 100 $\mu\text{m}^2$ )	
			VG1&2	VGAT	VG1&2	VGAT		VG1&2	VGAT	VG1&2	VGAT			VG1&2	VGAT
Lamina X	1	11	929	1015	210	330	9968.03	2.11	3.31	753	721	2326.00	26210.18	2.87	2.75
	2	17	1195	1119	260	408	23855.34	1.09	1.71	823	664	4009.40	40056.51	2.05	1.66
	3	12	567	866	149	273	8641.75	1.72	3.16	418	593	1896	22469.76	1.86	2.64
<b>Mean</b>							<b>1.64</b>	<b>2.73</b>						<b>2.26</b>	<b>2.35</b>
<b>SD</b>							<b>0.51</b>	<b>0.88</b>						<b>0.54</b>	<b>0.60</b>
<b>Intermediate</b>															
Laminae	1	17	2294	2144	434	606	20308.62	2.14	2.98	1860	1538	4369.40	55060.10	3.38	2.79
	2	15	1315	1491	361	518	28591.36	1.26	1.81	993	985	4195.40	48803.88	2.03	2.02
	3	17	677	1155	112	302	12464.05	0.90	2.42	565	853	2729.7	36384.30	1.55	2.34
<b>Mean</b>							<b>1.43</b>	<b>2.41</b>						<b>2.32</b>	<b>2.39</b>
<b>SD</b>							<b>0.64</b>	<b>0.59</b>						<b>0.95</b>	<b>0.39</b>
<b>Deep Dorsal</b>															
Laminae	1	9	1169	1601	247	465	13569.99	1.82	3.43	915	1143	3568.60	37184.69	2.46	3.07
	2	10	1307	1721	290	557	29354.21	0.99	1.90	909	1139	4915.90	54189.12	1.68	2.10
	3	8	824	1570	126	312	11649.20	1.08	2.68	698	1258	3347.2	56566.65	1.23	2.22
<b>Mean</b>							<b>1.30</b>	<b>2.67</b>						<b>1.79</b>	<b>2.47</b>
<b>SD</b>							<b>0.46</b>	<b>0.76</b>						<b>0.62</b>	<b>0.53</b>

### 5.3.1.2 Excitatory and inhibitory contacts on spinoreticular cells in cat

In all six cats, recordings were taken from many SRT cells identified antidromically by: collision of the antidromic spike evoked from the LRN and the Th stimulus; stimulating the peripheral nerve and thoracic spinal cord at a critical interval; as well as taking note of the anatomical location of recorded cells within Rexed lamina VI-VII. A detailed explanation of the selection criteria has already been explained in [Section 5.2.2 Aim 1b](#). The cells had stable recording and robust penetrations so that spikes proved that the recordings were intracellular, as shown in [Figure 5-2](#).

Electrophysiological recordings from a neuron representative of these spino-reticulo-cerebellar (SRC) neurons are shown in [Figure 5-2 \(1\)](#). Stimulation of the contralateral pyramidal tract (coPT) revealed EPSPs at latencies of 4.5ms, compatible with di or oligosynaptic input [Figure 5-2 \(2\)](#). Furthermore, the records illustrate strong inhibition from muscle afferents; Quadriceps nerve (Q) with a lack of excitatory inputs from this nerve<sup>5</sup>. In addition these SRT neurons receive cutaneous inhibitory inputs via the Saphenous nerve (Saph) but the most potent inhibition was from Q and SP [Figure 5-2 \(3\)](#). Some of the cells did not respond to primary afferent stimulation from the ipsilateral Tibial (Tib) and Superficial Peroneal (SP) or bilateral Quadriceps (Q) and Saphenous (Saph) nerves.

Out of 16 Neurobiotin-Rhodamine labelled cells, six were selected for detailed analysis on the basis of good cytoarchitecture. They were also chosen on the basis of anatomical location with a distance of at least 800µm in between two cells so that during reconstruction there was no confusion about overlapping dendrites. The soma locations of these neurons are shown as red dots within L4-L5 segments in [Figure 5-3](#), located in the mid lamina VII region.

These cells have a range of soma sizes, from 20µm to 65µm and have smaller dendritic arbors to quite extensive ones as shown in [Table 5-7](#). However, there is no set pattern to divide the cells up into subgroups based on morphological criteria.

<sup>5</sup> While the first cells we labelled had practically no excitation from peripheral nerves, there were cells later on that were excited albeit weakly, from Q.

As described in the methods section ([Section 5.2.2](#)), immunoreactivity to VGLUT-1 and VGLUT-2 was used to label excitatory glutamatergic contacts and VGAT to reveal inhibitory axonal terminals containing GABA and/or glycine. In addition two of the cells were also labelled with the post synaptic inhibitory marker gephyrin to confirm that the VGAT terminals associated with them made synapses.

The confocal images in [Figure 5-10](#) illustrate that the majority of the contacts are immunopositive for VGLUT-2 with some VGLUT-1 terminals interspersed among them especially along the dendrites. On the other hand the proportion of VGAT terminals to glutamatergic VGLUT-2 terminals is approximately equal. This is more clearly demonstrated in reconstructions of the individual cells in [Figures 5-11A to D](#). Images a, illustrate the relative distribution of VGLUT-2 (red) and VGAT (blue) on the neurons while images b, illustrate both of the excitatory terminals VGLUT-2 (red) and VGLUT-1 (green) on the cell bodies and dendrites for each of the reconstructed neurons. The emerging pattern clearly demonstrates an overwhelming abundance of VGAT and VGLUT-2 contacts and a smaller proportion of VGLUT-1 contacts.

The overall average contact densities of VGAT (inhibitory) and VGLUT-1&2 (excitatory) per  $100\mu\text{m}^2$  on both soma and dendrites together was  $2.67\pm 0.33$  and  $2.41\pm 0.9$  ([Table 5-7](#));  $p>0.05$ , [Figure 5-7C](#)). Although, somata had 1.4 times more VGAT boutons as compared to VGLUT-1&2 excitatory terminals ([Table 5-7](#)).

The results of the quantitative comparison of the distribution of VGAT and VGLUT-1 & 2 contacts at certain distances from the soma are summarised in [Figure 5-8B](#). They are based on Sholl analysis, where the number of contacts in concentric circles from the soma is plotted per  $25\mu\text{m}$  increments of distance from the soma. The average contact density of VGLUT-1 terminals/ $100\mu\text{m}^2$ , was  $0.42\pm 0.24$  on both soma and dendrites which was significantly lower than both the VGLUT-2 and VGAT contact densities (one way-Anova,  $p<0.001$ , [Figure 5-7C](#)).

The confocal scan seen in [Figure 5-12](#) clearly illustrates VGAT terminals in contact with gephyrin puncta (reconstructions in [Figures 5-13 A & B](#)).

### 5.3.1.3 Comparison of excitatory and inhibitory contacts on spinoreticular cells in the rat and cat

Tables 5-5 and 5-6 summarise data for retrogradely labelled SRT cells in the rat with the number and contact densities of glutamatergic and GABAergic contacts on these cells. Together with Table 5-7 for cat, it shows that the overall contact densities of these terminals in the rat were slightly lower than in the cat both on somata and dendrites. Although, the range of soma sizes for cat SRT neurons (20-65 $\mu$ m in diameter) and rat (20-50 $\mu$ m) within the intermediate laminae are comparable. As can be seen in the Sholl analysis in Figure 5-8A & B, although the cat cells have a much more extensive dendritic tree when compared to the rat which is probably due to intracellular filling of the cells; the results are still comparable with higher numbers of VGAT and VGLUT-2 contacts as opposed to VGLUT-1 terminals. Most glutamatergic contacts are, ~88% (cat) and ~90% (rat) VGLUT-2 positive. The proportions of inhibitory to excitatory contacts in the cat and rat are more or less the same, 59% to 55% VGAT and 41% to 45% VGLUT-1 & 2, in the cat and rat, respectively.

Hence, both species have more inhibitory contacts than excitatory ones (VGLUT-2) and both of these types of contact are significantly higher than VGLUT-1 ones. These results compare well with the electrophysiological data, that primary afferent inputs exert inhibitory changes on the SRT neurons (Figure 5-2, Panel 3), rather than monosynaptic excitatory.

Table 5-7 The number and densities of VGAT, VGLUT-1 and 2 (VG 1&2) axon terminals in apposition with the cell bodies and dendrites of intra intracellularly labelled Spinoreticular cat cells (n=6)

Spinoreticular neurons	Total contacts (n) soma and dendrites		Soma						Dendrite					
			Surface area		soma diameter( $\mu\text{m}$ )	Density		Total dendritic		Surface area ( $\mu\text{m}^2$ )	Density			
	Contacts (n)		( $\mu\text{m}^2$ )	( $\text{n}/100\mu\text{m}^2$ )		Contacts (n)		length ( $\mu\text{m}$ )	( $\text{n}/100\mu\text{m}^2$ )					
	VGAT	VG1&2		VGAT	VG1&2	VGAT	VG1&2		VGAT	VG1&2	VGAT	VG1&2		
cell 1	1501	1773	59	93	4921.49	39.59	1.20	1.89	1442	1650	4681.6	59021.33	2.44	2.80
cell 2	805	942	29	57	1312.34	20.44	2.21	4.34	776	885	2950	26686.16	2.91	3.32
cell 3	1160	1192	183	136	3247.76	32.16	5.63	4.19	977	1056	2462.6	35147.20	2.78	3.00
cell 4	2597	2386	162	66	4259.46	36.83	3.80	1.55	2435	2320	6213.9	86316.27	2.82	2.69
cell 5	6719	3709	445	144	13409.75	65.35	3.32	1.07	6274	3565	25557.4	293743.07	2.14	1.21
cell 6	4781	2422	584	279	12705.25	63.61	3.50	1.13	4197	2143	12368.6	163343.45	2.57	1.31
<b>Mean</b>							<b>3.28</b>	<b>2.36</b>					<b>2.61</b>	<b>2.39</b>
<b>SD</b>							<b>1.51</b>	<b>1.50</b>					<b>0.29</b>	<b>0.90</b>
	<b>VG-2</b>	<b>VG-1</b>	<b>VG-2</b>	<b>VG-1</b>			<b>VG-2</b>	<b>VG-1</b>	<b>VG-2</b>	<b>VG-1</b>			<b>VG-2</b>	<b>VG-1</b>
cell 1	1387	386	65	28	4921.49		1.32	0.57	1322	328		59021.33	2.24	0.61
cell 2	762	180	51	6	1312.34		4.95	2.13	711	174		26686.16	2.66	0.65
cell 3	1136	56	128	8	3247.76		3.94	0.25	1008	48		35147.20	2.87	0.14
cell 4	2134	252	66	0	4259.46		1.55	0	2068	252		86316.27	2.40	0.29
<b>Mean</b>							<b>2.94</b>	<b>0.74</b>					<b>2.54</b>	<b>0.42</b>
<b>SD</b>							<b>1.79</b>	<b>0.96</b>					<b>0.28</b>	<b>0.25</b>

### 5.3.2 AIM II What proportion of contacts on rat spinoreticular tract cells originate from myelinated primary afferents?

A total of 50 cells in the lumbar spinal cord were analysed for myelinated primary afferent contacts. This was accomplished by injecting CTb into the sciatic nerve and observing CTb labelled terminals in contact with SRT cells, ipsilaterally. FG injection sites reconstructed in [Figure 5-4](#) for each animal were mainly focused on the LRN but there was some spread dorsally into the ventral medullary reticular nucleus and the intermediate reticular nucleus. [Figure 5-4B](#) shows the pattern of CTb labelled primary afferent terminals in the lumbar spinal cord extending from the superficial dorsal horn to the deep dorsal laminae with sparser terminals in the medial part of the intermediate laminae and lamina X.

At least five cells each were selected from three areas of the mid-lumbar sections; deep dorsal laminae, intermediate laminae and lamina X for each rat. The confocal image in [Figure 5-14](#) illustrates a FG labelled SRT neuron with CTb contacts positive, for both parvalbumin as well as VGLUT-1, while some are immunoreactive to VGLUT-1 only. Double immunoreactivity for VGLUT-1 and PV was used as an indication of proprioceptive origin, as explained in the introduction. As there was no significant difference in the contacts to the soma and dendrites data are presented as total SRT contact densities as shown in [Table 5-8](#). There is no statistically significant difference in contacts associated with SRT cells in the three areas of the grey matter examined ([Figure 5-15](#)). Although CTb contacts that were positive for both VGLUT-1 as well as PV were sparse, the deep dorsal horn cells have comparatively more contacts from proprioceptors ( $0.04 \pm 0.02$  contact densities/ $100\mu\text{m}^2$ ; mean $\pm$ SD), as compared to lamina X ( $0.01 \pm 0.01$  contact densities/ $100\mu\text{m}^2$ ; mean $\pm$ SD) and lamina VII, VIII neurons ( $0.01 \pm 0.00$  contact densities/ $100\mu\text{m}^2$ ; mean $\pm$ SD). Furthermore the highest contact density of CTb terminals/ $100\mu\text{m}^2$ , with VGLUT-1 only, is present on lamina IV and V cells ( $0.15 \pm 0.05$ ; mean $\pm$ SD). Hence, the within group comparison for deep dorsal laminae shows significantly higher CTb/VGLUT-1 contact densities contacts when compared with CTb/PV/VGLUT-1 or purely CTb ( $p < 0.01$  and  $p < 0.001$ , respectively, post hoc *Tukey's*).

The pie-chart in [Figure 5-16](#) shows various proportions of the CTb primary afferent contacts on spinoreticular tract neurons. The proprioceptive input (CTb/VGLUT-1/PV) to all SRT cells is about 17% of all CTb terminals labelled by sciatic nerve injection ( $0.04 \pm 0.02$  contact densities/ $100\mu\text{m}^2$ ; mean $\pm$ SD). The majority of the primary afferents were of non-proprioceptive origin, presumably cutaneous. In addition there are a significant number of pure CTb contacts onto SRT cells ( $0.15 \pm 0.07$  contact densities/ $100\mu\text{m}^2$ ; mean $\pm$ SD).

Table 5-8 Primary afferent (CTb), VGLUT-1(VG1) and Parvalbumin (PV) positive contact densities on retrogradely labelled SRT cells in the rat mid-lumbar spinal cord (n=3)

	Animal	No. of cells	Contacts (n) (total number soma and dendrites)						Total Surface area ( $\mu\text{m}^2$ )	Density (n/ 100 $\mu\text{m}^2$ )					
			VG1	PV	CTb	VG1/CTb	VG1/PV	VG1/CTb/PV		VG1	PV	CTb	VG1/CTb	VG1/PV	VG1/CTb/PV
<b>Lamina X</b>	1	6	105	91	6	18	45	5	26167.13	0.40	0.35	0.02	0.07	0.17	0.02
	2	7	112	135	7	38	82	6	29861.04	0.38	0.45	0.02	0.13	0.27	0.02
	3	6	67	146	9	17	24	1	31977.19	0.21	0.46	0.03	0.05	0.08	0.00
<b>Mean</b>										<b>0.32</b>	<b>0.42</b>	<b>0.02</b>	<b>0.08</b>	<b>0.17</b>	<b>0.01</b>
<b>SD</b>										<b>0.10</b>	<b>0.06</b>	<b>0.00</b>	<b>0.04</b>	<b>0.10</b>	<b>0.01</b>
<b>Intermediate Laminae</b>	1	6	139	86	11	9	9	5	59258.02	0.23	0.15	0.02	0.02	0.02	0.01
	2	4	108	112	16	73	14	4	37443.05	0.29	0.30	0.04	0.19	0.04	0.01
	3	4	62	93	5	12	11	3	18504.08	0.34	0.50	0.03	0.06	0.06	0.02
<b>Mean</b>										<b>0.27</b>	<b>0.25</b>	<b>0.03</b>	<b>0.08</b>	<b>0.03</b>	<b>0.01</b>
<b>SD</b>										<b>0.05</b>	<b>0.18</b>	<b>0.01</b>	<b>0.09</b>	<b>0.02</b>	<b>0.00</b>
<b>Deep Dorsal Laminae</b>	1	6	175	154	3	53	5	23	36405.08	0.48	0.42	0.01	0.15	0.01	0.06
	2	6	175	165	10	101	45	16	49375.91	0.35	0.33	0.02	0.20	0.09	0.03
	3	5	131	140	8	59	24	18	59909.00	0.22	0.23	0.01	0.10	0.04	0.03
<b>Mean</b>										<b>0.33</b>	<b>0.32</b>	<b>0.01</b>	<b>0.15</b>	<b>0.05</b>	<b>0.04</b>
<b>SD</b>										<b>0.13</b>	<b>0.09</b>	<b>0.01</b>	<b>0.05</b>	<b>0.04</b>	<b>0.02</b>

### 5.3.3 AIM IV: What proportion of contacts, on spinoreticular tract cells, is from ChAT, CB and PV terminals in the rat lumbar spinal cord?

In addition to tract tracing, using CTb to retrogradely label spinoreticular cells in the lumbar spinal cord, immunohistochemistry was used to label choline acetyl transferase (ChAT) and calbindin (CB) spinal neurons. This was done in order to find the source of some of the intra-spinal terminals, i.e. ChAT and CB to SRT cells. The antibody combinations and concentrations used are listed in [Table 5-4](#). The stereotaxic injection sites as illustrated in [Figure 5-5](#) were more or less localised to the lateral reticular nucleus but there was some spread to the surrounding reticular tissue in the CVLM, MdV and IRt. Some of the retrogradely labelled SRT cells also labelled positively for calbindin (CB) and so this part of the experiment was further subdivided into two parts; CB & ChAT inputs to SRT cells labelled by CB and SRT cells negative for CB.

A confocal scan of a CTb labelled SRT cell in [Figure 5-17](#) is shown with contacts from both ChAT and CB sources. The cholinergic contact densities averaged  $0.16 \pm 0.04 / 100 \mu\text{m}^2$  (mean  $\pm$ SD), which was significantly higher (Anova  $p < 0.001$ , post hoc *Tukey's*) than the CB contact density of  $0.02 \pm 0.01 / 100 \mu\text{m}^2$  (mean  $\pm$ SD) ([Table 5-9 & Figure 5-18C](#)). The intermediate laminae within group comparison showed significantly greater cholinergic contacts than calbindin for both SRT cell groups (Anova,  $p < 0.01$ , post hoc *Tukey's*, [Figure 5-18A](#)).

The confocal image in [Figure 5-20](#) illustrates the second group of CTb labelled SRT cells that were also, CB positive. The contact densities to these cells are similar to the previous group, with an average ChAT contact density of  $0.13 \pm 0.02 / 100 \mu\text{m}^2$  (mean  $\pm$ SD) and a mean CB contact density of  $0.01 \pm 0.01 / 100 \mu\text{m}^2$  (mean  $\pm$ SD; Anova  $p < 0.001$ , post hoc *Tukey's*, ([Table 5-9, Figure 5-18C](#)). Furthermore there is no statistically significant difference in the ChAT or CB contacts to these CTb+CB cells in the three zones; lamina X, intermediate and deep dorsal laminae of the L4/L5 segments ([Figure 5-18B](#)). However, each group within these zones has significantly more ChAT input as compared to CB contacts (Anova  $p < 0.001$ ; lamina X,  $p < 0.01$ ; laminae VI and VII,  $p < 0.001$ ; laminae IV and V, post hoc *Tukey's*). Comparing both cell groups i.e.

CTb and CTb+CB labelled, in [Figure 5-18C](#); although there was no between group difference in the ChAT or CB contact densities, ChAT contact densities were significantly higher within the groups ( $p < 0.001$ , Anova post hoc *Tukey's*).

#### *Parvalbumin contacts to spinoreticular cells*

In investigating primary afferent contacts to rat spinoreticular cells it was noted that quite a large proportion of terminals contacting these cells were immunoreactive for PV ([see Tables 5-8 and 5-9](#)) with contact densities of  $0.42 \pm 0.06/100\mu\text{m}^2$  (mean $\pm$ SD) on both soma and dendrites. These PV terminals are principally from interneurons within the spinal cord. As shown in [Figure 5-19](#), parvalbumin densities are significantly greater than either ChAT or CB terminal densities (Anova,  $p < 0.001$ , post hoc *Tukey's*).

Table 5-9 Choline acetyltransferase (ChAT), calbindin (CB) and parvalbumin (PV) contact densities associated with spinoreticular cells (n=6)

SRT cells	Animal	No. of cells	Both Soma and Dendrite					Soma				Dendrite					
			Contacts (total number)		Total surface area ( $\mu\text{m}^2$ )	Density (n/ 100 $\mu\text{m}^2$ )		Contacts (n)		Density (n/ 100 $\mu\text{m}^2$ )		Contacts (n)		Density (n/ 100 $\mu\text{m}^2$ )			
			ChAT	CB		ChAT	CB	ChAT	CB	ChAT	CB	ChAT	CB	ChAT	CB		
Only CTb	1	12	51	10	28835.18	0.18	0.03	26	7	8497.50	0.31	0.08	25	3	20337.68	0.12	0.01
	2	12	70	5	37544.20	0.19	0.01	25	1	8700.85	0.29	0.01	45	4	28843.35	0.16	0.01
	3	11	57	7	46470.47	0.12	0.02	21	1	12081.61	0.17	0.01	36	6	34388.86	0.10	0.02
<b>Mean</b>											<b>0.26</b>	<b>0.03</b>				<b>0.13</b>	<b>0.02</b>
<b>SD</b>											<b>0.07</b>	<b>0.04</b>				<b>0.03</b>	<b>0.00</b>
CTb and CB	1	12	53	7	47694.48	0.11	0.01	8	2	7225.93	0.11	0.03	45	5	40468.55	0.11	0.01
	2	12	55	0	45296.58	0.12	0	11	0	8699.56	0.13	0.00	44	0	36597.02	0.12	0.00
	3	11	39	3	26153.32	0.15	0.01	7	2	5396.05	0.13	0.04	32	1	20757.27	0.15	0.00
<b>Mean</b>											<b>0.12</b>	<b>0.02</b>				<b>0.13</b>	<b>0.01</b>
<b>SD</b>											<b>0.01</b>	<b>0.02</b>				<b>0.02</b>	<b>0.01</b>
			<b>PV</b>			<b>PV</b>		<b>PV</b>			<b>PV</b>		<b>PV</b>			<b>PV</b>	
Only CTb	4	18	91		88739.33	0.35		33		26581.92	0.39		58		62157.41	0.33	
	5	17	135		109098.00	0.45		35		23051.61	0.49		108		86046.38	0.48	
	6	15	146		123863.37	0.46		35		30005.64	0.45		111		93857.73	0.46	
<b>Mean</b>					<b>0.42</b>					<b>0.44</b>					<b>0.42</b>		
<b>SD</b>					<b>0.06</b>					<b>0.05</b>					<b>0.08</b>		

**Figure 5-2 Electrophysiological identification of a spinoreticular neuron in the cat lumbar spinal cord with excitatory and inhibitory inputs from various sources**

**Panel 1 Identification of SRT neurons**

**A.** Upper trace shows extracellular records (averages of 10 or 20 single recordings) in a SRT neuron by antidromic stimulation of the contralateral LRN (coLRN) and the lower traces are from the cord dorsum. **B.** The upper trace now shows the recording intracellularly in the same spinoreticular neuron and the lower trace is from the cord dorsum. **C & D.** Train of five stimuli with collision test from coTh and antidromic stimulation of LRN.

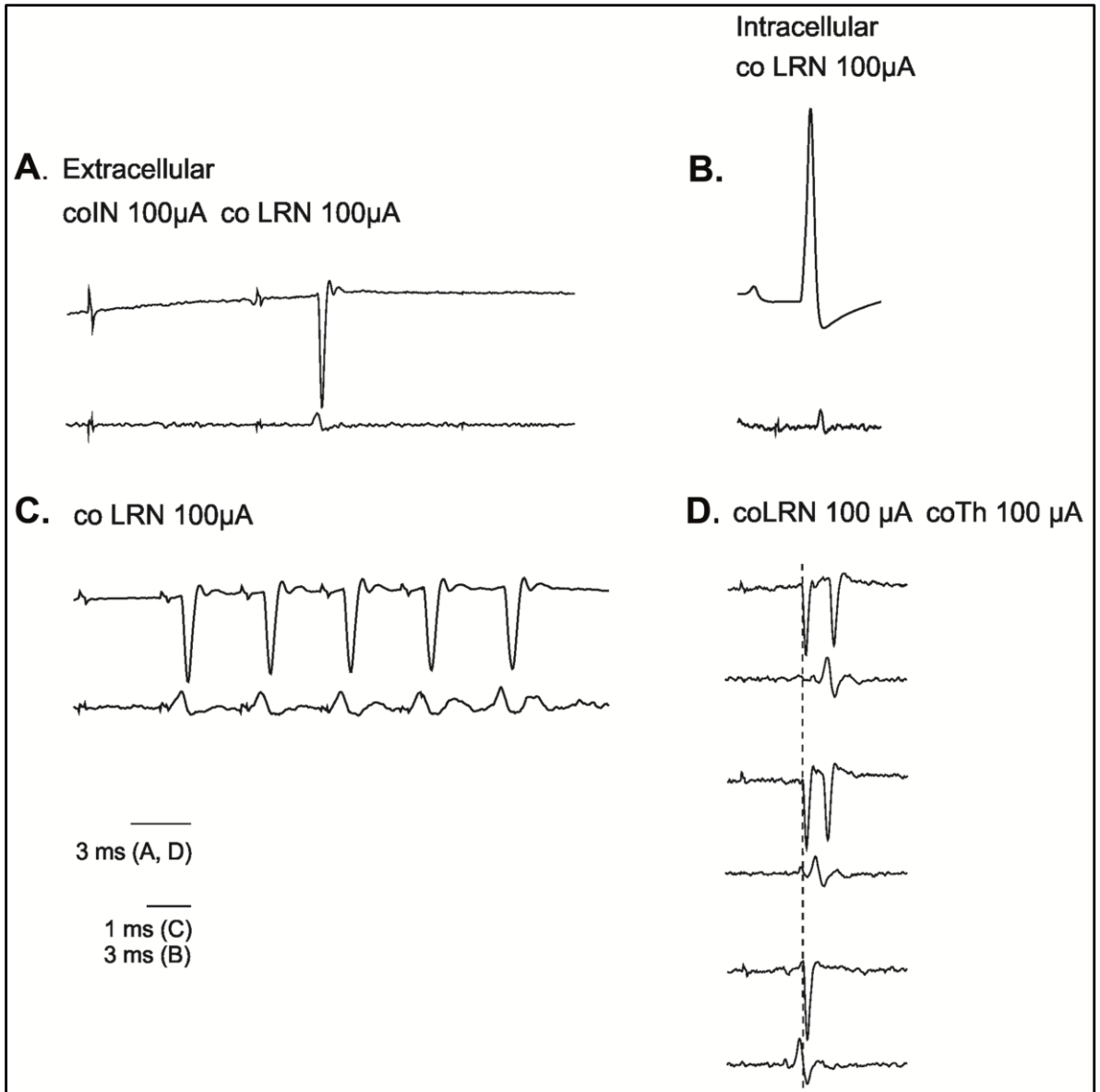
**Panel 2 Excitation by descending axons from the contralateral pyramidal tract**

**A.** Upper pair of traces shows extracellular records from an SRT neuron following stimulation of the contralateral pyramid and antidromic stimulation applied within the coLRN. Lower pair of traces shows intracellular records from the same cell. Lower traces in each pair show cord dorsum records. **B.** Excitatory effects with an increased number of antidromically evoked sub-threshold responses when preceded by stimulation of the coPT. Histograms are aligned with individual records with and without preceding coPT stimulation. Dashed horizontal line indicates the discrimination level used to create histograms online.

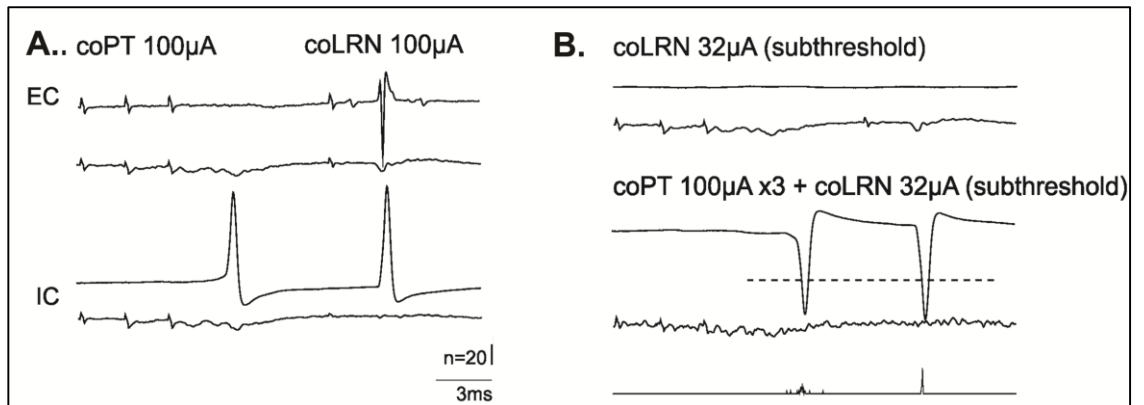
**Panel 3 Inhibition by peripheral afferents**

**A.** Records from a SRT neuron following stimulation of Saph 5T recorded extracellularly (upper trace) and the corresponding intracellular IPSP (middle trace) aligned with cord dorsum records (lower trace). **B.** No spikes evoked when preceded by stimulation with Saph 5T (grey) at the critical level as opposed to without Saph (black). Aligned with individual records are histograms created online illustrating the reduced number of evoked responses following Saph stimulation (grey). **C.** IPSPs evoked from Quadriceps (Q) at intensities 5 times the threshold (T). **D.** Di or Oligo synaptic IPSPs are evoked from the MLF. The lowest trace in each recording is the cord dorsum. The negativity is downward in intracellular records and upward in those from the cord dorsum.

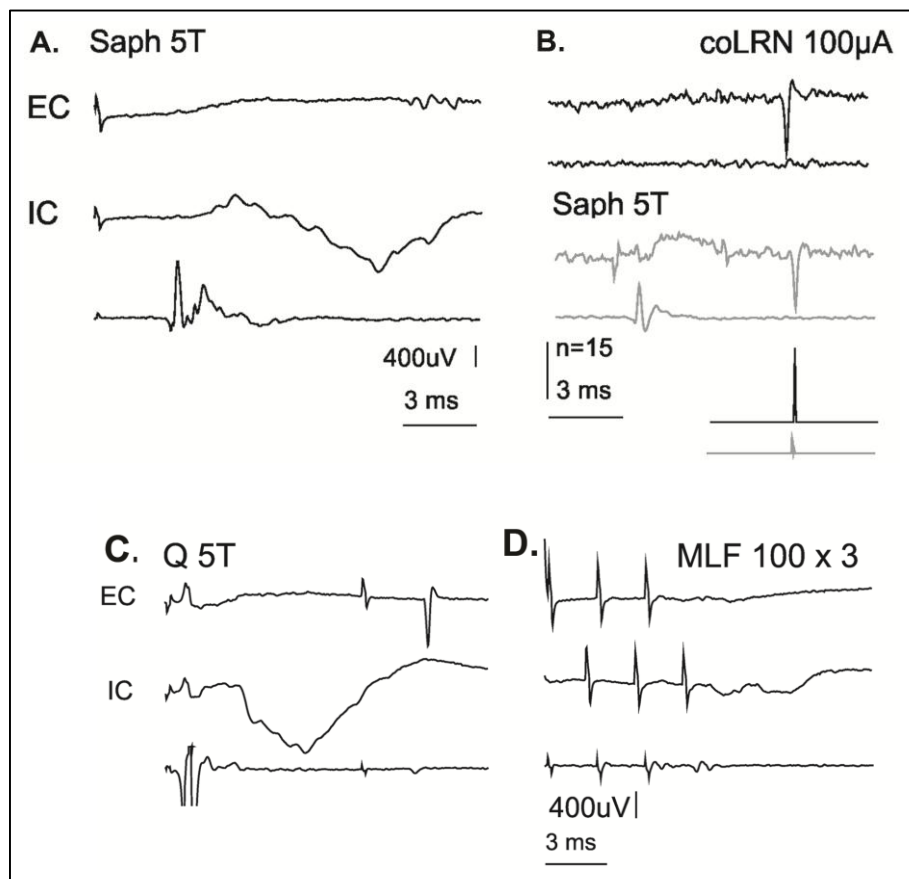
# 1. Identification of spinoreticular neurons



## 2. Excitatory inputs



## 3. Inhibitory inputs



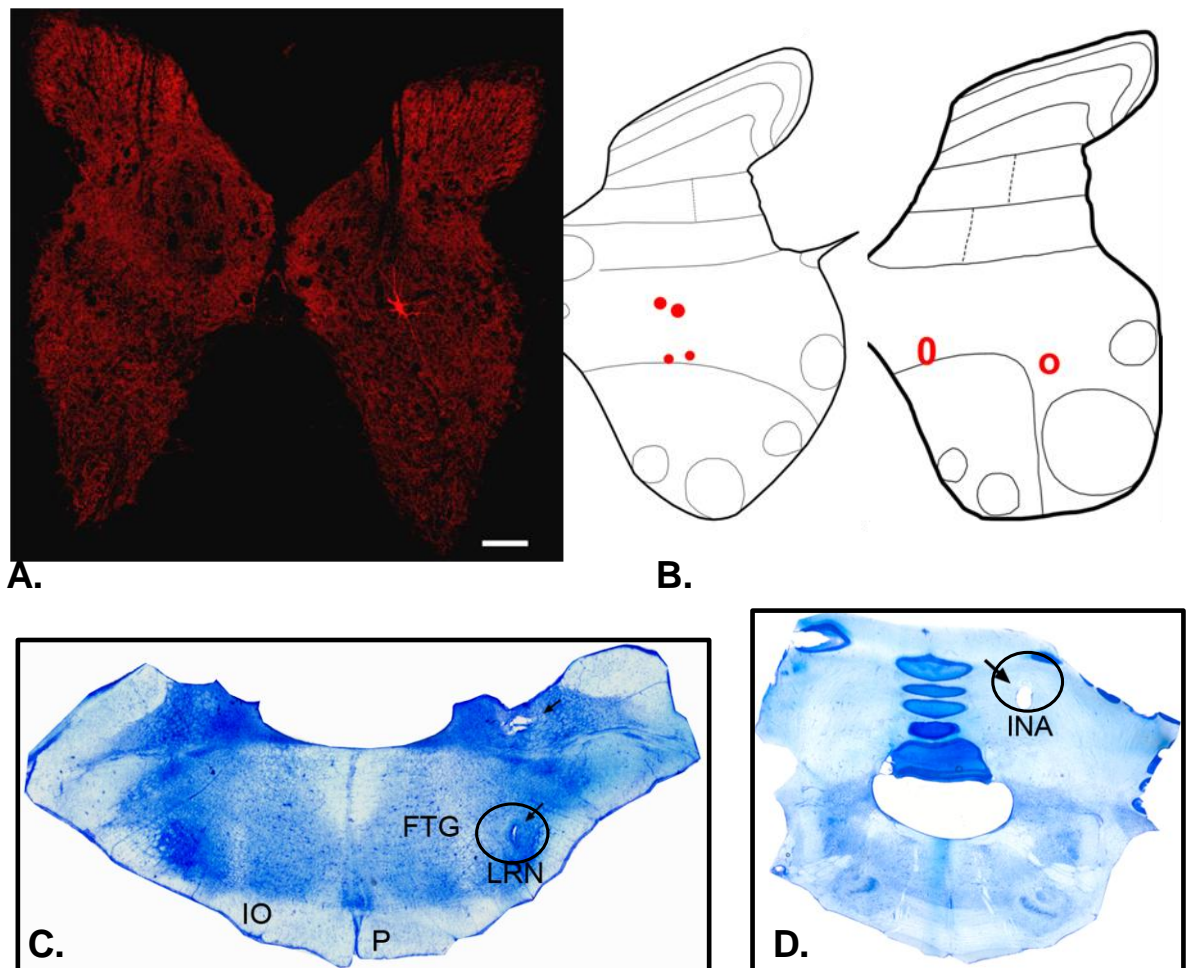


**Figure 5-3** Soma locations of all intracellularly labelled SRT cells in the lumbar segment of the cat and representative sections of the medulla and cerebellum with locations of the stimulated sites

**A.** Confocal scan of a transverse section of the L4 segment showing the location of a cat neurobiotin filled cell (scale 200µm).

**B.** Plotted soma locations of all six cat cells reconstructed in this study onto lumbar 4 & 5 maps. Filled red dots illustrate cells 1-4 (lumbar 4) and red rings refer to cells 5 & 6 (lumbar 5).

**C&D.** Cresyl violet stained coronal sections showing the location of stimulation sites in the lateral reticular nucleus and cerebellum of the cat brain (black circles).

LRN, lateral reticular nucleus; IO, inferior olivary nucleus; p, pyramid; FTG, gigantocellular tegmental field; INA, nucleus interpositus of the cerebellum.

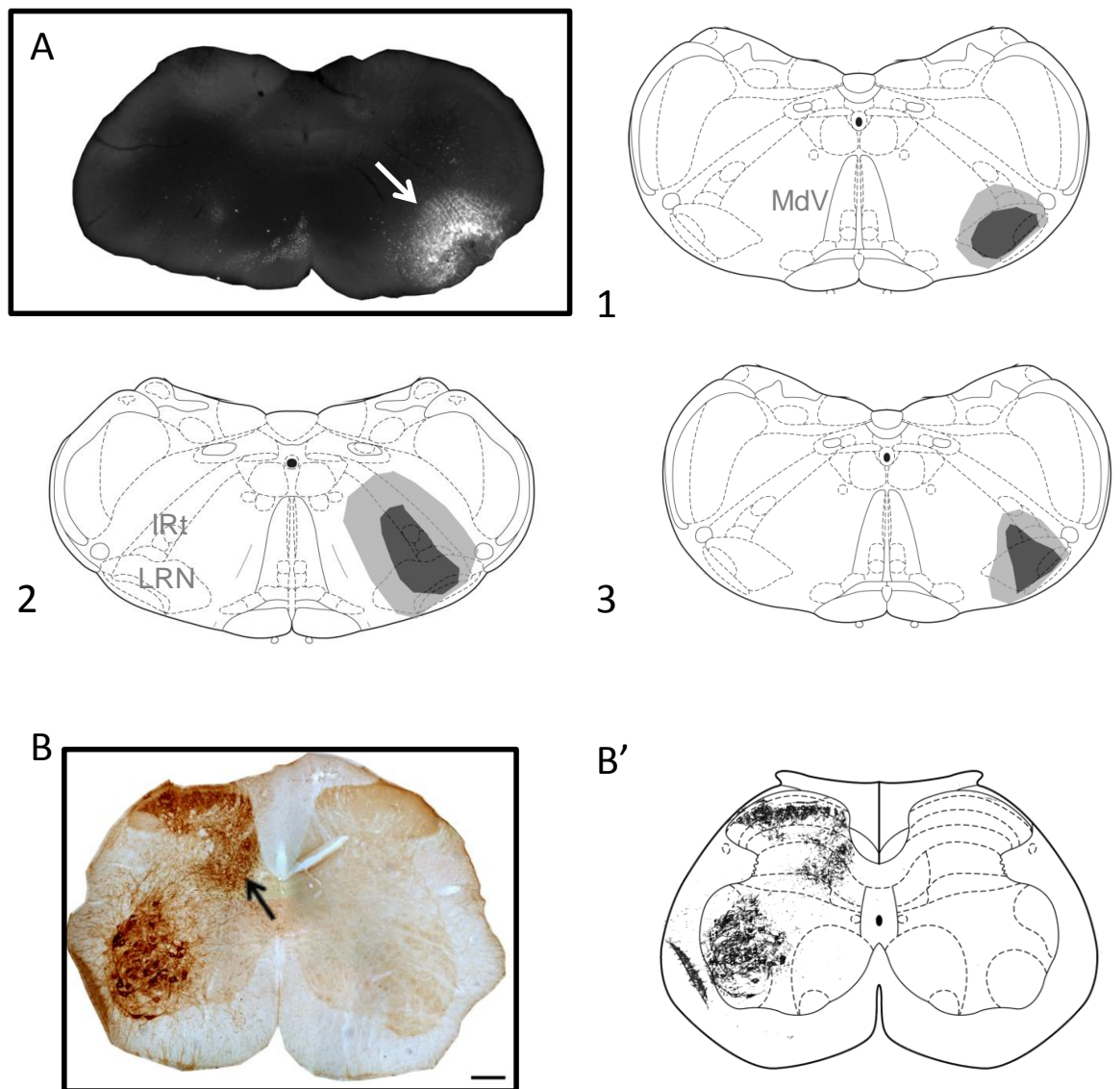


**Figure 5-4 Fluorogold injection into the right lateral reticular nucleus and injection of the b subunit of cholera toxin into the left sciatic nerve in the hind limb of the rat with myelinated terminals labelled in the lumbar segments**

**A.** A photomicrograph of a representative ultraviolet medullary section illustrating the FG injection site (white arrow).

**1, 2 & 3** Drawings of the injection sites onto coronal sections of the rat medulla for each animal, from Paxinos & Watson, 2005. The dark grey is the injection site with a light grey penumbra of tracer spread.

**B&B'** DAB image and corresponding reconstruction on a L4 map; illustrating the pattern of distribution of CTb labelled terminals by sciatic nerve injection (black arrow, scale bar 100µm).

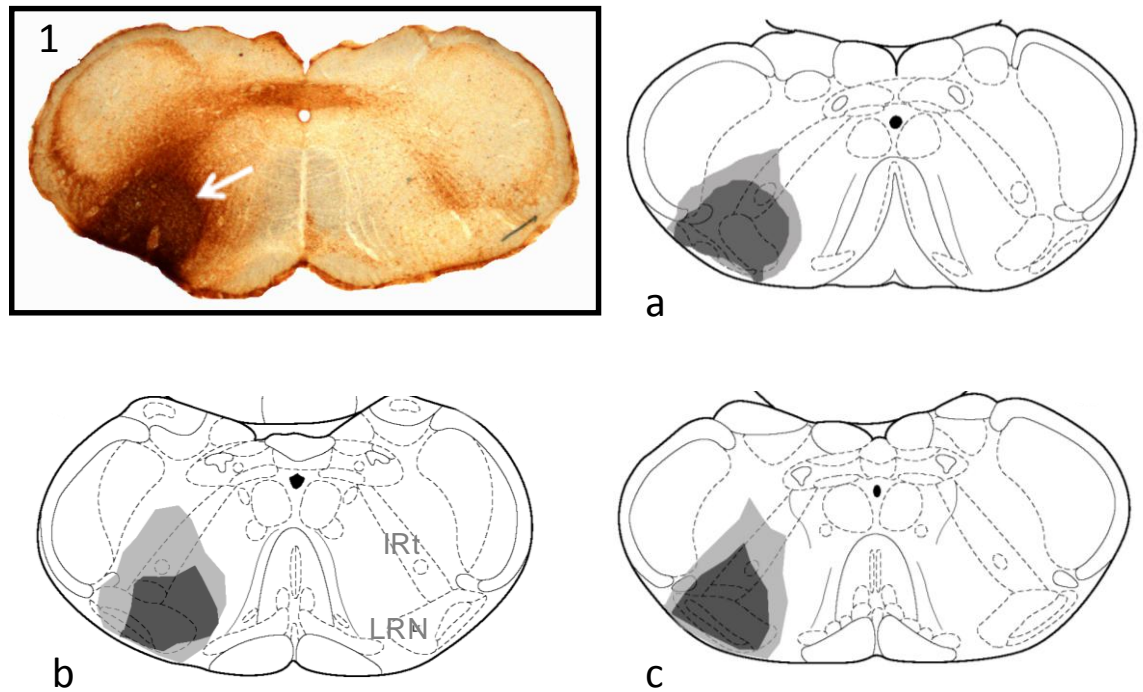


**Figure 5-5 CTb injection sites into the lateral reticular nucleus of the rat to retrogradely label SRT cells in the lumbar spinal cord**

1. Photomicrograph of a representative DAB transverse section of the medulla with the CTb injection site (white arrow).

a, b & c, Reconstructions onto brain maps (from Paxinos & Watson, 2005) illustrating the injection sites for each of the three animals used in these experiments. The dark grey shaded area shows the primary injection site of CTb and the light grey shaded area represents the spread of the tracer.

**Figure 5-6 Confocal image of a representative, retrogradely labelled spinoreticular rat neuron (red) with VGLUT-1 (blue) and VGLUT-2 (green) contacts (Large panel)**

**a to d** Magnified views of the inset illustrating a single optical section of the contacts on a dendrite of the cell.

**a.** CTb (Rhodamine red) labelled SRT dendrite.

**b.** VGLUT-2 (green, white arrows; Alexa 488) terminals in contact with the dendrite (CTb, Rh Red).

**c.** VGLUT-1 terminal (blue, arrow head; dylight 647) in contact with the dendrite (CTb, Rh Red).

**d.** Merged image showing the VGLUT-1 and 2 terminals making contact with the CTb labelled dendrite.

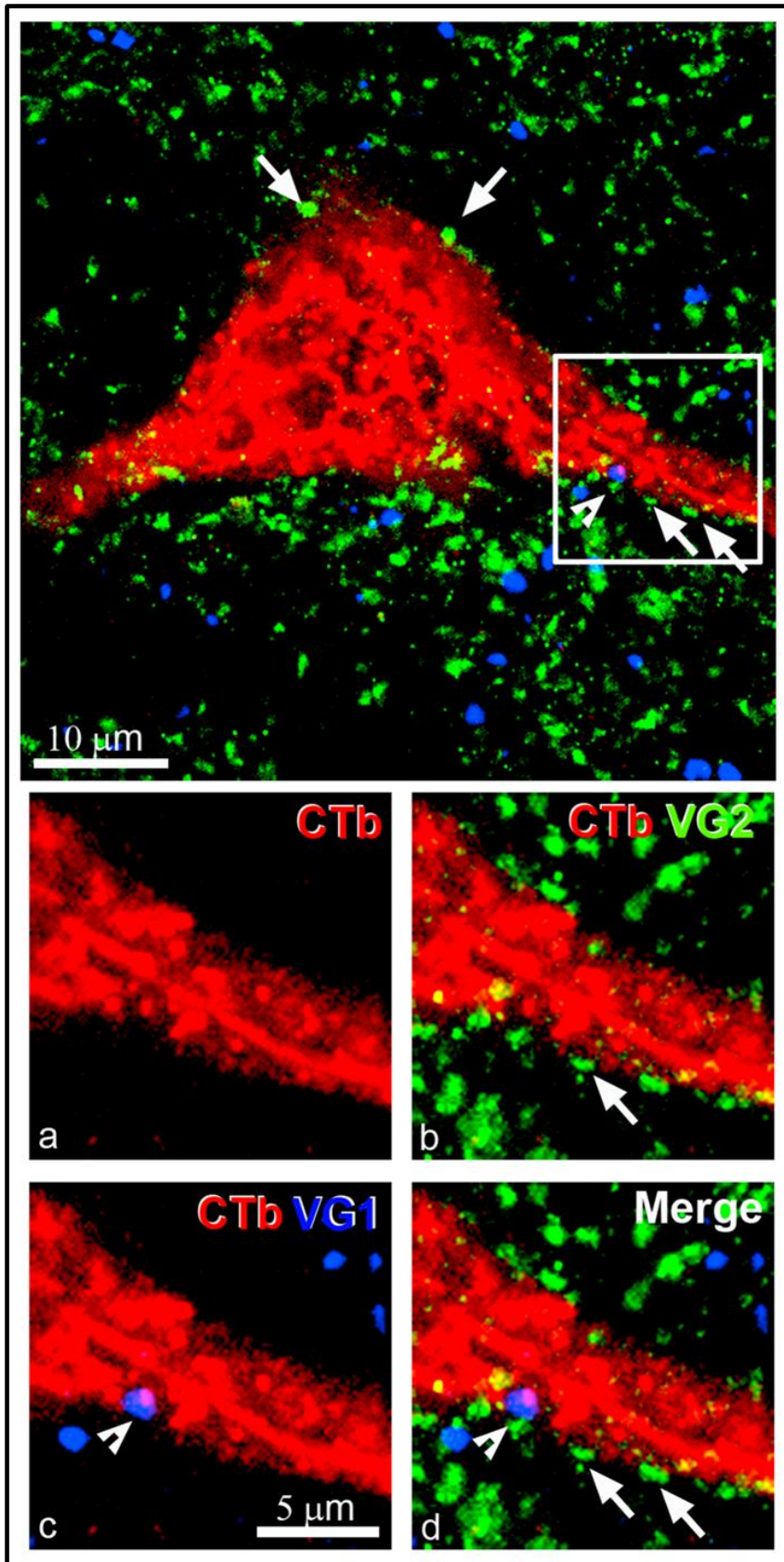


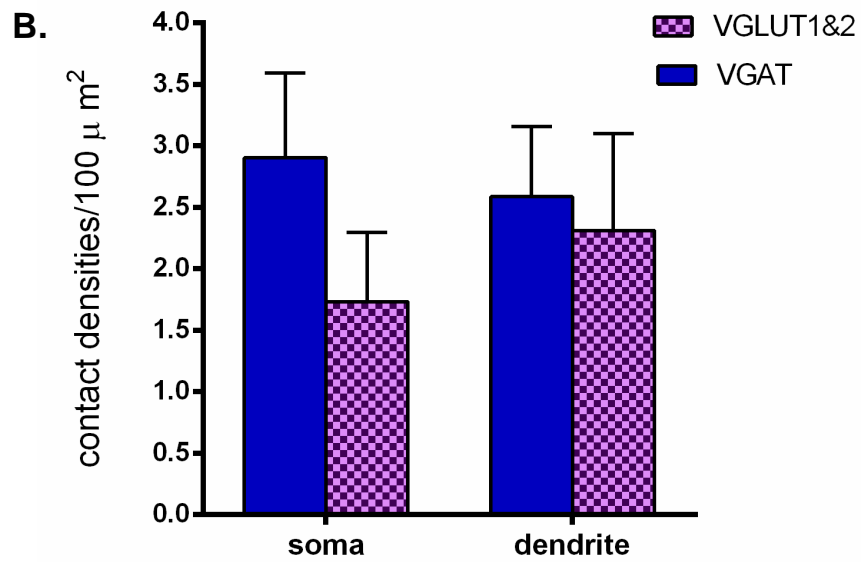
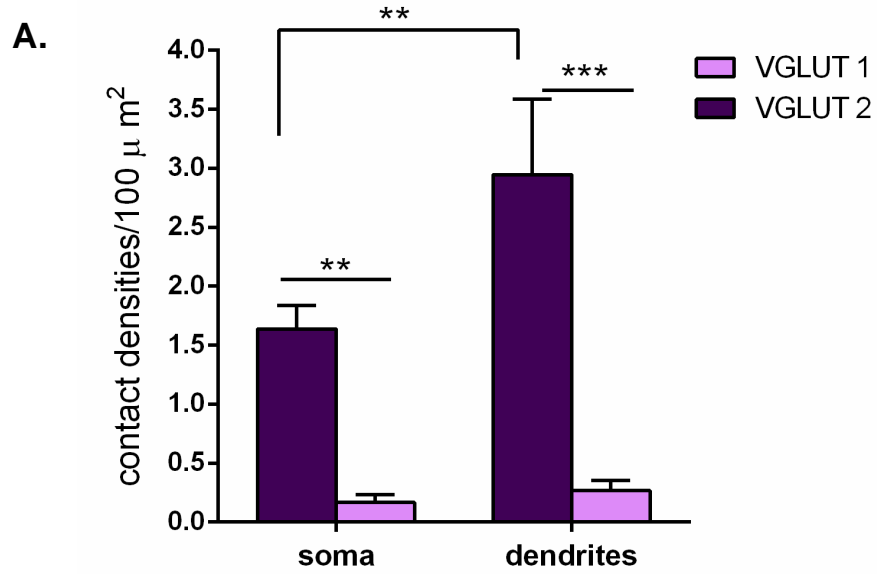
**Figure 5-7 Contact densities of excitatory and inhibitory inputs on spinoreticular tract neurons in rat (A-B) and cat (C) lumbar segments of the spinal cord**

**A.** In the rat, there is a significant difference in VGLUT-1 and VGLUT-2 contact densities on the soma,  $**p < 0.01$  and dendrites,  $***p < 0.001$ . The contact densities of VGLUT-2 terminals are also significantly higher in the dendrites as compared to the soma,  $**p < 0.001$  (post hoc *Tukey's*),  $n=3$ , cells=116 and data presented as mean $\pm$ SD.

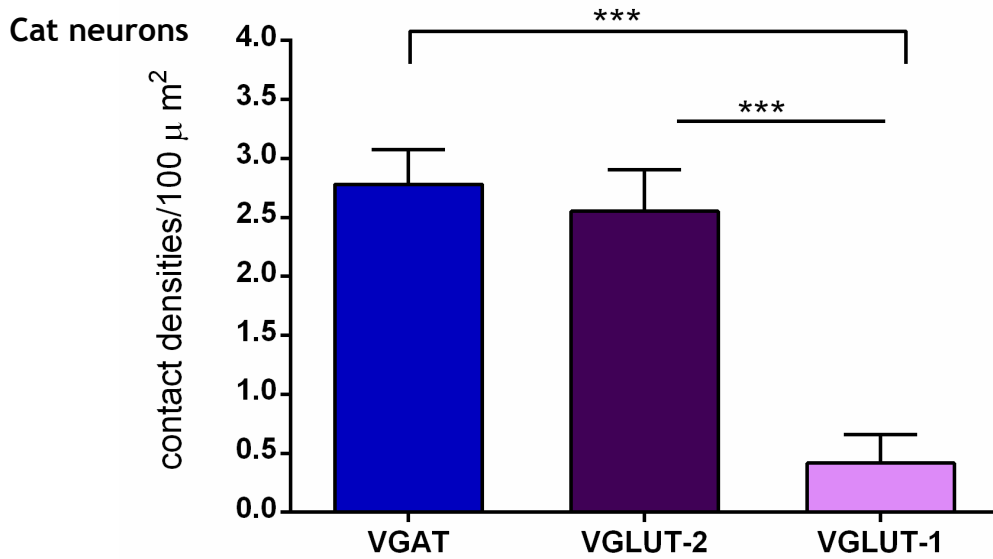
**B.** The contact densities of excitatory VGLUT 1& 2 terminals and inhibitory VGAT synapses on the soma and dendrites are not significantly different,  $p > 0.05$ . All experiments were carried out in three rats, cells=115 and data presented as mean $\pm$ SD.

**C.** In the cat there is a significant difference in contact densities of VGLUT-1 and VGLUT-2,  $***p < 0.001$  and also between VGAT and VGLUT-1,  $***p < 0.001$  (Anova, post hoc *Tukey's*),  $n=6$  and data is presented as mean $\pm$ SD.

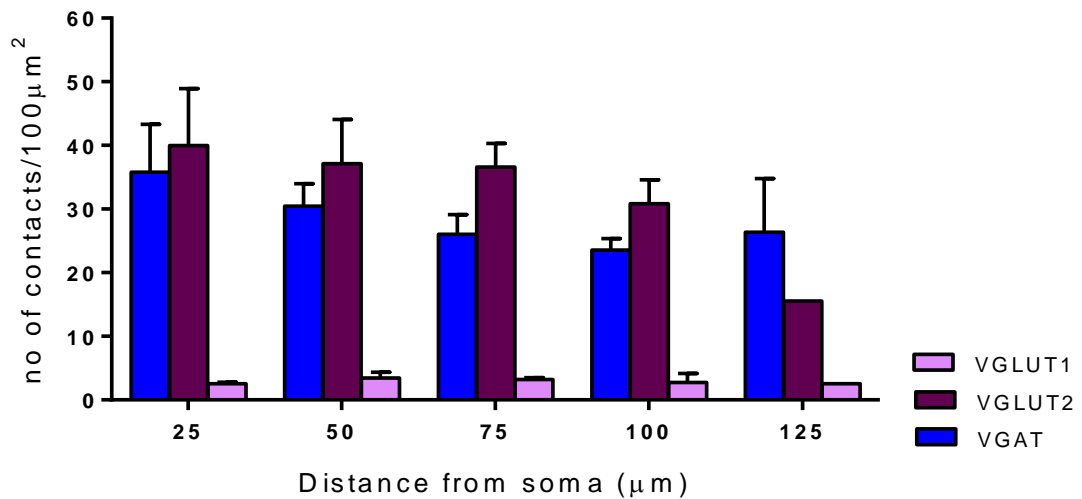
Rat neurons



**C.**



### A. Rat SRT neurons



### B. Cat SRT neurons

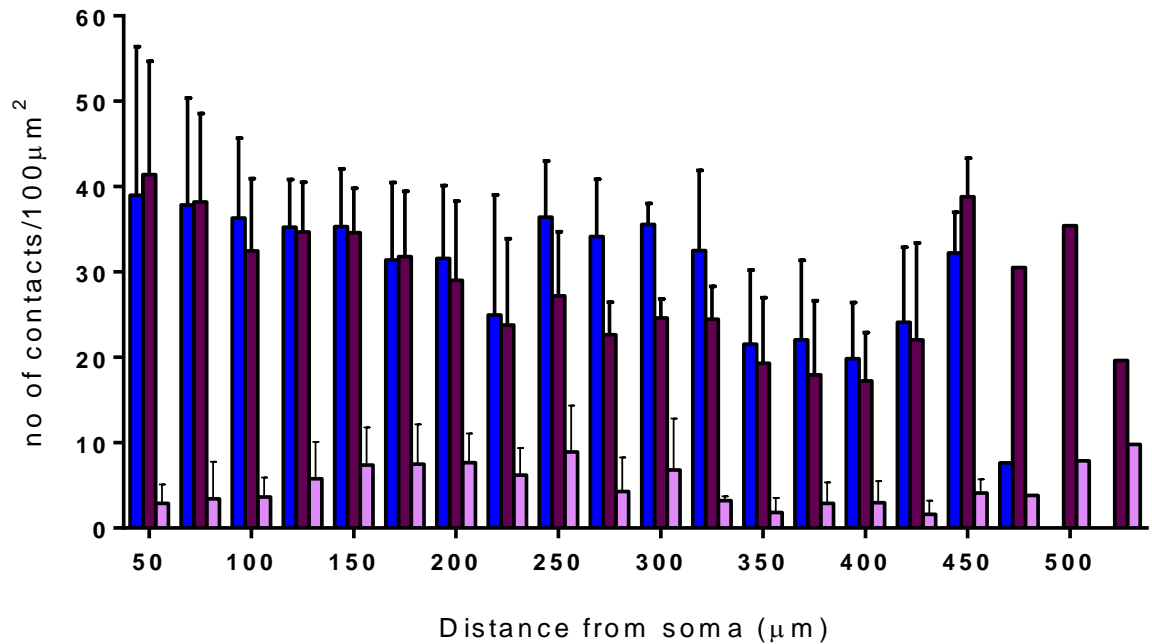


**Figure 5-8 Sholl analysis showing the mean number of excitatory and inhibitory contacts on both retrogradely labelled rat SRT neurons (A) and intracellularly labelled cat spinoreticular neurons (B)**

The plots show VGAT, VGLUT-1 and VGLUT-2 contacts per 100 μm dendritic length within concentric spheres of 25 μm radii increments from the soma centre. Bars (T) represent standard deviations.

**Figure 5-9 Confocal image of a representative, retrogradely labelled spinoreticular rat neuron (red) with excitatory inputs (VGLUT-1&2) and VGAT synapses**

**Large panel** Spinoreticular neuron (red, CTb; Rhodamine red) with excitatory (VGLUT-1&2, green; Alexa 488) and inhibitory terminals (VGAT, blue; Alexa 647) and with gephyrin puncta (yellow; Avidin Pacific blue)

**a to f** Magnified views of the inset illustrating a single optical section of contacts on a dendrite of the cell

- a. CTb labelled spinoreticular dendrite (red)
- b. VGLUT-1&2 contacts (green, white arrows) on a SRT dendrite (red, from inset)
- c. VGLUT-1&2 (green, white arrows) and VGAT contacts (blue, arrow heads)
- d. VGAT contacts (blue, arrow heads) on the SRT dendrite
- e. Gephyrin puncta (yellow, red arrows) along the same dendrite
- f. VGAT synapses with Gephyrin (yellow arrows) on the SRT dendrite

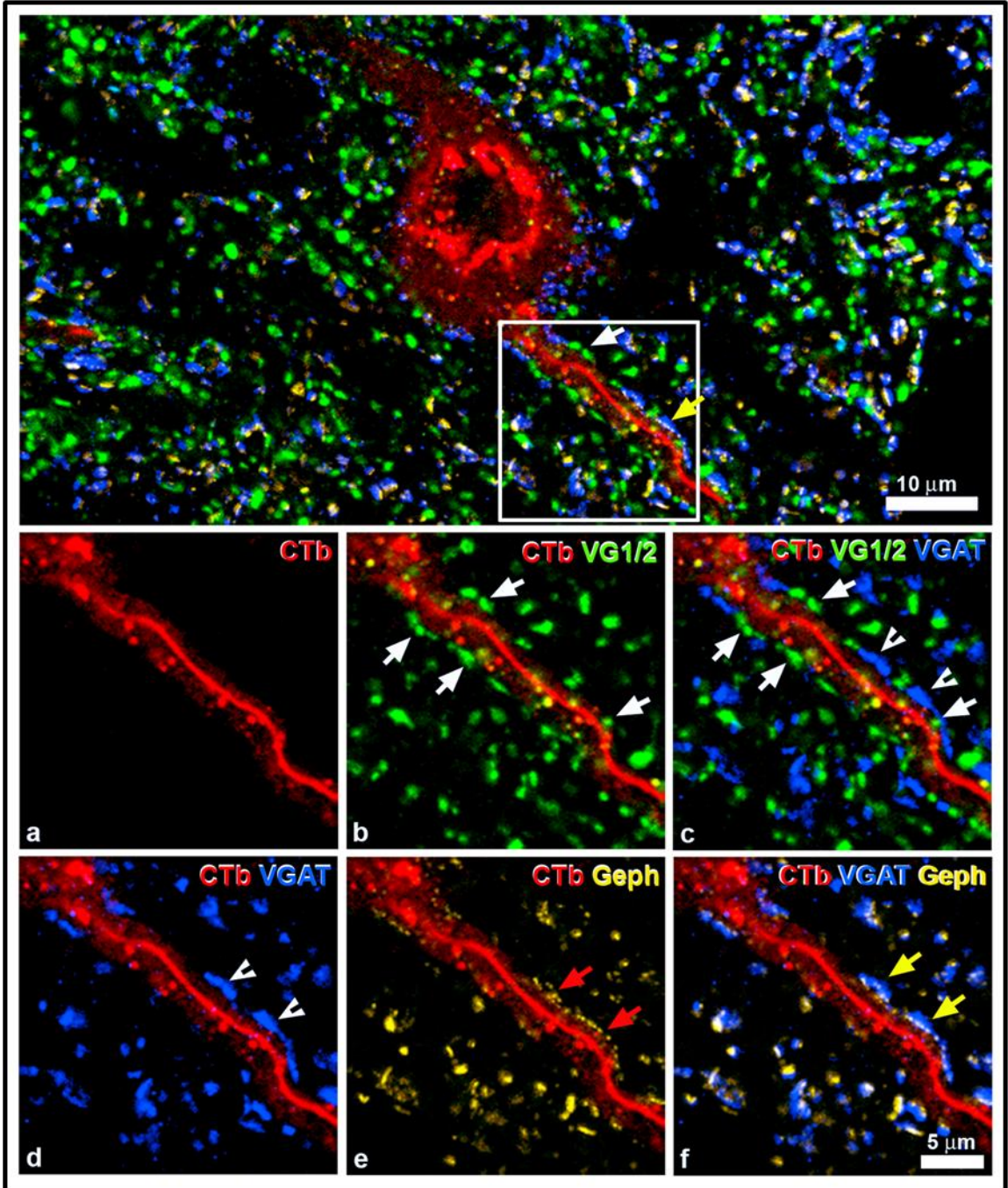


**Figure 5-10 A neurobiotin-rhodamine filled cat spinoreticular cell with excitatory (VGLUT-1&2) and inhibitory (VGAT) contacts**

**1. Large panel** on the left, neurobiotin-rhodamine filled SRT cell with VGLUT 1 (white arrows), VGLUT-2 (arrow head) and VGAT positive boutons (red arrow).  
**1a-e** Magnified views of the inset illustrating a single optical section of the contacts on soma of the cell.

**1a** White arrows point to VGLUT-1 (VG1, green, Alexa 488) contacts on the soma

**1b** Merged image of VGLUT-1 (VG1, green) and VGLUT-2 (VG2, magenta, arrow heads) contacts on the Avidin-Neurobiotin labelled soma

**1c** VGAT (blue, red arrow) contacts onto the soma

**1d** VGLUT-2 (VG2, magenta, arrow heads) terminals contacting the soma

**1e** Merged image of VGLUT-1 (VG1, green, white arrow) and VGAT (VGAT, blue, red arrow) contacts on the Avidin-Neurobiotin labelled soma

**2. Large panel** on the left, a dendrite of a neurobiotin-rhodamine filled SRT cell with, VGLUT-2 (arrow head) and VGAT positive boutons (red arrow).

**2a-e** Magnified views of the inset illustrating a single optical section of the contacts on a dendrite of the cell

**2a** No VGLUT-1 (VG1, green, Alexa 488) contacts on the dendrite

**1b** Merged image of VGLUT-1 (VG1, green) and VGLUT-2 (VG2, magenta, arrow heads) with only VG2 contacts on Avidin-Neurobiotin labelled dendrite

**1c** VGAT (blue, red arrow) contacts onto the dendrite

**1d** VGLUT-2 (VG2, magenta, arrow heads) terminals contacting dendrite

**1e** Merged image of VGLUT-2 (VG2, magenta, arrow heads) and VGAT (VGAT, blue, red arrow) contacts on the Avidin-Neurobiotin labelled dendrite

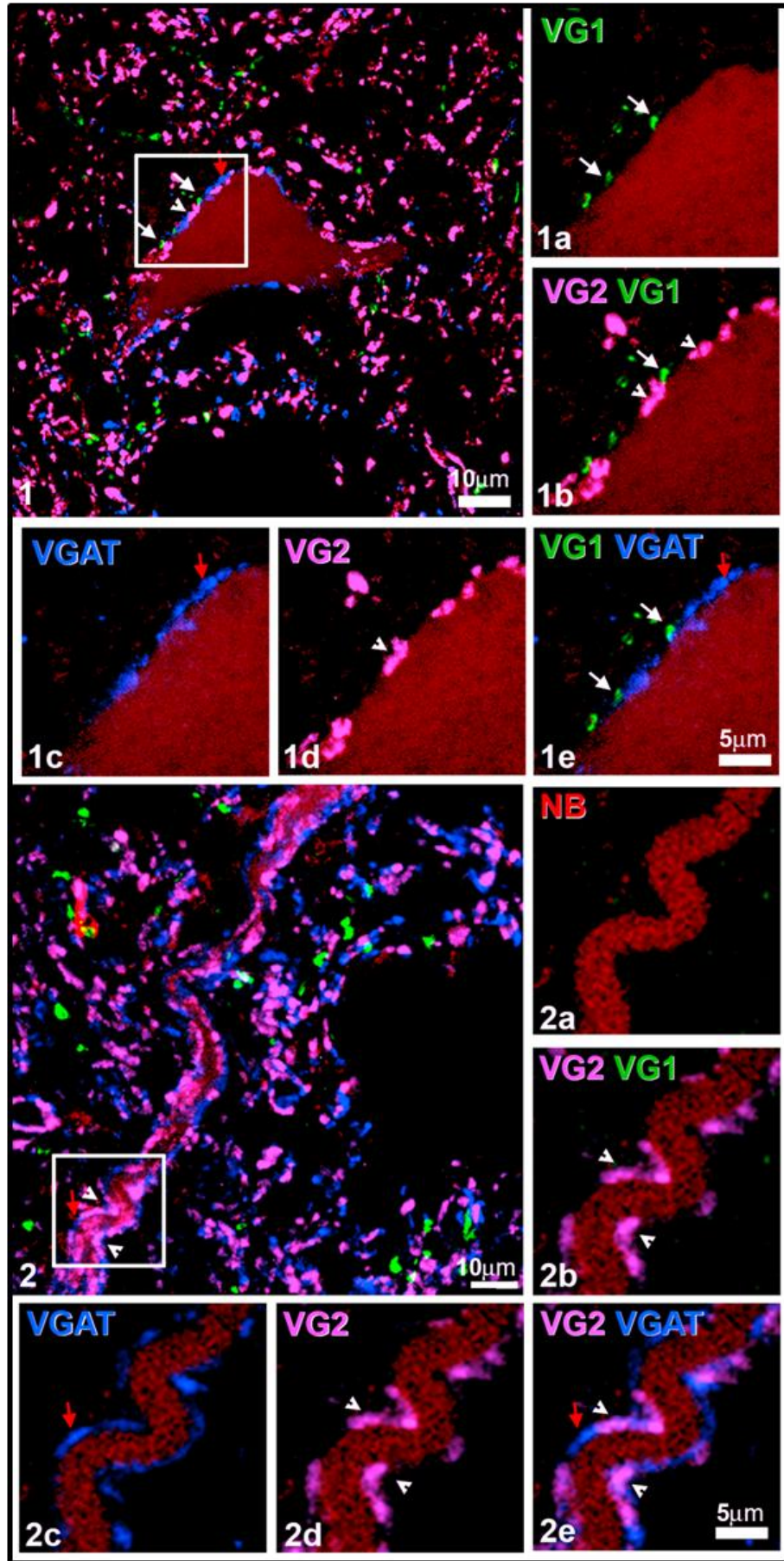


**Figure 5-11 Reconstructions of intracellularly labelled neurobiotin cat lumbar spinoreticular tract neurons illustrating the patterns of distribution of excitatory and inhibitory inputs**

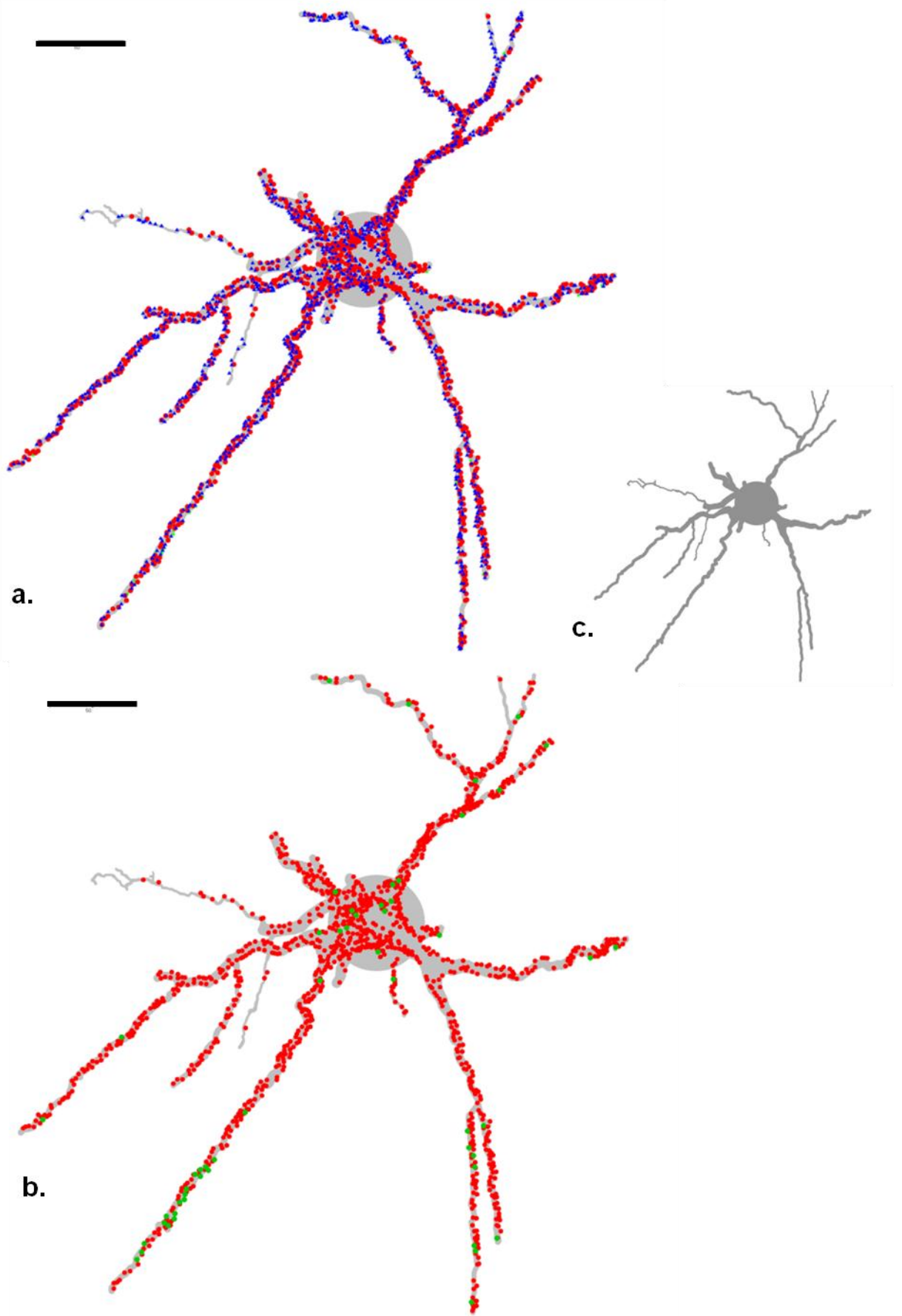
Illustrations of the first four SRT cells (A-D, Cell1 to 4) reconstructed in this study.

a VGLUT-2 (red dots) and VGAT (blue dots)

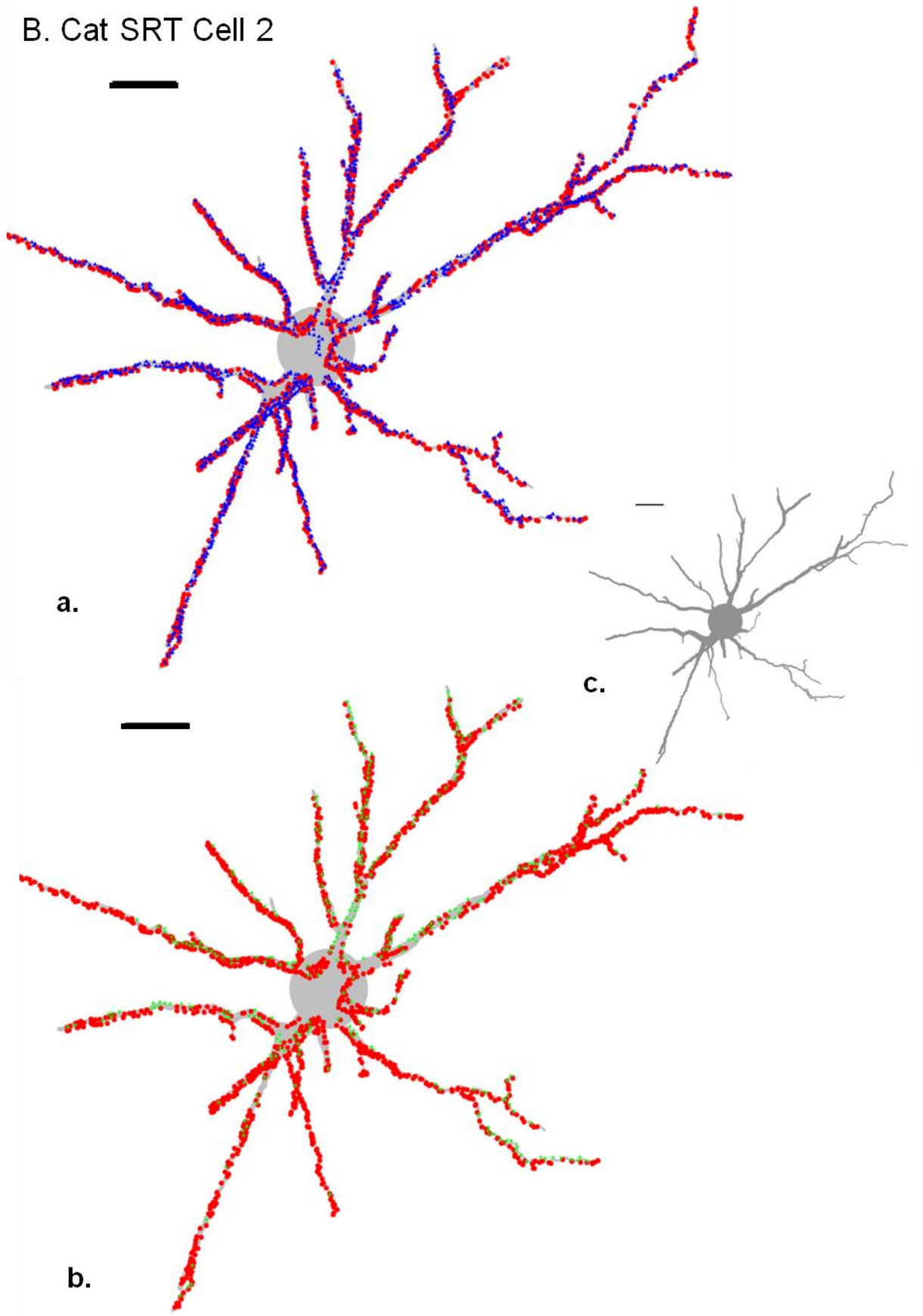
b VGLUT-1 (green dots) and VGLUT-2 (red dots)

c. Reconstruction of cell body and dendritic pattern (grey). Scale bar: 50µm

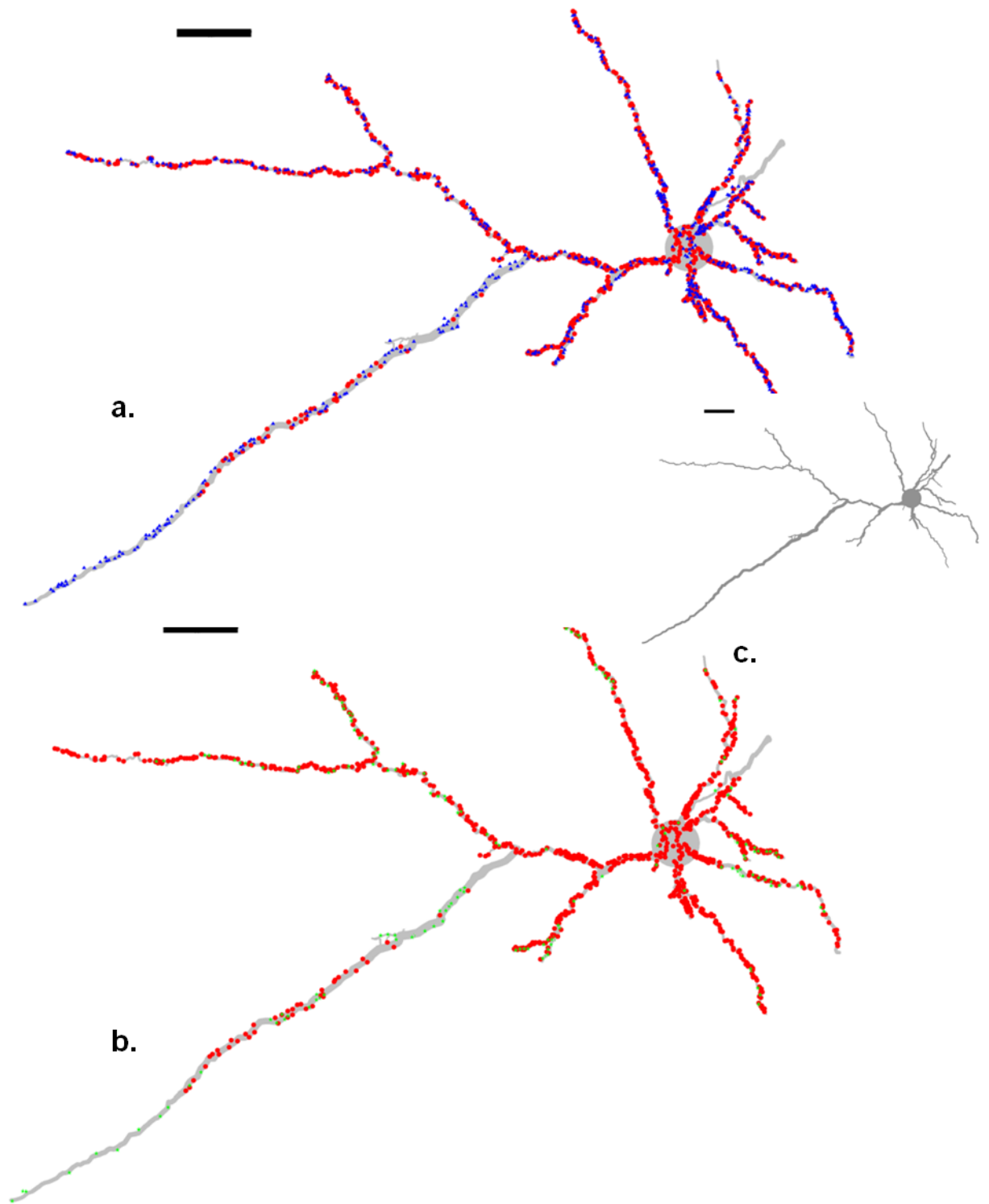
A. Cat SRT cell 1



B. Cat SRT Cell 2



C. Cat SRT cell 3



D. Cat SRT cell 4

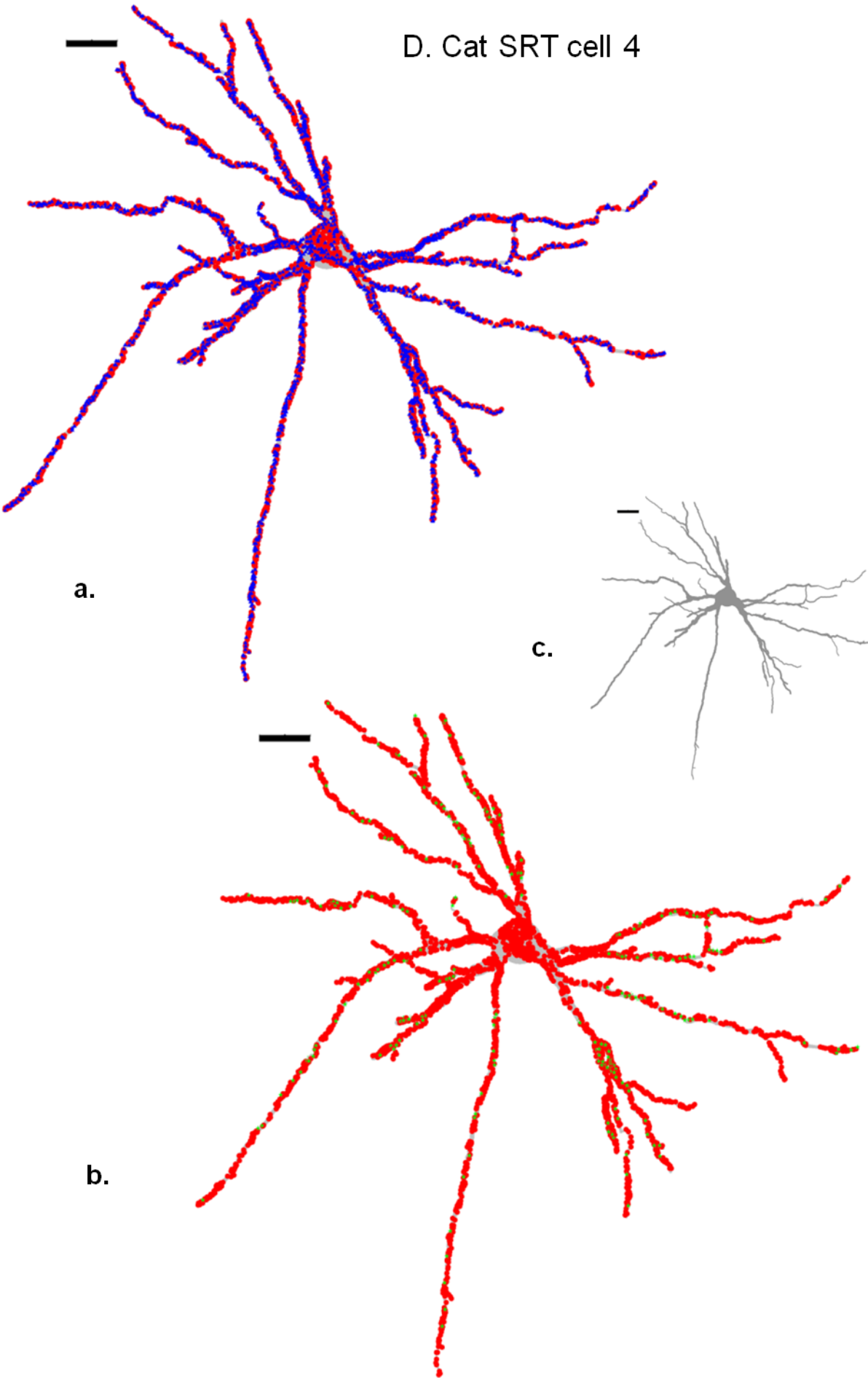


**Figure 5-12 A neurobiotin-rhodamine filled spinoreticular cat cell with VGAT synapses and VGLUT-1 and VGLUT-2 positive terminals**

**Large panel,** neurobiotin-rhodamine filled SRT cell with VGLUT 1&2 (arrow heads), VGAT (white arrows) positive boutons

**1a-c and 2a-c** magnified views of the inset illustrating a single optical section of the contacts on the soma of the SRT cell

**1a** Arrow heads point to VGLUT-1&2 (VG1/2, green, Alexa 488) contacts on the soma

**1b** VGAT (blue, white arrows) contacts to the soma

**1c** Merged image of VGLUT-1&2 (VG1/2, green) and VGAT (blue, white arrows) contacts on the Avidin-Neurobiotin labelled soma

**2a** Gephyrin puncta (yellow, red arrows) on the soma membrane

**2b** Merged image of VGAT (blue) terminals making synapses with the Gephyrin puncta (yellow) on the spinoreticular neuron (yellow arrows)

**2c** Merged image of VGLUT-1&2 contacts (green, arrow heads) and VGAT synapses (yellow arrows) on the SRT cell

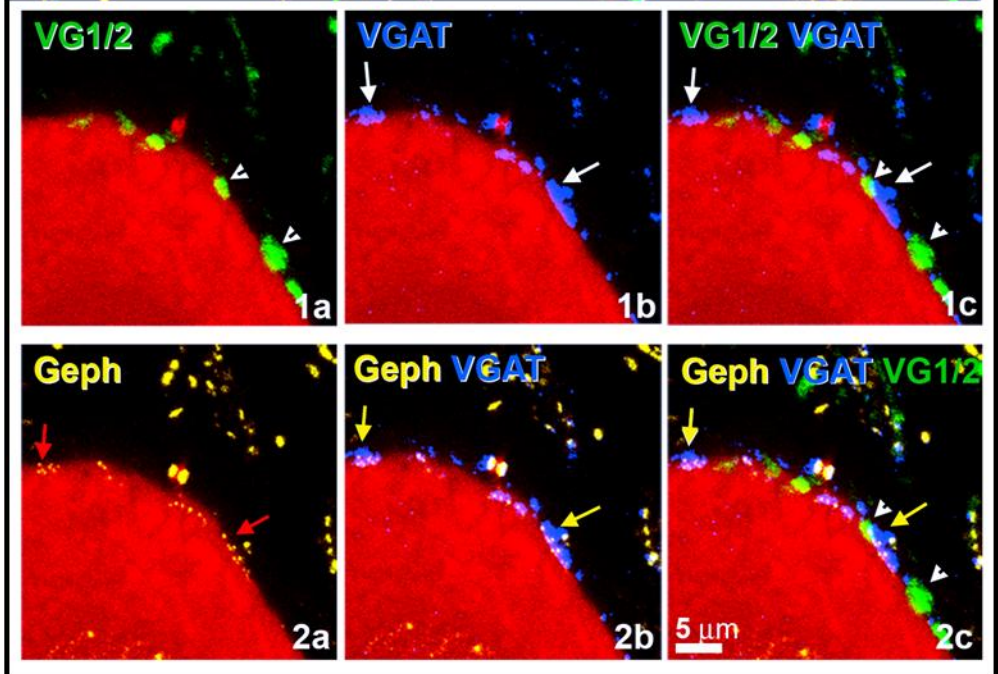
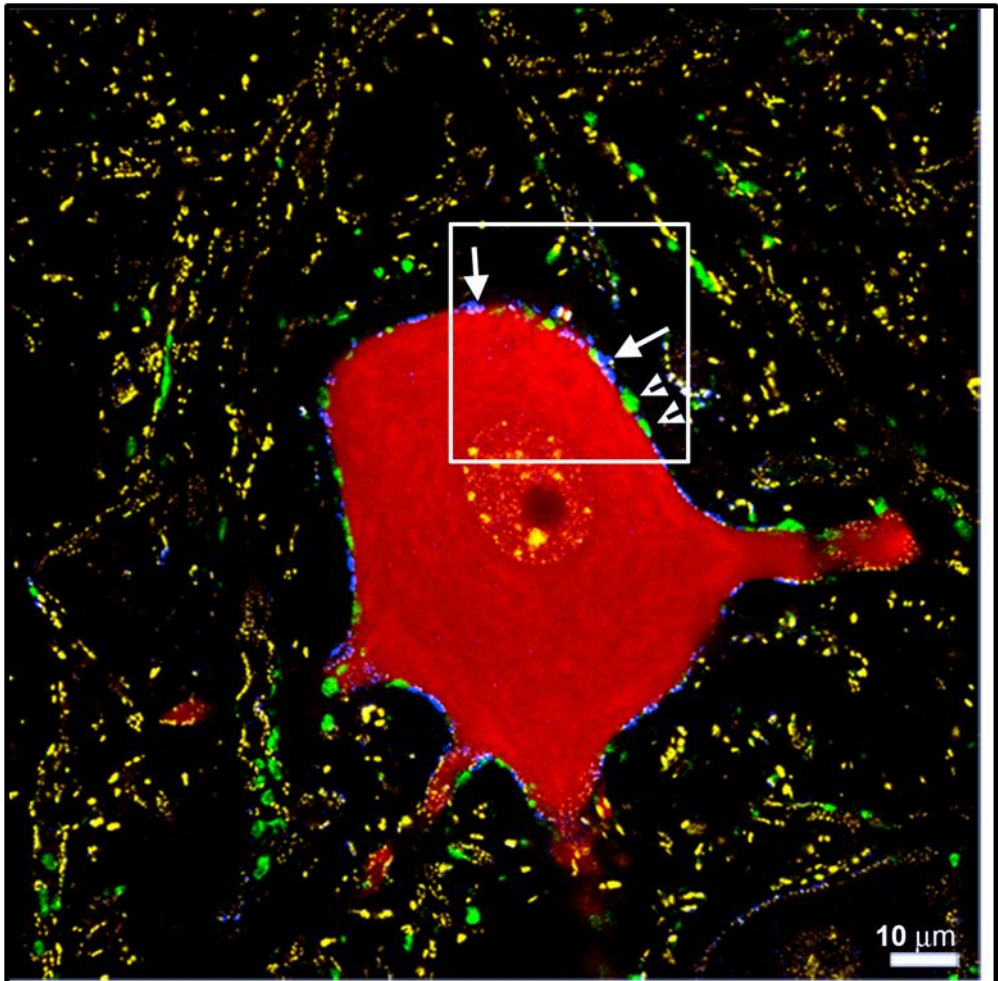


**Figure 5-13 Reconstructions of neurobiotin labelled cat spinoreticular tract neurons illustrating the patterns of distribution of excitatory inputs and inhibitory synapses**

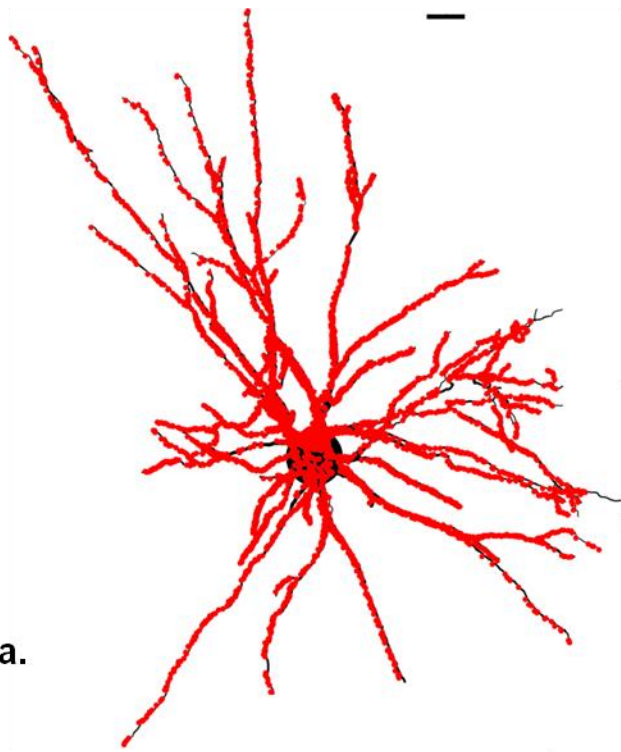
Illustrations of cell 5 and 6 SRT cells reconstructed in this study.

a VGLUT-1&2 (red dots)

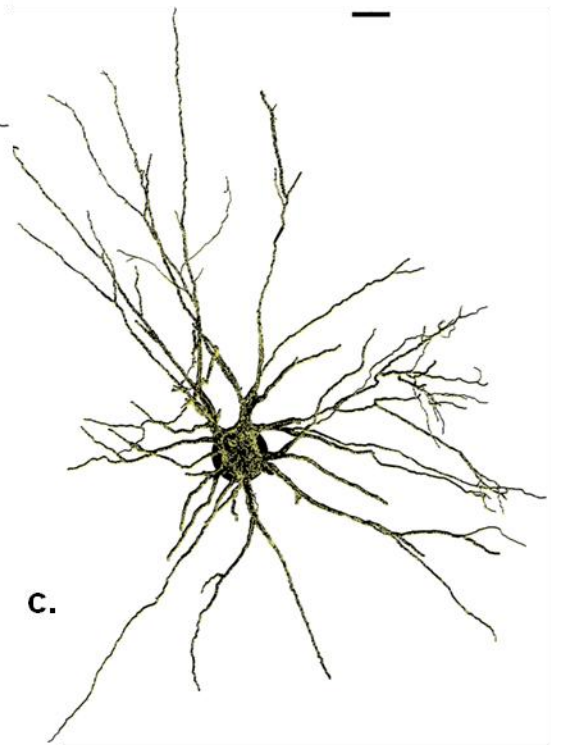
b VGAT (blue dots) and gephyrin (yellow dots)

c Reconstruction of cell body and dendritic pattern (black) with gephyrin (yellow). Scale bar: 50µm

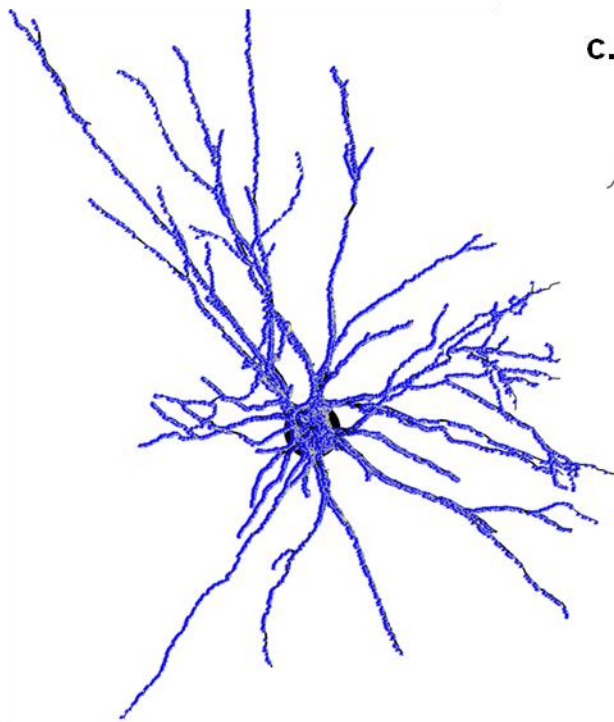
A. Cat SRT cell 5



a.



c.



b.

B. Cat SRT cell 6

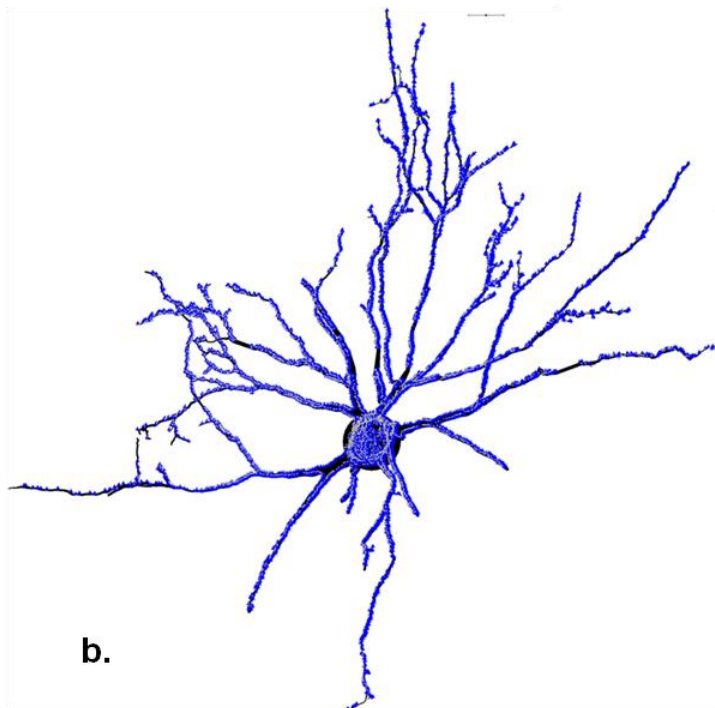
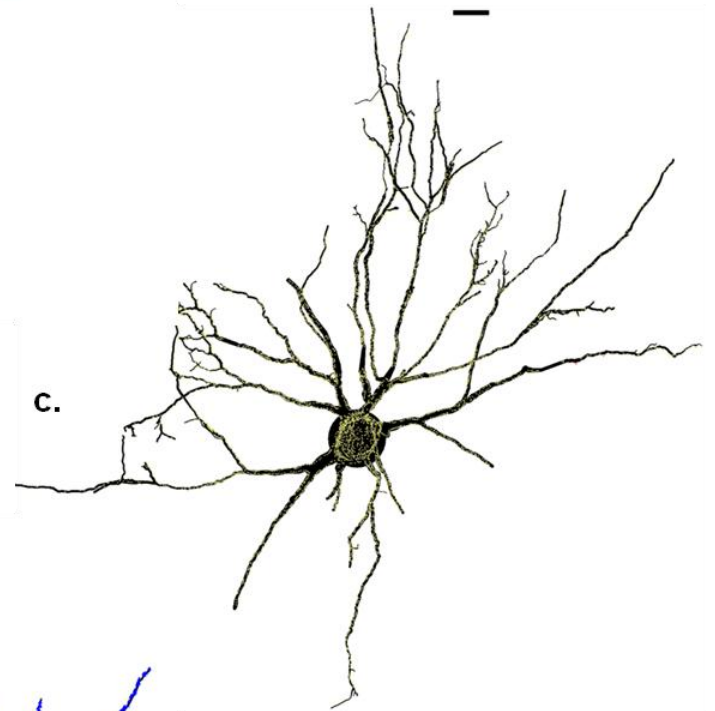
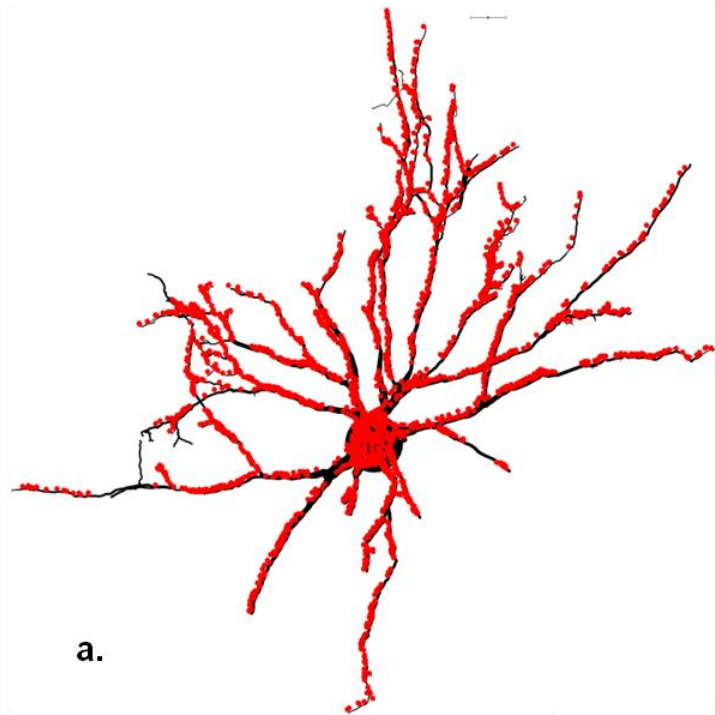


**Figure 5-14 Spinoreticular cells (FG, green) with myelinated primary afferent inputs (CTb, red)**

**Large panel,** Retrogradely labelled FG (green; Alexa 488) filled dendrites of a cell with CTb labelled terminals (red; Rhodamine)

The lower panels show a magnified view of inset 1.

**1a** Top to bottom, a white arrow points to a CTb labelled terminal (red; Rhodamine) onto a FG filled dendrite of the cell (green; Alexa 488).

**1b** A parvalbumin terminal (yellow; PV, Alexa ) onto the same FG filled dendrite (green)

**1c** VGLUT-1 bouton (VG1, blue; Av. pacific blue) contacting the dendrite.

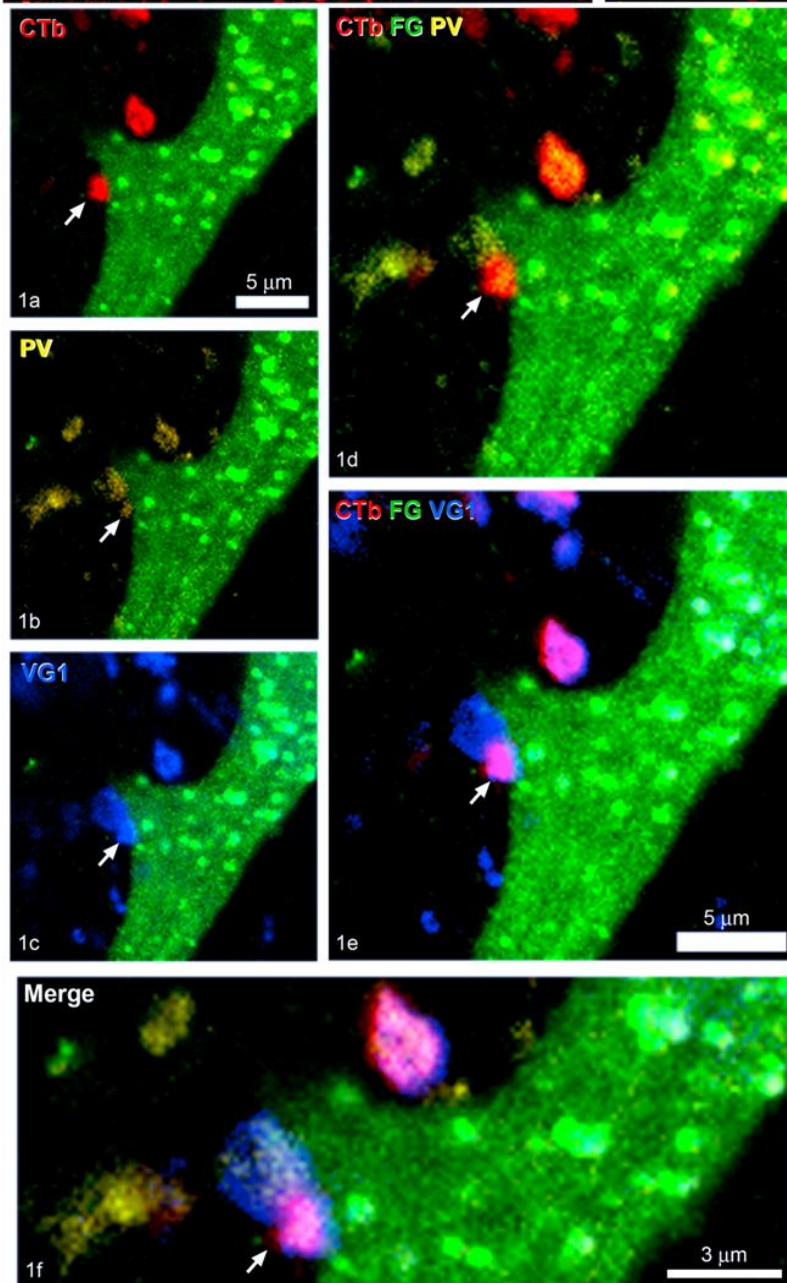
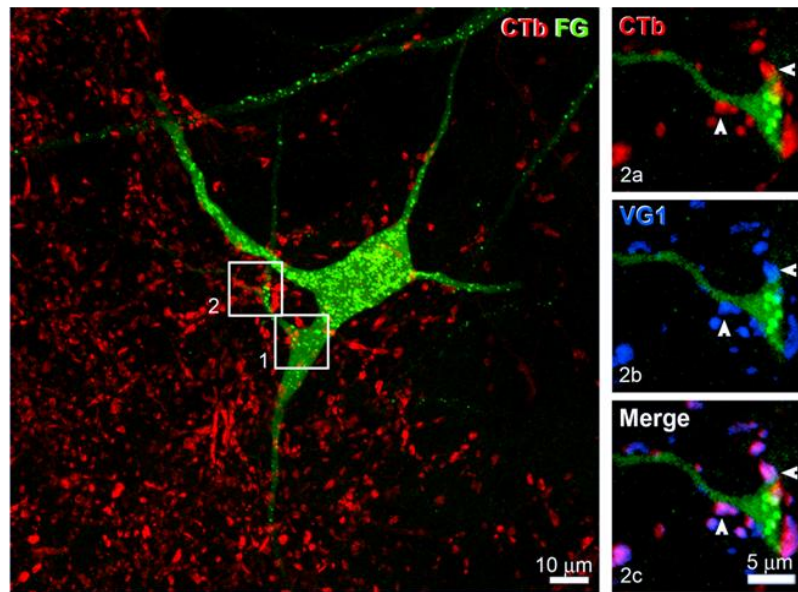
**1d** Merged image illustrating the same CTb terminal now co-localised with PV (orange, white arrow)

**1e** Merged image illustrating the same CTb terminal co-localised with VGLUT-1 (magenta, white arrow)

**1f** Final merged image showing CTb/PV/VG1 terminal (white arrow) onto fluorogold filled dendrite of the SRT cell

The right smaller panels show a magnified view of inset 2

**2a-c** From the top, CTb labelled terminals (red; Rhodamine) onto FG (green; Alexa 488) filled dendrite of the cell co-localised with VGLUT-1 (VG1, blue, Alexa 647) and so appearing magenta (white arrow heads)



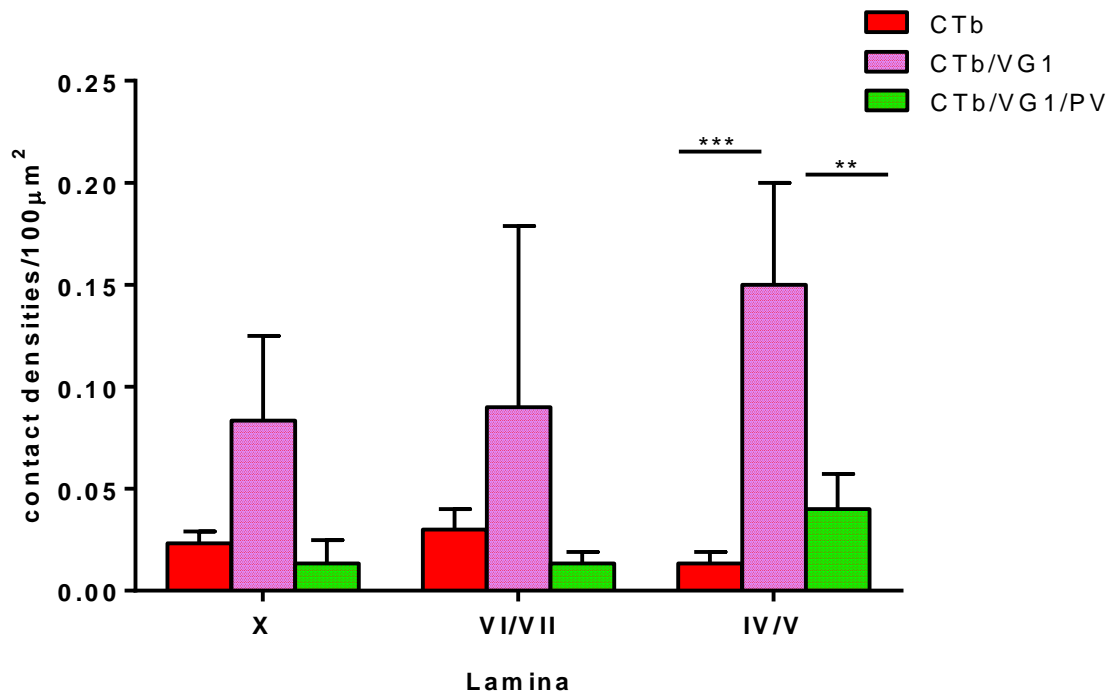


**Figure 5-15 Mean contact densities of CTb inputs onto spinoreticular cells distributed in the rat lumbar spinal cord**

In Lamina IV/V (deep dorsal lamina), the contact densities of CTb/VG1 are significantly more than CTb and CTb/VG1/PV contact densities, \*\*\* $p < 0.001$  and \*\* $p < 0.01$ , respectively (2 way Anova, post hoc *Tukey's*). There is no significant difference in the contact densities in lamina VI/VII (intermediate area) and lamina X SRT neurons,  $p > 0.05$ . Data expressed as mean $\pm$ SD (T),  $n=3$ , cells=50.

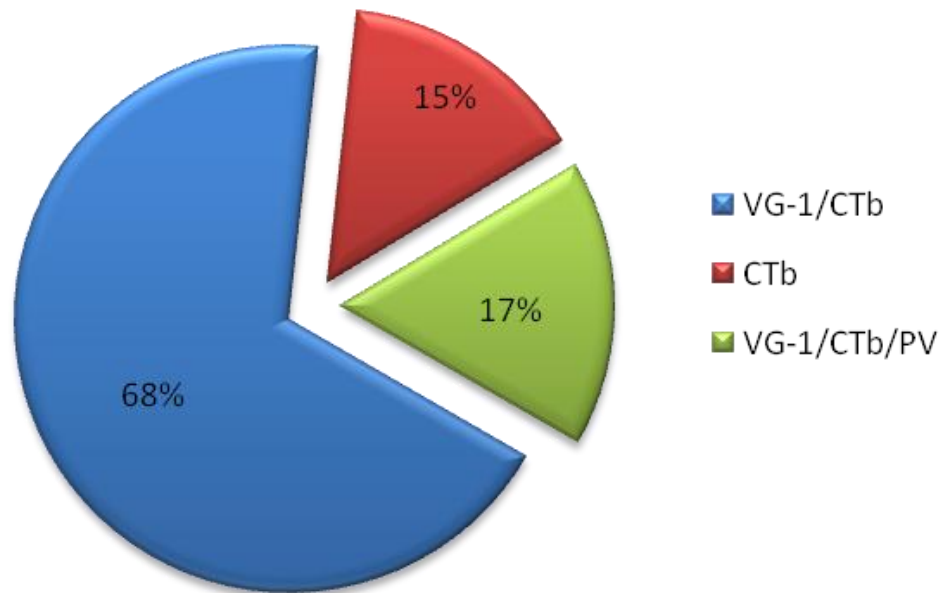


**Figure 5-16 Percentage of primary afferent CTb positive contacts on rat spinoreticular neurons**

Most CTb contacts are VG-1 positive, which are significantly higher than contacts that are CTb, VGLUT-1 as well as PV positive,  $p < 0.05$  (Anova,  $n = 3$  animals, cells = 50. CTb, b subunit of cholera toxin; VG-1, VGLUT 1; PV, parvalbumin.

**Figure 5-17** A single optical section of a retrogradely labelled spinoreticular cell in the rat lumbar spinal cord with calbindin (CB) and choline acetyltransferase (ChAT) inputs

**1a** A magnified view of inset 1 in the large panel, with a CTb labelled dendrite (blue) of SRT cell. Scale bar 5 $\mu$ m

**1b** ChAT contacts (red, arrows) to the CTb labelled dendrite

**1c** CB contacts (green, arrow heads) to the same dendrite

**1d** Merged image with both ChAT (red, white arrows) and CB terminals (green, arrow heads) in contact with the CTb labelled dendrite of the SRT cell. Scale bar 3 $\mu$ m

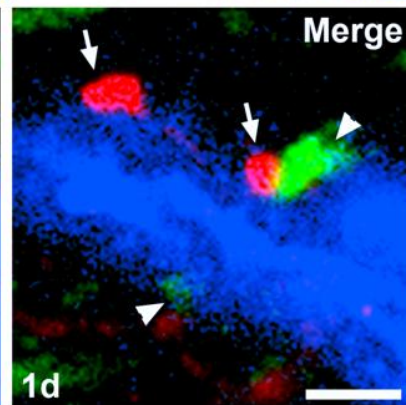
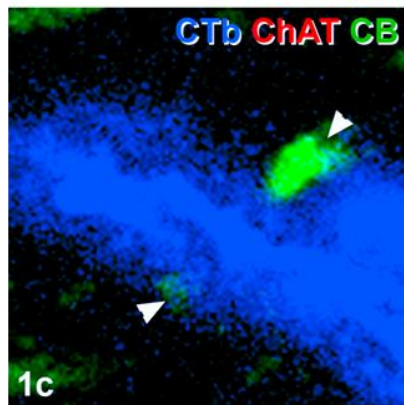
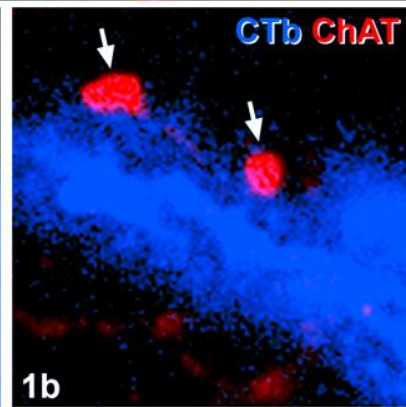
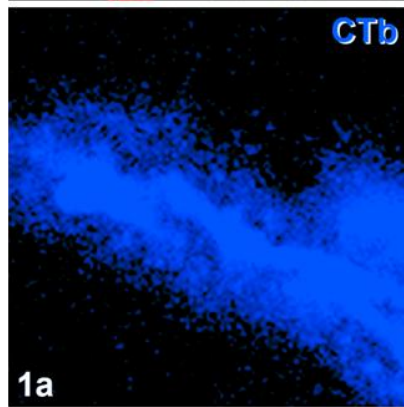
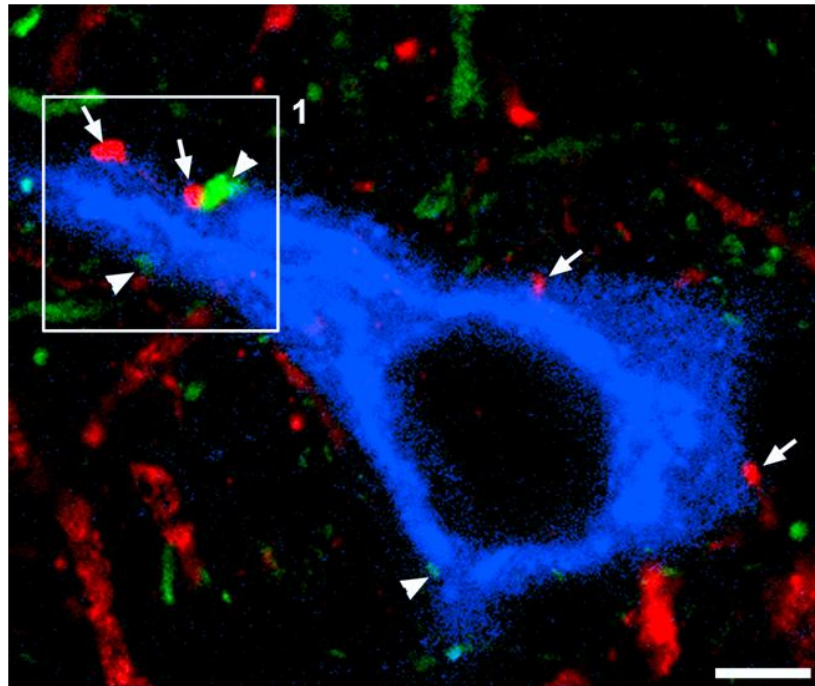


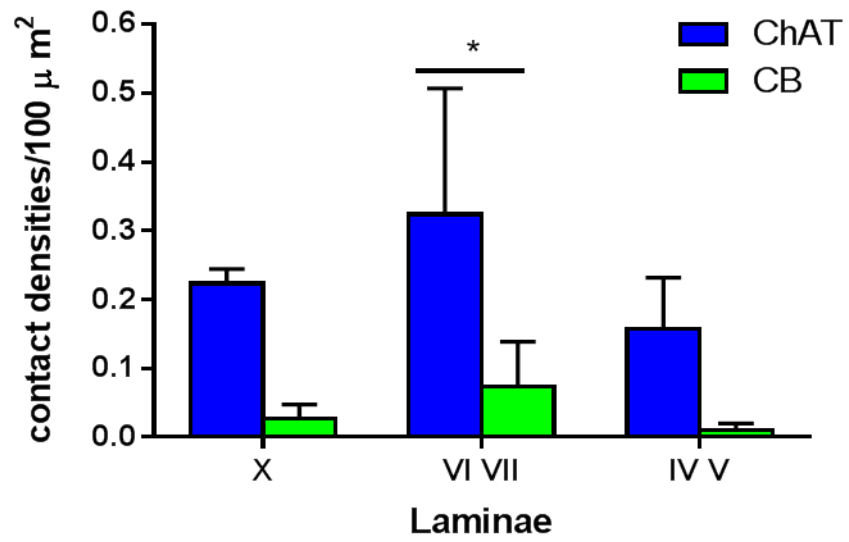
**Figure 5-18 Bar graphs showing choline acetyltransferase (ChAT) and calbindin (CB) contact densities onto two sub-populations of spinoreticular cells (SRT)**

**A.** ChAT and CB terminal densities on CTb labelled SRT cells in the three laminar zones; lamina X, intermediate laminae (VI, VII) and deep dorsal laminae (IV, V). There is a significantly higher contact density of ChAT terminals to these cells as compared to CB contacts in case of lamina VI,VII; \* $p < 0.05$  (2 way Anova, post hoc *Tukey's*).

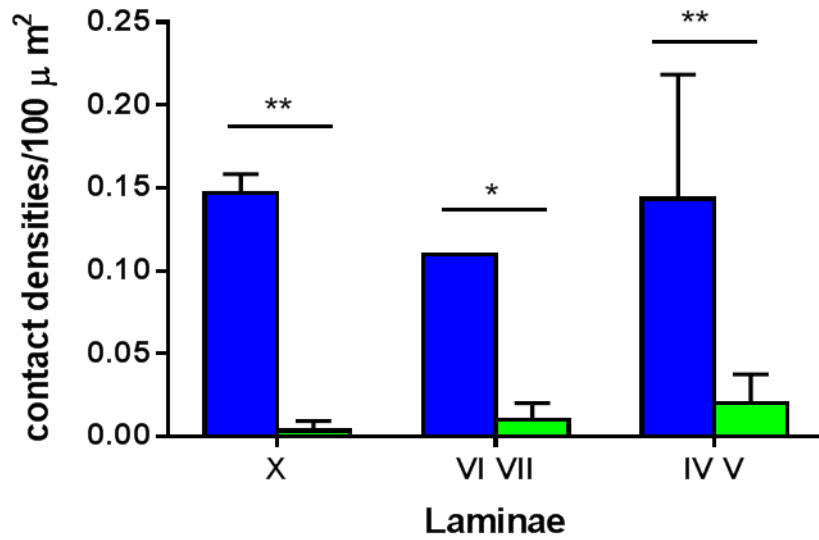
**B.** ChAT and CB terminal densities on CTb/CB labelled SRT cells in the three laminar zones; lamina X, intermediate laminae (VI, VII) and deep dorsal laminae (IV, V). There is a significantly higher density of ChAT terminals to these cells as compared to CB contacts in each of the three zones; lamina X, \*\* $p < 0.01$ ; lamina VI & VII, \* $p < 0.05$  and lamina IV & V, \*\* $p < 0.01$  (2 way Anova, post hoc *Tukey's*).

**C.** This graph shows the comparison between CTb only and CTb/CB spinoreticular cells. In a within group comparison of CTb only SRT cells and CTb/CB positive SRT there is a significantly higher ChAT density as compared to CB contacts, \*\*\* $p < 0.001$  and \*\*\* $p < 0.001$ , respectively (2 way Anova, post hoc *Tukey's*). Data expressed as mean $\pm$ SD, n=3 animals, cells=35 each.

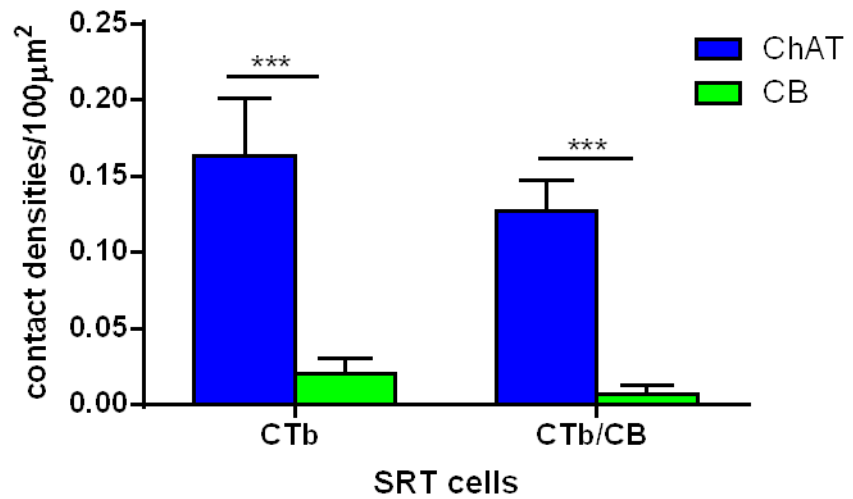
**A. CTb labelled SRT cells**



**B. CTb /CB labelled SRT cells**



**C.**



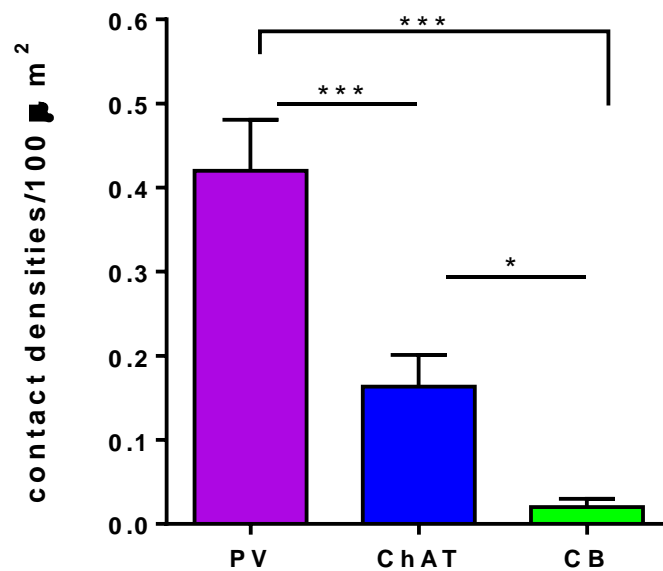


**Figure 5-19** Bar graph showing a comparison of PV, ChAT and CB contact densities on Spinoreticular cells in rat lumbar spinal cord

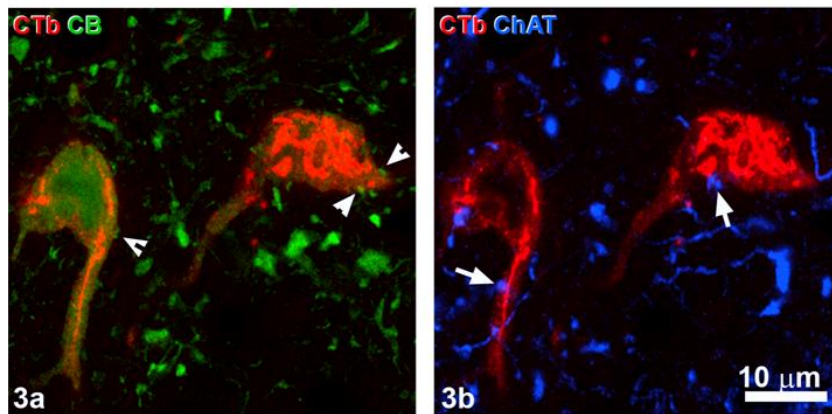
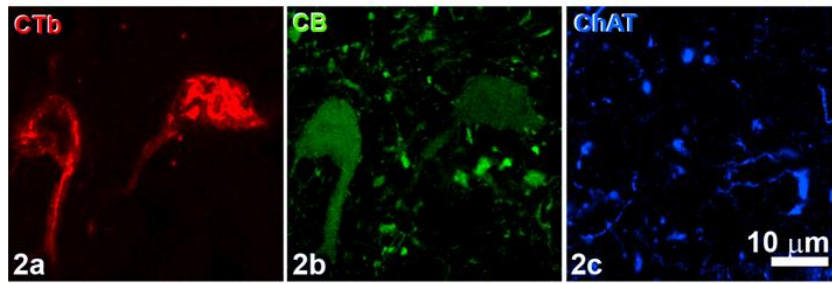
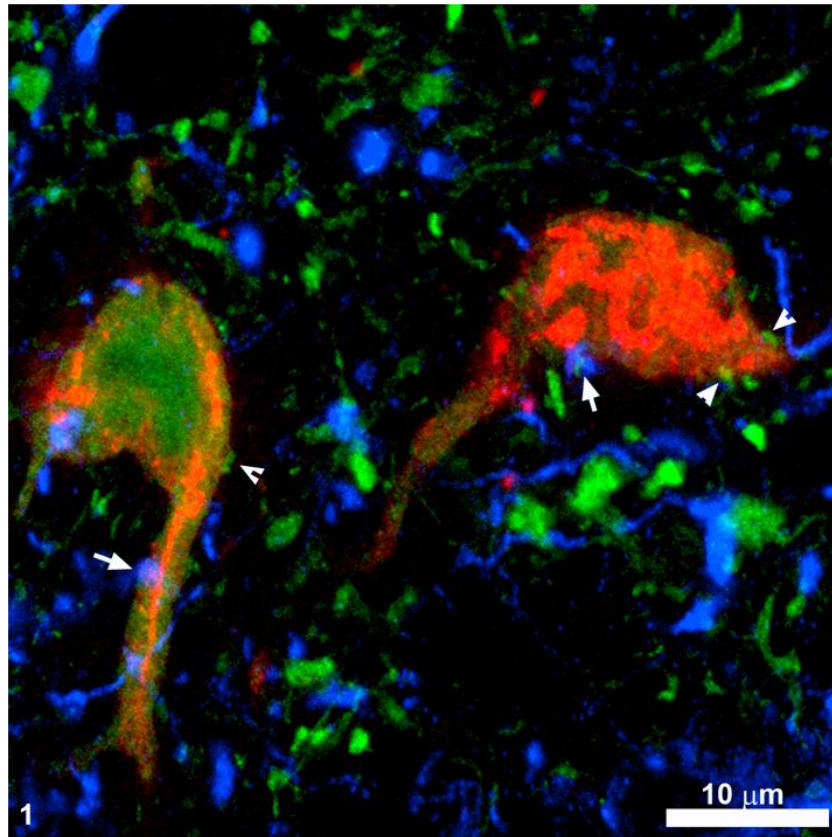
There are significantly higher PV (parvalbumin) contact densities to spinoreticular cells as compared to ChAT (choline acetyl-transferase) as well as CB (calbindin) contact densities,  $***p < 0.001$  and  $***p < 0.001$ , respectively (One way Anova, post hoc *Tukey's*). There are, in addition significantly more ChAT contacts as compared to CB,  $*p < 0.05$ . Data expressed as mean  $\pm$  SD (T), n= 6 animals.

**Figure 5-20 Confocal scans of some retrogradely labelled rat spinoreticular cells positive for calbindin, with both calbindin (CB) and choline acetyltransferase (ChAT) inputs**

**1** Merged magnified view of two CTb+CB cells (orange) with ChAT (blue; Dylight 647, white arrows) and CB contacts (green; Alexa 488, arrow heads).

**2 a-c** Lower panel split views of the same cells, from left to right CTb labelled cells (red; rhodamine), CB labelled cells (green; Alexa 488) with no ChAT (blue; dylight 647) reactivity

**3 a-b** CTb+CB cells with CB (arrow heads, green; Alexa 488) and ChAT contacts (white arrows, blue; Alexa 649)



## 5.4 Discussion

The present investigation, using a combination of techniques including retrograde tract tracing, intracellular labelling of cat cells, electrophysiological recordings and immunohistochemical reactions provides some insight into the contacts on spinoreticular cells in two species, rat and cat. In both species, these cells receive predominantly inhibitory contacts (VGAT) in addition to excitatory glutamatergic contacts that are overwhelmingly VGLUT-2 positive. Thus, it appears that most contacts on these cells are from intraspinal neurons. In addition SRT neurons in rat receive a sizeable proportion of proprioceptive input (CTb/VGLUT-1/PV positive) but in cat these cells do not seem to be monosynaptically activated by somatic nerves i.e. Quadriceps. Furthermore, the vast majority of primary afferent terminals contacting rat SRT cells appear to originate from myelinated cutaneous afferents. These cells also receive contacts from sub-groups of spinal neuronal cells; PV and ChAT cells with hardly any from calbindin cells. [Figure 5-21](#) (at the end of this chapter) illustrates a simplified diagram of these results.

### 5.4.1 Technical considerations

The pros and cons, regarding the tract tracing technique and use of CTb and FG as tracers to retrogradely label cells in the lumbar spinal cord in the rat, have been discussed in the previous two chapters ([Sections 3-5 and 4-5](#), technical considerations). All these factors were kept in mind, especially spread of the tracers and uptake by axons of passage, while interpreting the results. In addition, during the sciatic nerve injections, care was taken to place the tracer centrally after identification of the trifurcation of the nerve and also not to puncture the perineurium on the opposite side to prevent any extravasation. The labelling pattern of myelinated primary afferent terminals from sciatic nerve injection was similar to previous studies (Olave MJ et al., 2002, Shehab SA and Hughes DI, 2011).

In some of the protocols a combination of VGLUT-1 and VGLUT-2 was used to label as many excitatory contacts as possible to compare them with inhibitory contacts. In addition, terminals with glycine, GABA or those co-expressing

glycine and GABA, were labelled with an antibody against VGAT which is highly expressed in both GABAergic and glycinergic nerve endings (Burger PM et al., 1991, Chaudhry FA et al., 1998). This approach enabled us to maximise labelling of both excitatory and inhibitory terminals and thus allowed the proportions of these terminals to be defined with confidence. The excitatory terminal contact densities on cat spinoreticular cells were approximately twice as high on the soma when compared with rat cells. While the exact reason for this difference is unclear, at least part of the explanation is that cell bodies of the rat spinoreticular neurons are smaller than those in the cat and therefore they may require less excitatory drive to activate them. The dendrites of rat SRT cells had considerably lower densities for VGLUT-1 when compared with their cat counterparts. This may be because of the incomplete labelling of dendritic arbors of retrogradely labelled cells. Sholl analysis of cat SRT dendrites reveals that even the most distal dendrites had substantial labelling of VGLUT-1 contacts and as the surface areas of these dendrites are considerably smaller, there is a spike in contact densities distally and thus the mean values of contact densities will therefore be higher in cats (see Figure 5-7).

Another issue that requires consideration is the small sample size of intracellularly labelled cat neurons used for analysis. It should, however, be kept in mind that intracellularly labelled neurons have an advantage over retrogradely labelled cells because they are identified electrophysiologically and thus morphology can be related to function with greater confidence. In addition intracellular labelling allows a more complete visualisation of the dendritic arbors of these cells. These advantages, to some extent, would compensate for the unavoidably restricted numbers of cat neurons although qualitatively the results from both small (cat cells) and larger (rat cells) populations for the various contacts are somewhat similar.

#### **5.4.2 Excitatory contacts on spinoreticular cells in the rat and cat lumbar spinal cord and primary afferent contacts**

The type of vesicular transporter in terminals contacting spinoreticular cells provides an indication of the potential sources of these contacts. In this study, approximately 90% of the excitatory contacts onto SRT cells, of both species, are

VGLUT-2 positive. Thus it can be inferred that the majority of excitatory contacts on these cells originate from the intraspinal neurons, as VGLUT-2 is the principal glutamate transporter in interneuronal boutons (Aihara Y et al., 2000, Fremeau RT et al., 2001, Varoqui H et al., 2002, Todd AJ et al., 2003, Alvarez FJ et al., 2004). For review see (Reimer RJ et al., 2001).

Another source of VGLUT-2 contacts on SRT cells are the descending systems; the lateral vestibulospinal, rubrospinal and reticulospinal tracts (Du Beau A et al., 2012, Shrestha SS et al., 2012, Huma Z et al., 2014). As mentioned earlier in Chapter 4, rat SRT cells receive some excitatory reticulospinal contacts (VGLUT-2), which form a small proportion of all excitatory contacts. This corresponds well with electrophysiological data obtained from cat that show mostly polysynaptic actions in these neurons in response to MLF stimulation.

Both rat and cat spinoreticular cells receive a substantial proportion of excitatory contacts that are VGLUT-1 positive. VGLUT-1 is present in all primary afferent boutons within the deeper laminae of the spinal cord as well as terminals of the corticospinal tract (Oliveira AL et al., 2003, Todd AJ et al., 2003, Alvarez FJ et al., 2004, Du Beau A et al., 2012, Shrestha SS et al., 2012). So although spinoreticular cells receive contacts mostly from excitatory interneurons there is significant input from primary afferents as well. Approximately 15% of the primary afferents in contact with SRT cells in rats are labelled by VGLUT-1 and thus potential sources of these contacts may be from myelinated cutaneous afferents presumably A $\beta$  low threshold mechanoreceptors (Menetrey D et al., 1984, Molander C and Grant G, 1987, Todd AJ, 2010a). In agreement with Haber et al (1982) electrophysiological data from cat showed that most SRT cells are either unresponsive to peripheral stimulation or respond to polysynaptic inhibitory inputs. This is in contrast to the anatomical data from both cat and rat that show significant VGLUT-1 contacts. It may be, however, that spinoreticular cells are particularly sensitive to anaesthetics and thus are not as excitable under anaesthesia (Fields HL et al., 1977, Haber LH et al., 1982). Another explanation for the lack of peripheral receptive fields would be a strong tonic descending inhibition or inputs from structures that were not stimulated (e.g. viscera).

In addition to cutaneous contacts these cells receive contacts from proprioceptive afferents as demonstrated by co-localisation of parvalbumin with VGLUT-I in terminals (Celio MR, 1990, Zhang JH et al., 1990, Ichikawa H et al., 1994, Clowry GJ et al., 1997, Varoqui H et al., 2002, Ichikawa H et al., 2004). Myelinated Group Ia, Ib and group II fibres are present in the intermedio-ventral laminae and are involved in a variety of motor functions from maintenance of posture, to limb co-ordination, stepping and general flexion reflex (Brown AG and Fyffe RE, 1978). Furthermore cutaneous afferents from various peripheral nerves as well as high threshold muscle afferents evoke excitatory and inhibitory effects in the neurons of the reticular formation (Giaquinto S and Pompeiano O, 1963, Oscarsson O and Rosén I, 1966, Thies R, 1985) and are likely candidates for the exercise pressor reflex (Degtyarenko AM and Kaufman MP, 2002). Thus SRT neurons in the lumbar cord may play a role in integrating proprioceptive inputs via Group I and possibly Group II afferents and relay this information to the LRN, to be forwarded to the cerebellum, thus modifying motor responses.

In contrast to other studies that also used CTb to label primary afferents from the sciatic nerve, we observed some primary afferent fibres with neither VGLUT-1 nor parvalbumin labelling (Olave MJ et al., 2002, Todd AJ et al., 2003, Shehab SA and Hughes DI, 2011). One reason behind this apparent aberration might be inadequate labelling by VGLUT-1 as some of these terminals had ambiguous VGLUT-1 staining and were not included in the final quantitative analysis. Injury to some of the sciatic nerve axons during placement of the pipette may be another factor, as axotomy studies have shown VGLUT-1 is depleted from central terminals of transected primary afferents. This loss is more severe in proprioceptive rather than cutaneous afferents (Shehab SA et al., 2003, Hughes DI et al., 2004).

### **5.4.3 Inhibitory contacts to spinoreticular cells in the rat and cat lumbar spinal cord**

In both rats and cats there is no significant difference in the percentage of inhibitory (VGAT), compared with excitatory terminals (both VGLUTs) in contact with somata and dendrites of SRT cells. As previously explained, VGAT labels all inhibitory terminals containing GABA and/or Glycine (Todd AJ and Sullivan AC,

1990, Chaudhry FA et al., 1998, Wojcik SM et al., 2006). With the addition of gephyrin we can deduce that most, if not all, of these contacts are actual synapses on the cells as there is strong evidence for the presence of gephyrin within the post synaptic densities of GABAergic/glycinergic synapses (Mitchell K et al., 1993, Todd AJ et al., 1995). There are two potential sources of inhibitory contacts to these cells, inhibitory interneurons within the spinal grey and descending systems from the brain.

The only known descending system with inhibitory terminals in the lumbar spinal cord is from ReST neurons (Holstege G, 1991, Du Beau A et al., 2012, Huma Z et al., 2014). As mentioned in the previous chapter, small but significant numbers of these reticulospinal terminals contact SRT cells in the rat. This is in contrast to the findings for cat SRT neurons, where a descending inhibitory input was not detected electrophysiologically, possibly because of sparse contact densities and hence a weak input. Furthermore in cat, the source of inhibitory terminals may be limited to spinal interneurons or propriospinal neurons, in view of lack of evidence of supraspinal direct inhibitory inputs to these neurons in the lumbar segments (Hammar I et al., 2011).

Thus the most likely source of inhibitory synapses on both the rat and cat cells is from local intraspinal inhibitory neurons. Spinoreticular neurons concerned with the bVFRT receive bilateral excitatory as well as inhibitory inputs by stimulation of peripheral afferents (i.e. the so called flexor reflex afferents)(Holmqvist B, 1960, Lundberg A and Oscarsson O, 1962b, Oscarsson O and Rosén I, 1966, Rosén I and Scheid P, 1973a, Clendenin M et al., 1974 b, Illert M et al., 1978, Alstermark B et al., 1981, Ekerot CF, 1990c). These polysynaptic IPSPs from ipsilateral FRAs would be mediated by intervening inhibitory interneurons (Eccles JC et al., 1961, Lundberg A and Weight F, 1971, Jankowska E and Edgley SA, 2010b). The finding of several hundred to thousands of VGAT synapses onto individual rat (~100/cell) and cat cells (~3000/cell) suggests two possible models of inhibitory interneuronal contacts to these cells; these are either multiple contacts from individual interneurons or are individual contacts from a large group of interneurons. Either way as these interneurons mediate inhibition from several sources, it suggests a convergence of many spinal circuits onto these cells, thus modifying signals to the brain stem (Alvarez FJ et al., 2005,

Jankowska E and Edgley SA, 2010b, Liu TT et al., 2010b). Jankowska and Edgley (2010) in their review on the functional properties of spinal interneurons refer to two groups of inhibitory glycinergic interneurons in the deep dorsal and ventral horn with axonal projection fields extending into the deep dorsal, intermediate and ventral laminae (see Figure 3 in (Jankowska E and Edgley SA, 2010a). These interneurons are activated by Group I and II muscle and joint afferents as well as descending cortico-, rubro-, vestibulo- and reticulospinal tracts. Thus, it is likely that a potential source of the inhibitory contacts to SRT neurons is from these interneurons mediating Group I and II primary afferent inputs. This agrees with the electrophysiological findings from cat SRT cells in this study, which have polysynaptic inhibitory inputs from Group II proprioceptors.

#### **5.4.4 Choline acetyltransferase, parvalbumin and calbindin contacts on SRT neurons**

Neurochemical markers have been used extensively to identify functionally discrete groups of neurons in the spinal cord, be they projection neurons or interneurons. As most of the contacts onto the SRT appear to be from interneuronal populations it is safe to assume that SRT cells would be potential targets for these neurochemically identifiable interneuronal cells. In this study a substantial number of contacts were parvalbumin positive along with moderate contacts from choline acetyltransferase but sparser calbindin contacts.

There is a variety of potential sources of calbindin, calretinin or parvalbumin immunoreactive terminals on the SRT cells; from descending systems, collaterals from projection neurons, primary afferents and interneurons. Calcium binding proteins CB, CR and PV are widely distributed in the neurons and terminals of the spinal cord grey matter (Antal M et al., 1990, Celio MR, 1990, Antal M et al., 1991, Ichikawa H et al., 1994, Ren K and Ruda MA, 1994). In this study as well as previous work it has been shown that CB is present in some SRT neurons (Menetrey D et al., 1992) in addition to other neurons of origin of spinothalamic and spinomesencephalic tracts (Craig AD et al., 2002, Morona R et al., 2007). In addition Rubrospinal fibres immunoreactive for CB as well as PV are distributed in the spinal grey (Wang YJ et al., 1996). Although CB immunoreactive terminals do not seem to originate from primary afferents, proprioceptive primary

afferent contacts are immunoreactive for PV. In spite of this, PV contact densities on these cells far outnumber all VGLUT-1 contact densities; it is therefore proposed that most of these PV-ir terminals are from interneurons within the spinal cord. There are almost no calbindin contacts on SRT cells; hence it appears that these terminals do not form a significant component of SRT neuronal circuitry.

So what is the significance of these PV immunoreactive terminals on the spinoreticular cells? Distinct cell types derived from genetically discrete populations of embryonic neurons have been identified in the spinal cord. Alvarez et al (2005) identified groups of ventral interneurons labelled by CABPs, mostly PV and CB, with the largest proportion being PV immunoreactive. These interneurons have contacts from proprioceptive primary afferents. Thus, a cautious interpretation pertaining to SRT cells is that the presence of these PV contacts suggests that, in addition to the direct proprioceptive input, there is an indirect input via intervening interneurons. Subgroups of PV/GABA immunoreactive interneurons have been defined in the deep dorsal horn as well as ventral horn (Antal M et al., 1991, Alvarez FJ et al., 2005). Further tests to find out if PV inputs to SRT cells are inhibitory would be interesting as it would explain one possible neurochemical pathway of the polysynaptic inhibitory input from muscle afferents seen in the electrophysiological records in cat SRT neurons.

In addition to CABPs, a significant proportion of contacts on SRT cells are ChAT immunoreactive. In principle, these cholinergic contacts could arise from intrinsic spinal neurons as well as descending cholinergic innervation or primary afferents. There is general agreement on the absence of descending cholinergic innervation (Kanazawa I et al., 1979, Woolf NJ and Butcher LL, 1989, Sherriff FE et al., 1991). Although there is some controversy regarding the existence of cholinergic primary afferents, by using different antibodies, some studies have concluded that dorsal root ganglion cells (DRG) do not express ChAT (Barber RP et al., 1984, Borges LF and Iversen SD, 1986, Mesnage B et al., 2011) while others show evidence of ChAT positive DRG cells (Matsumoto M et al., 2007). The presence of cholinergic dendrites within laminae II and III indicates that they arise, at least in part from intrinsic spinal neurons with cell bodies in lamina III

and IV (Ribeiro-Da-Silva A and Cuello AC, 1990, Pawlowski SA et al., 2013). Spinoreticular cells in all three zones (deep dorsal, intermediate, lamina X) have ChAT contacts and it is probable that they originate exclusively from local interneurons within these respective laminae. Acetylcholine (ACh) levels in the spinal cord critically control nociceptive behaviour by a balance between acetylcholine esterase (AChE) and ChAT as well as activation of nicotinic and muscarinic Ach receptors; nociceptive versus analgesic action (Hama A and Menzaghi F, 2001, Rashid MH and Ueda H, 2002). Thus SRT cells in the deep dorsal horn may be influenced by these ChAT interneurons and thus play a role in sensory modification of these neurons to acute pain. Furthermore a study by Todd in 1991 showed the presence of inhibitory markers GABA/glycine within ChAT positive terminals in the deep dorsal horn. Such terminals may further suppress the excitability of SRT neurons involved in nociception by post synaptic inhibition.

In addition, along with the deep dorsal neurons described above, Borges and Iversen (1986) described two other cholinergic systems within the spinal cord: motor neurons innervating muscles with collaterals influencing neighbouring ventral horn cells; and lamina X interneurons projecting to dorsal, intermediate and the ventral grey matter neurons (Borges LF and Iversen SD, 1986, Liu TT et al., 2010b, Arber S, 2012). The proposed roles for these interneurons are sensory processing and motor output (Barber RP et al., 1984, Huang A et al., 2000). Later studies using retrograde double-virus infection from defined target muscles in mice have shown that the majority of ipsilateral ChAT interneurons (to muscular injections) are found in laminae VI, VII and X, while contralateral interneurons are mainly confined to ventromedial lamina VII and laminae VIII (Stepien AE et al., 2010). Neurons in this domain are known to receive input from the reticular formation and contain both excitatory and inhibitory commissural interneurons with direct connections to contralateral motor neurons (Bannatyne BA et al., 2003, Jankowska E et al., 2003). Hence, SRT cells in these laminae may have cholinergic contacts from these commissural ChAT interneurons and may be indirectly influenced by descending reticulospinal projections. Thus, it may be one of the pathways through which the brainstem modifies sensori-motor output. Furthermore, cholinergic neurons within the dorsal and intermediate grey influence sensory input from the dorsal horn as

well as autonomic output (Rexed B, 1952, Brezenoff HE, 1984, Borges LF and Iversen SD, 1986). In conclusion, as ChAT cells in various laminae have functionally defined roles of sensory, motor or autonomic functions it is possible that SRT cells within these laminae subserve similar roles and it would be interesting to find out where the source of these inputs were located from a functional point of view. These contacts to the SRT neurons may in turn form part of several, overlapping levels of regulation not only within the spinal cord but to the higher centres in the brain as well.

Although this part of the study sheds light on some neurochemically distinct terminals contacting SRT neurons further work needs to be done in defining the sources of these markers to try and identify functional implications of these spinal circuits.

#### **5.4.5 Functional considerations**

This part of my study has an extra dimension because information is not only provided by a comparison between two different species (rat and cat) but also because some functional data is provided by recordings from cat SRT neurons. Taken together, these findings provide a new basis for understanding the organisation and functional connectivity of spinoreticular cells in the lumbar enlargement of the cat and rat. The anatomical pattern of excitatory and inhibitory contacts on SRT neurons is in agreement with previous electrophysiological data as discussed above. Results of the present study provide further evidence that excitatory and inhibitory contacts to spinoreticular neurons have specific and overlapping origins from the periphery, spinal and supraspinal levels. Thus such an of assimilation of information by these cells, particularly as regards contacts from interneurons and propriospinal neurons provides an indication of their role in the spinal circuitry at a segmental level. As is seen in co-ordinating movements between forelimbs and hindlimbs in the spinalised cat (Haber LH et al., 1982, Barbeau H and Rossignol S, 1987, Alstermark B et al., 1990, De Leon RD et al., 1998, Matsuyama K et al., 2004).

These spinoreticular cells form a part of the indirect spino-reticulo-cerebellar pathway that convey proprioceptive as well as tactile information to the

cerebellum to modify movement, adjust posture and prevent injury (Alstermark B and Ekerot CF, 2013). Although there is a descending component of this spino-cerebellar loop via a substantial ReST pathway to the lumbar spinal cord, the fibres contacting SRT neurons directly is sparse. An alternative path therefore is likely to be via polysynaptic inputs from intervening interneurons that may augment ReST signals to SRT neurons. The cerebellum would receive this integrated information likely to help in adjusting descending commands accordingly, for example, in posture adjustments during withdrawal reflex (Arshavsky YI et al., 1978 a, Peterson BW, 1979a, Leblond H et al., 2000, Habaguchi T et al., 2002, Jankowska E et al., 2003).

It has been proposed that the bVFRT pathway may signal information regarding activity in spinal circuits regulating posture during standing, locomotion and scratching (Clendenin M et al., 1974 b). A question typically asked in correlating electrophysiological data to anatomical is that: are some of these spinoreticular cells a component of the bVFRT, i.e. activated by flexor reflex afferents? A cautious answer would be that although some of the features of these cells fit the bVFRT profile these neurons seem to be a different group altogether. Anatomically, they are located in the ventromedial laminae, responding to cutaneous as well as muscular afferents with a small but significant input from the ReST pathway and are likely to play a key role in anticipating peripherally derived sensory feedback and relaying this information to the cerebellum via the lateral reticular nucleus. However, electrophysiologically these cells do not appear to have the extensive bilateral excitatory and inhibitory field of the bVFRT and in addition they are polysynaptically inhibited by descending supraspinal input.

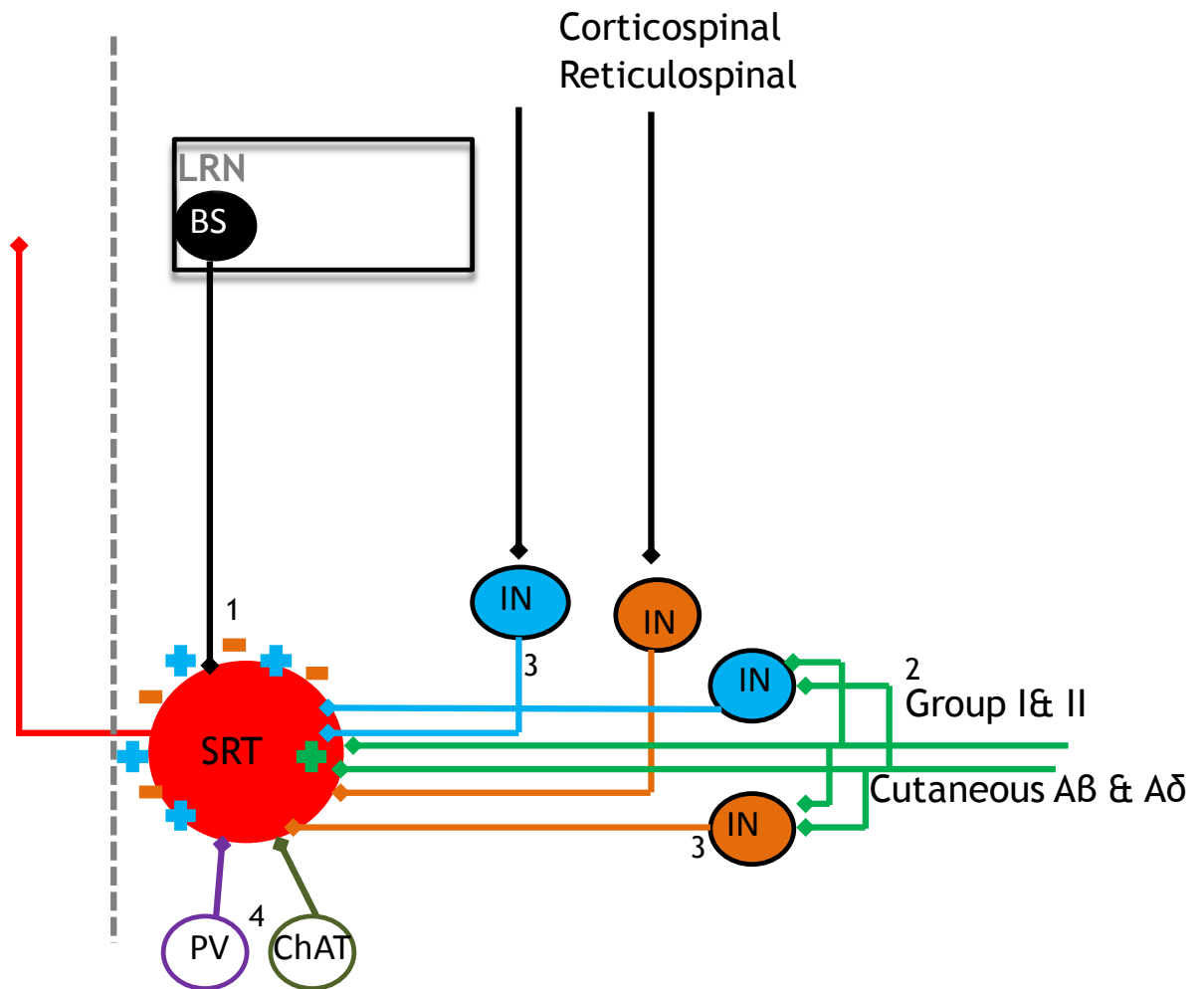


**Figure 5-21 Summary of excitatory and inhibitory inputs to spinoreticular cells**

A spinoreticular cell (red circle) with VGLUT-2 (blue crosses), VGLUT-1 (green crosses) and VGAT contacts (orange hyphen). Potential sources of these inputs are:

- 1) Descending bulbospinal (BS, black circle and line);
- 2) Cutaneous and proprioceptive afferents, Group I & II (green lines);
- 3) Excitatory interneurons (blue circles and lines, VGLUT-2) and inhibitory interneurons (orange circles and lines); and
- 4) Choline acetyltransferase (ChAT) and parvalbumin (PV) contacts.

# Chapter 6

## 6 Spinoreticular neurons; neurochemical phenotypes and response to noxious stimulus

### 6.1 Introduction

In the spinal cord populations of neurochemically defined neurons have been recognised based on the expression of neuropeptides and various proteins (Antal M et al., 1991, Todd AJ and Spike RC, 1993, Al Ghamdi KS et al., 2009). Thus neurochemistry may be used to define subpopulations of cells as well as provide an indication of the possible functional role that some of these neurons carry out.

It has been demonstrated that the calcium binding proteins (CABPs) calbindin and calretinin either singly or in combination are markers of separate neuronal populations (Menetrey D et al., 1992, García-Larrea L et al., 1993, Ren K and Ruda MA, 1994, Anelli R and Heckman CJ, 2005). The precise physiological function of calbindin and calretinin is still not known however recent investigations favour a role in  $Ca^{+2}$  homeostasis and that they perform a subtle regulation and timing of  $Ca^{+2}$  signals pre and post-synaptically (Vecellio M et al., 2000, Blatow M et al., 2003, Cheron G et al., 2004). Studies have identified interactions between  $Ca^{+2}$  and the extracellular signal regulated kinase (ERK) cascades in mitogen-activated protein kinase (MAPK) pathways that show an increase in intracellular free  $Ca^{+2}$  concentrations leading to increased ERK phosphorylation (Rosen LB et al., 1994, Agell N et al., 2002).

Choline acetyltransferase (ChAT) is an enzyme responsible for the formation of the essential neurotransmitter acetylcholine (ACh) and has been used extensively to define cholinergic neurons (Barber RP et al., 1984, Huang A et al., 2000). In rodents, spinal ACh is known to be a modulator of nociceptive transmission in the spinal cord (Zhuo M and Gebhart GF, 1991, Rashid MH and Ueda H, 2002, Matsumoto M et al., 2007). Furthermore activation of the cholinergic system in the spinal cord depolarises motor neurons (Zieglgansberger W and Reiter C, 1974) and is involved in the generation of programmed motor responses (Cowley KC and Schmidt BJ, 1994).

The anterolateral quadrant (ALQ) of the spinal cord conveys noxious mechanical and heat sensitivities to the brain. In addition to the spinothalamic tract, the spinoreticular tract is one of the principal somatosensory pathways in the ALQ (García-Larrea L et al., 1993). For review see (Fields HL and Basbaum AI, 1978). Hence the spinoreticular system plays a critical role in the central processing of noxious stimuli (Fields HL et al., 1977, Haber LH et al., 1982, Kevetter GA et al., 1982). Electrophysiological experiments have shown that spinoreticular neurons in the deep dorsal and intermediate laminae respond to high threshold stimuli presumably from A $\delta$  or C fibres evoked by noxious pinch (Fields HL et al., 1977, Haber LH et al., 1982, Kevetter GA et al., 1982). These primary afferents release glutamate to activate neurochemically and physiologically distinct populations of spinal projection neurons (Todd AJ et al., 2000, Todd AJ et al., 2002b, Sardella TC et al., 2011). For review see (Basbaum AI and Braz JM, 2010).

There are a number of known mechanisms involved in the transmission of nociceptive information. Many small diameter primary afferents contain Substance P (SP) which act on neurokinin 1 (NK-1r) receptors on certain neurons (Helke CJ et al., 1990, Brown JL et al., 1995, Littlewood NK et al., 1995). All SP containing afferents appear to be nociceptive as the peptide is released following noxious stimulation (Light AR and Perl ER, 1979, Duggan AW and Hendry IA, 1986, Sugiura Y et al., 1986, Lawson SN, 1995) and this results in internalisation of NK-1 receptors (Mantyh P et al., 1995, Polgár E et al., 2010). Nitric oxide (NO) produced by nNOS plays an essential role in inflammatory and neuropathic pain states (Schmidtko A et al., 2009). It is therefore important to determine which neurons express nNOS, as specific pharmacological inhibitors can be targeted to these cells to relieve neuropathic pain, for example, nitroimidazole (Southan GJ and Szabó C, 1996).

One of the signal transduction mechanisms of primary afferent neurons responsible for the modulation of pain transmission is through activation of ERKs by noxious mechanical stimulation via membrane depolarisation and calcium influx (Khasar SG et al., 1999, Aley KO et al., 2001, Chang KT and Berg DK, 2001, Karim F et al., 2001, Dai Y et al., 2002). pERK activates NMDA or metabotropic glutamate receptors which via transcriptional activation of NK-1 lead to central or peripheral sensitisation (Ji RR et al., 2002).

However, there is a paucity of information regarding the relationship between neurochemical phenotypes of spinoreticular neurons and their role in nociception. Throughout this thesis it has been shown that spinoreticular neurons form an integral part of the spinal circuitry and are involved in a variety of sensorimotor activities that are activated and modified not only by the descending systems but also directly and indirectly by primary afferents. The aim of this study was to provide support for the proposal that there are various subgroups of neurochemically identifiable SRT neurons in the lumbar spinal cord and to determine if particular chemical subtypes respond to noxious stimuli. Such cells could play a critical role in the central processing of nociception by providing information to the reticular formation concerning the activation of nociceptors. The reticular formation in turn would influence higher centres in the brain and participate in the descending control of this nociceptive input through projections to the spinal cord.

To achieve this, two major aims were formulated:

- Aim I: to identify subgroups of SRT cells using neurochemical markers; NK-1r, nNOS, CB, CR and ChAT; and
- Aim II: to find out whether chemical subtypes of SRT cells respond to acute noxious mechanical stimulus.

## 6.2 Methods

In total eleven adult male Sprague Dawley rats (Harlan, Bicester, UK) were injected with CTb into the left LRN (inter-aural co-ordinates -4.8mm; 1.8, medio-lateral and dorso-ventral, -0.4,(Paxinos G and Watson C, 1997). The details of the stereotaxic injection, perfusion and subsequent dissection and processing for immunohistochemistry have already been given in [Chapter 2](#).

Following a six day interval, seven of these animals were deeply anaesthetised (tested by the absence of the corneal reflex) with Urethane 3ml-5ml i.p (Sigma-Aldrich Co., UK). A noxious mechanical stimulus, in the form of pinching of folds of skin with a Kocher's forceps with toothed jaws, was applied for 2mins on the dorsal and plantar aspects of the right hind paw (contralateral to the LRN injection site, [Figure 6-1C](#)). The stimulus was applied at five selected sites of the foot pad as well as the dorsum of the foot with each site having ~20sec of stimulation. These animals were perfused after an interval of 5mins, from the end of the last stimulus, with 4% Paraformaldehyde in 0.1M PB. The spinal cord and brain were removed and post-fixed in the same fixative overnight at 4° C.

Coronal sections of the medulla (100µm) were cut with a freezing microtome for histological examination of the injection site and the sites were visualised by using DAB as a chromogen ([Figure 6-1A](#)). Sections from Lumbar 3, 4 & 5, were cut into 50µm thick transverse sections with a vibrating microtome and further immunohistochemical reactions carried out as shown in [Table 6-1](#).

In the first phase of this experiment, sections were incubated in two groups, to find out what proportion of CTb labelled SRT neurons were labelled for calbindin and calretinin ([Group A, Table 6-1](#)) or calbindin and ChAT ([Group B](#)) and subsequently incubated in secondary antibodies 48hrs later. Three channels of a confocal laser scanning microscope (Bio-Rad Radiance 2100, Hemmel Hempstead, UK) were used to identify CTb, CB, CR or ChAT.

In the second phase, for animals with a noxious stimulus applied to the hind paw, all sections were prepared for immunofluorescence by incubating them in primary antisera to CTb and pERK and then divided into subgroups with

immunoreactions for NK-1r, CB, CR, nNOS or ChAT to determine which of these neurochemical groups of SRT cells are activated by noxious stimuli (Groups A-E, Table 6-2).

Three sections per segment (L3, L4 and L5) were selected randomly from each group and entire sections were systematically scanned at a magnification of x10, to obtain a complete series of images in order to make a montage. Image stacks were analysed with Neurolucida. All retrogradely labelled cells in three zones, deep dorsal horn (laminae IV and V), intermediate grey matter (laminae VI and VII) and lamina X, both ipsi and contralateral to the LRN injection site, were counted and examined for immunoreactivity.

### **6.2.1 Data analysis**

Data are expressed as mean%  $\pm$  standard deviation (SD) and multi group comparisons were made by using an analysis of variance test (ANOVA) followed by a post hoc *Tukey's* analysis, as appropriate. Two variable comparisons among the same population were made by using Student's *t* test. A  $p < 0.05$  was considered as to be statistically significant.

**Table 6-1 Primary and secondary antibody combinations and concentrations used to find out neurochemical phenotypes of SRT neurons**

<b>Group</b>	<b>Primary antibody combination</b>	<b>Primary antibody concentration</b>	<b>Supplier</b>	<b>Secondary antibody combination</b>	<b>Secondary antibody concentration</b>	<b>Supplier</b>
<b>A</b>	mo CTb	1:250	Annika Wilkstrom, Göteborg, Sweden	Rh. Red	1:100	Jackson ImmunoResearch, West Grove, USA
	gt CR	1:1000	Swant, Switzerland	Dylt. 649	1:500	Molecular probes, Eugene, USA
	rbt CB	1:1000	Swant, Switzerland	Alexa 488	1:500	Molecular probes, Eugene, USA
<b>B</b>	mo CTb	1:250	Annika Wilkstrom, Göteborg, Sweden	Rh. Red	1:100	Jackson ImmunoResearch, West Grove, USA
	gt ChAT	1:100	Chemicon/Millipore, Harlow, USA	Dylt. 649	1:500	Molecular probes, Eugene, USA
	rbt CB	1:1000	Swant, Switzerland	Alexa 488	1:500	Molecular probes, Eugene, USA

All secondary antibodies were raised in donkey and conjugated to Rh. Red, Rhodamine Red; Dylt 649, Dylight 649; Alexa 488, Alexa-fluor 488; gt, goat; rbt, rabbit; mo, mouse; CTb, b subunit of cholera toxin; CR, calretinin; CB, calbindin; ChAT, choline acetyl transferase; \*pERK, phosphorylation of extracellular signal regulated kinases; NK-1r (Neurokinin-1 receptor) or nNOS (neuronal nitric oxide synthase).

**Table 6-2 Primary and secondary antibody combinations and concentrations used to investigate response to noxious stimulus by SRT neurons (n=7)**

<b>Group</b>	<b>Primary antibody combination</b>	<b>Primary antibody concentration</b>	<b>Supplier</b>	<b>Secondary antibody combination</b>	<b>Secondary antibody concentration</b>	<b>Supplier</b>
<b>A</b>	gt CTb	1:5000	List (Quadragech), Campbell, USA.	Rh. Red	1:100	Jackson Immunoresearch, West Grove, USA
	mo pERK	1:500	Cell signalling/Millipore,UK	Alexa 488	1:500	Molecular probes, Eugene, USA
	rbt NK-1r	1:10000	Sigma ,USA	Dylt 649	1:500	Molecular probes, Eugene, USA
<b>B</b>	gt CTb	1:5000	List (Quadragech), Campbell, USA.	Rh. Red	1:100	Jackson Immunoresearch, West Grove, USA
	mo pERK	1:500	Cell signalling/Millipore,UK	Alexa 488	1:500	Molecular probes, Eugene, USA
	rbt CB	1:1000	Swant, Switzerland	Dylt 649	1:500	Molecular probes, Eugene, USA
<b>C</b>	gt CTb	1:5000	List (Quadragech), Campbell, USA.	Rh. Red	1:100	Jackson Immunoresearch, West Grove, USA
	mo pERK	1:500	Cell signalling/Millipore, UK	Alexa 488	1:500	Molecular probes, Eugene, USA
	rbt CR	1:1000	Swant, Switzerland	Dylt 649	1:500	Molecular probes, Eugene, USA
<b>D</b>	gt CTb	1:5000	List (Quadragech), Campbell, USA.	Rh. Red	1:100	Jackson Immunoresearch, West Grove, USA
	mo pERK	1:500	Cell signalling/Millipore, UK	Alexa 488	1:500	Molecular probes, Eugene, USA
	rbt nNOS	1:2000	Chemicon/Millipore, USA	Dylt 649	1:500	Molecular probes, Eugene, USA
<b>E</b>	rbt CTb	1:2000	Sigma ,USA	Rh. Red	1:100	Jackson Immunoresearch, West Grove, USA
	mo pERK	1:500	Cell signalling/Millipore, UK	Alexa 488	1:500	Molecular probes, Eugene, USA
	gt ChAT	1:100	Chemicon/Millipore, USA	Dylt 649	1:500	Molecular probes, Eugene, USA

## 6.3 Results

### 6.3.1 Aim I: To investigate the neurochemical phenotypes of spinoreticular neurons in the rat lumbar spinal cord

In this part of the investigation neurochemical properties of SRT cells were examined by immunoreacting them for CB, CR, ChAT, NK-1r and nNOS.

The CTb injection sites, for retrograde labelling of SRT cells in the lumbar spinal cord, were centred on the lateral reticular nucleus with some slight spread to the adjacent reticular tissue (Figure 6-1).

#### *Calcium binding proteins; calbindin and calretinin*

Approximately 20% of CTb labelled cells were immunoreactive for calbindin, calretinin or in some cases for both calbindin and calretinin in varying proportions throughout the deep dorsal, the intermediate laminae and lamina X (Figure 6-3). The pattern of distribution of these double and triple labelled cells can be seen in the confocal image in Figure 6-2. In addition the cells were distributed equally bilaterally in the lumbar spinal cord with some slight differences in the ratios of calretinin to calbindin positive cells; more calretinin on the ipsilateral side as compared to calbindin on the contralateral side (Table 6-3). The average percentage ( $\pm$ SD) of neurons with calbindin or calretinin expressed as a proportion of the total number of CTb labelled neurons is  $8.7\% \pm 4.68$  to  $9.31\% \pm 3.17$ , respectively. The laminar distribution of CB positive cells is more or less even throughout the three areas (deep dorsal, intermediate and lamina X) whereas relatively more CR positive cells were present in the deep dorsal laminae (Figure 6-3).

Although spinoreticular cells immunoreactive for either calbindin or calretinin were present in similar proportions they were both 4.5 times more numerous than cells that were labelled for both CABPs. Most of these double labelled cells (both CB and CR) were present in the deep dorsal laminae. The percentage of these cells on the ipsilateral side was  $3.1 \pm 1.22$  ( $\pm$ SD) as compared to  $1 \pm 1.57$  ( $\pm$ SD) contralateral to the injection site (Table 6-3)

*Neurokinin-1 receptors (NK-1r, neuronal nitric oxide synthase (nNOS) and choline acetyltransferase (ChAT)*

Confocal scans in [Figure 6-4](#) illustrate some of the retrogradely labelled CTb cells that are immunoreactive to NK-1r, nNOS and ChAT and the proportions of these subgroups of SRT cells are shown in [Table 6-4](#).

Approximately 27% of the spinoreticular cells express NK-1 receptors which extended along the soma membrane and onto proximal dendrites. In fact NK-1 receptors could be visualised on second order dendrites where the CTb labelling was getting fainter. Some of these cells also showed internalisation of the NK-1 receptor following noxious stimulation as is illustrated in [Figure 6-4, 4a-c](#). The percentage of CTb NK-1r positive cells ( $20.9 \pm 5.33$ ) when compared with both nNOS and ChAT ( $2.53 \pm 1.45$  to  $0.22 \pm 0.39$ ) was significantly greater ([Figure 6-5A](#)). In addition, there were also significantly more NK-1r positive cells than those immunoreactive for calbindin ( $14.5 \pm 7.01$ ) and calretinin ( $14.3 \pm 4.1$ ) ([Table 6-4](#)).

Neuronal nitric oxide labelled SRT cells only make ~3% of all CTb labelled cells and were distributed in all three zones, the deep dorsal, intermediate laminae and lamina X, in approximately equal proportions ([Figure 6-5B](#)). However most SRT neurons are not cholinergic and the few ChAT labelled cells (~0.2%) were relatively small in size (~8 $\mu$ m in diameter, [Figure 6-4](#)) in the ventromedial part of lamina VII and might represent a distinct population of SRT cells.

**Table 6-3 Percentages of spinoreticular cells immunoreactive for calbindin (CB) and/or calretinin (CR) ipsi and contralateral to the LRN injection**

IPSILATERAL					
Animal	Total no. of SRT neurons	CTb only	CTb/CB	CTb/CR	CTb/CB/CR
1	98	86.7	6.1	5.1	2
2	158	74.7	7	13.9	4.4
3	71	80.3	5.6	11.3	2.8
	Mean%	<b>80.6</b>	<b>6.2</b>	<b>10.1</b>	<b>3.1</b>
	±SD	6.03	0.67	4.53	1.22

CONTRALATERAL					
Animal	Total no. of SRT neurons	CTb only	CTb/CB	CTb/CR	CTb/CB/CR
1	185	75.7	18.4	5.9	0
2	281	82.2	5.7	9.3	2.8
3	352	82.4	6.0	11.4	0.3
	Mean%	<b>80.1</b>	<b>10</b>	<b>8.9</b>	<b>1</b>
	±SD	3.82	7.25	2.73	1.57

**Table 6-4 Percentages of SRT cells labelled by neurochemical markers; NK-1r, nNOS, CB, CR and ChAT**

Animals	NK-1r+	nNOS+	CB+	CR+	ChAT+
1	30.5	1.6	9.4	19	0.67
2	29.7	1.8	22.5	12	0
3	20.9	4.2	11.6	11.8	0
Mean%	<b>27.03</b>	<b>2.53</b>	<b>14.5</b>	<b>14.27</b>	<b>0.22</b>
±SD	5.33	1.45	7.01	4.10	0.39

### 6.3.2 Aim II: Do some subtypes of SRT cells express pERK in response to acute mechanical noxious stimuli?

In this second phase of the study seven Sprague-Dawley rats were given a noxious mechanical stimulus, in the form of pinch to the right hind paw. [Figure 6-1A](#) shows a CTb injection site in the lateral reticular nucleus and [Figure 6-1B](#) illustrates the distribution of somatotopically appropriate pattern of pERK immunoreactivity seen in the superficial dorsal horn ipsilateral to the stimulus and was regarded as proof that the stimulation was adequate (Dai Y et al., 2002, Todd AJ, 2002, Polgár E et al., 2007). The five series of immunoreactions (A to E) carried out to investigate the response of spinoreticular cells to noxious stimulus by phosphorylation of extracellular signal regulated kinase, pERK are listed in [Table 6-2](#).

Approximately 9% of all CTb labelled cells expressed phosphorylation of ERK within somata and dendrites after mechanical noxious stimulation in ipsilateral laminae IV, V, VI, VII and X ([Figure 6-10A & B](#)). The pattern of distribution within the spinal grey matter is also illustrated in a confocal image of a lumbar section in [Figure 6-6](#). [Table 6-5](#) provides details of the proportion of neurochemical subtypes of SRT cells that respond to noxious stimulus by phosphorylation of ERK. Confocal images in [Figure 6-7](#) illustrate spinoreticular cells responsive to phosphorylation of ERK, in addition to showing immunoreactivity to NK-1r, CB, CR, nNOS as well as ChAT and various proportions are illustrated in the bar graphs in [Figure 6-9](#) as percentages of SRT cells.

Neurokinin 1 receptors are present in ~15% of SRT cells responding to pERK ( $\pm 4.95$ , SD) which is significantly greater than CTb/pERK neurons with no NK1-r immunolabelling ( $5.3 \pm 5.0$ ,  $p < 0.05$ , Anova, post hoc *Tukey's*). Hence, more than half of the spinoreticular NK-1r reactive cells (~60%) respond to acute noxious stimulus in the form of pERK expression ([Table 6-5](#)). Most of the cells appeared to be located in the reticular part of lateral lamina V as well as the medio-ventral area of the intermediate laminae and lamina X. [Figure 6-7 panel \(1a-d\)](#) illustrates a SRT/NK-1r positive cell, responsive to pERK.

Calcium binding proteins were also expressed by discreet subgroups of SRT neurons within the spinal laminae. The confocal montage in [Figure 6-7, panels 2 & 3 \(a-d\)](#) illustrates spinoreticular cells that are immunopositive for calbindin and calretinin as well as some that are also pERK positive. However, as the images illustrate, not all SRT cells reactive to CABPs are also responsive to phosphorylation of ERK. In fact only a very small number of these cells show phosphorylation of ERK; 1.9% CB positive ( $\pm 0.73$ , SD) and 1.1% CR positive ( $\pm 0.92$ , SD, [Table 6-5, Figure 6-9 B & C](#)). It is worth noting that there were no pERK responsive SRT/CB cells in lamina X. Whereas, in the deep dorsal laminae, SRT neurons responsive to pERK with no CB/CR labelling were significantly more ( $13 \pm 3.22$ ) than either pERK/CB ( $1.23 \pm 1.47$ ) or pERK/CR cells ( $2.4 \pm 2.14$ ) ([Figure 6-10](#)).

Hardly any pERK immunoreactive SRT cells showed reactivity for nNOS as shown in [Figure 6-9D and Table 6-5](#). Furthermore only ~2% ( $\pm 0.97$ , SD) of SRT cells were labelled by nNOS within intermediate laminae and no pERK/nNOS positive cells were found within either the deep dorsal laminae or lamina X ([Figure 6-10B](#)). [Figure 6-8](#) illustrates a confocal scan with a field view of SRT cells and magnified views of cells with nNOS immunolabelling but no pERK and with pERK but no nNOS labelling.

No ChAT cells expressed pERK. [Figure 6-7 \(5a-d\)](#) shows an example of SRT cells responding to noxious stimulation by the presence of pERK with no reactivity to ChAT.

In all five sub-groups of cells investigated, the percentage of pERK/NK-1r cells is significantly higher than pERK positive nNOS, CB or CR cells ( $p < 0.001$ , [Figure 6-10A](#)). In a comparison between spinoreticular cells that were pERK positive or negative for each of the subgroups of cells; NK-1r, nNOS, CB, CR or ChAT, a within group comparison showed significantly more pERK negative CB and CR cells when compared with pERK positive CB and CR cells ( $p < 0.01$ , [see Figure 6-11](#)).

**Table 6-5 Percentage of various subpopulations of retrogradely labelled spinoreticular cells (SRT/CTb) in response to noxious stimulation**

<b>A</b>	<b>SRT neurons</b>	<b>CTb</b>	<b>CTb/pERK</b>	<b>CTb/NK-1</b>	<b>CTb/pERK/NK-1</b>
1	128	58.6	10.9	11.7	18.8
2	37	62.2	8.1	10.8	18.9
3	72	77.8	1.4	5.6	15.3
4	267	83.3	0.8	7.5	8.3
	Mean%	<b>70.5</b>	<b>5.3</b>	<b>8.9</b>	<b>15.3</b>
	±SD	11.96	5.00	2.87	4.95
<b>B</b>	<b>SRT neurons</b>	<b>CTb</b>	<b>CTb/pERK</b>	<b>CTb/CB</b>	<b>CTb/pERK/CB</b>
1	266	85.3	5.3	6.8	2.6
2	254	74.0	3.5	21.3	1.2
3	207	77.8	10.6	9.7	1.9
	Mean%	<b>79.0</b>	<b>6.5</b>	<b>12.6</b>	<b>1.9</b>
	±SD	5.77	3.70	7.67	0.73
<b>C</b>	<b>SRT neurons</b>	<b>CTb</b>	<b>CTb/pERK</b>	<b>CTb/CR</b>	<b>CTb/pERK/CR</b>
1	274	72.6	8.4	17.5	1.5
2	274	84.7	3.3	12.0	0.0
3	218	72.5	13.8	10.1	1.7
	Mean%	<b>76.6</b>	<b>8.5</b>	<b>13.2</b>	<b>1.1</b>
	±SD	7.00	5.24	3.85	0.92
<b>D</b>	<b>SRT neurons</b>	<b>CTb</b>	<b>CTb/pERK</b>	<b>CTb/nNOS</b>	<b>CTb/pERK/nNOS</b>
1	253	90.9	7.5	1.6	0.0
2	217	91.7	6.5	1.8	0.0
3	267	85.0	10.9	3.4	0.8
	Mean%	<b>89.2</b>	<b>8.3</b>	<b>2.3</b>	<b>0.3</b>
	±SD	3.65	2.30	0.97	0.43

**Figure 6-1 Injection site of CTb into the lateral reticular nucleus of the rat retrogradely labelling SRT cells (red) and distribution of pERK stimulation (green)**

**A.** Photomicrograph of a representative DAB transverse section of the medulla with the CTb injection site (black arrow).

**1 to 3** Reconstructions onto brain maps from Paxinos & Watson, 2005, illustrating the injection sites for three of the animals used in these experiments. The dark grey shaded area shows the primary injection site of CTb and the light grey shaded area represents the spread of the tracer.

**B.** A low magnification confocal scan of a transverse section of L4 of the spinal cord illustrating in green the pattern of distribution of the pERK signal (phosphorylation of extracellular signal regulated kinases) in the dorsal horn (white arrow) and SRT cell (red) with pERK, in the intermediate lamina (arrow head, scale bar 200µm).

**C.** Noxious mechanical stimulation to the right hind paw of the rat.

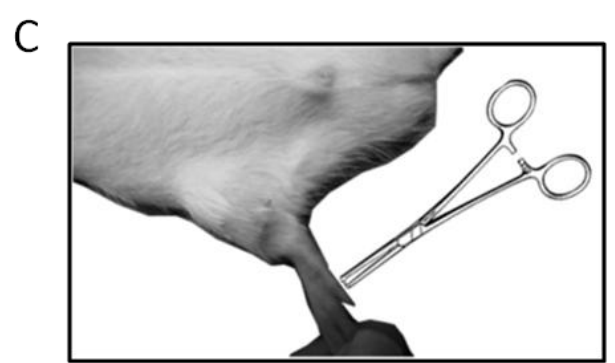
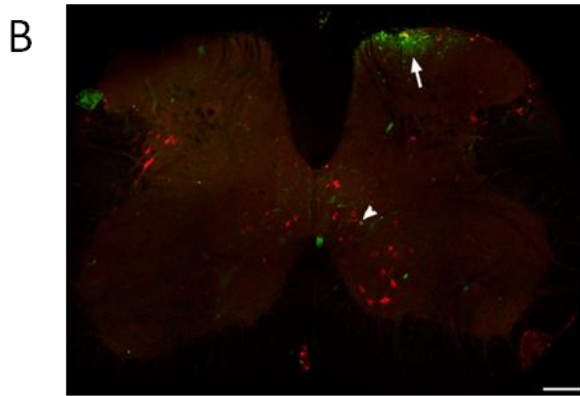
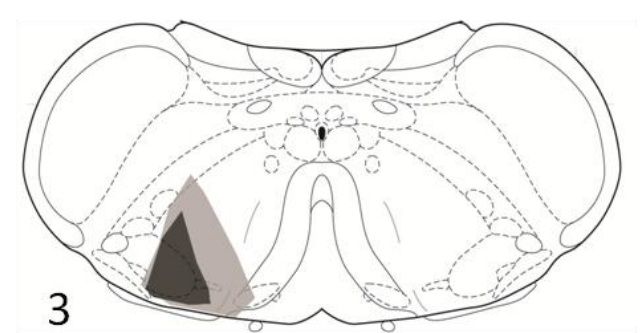
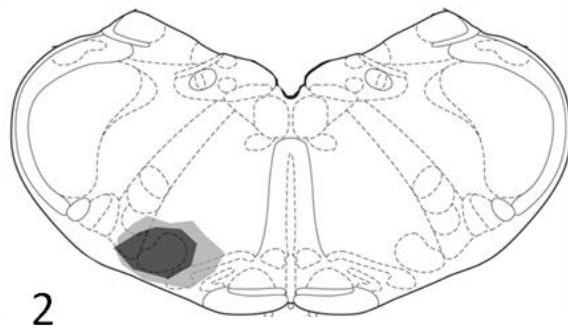
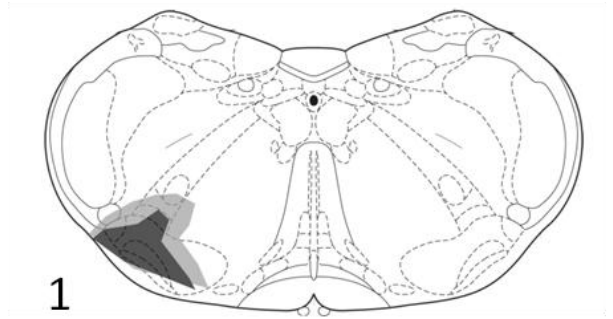
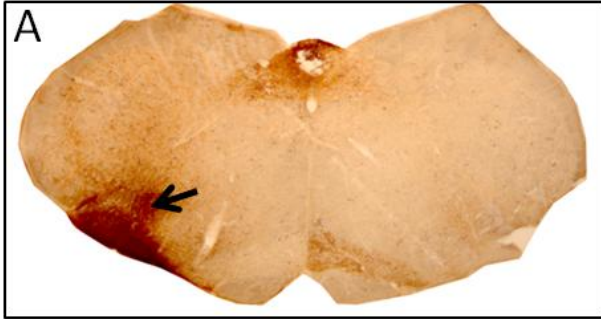
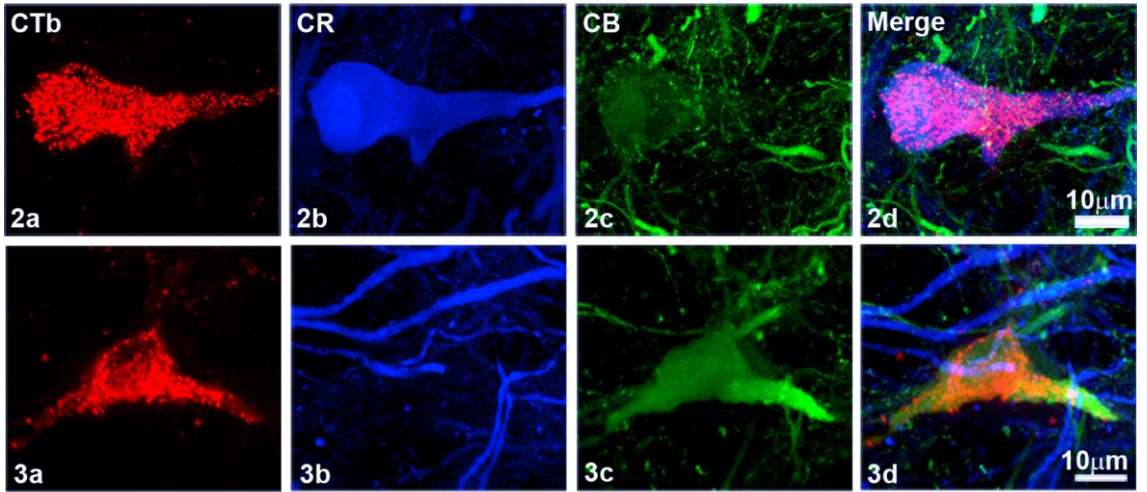
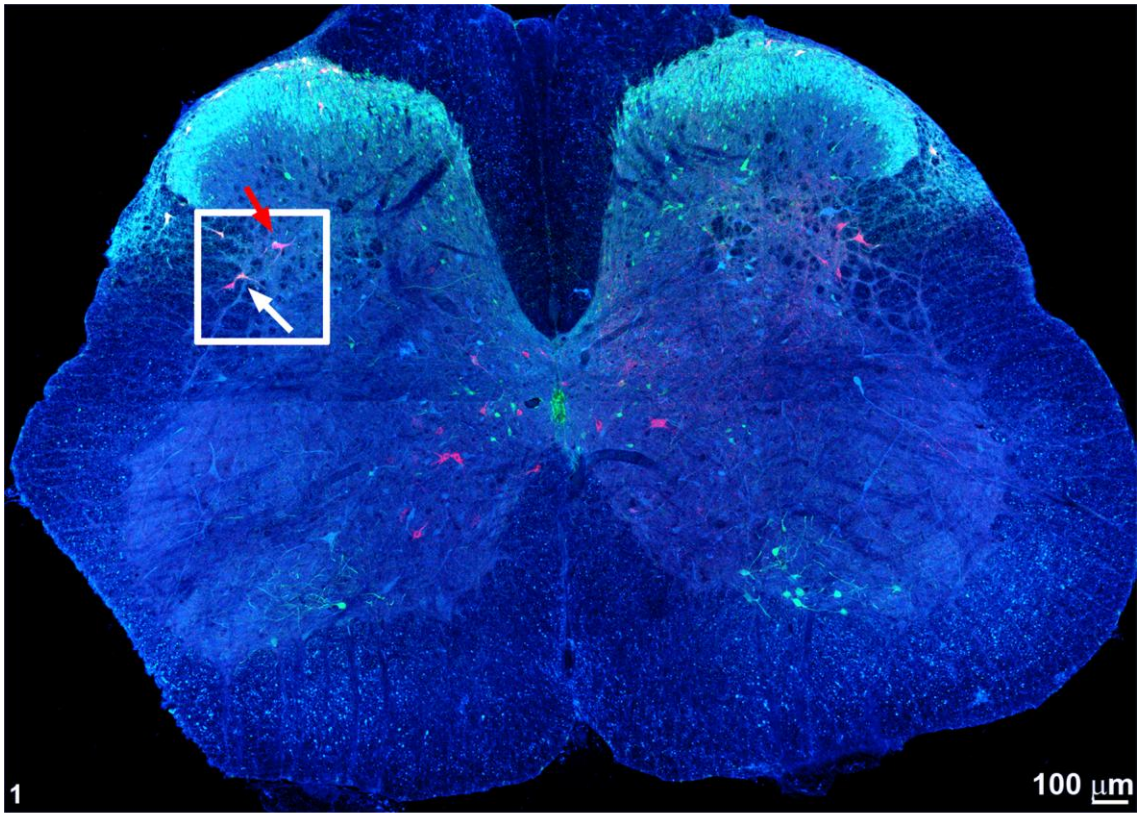


**Figure 6-2 Distribution of spinoreticular cells in the lumbar spinal cord immunoreactive for calcium binding proteins**

**1. Top large panel,** A maximum intensity projected confocal scan of a transverse section of the lumbar spinal cord showing the distribution patterns of the SRT cells (red) with calbindin (green) and calretinin (blue) SRT. The inset shows a representative CTb and calbindin positive cell (white arrow) and a CTb and calretinin cell with weak calbindin (red arrow).

**2a-d, Middle panel,** from left to right, shows a CTb labelled cell (2a, red) that is calretinin positive (2b, blue) and weakly positive for calbindin (2c, green), merged cell (2d, magenta).

**3a-d, Lower panel** from left to right illustrates a CTb labelled cell (3a, red; Rhodamine) with no co-localisation for calretinin (3b, blue; Dylight 649), but has calbindin positive labelling (3c, green; Alexa 488), merged CTb and calbindin cell (3d, orange).



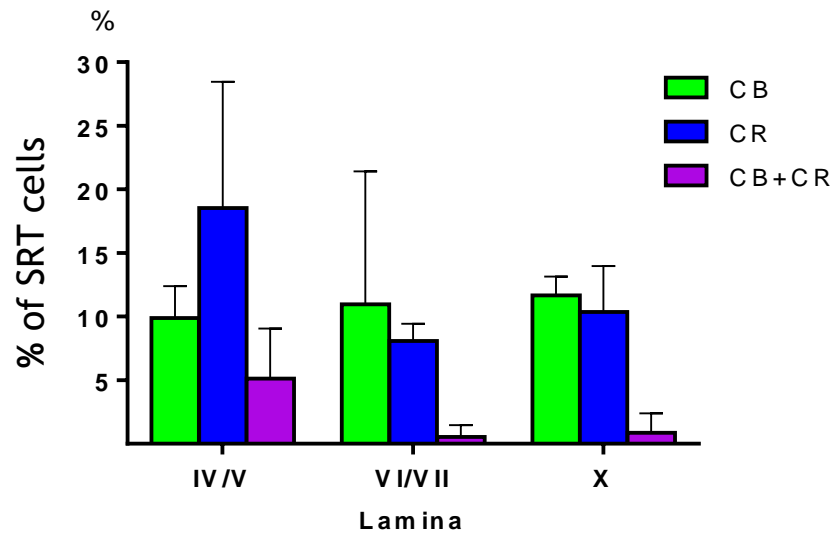


**Figure 6-3 Laminar distribution of SRT cells immunoreactive for calcium binding proteins**

This graph shows the mean percentage of SRT cells in three sections of the lumbar spinal cord both ipsilateral and contralateral to the injection site in the brain. The deep dorsal horn has more calretinin and both calbindin and calretinin positive neurons (ANOVA,  $p > 0.05$  post hoc *Tukey's*,  $n = 3$  animals, cells = 633). T=SD.

**Figure 6-4 Neurochemical phenotypes of spinoreticular cells in the rat lumbar spinal cord**

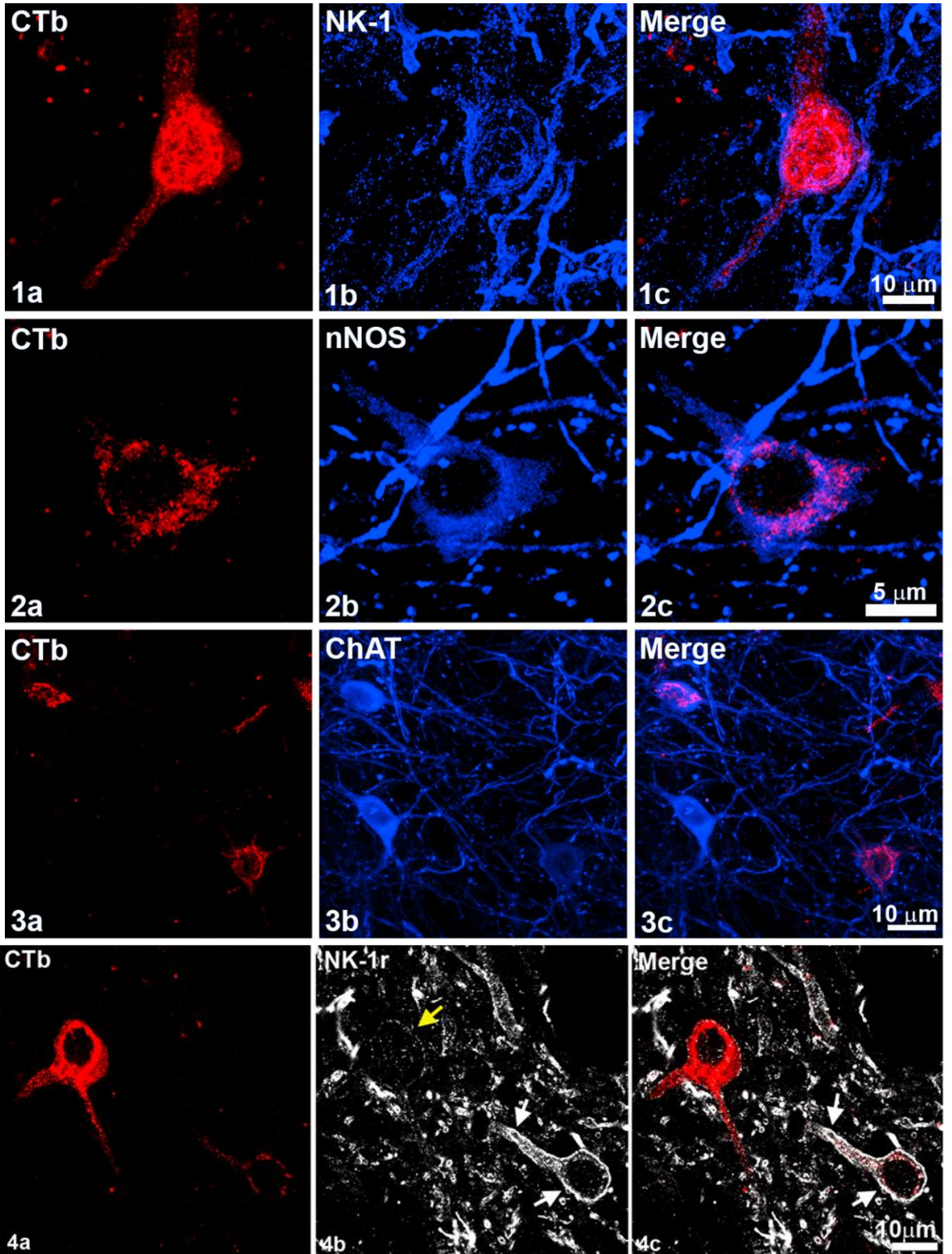
These confocal scans are maximum intensity projections of spinoreticular cells (CTb) that are labelled by markers for neurokinin-1 receptors (NK-1), nitric oxide synthase (nNOS) and choline acetyltransferase (ChAT).

**1a,b** Left to right illustrates a CTb labelled cell (red, Rhodamine red) with the presence of NK-1 receptors (blue, Dylight 649), **(c)** merged image (magenta)

**2a,b** Left to right illustrates a CTb labelled cel (red, Rhodamine red) with the presence of nNOS (blue, Dylight 649) **(c)** merged image (magenta)

**3a,b** Left to right illustrates CTb labelled cells (red, Rhodamine red) with the presence of ChAT (blue, Dylight 649) **(c)** merged image (magenta)

**4a,b** Left to right illustrates CTb labelled cells (red, Rhodamine red) with the presence of NK-1 receptors (grey, Dylight 649), white arrows indicate internalisation of NK-1receptors, yellow arrow shows NK-1 receptors without internalisation **(c)** merged image



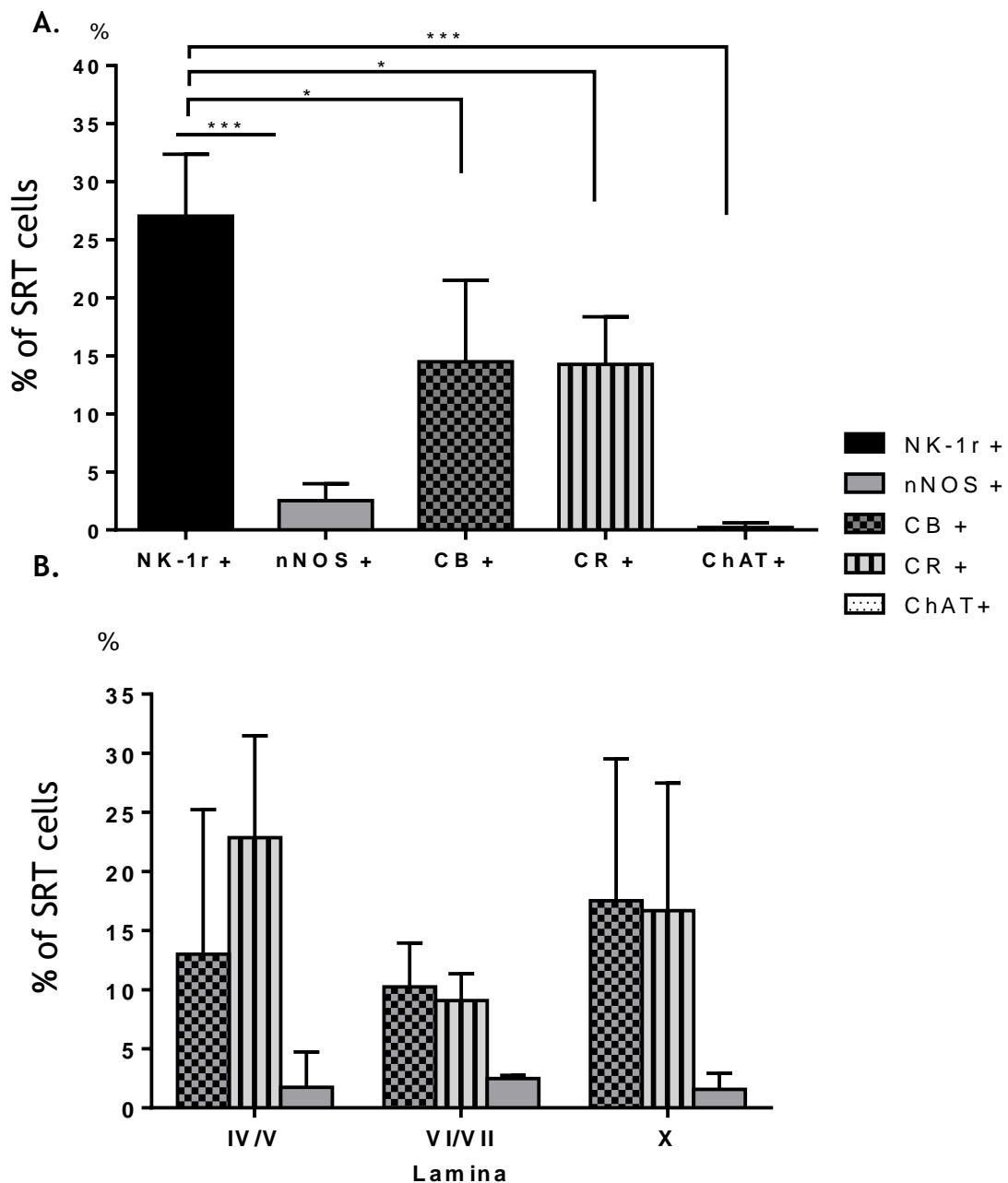


**Figure 6-5 A. Percentage of spinoreticular cells immunoreactive to NK-1r, nNOS, CB, CR and ChAT; B. Laminar distribution of double labelled cells**

A. Percentage of NK-1r positive SRT cells is significantly higher than either the nNOS or ChAT labelled cells (Anova,  $***p < 0.001$ , post hoc *Tukey's*) as well as the calcium binding proteins, CB and CR (Anova,  $*p < 0.05$ , post hoc *Tukey's*).

B. The percentages of both CB and CR are more than nNOS cells in all the three zones.  $n=4$  and  $T = SD$ .

**Figure 6-6 Distribution of Spinoreticular cells (CTb, red) responding to noxious pinch in the rat lumbar spinal cord**

**Large panel,** A maximum intensity projection of a confocal scan of a section of the rat lumbar spinal cord, illustrating retrogradely labelled CTb SRT cells (red, Rhodamine) with pERK immunoreactivity (green, Alexa 488) in the intermediate laminae (Inset 1&3) and the deep dorsal laminae (Inset 2) contralateral to the LRN injection site.

**1a-c,** A magnified view of inset 1 in the intermediate lamina, from left to right, CTb labelled cells that are pERK positive (white arrows, orange), CTb labelled cells that are pERK negative (arrow heads). The yellow arrow points to a pERK responsive cell that is not CTb labelled.

**2a-c,** A magnified view of inset 2 in the deep dorsal lamina from left to right, CTb labelled cell that is pERK positive (white arrow, orange), CTb labelled cell that is pERK negative (arrow heads). The yellow arrow points to a pERK responsive cell that is not CTb labelled.

**3a-c,** A magnified view of two CTb labelled cells from inset 3, pERK positive (white arrow) and pERK negative (arrow head).

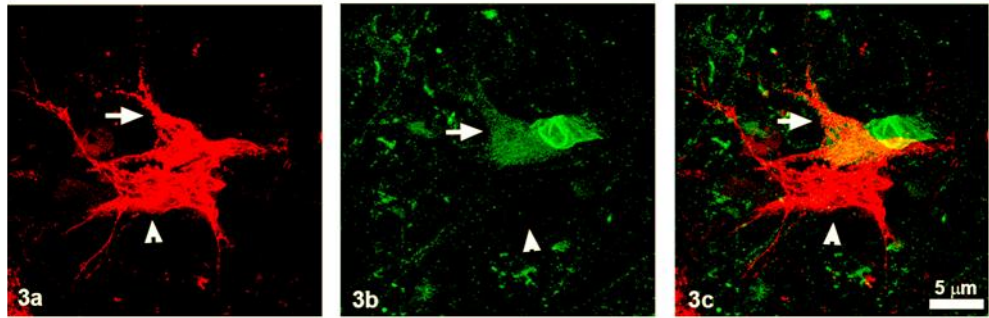
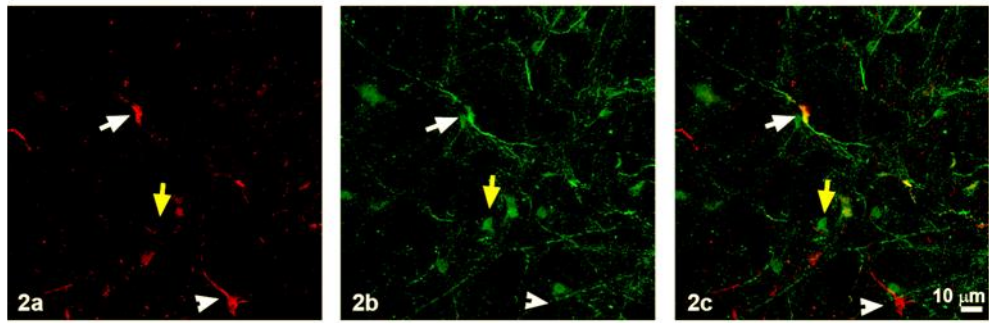
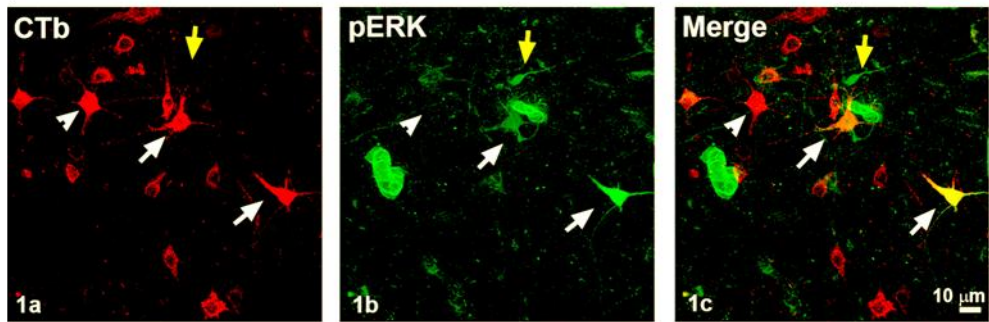
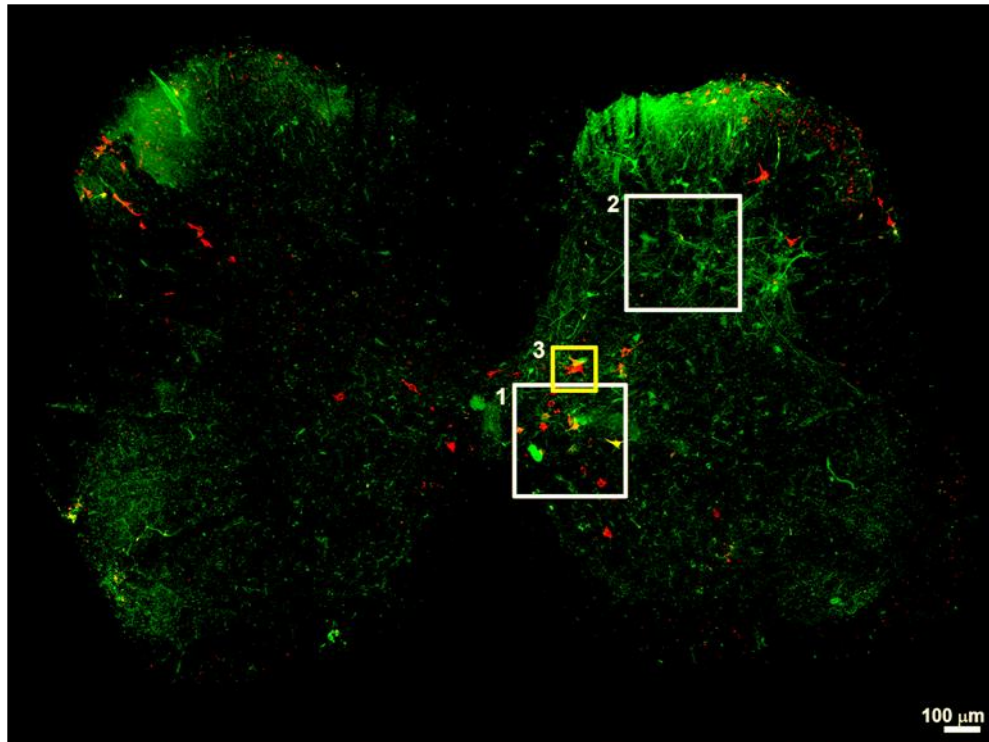


**Figure 6-7 Sub-groups of spinoreticular cells (CTb,red) that are responsive to noxious stimuli by the phosphorylation of ERK**

**1a-d** The cell body of CTb labelled SRT neuron (1a, red; rhodamine red) with the presence of pERK (1b, green; Alexa 488) and NK-1r (1c, blue; dylight 647), 1d merged image.

**2a-d**, Two types of CTb labelled SRT neurons (2a, red) one pERK+ (2b, green, white arrow) and calbindin +ve (1c, blue, white arrow) and the other only calbindin +ve (arrow head), 1d merged image.

**3a-d**, This scan illustrates two types of spinoreticular cells (3a, red) both showing the presence of pERK (3b, green) but one with calretinin (3c, blue, white arrow) and the other pERK (2d, merged, arrow head).

**4a-d**, Soma of a CTb labelled SRT cell (red) that expresses pERK (green) but is not immunoreactive to nNOS (blue), 1d, merged image.

**5a-d**, Illustrates two types of Spinoreticular cells (5a, red; Rhodamine red) one showing phosphorylation of ERK (5b, green, white arrow head; Alexa 488) but negative for ChAT and the other, ChAT positive but pERK-ve (5c, blue, white arrow; dylight 647).

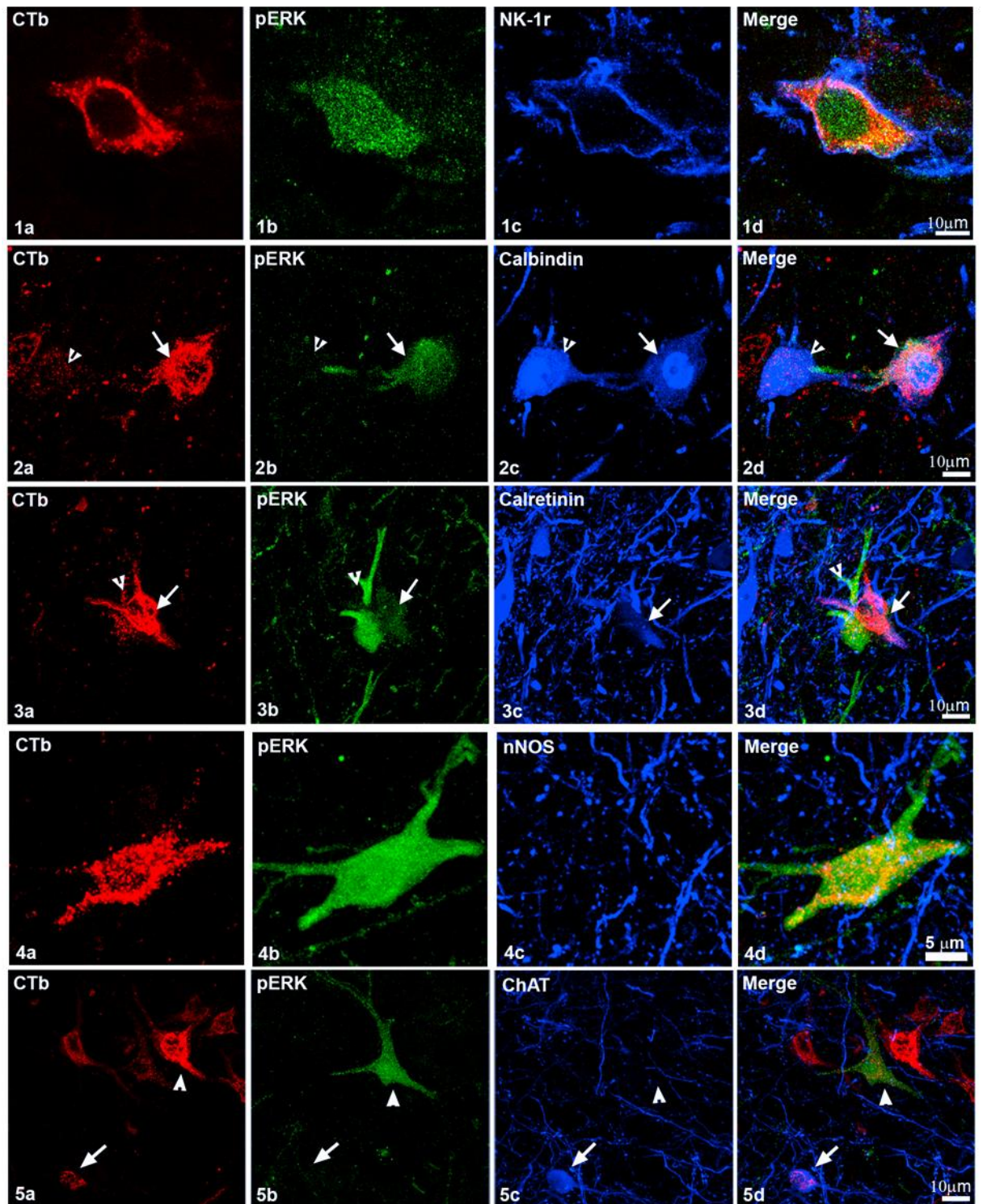


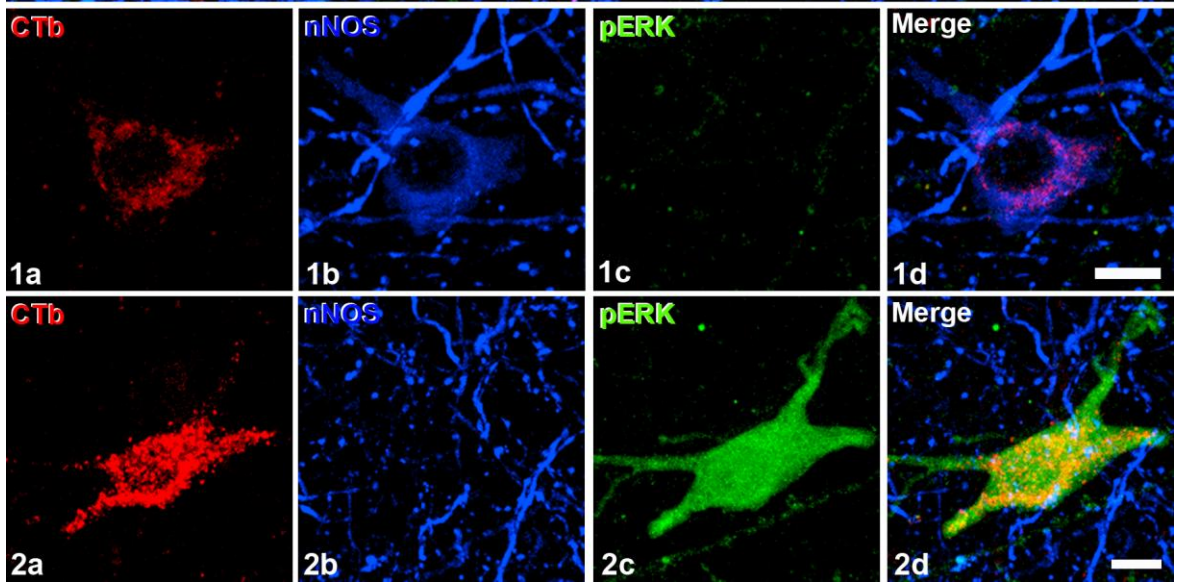
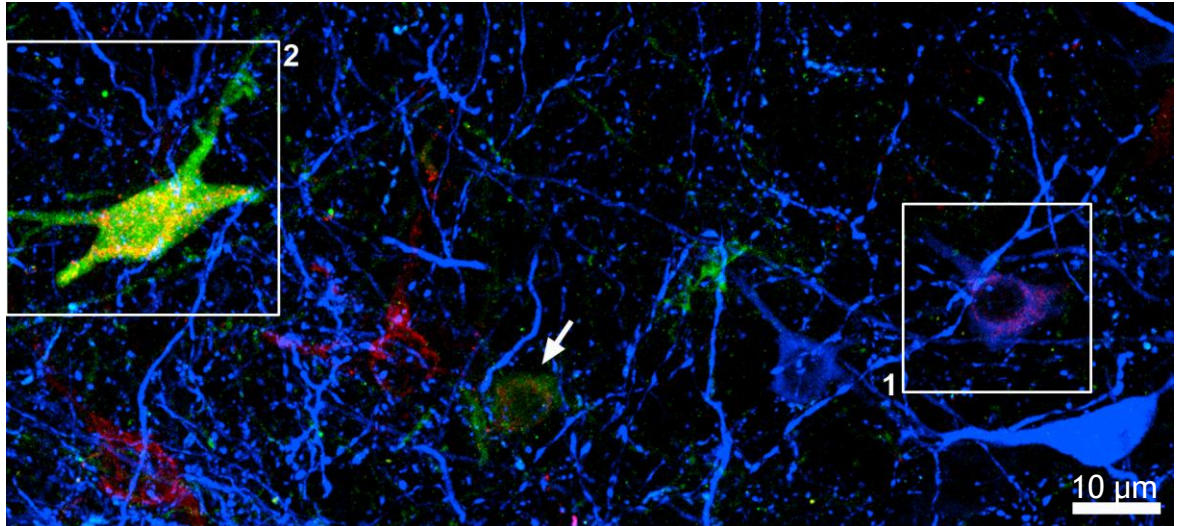
**Figure 6-8 Spinoreticular cells illustrating phosphorylation of extracellular signal regulated kinase and negative for nNOS**

Top panel SRT with pERK (orange, inset 2 and arrow) and SRT cell with the presence of neuronal nitric oxide synthase (nNOS, magenta, inset 1).

Middle panel (1a-d), shows the cell body of a CTb labelled SRT neuron (1a, red; Rhodamine red) and its immunoreactivity with nNOS (1b, blue, arrow; Dylight 647) and negative for pERK (1c, green, Alexa 488). Merged image CTb/nNOS (magenta). Scale bar 5µm.

\*Lower panel (2a-d), illustrates another type of spinoreticular cell (2a, red; Rhodamine) showing the presence of pERK (2c, green; Alexa 488), but no nNOS (2c, blue, arrow; Dylight 647) and 2d, orange, merged). Scale bar 5µm.

\*This is a repeat of Figure 6-7, a-d and has been shown here to illustrate pERK cells in the field.



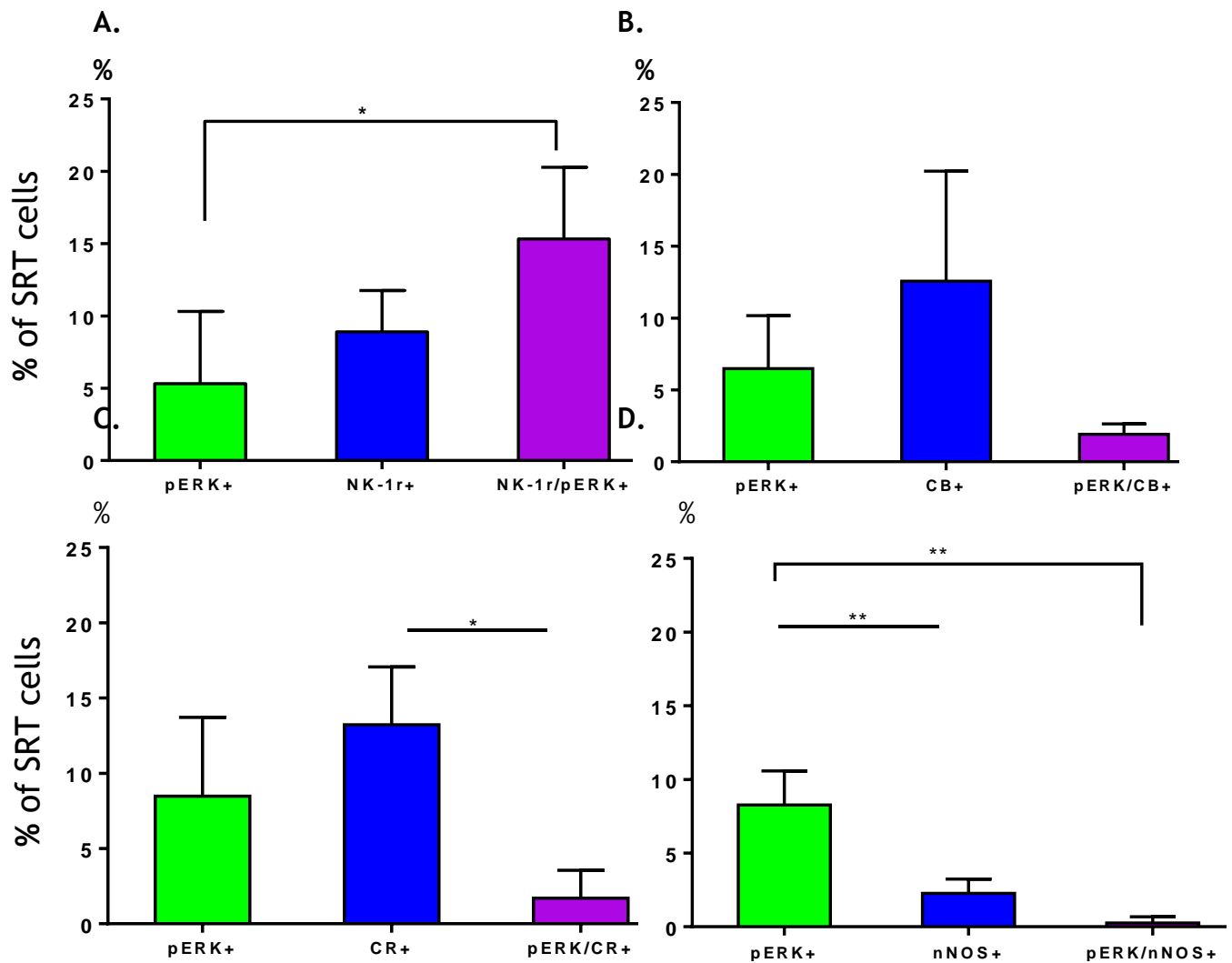


**Figure 6-9 Percentages of spinoreticular cells expressing pERK, NK-1r, CB, CR and nNOS**

**A.** SRT cells with pERK as well as NK-1r are significantly greater than cells labelled by pERK only (Anova,  $**p < 0.05$ , post hoc *Tukey's*),  $n=4$ , SRT cells =504. T =SD

**B.** No significant difference between SRT cells labelled by pERK, CB or both pERK/CB (Anova,  $p > 0.05$ , post hoc *Tukey's*),  $n=3$ , SRT cells=727. T =SD

**C.** SRT cells that are labelled by both pERK & CR are significantly fewer than cells with CR only (Anova  $p < 0.05$ , post hoc *Tukey's*),  $n=3$ , SRT cells=766. T =SD

**D.** The percentage of SRT pERK immunoreactive cells is significantly higher than only nNOS cells (Anova,  $p < 0.01$ , post hoc *Tukey's*) and cells labelled by both pERK and nNOS (Anova,  $p < 0.01$ , post hoc *Tukey's*),  $n=3$ , SRT cells=737. T =SD.

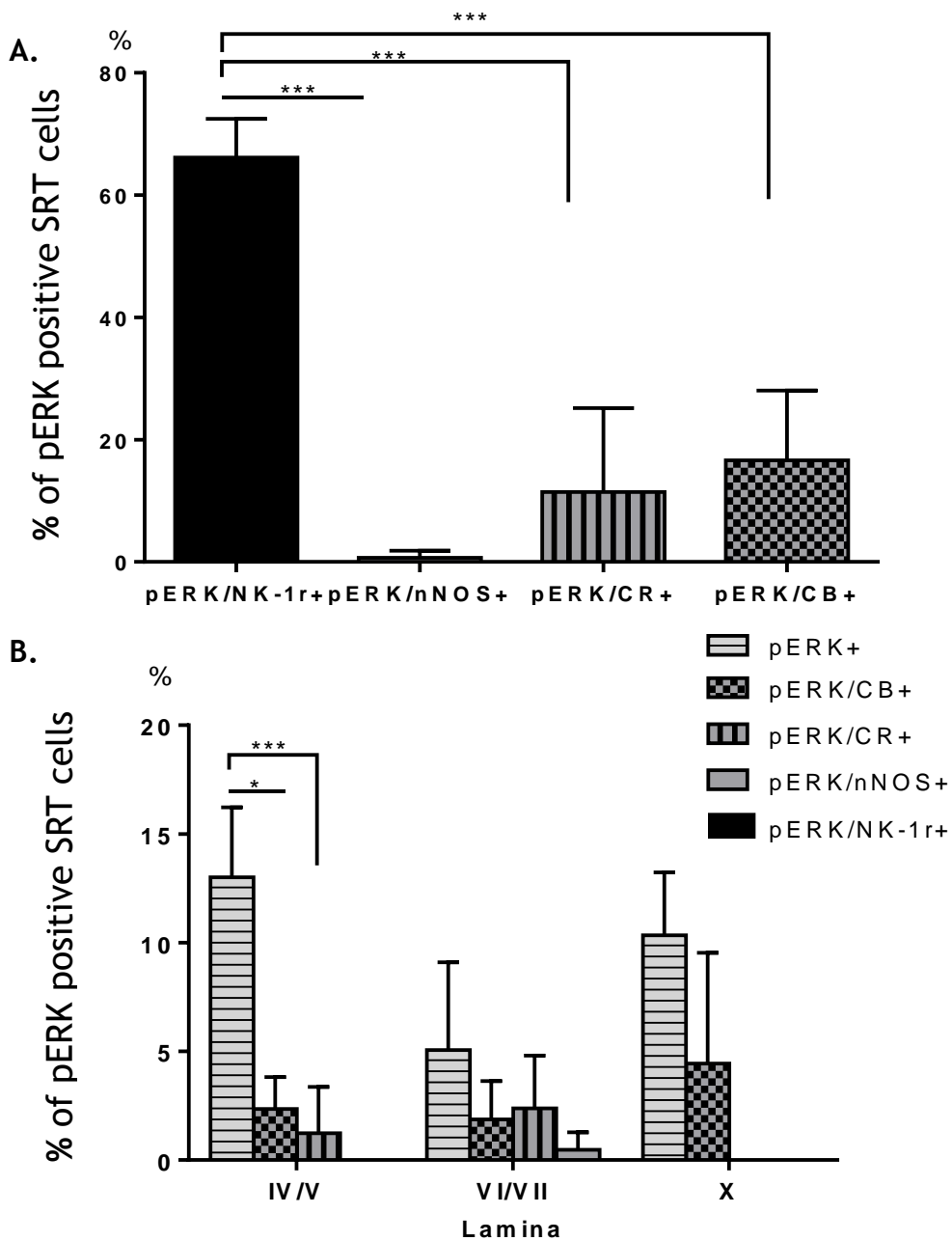


**Figure 6-10 A.** Comparison of sub-groups of spinoreticular cells (SRT) that have pERK and are labelled by NK-1r, CB, CR or ChAT; **B.** Laminar distribution of the cells

**A.** The largest population of SRT neurons expressing pERK also express neurokinin-1 receptors (NK-1r). They are significantly more than any of the other sub-groups, nNOS, CB, or CR (Anova,  $p < 0.001$ , post-hoc *Tukey's*).  $T = SD$

**B.** There are significantly greater numbers of pERK positive SRT cells than pERK cells labelled with CB or CR in deep dorsal laminae, IV/V (Anova,  $*p < 0.05$  and  $***p < 0.001$ , post hoc *Tukey's*).  $T = SD$

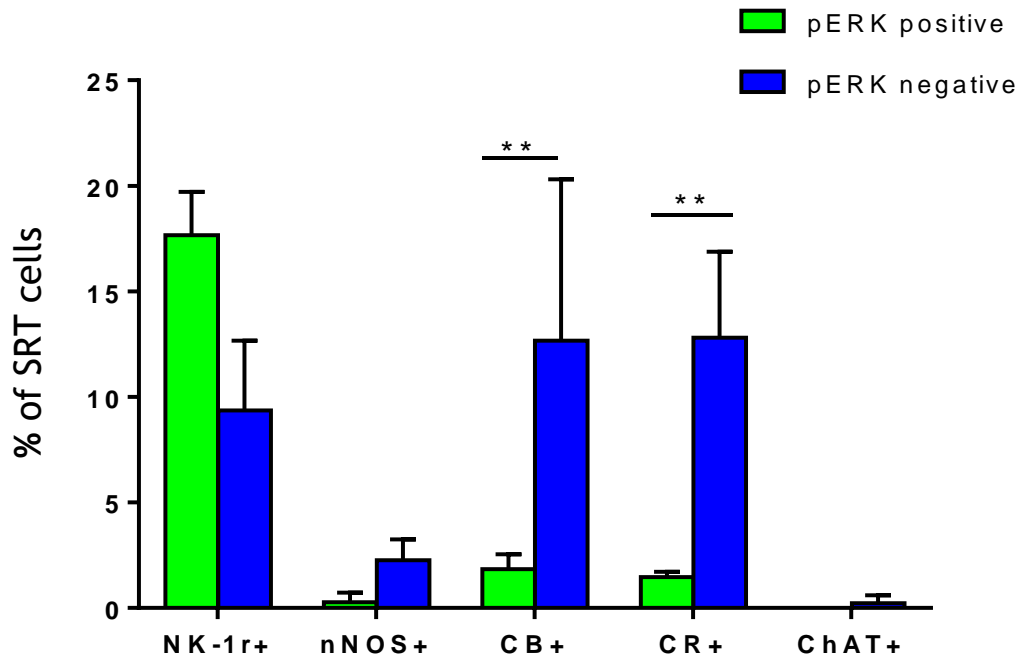


Figure 6-11 A comparison of SRT cells that are pERK positive within the NK-1r, nNOS, CB, CR and ChAT immunoreactive sub-populations

Calbindin and calretinin within group comparisons show a significant difference between cells that respond to noxious stimulus by phosphorylation of ERK and those that do not (Anova,  $**p < 0.01$ , post hoc *Tukey's*,  $n=11$ ). T =SD

## 6.4 Discussion

This study demonstrates the heterogeneity of spinoreticular neurons in terms of labelling by neurochemical markers as well as their responses to noxious stimulation and thus provides an insight into the spinal circuitry and function of spinoreticular neurons. Many SRT neurons in laminae IV to VII and X express NK-1 receptors along with a smaller group that are immunolabelled with nNOS which indicates a possible role in nociception (Naim MM et al., 1998, Polgár E et al., 2007, Schmidtko A et al., 2009). In addition to these a number of SRT neurons were immunoreactive for the calcium binding proteins, CB and CR with some double labelled for both CB and CR. However, hardly any cells were labelled for ChAT.

Furthermore, a significant number of SRT cells in deep dorsal laminae, intermediate laminae and lamina X expressed phosphorylation of ERK in response to acute noxious mechanical stimulation. A majority of these cells expressed NK-1r, while a moderate number expressed CB or CR with hardly any labelled for nNOS. Thus phosphorylation of ERK is one of the mechanisms used principally by NK-1r sub-group of SRT cells in the processing of nociceptive information.

### 6.4.1 Technical considerations

The benefits and pitfalls in the use of b subunit of cholera toxin as a tracer to retrogradely label spinoreticular cells have been discussed in the previous chapters ([Sections 3-4](#), [4-4](#) and [5-4](#)). All factors concerning spread of the tracer and uptake by axons of passage were taken into consideration when interpreting the results.

The validity of anaesthetic use in experiments investigating the response of neurons to noxious stimulus raises questions about the effect of these anaesthetics on the circuitry of pain in processing nociceptive information. Some anaesthetics, to a certain extent, have weak analgesic effects, for example barbiturates and nitrous oxide (Dundee JW, 1960, Banks WA et al., 1988). Banks et al. (1988) reported that anaesthesia may influence the responses of neurons by minimising the effects of intra-individual variability seen while measuring

responses in un-anesthetised rats that are awake. In this study, Urethane was used as the anaesthetic and a large number of pERK-positive neurons were seen in the superficial dorsal horn after noxious stimulation. Thus the use of Urethane is less likely to lead to an under estimation of neurons activated by noxious stimulation at the spinal levels. On the other hand it has been reported that anaesthesia may cause false positive results but this phenomenon has been reported only in supraspinal areas, after prolonged inhalational anaesthesia and in some cases, with intra-peritoneal Urethane injections (Bullitt E, 1990, Strassman AM et al., 1993). However, this effect has not been documented in the spinal cord (Lanteri-Minet M et al., 1993). In the present study most of the pERK positive cells were found exclusively on the ipsilateral side of the stimulus and the pattern of somatotopically appropriate labelling of the superficial dorsal horn cells, as seen in [Figure 6-6](#) further suggests that the use of Urethane as an anaesthetic appears to have no obvious effect in evoking false positive results.

The various components of the mechanical stimulus were kept as constant as possible including; the site, the duration of stimulus as well as application of force using the same Kocher's forceps locked to the maximum. In spite of this, there was still some variability in the number of cells responding to the noxious stimulus in part due to the stimulus intensity but nevertheless all rats had a more or less similar labelling pattern of pERK positive cells in the spinal grey matter.

#### **6.4.2 Neurochemical phenotypes of spinoreticular neurons**

The present neurochemical analysis reveals that ~20% of the SRT neurons in the deep dorsal, intermediate and lamina X are immunoreactive for the calcium binding proteins, CB or CR with a small percentage labelled by both CB and CR. This is in agreement to what Menetrey et al. (1992) demonstrated, regarding retrogradely labelled cells from the LRN, that were calbindin positive in the deep dorsal and intermediate laminae, although, in contrast to our findings, they showed a higher percentage of CB positive SRT cells in lamina X (25%) as opposed to our findings of ~12%. A possible reason for this difference is variability of the injection sites between the two studies. Furthermore, there was some variability in the percentage of calbindin positive SRT cells between

the animals (10.5 to 13.3%) but this percentage was not as great as that reported by Menetrey et al. (6 to 32%). In addition approximately equal percentages of CR and CB positive SRT cells were present in the spinal grey as well as some cells positive for both calbindin and calretinin on both sides of the central canal. These results help to fill up some of the gaps regarding the presence of CR in SRT cells projecting to the LRN. Functional groups of other neurons with CABPs have been recognised in the spinal grey matter based on the expression of various neurochemicals (Celio MR, 1990, Antal M et al., 1991, Baimbridge KG et al., 1992, Ichikawa H et al., 1994, Ren K and Ruda MA, 1994, Alvarez FJ et al., 2005). Thus although this differential expression of CABPs is interesting from a morphological point of view, it is difficult to assign any functional relevance to these cells as regards the presence or absence of CB or CR. Calcium binding proteins regulate the excitability of cellular membranes via  $Ca^{+2}$  signals and thus play a role in the release of neurotransmitter substances into the synaptic cleft (Augustine GJ et al., 1987). In recent years,  $Ca^{+2}$  ions have been implicated in a plethora of post-synaptic phosphorylation activities through the activation of various protein kinases including ERK (Augustine GJ et al., 1987, Rosen LB et al., 1994, Agell N et al., 2002). Thus it is logical to deduce that calbindin and calretinin may well be important in controlling the excitability of SRT cells that form the second order elements for the transmission of sensory information including noxious stimuli to the higher centres in the brain. The present study shows a high proportion of CB and/or CR containing cells that send axons to the CVLM, that is involved in processing information derived from sensory perception including nociception and visceronociception (Janss AJ and Gebhart GF, 1988, Lima D et al., 1991, Ness TJ et al., 1998, Tavares I and Lima D, 2002). Although the significance of SRT cells with different CABPs and some with both CB and CR is not fully understood each of these different types of cells might be involved in subtly different pathways of neuronal transmission.

Extensive work has been carried out in our lab on projection neurons located in the superficial and deep dorsal horns, that possess NK-1 receptors (Sakamoto H et al., 1999, Al Ghamdi KS et al., 2009, Polgár E et al., 2010, Sardella TC et al., 2011), as most substance P containing nociceptive primary afferents terminate within these areas (Light AR and Perl ER, 1979, Duggan AW and Hendry IA, 1986, Lawson SN, 1995, Todd AJ, 2002). In agreement with a study by Todd et al.

(2000), this study shows that in addition to SRT cells that are NK-1r positive in the deep dorsal laminae, there are some NK-1 labelled SRT neurons in medial laminae VI and VII as well as some in lamina X. The presence of NK-1 receptors in these cells may indicate a role in nociceptive processing. Although few SP positive fibres terminate in these deep regions, these cells are most likely to be activated by diffusion of SP from the dorsal horn (Duggan AW and Hendry IA, 1986, Littlewood NK et al., 1995, Marshall GE et al., 1996, Todd AJ et al., 1998, Todd AJ et al., 2000). Electrophysiological records show that although a few spinoreticular neurons have discrete receptive fields and could, therefore, carry information related to stimulus location, many spinoreticular neurons in lamina VII and VIII have large or complex receptive fields (cutaneous, deep and extensive complex) that transmit nociceptive information (Fields HL et al., 1977, Fields HL and Basbaum AI, 1978, Maunz RA et al., 1978).

Furthermore, a small but significant percentage of CTb labelled cells were found to be immunoreactive to nNOS, particularly in intermediate laminae VI and VII. A large body of evidence indicates that nitric oxide (NO), produced by nNOS, essentially contributes to the processing of nociceptive signals in the spinal cord mainly in inflammatory and neuropathic pain sensitisation (Woolf CJ, 2004, Di Meglio T et al., 2008). For review, see (Meller ST and Gebhart GF, 1993, Scholz J and Woolf CJ, 2002). One of the known pathways used by NO for signalling is activation of NO-sensitive guanyl cyclase (NO-GC) which inhibits  $Ca^{+2}$  entering into the cell. In the spinal cord, NO-GC is expressed by NK-1r projection neurons as well as inhibitory interneurons in the superficial dorsal horn (Schmidtke A et al., 2009). Thus deeper SRT neurons that are NK-1r positive may also transmit nociceptive information via a NO dependent pathway that can be prevented by a NOS inhibitor. Furthermore, a retrograde labelling study by Kayalioglu et al (1999) did not find any neurons projecting to the periaqueductal grey (PAG), thalamus or hypothalamus in the spinal cord to be immunoreactive for nNOS. Thus nNOS spinoreticular cells, with fibres within the ALQ conveying nociceptive information to the brain, could be selectively inhibited by nNOS inhibitors as a possible therapeutic use (Southan GJ and Szabó C, 1996).

Hardly any SRT cells were immunoreactive to choline acetyltransferase but as we demonstrated in the previous chapter, SRT cells receive a significant input

from ChAT positive terminals. In addition Zhuo et al (1990) showed that intrathecal administration of Pirenzepine, a selective muscarinic receptor antagonist, increased the response to noxious mechanical stimulation, suggesting that the spinal cholinergic system exerts its tonic inhibitory effect on noxious mechanical spinal transmission. Although these cells are predominantly non-cholinergic and thus they may not be involved in the suppression of painful stimulus, they may, in turn, be suppressed by cholinergic contacts, thereby modifying their excitability to noxious stimuli.

Thus, there are a number of subgroups of SRT neurons in the lumbar spinal cord of the rat that are neurochemically distinct. What this means in functional terms is harder to define for all the subgroups, but it can safely be surmised that the NK-1r cells and possibly the nNOS cells, are involved in the transmission of pain related information via the LRN to the cerebellum.

### **6.4.3 Response to noxious stimulus**

Several studies have shown activity dependant and stimulus specific phosphorylation of ERK in spinal cord neurons (Ji RR et al., 1999, Polgár E et al., 2007). pERK can be induced within a minute of noxious stimulation in several sub-cellular structures such as nuclei, cytoplasm, axons and dendrites, which correlates well with the development of pain hypersensitivity (Ji RR et al., 1999, Gao YJ and Ji RR, 2009). In this study, application of an acute noxious mechanical stimulus resulted in the expression of pERK in the superficial dorsal laminae, deep dorsal, ventromedial lamina VI and VIII as well as lamina X in the spinal grey matter. Approximately 9% of SRT neurons expressed pERK, not only in the deep dorsal laminae but also in lamina VI, VII and X. Previous studies focusing predominantly on the superficial dorsal horn have also demonstrated pERK responsive cells in lamina V and VI (Polgár E et al., 2007). Most studies on the response of SRT cells to innocuous as well as noxious stimuli have been done using electrophysiology and applying electrical stimuli to peripheral nerves (Fields HL et al., 1977, Haber LH et al., 1982, Kevetter GA et al., 1982). These studies reveal that spinoreticular cells in the deep dorsal and intermediate laminae have varying responses to peripheral stimulus but most of these cells

respond to high threshold stimuli from A $\delta$  as well as C fibres and these responses are also evoked by applying noxious pinch.

Our study defines some of the neurochemical pathways that are involved in the transmission of these nociceptive influences. In this part of the project based on findings of Ji (1999) as well as Polgar (2007), the animals were perfused 5 minutes after the last exposure to noxious stimulation and pERK was used as the marker of neuronal activity. One of the advantages of ERK phosphorylation is the short period of time required for it to be manifested after stimulation, as well as its presence in the soma and dendrites of the neurons (Gao YJ and Ji RR, 2009). pERK is one of the intracellular signalling pathways involved in neuronal plasticity (Fields HL et al., 1977, Impey S et al., 1999) and studies have shown that nociceptive stimuli induce ERK phosphorylation in the spinal dorsal horn (Ji RR et al., 1999, Karim F et al., 2001).

Most of the SRT cells responding to noxious stimulus were predominantly NK-1 receptor positive. NK-1 is the post-synaptic receptor for substance P, which is principally released by nociceptive primary afferents as well as some SP interneurons (Duggan AW and Hendry IA, 1986, Helke CJ et al., 1990, Brown JL et al., 1995, Littlewood NK et al., 1995). For review, see (Fields HL and Basbaum AI, 1978). However, a number of SRT/NK-1r cells do not show phosphorylation of ERK but they do show internalisation of the NK-1 receptors in soma and dendrites and this suggests that these cells have a different signalling pathway for processing noxious stimuli, as demonstrated by previous studies on noxious stimulation in anaesthetised animals (Mantyh P et al., 1995, Allen BJ et al., 1999, Polgár E et al., 2007). The probability is that they are activated by glutamate which is a manifestation of fast synaptic transmission as opposed to slow (SP) transmission (De Biasi S and Rustioni A, 1988, Chen W et al., 2010). Whereas previous studies have concentrated on lamina I projection neurons (Todd AJ, 2002) and lamina III and IV neurons (Polgár E et al., 2007), this study extends this work further to show that there are deeper projection neurons in lamina V, VI, VII and X that have internalised NK-1 receptors after noxious mechanical stimulation, together with the phosphorylation of ERK. In addition to its involvement in acute pain, ERK phosphorylation involves activation of NMDA or metabotropic glutamate receptors followed by transcriptional activation of NK-1

leading to central or peripheral sensitisation; thus contributing to hyperalgesia and allodynia (Ji RR et al., 1999, Galan A et al., 2002, Ji RR et al., 2002).

Indeed, nNOS has been implicated in inflammatory or neuropathic pain (Meller ST and Gebhart GF, 1993, Schmidtke A et al., 2009). Thus it is hardly surprising that not many nNOS SRT cells were pERK positive, considering the mode of stimulus as acute mechanical rather than chronic. Nevertheless, the presence of nNOS in some of the spinoreticular cells suggests that some of these cells may be involved in the development and maintenance of hyperalgesia in inflammatory and neuropathic pain states by the production of NO. NO acts by diffusing from its site of production and its effects are dependent on the distance it can travel to NO-GC as explained above. The only SRT neurons labelled by nNOS with phosphorylation of ERK were localised in the deep dorsal laminae. These may be part of the intermediate wide dynamic range neurons with large cutaneous receptive fields stimulated by low and high threshold cutaneous afferents described by Sahara et al. (1990).

In conclusion, some SRT cells respond to acute nociceptive mechanical stimuli and convey this information via the LRN to the cerebellum.

#### **6.4.4 Functional aspects**

Nociception refers to the neural processes involved in encoding and processing noxious stimuli. While acute nociception is protective as a warning system, chronic pain lacks an obvious protective function and can be disabling and intractable. Accumulating evidence suggests that separate kinds of pain may be mediated and modulated in different ways in the central nervous system (Julius D and Basbaum AI, 2001, Scholz J and Woolf CJ, 2002). An important consideration is that variable nociceptive processes activate various signal molecules in the central nervous system differently.

This study supports the proposal that the spinoreticular tract neurons play a role in the spinal circuitry of pain by conveying information to the reticular formation concerning the acute activation of nociceptors in the skin and other tissues of the body. The processing of nociceptive input that occurs at the spinal level represents the first stage of effective control over its access to higher regions of

the central nervous system. Thus the spinothalamic neurons may play a critical role in the central processing of noxious stimuli (Fields HL et al., 1977, Menetrey D et al., 1980, Haber LH et al., 1982, Kvetter GA et al., 1982). However these neurons due to their complex receptive fields and polymodal responses are unlikely to be involved in discriminative functions rather in the motivational affective aspects of pain or by influencing motor activity through the cerebellum (Maunz RA et al., 1978).

Neurons in the LRN and adjacent areas respond to nociceptive inputs (Ness TJ et al., 1998). Duggan et al. (1986) have shown that small bilateral lesions in the ventral lateral medulla in the region of the LRN produced a complete loss of tonic inhibition in the spinal cord. Inversely stimulation of this region can inhibit spinal dorsal horn neurons (Morton CR et al., 1983). As Hall et al (1982) in turn suggested that this tonic inhibition of the dorsal horn cells was in response to impulses in C fibre afferents, i.e. nociceptive inputs. It is possible that SRT cells, by conveying acute nociceptive information to the LRN, produce analgesic effects via descending pathways from the LRN.

A natural motor response to a noxious stimulus is to withdraw the affected area from the source of irritation thus reducing chances of further tissue damage. Therefore, SRT cells transmit information regarding acute noxious activity to the LRN which then integrates and conveys this information to the cerebellum via reticulo-cerebellar fibres. Thus influencing the motor response to pinch, resulting in a withdrawal reflex, but this response is, in turn, further modified by a 'diffuse noxious inhibitory control (DNIC)' by supraspinal structures. This prevents any exaggerated first response to pain, thus preventing further injury. Furthermore, García-Larrea et al. (1993), following depression of the flexion reflex after anterolateral cordotomy in man, suggested that this nociceptive spinal reflex involves the spinothalamic tract and not the spinothalamic tract.

This ascending and descending loop to the LRN would thus form a spino-bulbo-spinal anti-nociceptive loop (Basbaum AI et al., 1978, De Broucker T et al., 1990, Tavares I and Lima D, 2002) modifying the response of spinal neurons to painful stimuli by an inherent analgesic system. A better understanding of these

nociceptive anti-nociceptive pathways and the various neurochemical markers may help in the development of target specific analgesics.

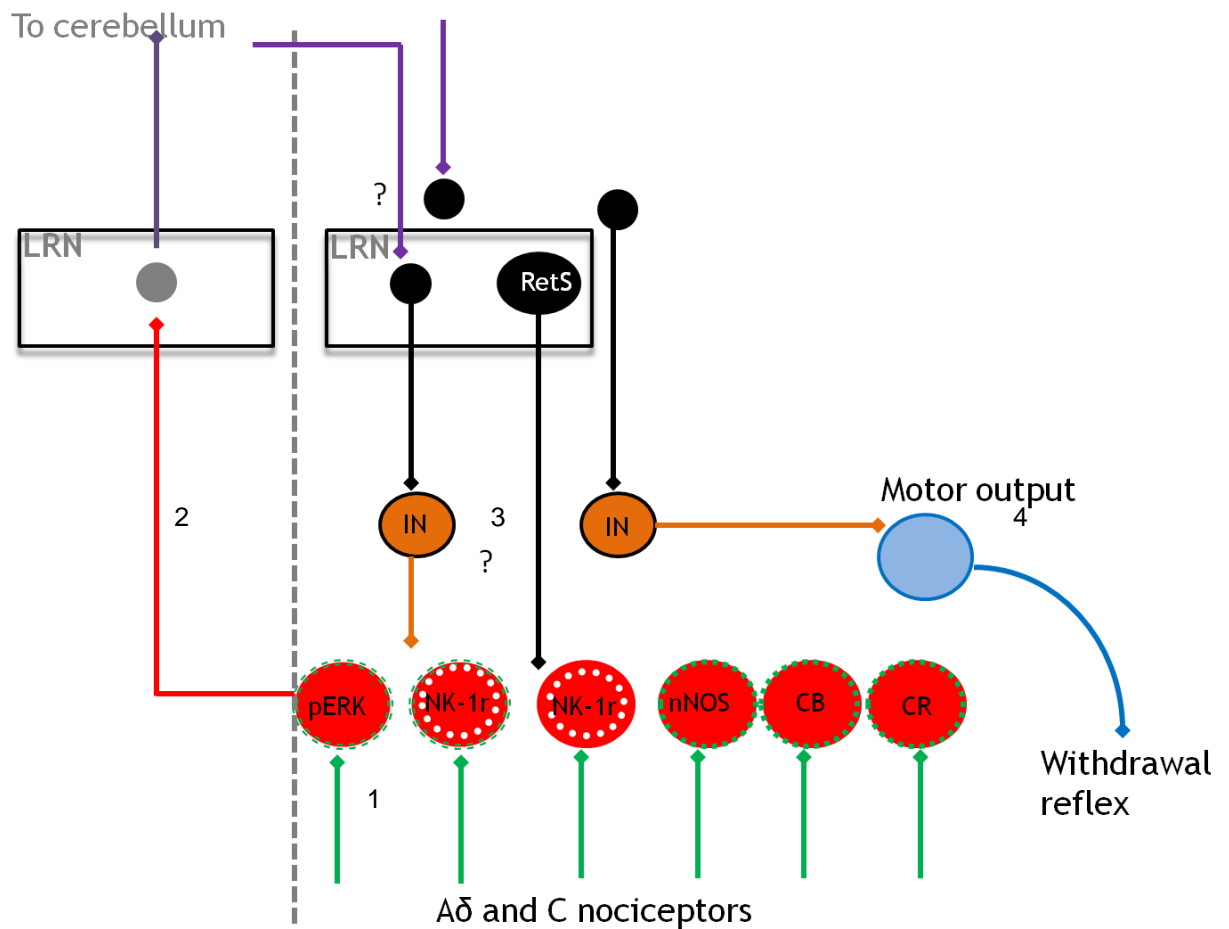


**Figure 6-12 Summary of the role of spinothalamic cells in the spinal circuitry of pain**

- 1) Sub-groups of spinothalamic cells (red circles) with pERK (green halos) and NK-1 receptors (white halos) stimulated by noxious stimulus A $\delta$  and C nociceptors (green lines).
- 2) Projection of SRT neurons to LRN pre-cerebellar cells (grey circle) and then to the cerebellum (purple line).
- 3) Descending projections (black circles and lines) to inhibitory interneurons (orange circles) and then to motor neurons (blue circle)
- 4) Eliciting a withdrawal reflex (blue arc). ? Unknown connections.

# Chapter 7

## 7 Concluding remarks

Essentially all data generated in this research revolves around spinoreticular neurons, in not only defining the role of these neurons within the spinal circuitry but as components of an ascending descending loop (Figure 7-1). Although the functional involvement of these neurons in locomotion, sleep-arousal and processing nociceptive stimuli, has been historically established in electrophysiological experiments conducted mainly in cat. The relative contribution of afferent fibres and spinal neurons to their input, their organisation and mechanisms of control of transmission has only been estimated approximately so far.

This study provides key contributions in increasing scientific knowledge in the field of neuroscience by confirming and extending previous observations, by suggesting that:

- SRT cells project to the LRN not only as crossed and uncrossed pathways but some of these cells project bilaterally, modulating cerebellar output by both excitatory and inhibitory mechanisms and thus demonstrating a degree of integration within the LRN (Figure 7-1, 1);
- although bulbospinal neurons, at the origin of the two major descending pathways via the MLF and CVLM, have overlapping spatial distributions mostly within the pontomedullary reticular formation; the BS cells projecting via the CVLM are a separate distinctive pathway with possibly a role in harmonising motor activity with sensory activity in the spinal cord (Figure 7-1, 2);
- these projection neurons play an important role not only in the transmission of sensory information to their supraspinal targets but their inputs from spinal interneurons, cutaneous and proprioceptive afferents, as well as descending systems, are important in processing sensory and motor information at the segmental level (Figure 7-1, 3);

- Because these SRT neurons respond to painful stimulus they play a role in modifying the cerebellar response by, for example, posture adjustment during the withdrawal and SBS reflexes. As these cells exhibit a variety of neurochemical pathways in the nociceptive process, indicating distinct sensory modalities transmitted through different pathways; pharmacological agents maybe developed targeting specific circuits in pain modulation (Figure 7-1, 4).

Thus, this thesis provides a new, deeper insight into the anatomical pathways and neurochemistry in mapping out a spino-bulbar spinal loop. However, some aspects of this circuitry are still unknown and require further investigation; what is the anatomical circuitry in the brainstem connecting the ascending and descending components of this loop and sparse descending contacts from the CVLM to SRT cells indicate the involvement of other circuits at the spinal level or possibly other sources of descending reticulospinal fibres contacting these cells. The present study was done by combining retrograde labelling in rats /intracellular labelling of electrophysiologically characterized cells in cats and immunohistochemistry using various neurochemical markers. It would be interesting to use viral tract tracing to label chains of synaptically linked networks of neurons or transgenic expression of tract tracing molecules, to address these issues further on. As clearly, a better understanding of the circuits engaged by these remarkably diverse populations of spinoreticular neurons is essential to the development of more selective modes of regulating neuronal circuitry.

In conclusion, the data presented in this thesis will hopefully contribute to progress in this area by providing an understanding of the normal to treat the pathological, for example, lesions in the LRN which may cause disruption of posture and balance or even severe limb and gait ataxia as seen in Machado-Joseph disease (spinocerebellar ataxia type 3) (Corvaja N et al., 1977b, Rub U et al., 2002).

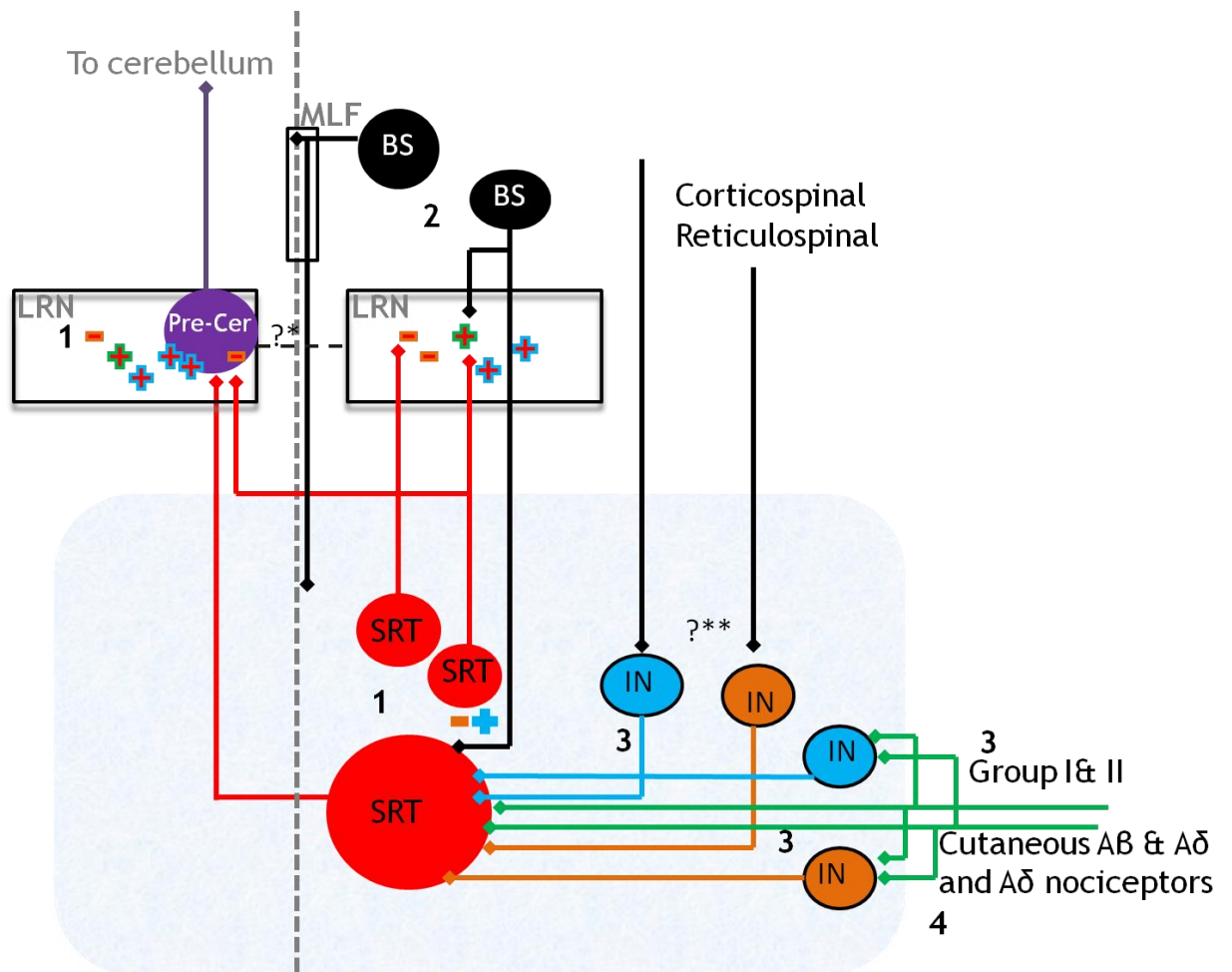


**Figure 7-1 Summary of the connectivity of spinoreticular cells as a component of an ascending descending loop**

1) Spinoreticular cells (in red circles and lines) project ipsi-, contra- and bilaterally to LRN. A convergence of spinoreticular excitatory (VGLUT 2, red cross blue outline) and inhibitory contacts (orange hyphen) on pre-cerebellar cells in the LRN (purple circle, Pre-Cer).

2) Black circles represent Bulbospinal neurons (BS) projecting via medial longitudinal fasciculus (MLF) and caudal ventrolateral medulla (CVLM).

3) Excitatory (VGLUT-2, blue cross and diamonds) and inhibitory inputs (VGAT, orange hyphen and diamonds) to SRT cells from the; BS neurons via the descending CVLM path (black line), cutaneous and proprioceptive afferents (green lines, VGLUT-1), and spinal interneurons (IN) both excitatory (blue circles and lines, VGLUT 2) and inhibitory (orange circles and lines, VGAT).

4) Noxious stimulus via A $\delta$  nociceptors.

?\* Unknown connections in the brain stem between ascending and descending paths, ?\*\* Unknown circuitry of descending inputs to SRT cells.

## References

- Agell N, Bachs O, Rocamora N & Villalonga P(2002). "Modulation of the Ras/Raf/MEK/ERK pathway by Ca(2+), and calmodulin". Cell Signal, 14, 649-54.
- Aibf. 2014." Allen Institute for Brain Science, Allen Mouse Brain Atlas [Internet]" [Online]. Available: <http://www.brain-map.org>.
- Aihara Y, Mashima H, Onda H, Hisano S, Kasuya H, Hori T, Yamada S, Tomura H, Yamada Y, Inoue I, Kojima I & Takeda J(2000). "Molecular cloning of a novel brain-type Na(+)-dependent inorganic phosphate cotransporter". Journal of neurochemistry, 74, 2622-5.
- Al Ghamdi KS, Polgár E & Todd AJ(2009). "Soma size distinguishes projection neurons from neurokinin 1 receptor-expressing interneurons in lamina I of the rat lumbar spinal dorsal horn". Neuroscience, 164, 1794-804.
- Alaynick WA, Jessell TM & Pfaff SL(2011). "SnapShot: spinal cord development". Cell, 146, 178-178 e1.
- Aley KO, Martin A, McMahon T, Mok J, Levine JD & Messing RO(2001). "Nociceptor sensitization by extracellular signal-regulated kinases". J Neurosci, 21, 6933-9.
- Allen AM, Chai SY, Clevers J, McKinley MJ, Paxinos G & Mendelsohn FaO(1988). "Localization and characterization of angiotensin II receptor binding and angiotensin converting enzyme in the human medulla oblongata". The Journal of Comparative Neurology, 269, 249-264.
- Allen BJ, Li J, Menning PM, Rogers SD, Ghilardi J, Mantyh PW & Simone DA(1999). "Primary Afferent Fibers That Contribute to Increased Substance P Receptor Internalization in the Spinal Cord After Injury". Journal of Neurophysiology, 81, 1379-1390.
- Almeida A, Cobos A, Tavares I & Lima D(2002). "Brain afferents to the medullary dorsal reticular nucleus: a retrograde and anterograde tracing study in the rat". The European journal of neuroscience, 16, 81-95.
- Alstermark B & Ekerot CF(2013). "The lateral reticular nucleus: a precerebellar centre providing the cerebellum with overview and integration of motor functions at systems level. A new hypothesis". The Journal of physiology, 591, 5453-5458.
- Alstermark B, Górska T, Lundberg A, Pettersson LG & Walkowska M(1987). "Effect of different spinal cord lesions on visually guided switching of target-reaching in cats". Neuroscience Research, 5, 63-67.
- Alstermark B, Isa T & Tantisira B(1990). "Projection from excitatory C3-C4 propriospinal neurones to spinocerebellar and spinoreticular neurones in the C6-Th1 segments of the cat". Neuroscience research, 8, 124-30.
- Alstermark B, Lindstrom AL, A. & Sybirska E(1981). "Integration in descending motor pathways controlling the forelimb in the cat. 8. Ascending Projection to the Lateral Reticular Nucleus from C3-C4 Propriospinal Neurones also Projecting to Forelimb Motoneurones". Experimental Brain Research, 42, 282-298.
- Alstermark B, Lundberg A & Sasaki S(1984). "Integration in descending motor pathways controlling the forelimb in the cat. 10. Inhibitory pathways to forelimb motoneurones via C3-C4 propriospinal neurones". Experimental brain research. Experimentelle Hirnforschung. Experimentation cerebrale, 56, 279-92.

- Alstermark B, Lundberg A & Sasaki S(1984 a).** "Integration in descending motor pathways controlling the forelimb in the cat. 11. Inhibitory pathways from higher motor centres and forelimb afferents to C3-C4 propriospinal neurones.". Experimental Brain Research, 56, 293-307.
- Alstermark B, Lundberg A & Sasaki S(1984 b).** "Integration in descending motor pathways controlling the forelimb in the cat.12 Interneurones which mediate descending feed-forward inhibition and feed back inhibition from the forelimb to C3-C4 propriospinal neurones.". Experimental Brain Research, 56, 308-322.
- Alstermark B, Pinter MJ & Sasaki S(1992).** "Descending pathways mediating disynaptic excitation of dorsal neck motoneurons in the cat: brain stem relay". Neuroscience Research, 15, 42-57.
- Alvarez FJ, Jonas PC, Sapir T, Hartley R, Berrocal MC, Geiman EJ, Todd AJ & Goulding M(2005).** "Postnatal phenotype and localization of spinal cord V1 derived interneurons". J Comp Neurol, 493, 177-92.
- Alvarez FJ, Villalba RM, Zerda R & Schneider SP(2004).** "Vesicular glutamate transporters in the spinal cord, with special reference to sensory primary afferent synapses". The Journal of comparative neurology, 472, 257-80.
- Ammons WS(1987).** "Characteristics of spinoreticular and spinothalamic neurons with renal input". Journal of neurophysiology, 58, 480-95.
- Andrezik JA & King JS(1977).** "The lateral reticular nucleus of the opossum (*Didelphis virginiana*). I. Conformation, cytology and synaptology". The Journal of Comparative Neurology, 174, 119-149.
- Anelli R & Heckman CJ(2005).** "The calcium binding proteins calbindin, parvalbumin, and calretinin have specific patterns of expression in the gray matter of cat spinal cord". Journal of neurocytology, 34, 369-85.
- Angelucci A, Clascá F & Sur M(1996).** "Anterograde axonal tracing with the subunit B of cholera toxin: a highly sensitive immunohistochemical protocol for revealing fine axonal morphology in adult and neonatal brains". Journal of Neuroscience Methods, 65, 101-112.
- Antal M, Freund TF & Polgár E(1990).** "Calcium-binding proteins, parvalbumin- and calbindin-D 28k-immunoreactive neurons in the rat spinal cord and dorsal root ganglia: a light and electron microscopic study". J Comp Neurol, 295, 467-84.
- Antal M, Polgár E, Chalmers J, Minson JB, Llewellyn-Smith I, Heizmann CW & Somogyi P(1991).** "Different populations of parvalbumin- and calbindin-D28k-immunoreactive neurons contain GABA and accumulate 3H-D-aspartate in the dorsal horn of the rat spinal cord". J Comp Neurol, 314, 114-24.
- Antonino-Green DM, Cheng J & Magnuson DS(2002).** "Neurons labeled from locomotor-related ventrolateral funiculus stimulus sites in the neonatal rat spinal cord". The Journal of comparative neurology, 442, 226-38.
- Araki T, Yamano M, Murakami T, Wanaka A, Betz H & Tohyama M(1988).** "Localization of glycine receptors in the rat central nervous system: An immunocytochemical analysis using monoclonal antibody". Neuroscience, 25, 613-624.
- Arber S(2012).** "Motor circuits in action: specification, connectivity, and function". Neuron, 74, 975-989.
- Arshavsky YI, Gelfand IM, Orlovsky GN & Pavlova GA(1978 a).** "Messages conveyed by spinocerebellar pathways during scratching in the cat. I. Activity of neurons of the lateral reticular nucleus". Brain research, 151, 479-491.

- Arshavsky YI, Gelfand IM, Orlovsky GN & Pavlova GA(1978 b). "Messages conveyed by spinocerebellar pathways during scratching in the cat. II. Activity of neurons of the ventral spinocerebellar tract". Brain research, 151, 493-506.
- Arshavsky YI, Orlovsky GN, Pavlova GA & Popova LB(1986). "Activity of C3-C4 propriospinal neurons during fictitious forelimb locomotion in the cat". Brain Research, 363, 354-357.
- Arshavsky Yu I, Gelfand IM, Orlovsky GN, Pavlova GA & Popova LB(1984). "Origin of signals conveyed by the ventral spino-cerebellar tract and spino-reticulo-cerebellar pathway". Experimental brain research. Experimentelle Hirnforschung. Experimentation cerebrale, 54, 426-31.
- Augustine GJ, Charlton MP & Smith SJ(1987). "Calcium action in synaptic transmitter release". Annual review of neuroscience, 10, 633-93.
- Baimbridge KG, Celio MR & Rogers JH(1992). "Calcium-binding proteins in the nervous system". Trends in neurosciences, 15, 303-8.
- Bankoul S & Neuhuber WL(1992). "A direct projection from the medial vestibular nucleus to the cervical spinal dorsal horn of the rat, as demonstrated by anterograde and retrograde tracing". Anat Embryol (Berl), 185, 77-85.
- Banks WA, Trentman TL, Kastin AJ & Galina ZH(1988). "The general anesthesia induced by various drugs differentially affects analgesia and its variability". Pharmacol Biochem Behav, 31, 397-403.
- Bannatyne BA, Edgley SA, Hammar I, Jankowska E & Maxwell DJ(2003). "Networks of inhibitory and excitatory commissural interneurons mediating crossed reticulospinal actions". The European journal of neuroscience, 18, 2273-84.
- Bannatyne BA, Liu TT, Hammar I, Stecina K, Jankowska E & Maxwell DJ(2009). "Excitatory and inhibitory intermediate zone interneurons in pathways from feline group I and II afferents: differences in axonal projections and input". The Journal of Physiology, 587, 379-399.
- Barbeau H & Rossignol S(1987). "Recovery of locomotion after chronic spinalization in the adult cat". Brain Res, 412, 84-95.
- Barber RP, Phelps PE, Houser CR, Crawford GD, Salvaterra PM & Vaughn JE(1984). "The morphology and distribution of neurons containing choline acetyltransferase in the adult rat spinal cord: An immunocytochemical study". The Journal of comparative neurology, 229, 329-346.
- Basbaum AI & Braz JM (2010). "Transgenic Mouse Models for the Tracing of "Pain" Pathways  
Translational Pain Research: From Mouse to Man", Boca Raton, FL, LLC.
- Basbaum AI, Clanton CH & Fields HL(1978). "Three bulbospinal pathways from the rostral medulla of the cat: An autoradiographic study of pain modulating systems". The Journal of Comparative Neurology, 178, 209-224.
- Basbaum AI & Fields HL(1979). "The origin of descending pathways in the dorsolateral funiculus of the spinal cord of the cat and rat: further studies on the anatomy of pain modulation". J Comp Neurol, 187, 513-31.
- Bing Z, Villanueva L & Le Bars D(1990). "Ascending pathways in the spinal cord involved in the activation of subnucleus reticularis dorsalis neurons in the medulla of the rat". Journal of neurophysiology, 63, 424-38.
- Blakeslee GA, Freiman IS & Barrera SE(1938). "The nucleus lateralis medullae: An experimental study of its anatomic connections in macacus rhesus". Archives of Neurology & Psychiatry, 39, 687-701.

- Blatow M, Caputi A, Burnashev N, Monyer H & Rozov A(2003).** "Ca<sup>2+</sup> buffer saturation underlies paired pulse facilitation in calbindin-D28k-containing terminals". Neuron, 38, 79-88.
- Blomqvist A & Berkley KJ(1992).** "A re-examination of the spino-reticulo-diencephalic pathway in the cat". Brain Research, 579, 17-31.
- Borges LF & Iversen SD(1986).** "Topography of choline acetyltransferase immunoreactive neurons and fibers in the rat spinal cord". Brain Res, 362, 140-8.
- Bouhassira D, Le Bars D, Bolgert F, Laplane D & Willer JC(1993).** "Diffuse noxious inhibitory controls in humans: a neurophysiological investigation of a patient with a form of Brown-Sequard syndrome". Annals of neurology, 34, 536-543.
- Boulland J-L, Jenstad M, Boekel AJ, Wouterlood FG, Edwards RH, Storm-Mathisen J & Chaudhry FA(2009).** "Vesicular Glutamate and GABA Transporters Sort to Distinct Sets of Vesicles in a Population of Presynaptic Terminals". Cerebral Cortex, 19, 241-248.
- Bowker RM & Abbott LC(1990).** "Quantitative re-evaluation of descending serotonergic and non-serotonergic projections from the medulla of the rodent: evidence for extensive co-existence of serotonin and peptides in the same spinally projecting neurons, but not from the nucleus raphe magnus". Brain Research, 512, 15-25.
- Brezenoff HE(1984).** "Cardiovascular regulation by brain acetylcholine". Fed Proc, 43, 17-20.
- Brinkman J & Kuypers HGJM(1973).** "Cerebral control of contralateral and ipsilateral arm, hand and finger movements in the split brain rhesus monkey". Brain, 96, 653-674.
- Brodal A(1949).** "Spinal afferents to the lateral reticular nucleus of the medulla oblongata in the cat; an experimental study". The Journal of comparative neurology, 91, 259-95, incl 2 pl.
- Brodal A & Courville J(1973).** "Cerebellar corticonuclear projection in the cat. Crus II. An experimental study with silver methods". Brain Research, 50, 1-23.
- Brodal A, Walberg F & Blackstad T(1950).** "Termination of spinal afferents to inferior olive in cat". J Neurophysiol, 13, 431-54.
- Brodal P(1975).** "Demonstration of a somatotopically organized projection onto the paramedian lobule and the anterior lobe from the lateral reticular nucleus: An experimental study with the horseradish peroxidase method". Brain Research, 95, 221-239.
- Brown AG & Fyffe RE(1978).** "The morphology of group Ia afferent fibre collaterals in the spinal cord of the cat". The Journal of Physiology, 274, 111-27.
- Brown JL, Liu H, Maggio JE, Vigna SR, Mantyh PW & Basbaum AI(1995).** "Morphological characterization of substance P receptor-immunoreactive neurons in the rat spinal cord and trigeminal nucleus caudalis". J Comp Neurol, 356, 327-44.
- Brumovsky PR(2013).** "VGLUTs in Peripheral Neurons and the Spinal Cord: Time for a Review". ISRN neurology, 2013, 829753.
- Bullitt E(1990).** "Expression of c-fos-like protein as a marker for neuronal activity following noxious stimulation in the rat". J Comp Neurol, 296, 517-30.

- Burger PM, Hell J, Mehl E, Krasel C, Lottspeich F & Jahn R(1991). "GABA and glycine in synaptic vesicles: storage and transport characteristics". Neuron, 7, 287-293.
- Burgess PR & Perl ER(1967). "Myelinated Afferent Fibres Responding Specifically To Noxious Stimulation Of Skin". Journal Of Physiology-London, 190, 541-&.
- Burstein R, Cliffer KD & Giesler GJ(1990). "Cells of origin of the spinothalamic tract in the rat". The Journal of comparative neurology, 291, 329-44.
- Buttner-Ennever JA(1992). "Patterns of Connectivity in the Vestibular Nucleia". Annals of the New York Academy of Sciences, 656, 363-378.
- Cabaj A, Stecina K & Jankowska E(2006). "Same spinal interneurons mediate reflex actions of group Ib and group II afferents and crossed reticulospinal actions". Journal of neurophysiology, 95, 3911-22.
- Carlton SM, Chung JM, Leonard RB & Willis WD(1985). "Funicular trajectories of brainstem neurons projecting to the lumbar spinal cord in the monkey (Macaca fascicularis): a retrograde labeling study". The Journal of comparative neurology, 241, 382-404.
- Celio MR(1990). "Calbindin D-28k and parvalbumin in the rat nervous system". Neuroscience, 35, 375-475.
- Cervero F, Handwerker HO & Laird JM(1988). "Prolonged noxious mechanical stimulation of the rat's tail: responses and encoding properties of dorsal horn neurones". The Journal of Physiology, 404, 419-36.
- Cervero F & Wolstencroft JH(1984). "A positive feedback loop between spinal cord nociceptive pathways and antinociceptive areas of the cat's brain stem". Pain, 20, 125-38.
- Chang KT & Berg DK(2001). "Voltage-gated channels block nicotinic regulation of CREB phosphorylation and gene expression in neurons". Neuron, 32, 855-65.
- Chaouch A, Menetrey D, Binder D & Besson JM(1983). "Neurons at the origin of the medial component of the bulbopontine spinoreticular tract in the rat: An anatomical study using horseradish peroxidase retrograde transport". The Journal of comparative neurology, 214, 309-320.
- Chaudhry FA, Reimer RJ, Bellocchio EE, Danbolt NC, Osen KK, Edwards RH & Storm-Mathisen J(1998). "The vesicular GABA transporter, VGAT, localizes to synaptic vesicles in sets of glycinergic as well as GABAergic neurons". The Journal of neuroscience : the official journal of the Society for Neuroscience, 18, 9733-50.
- Chen S & Aston-Jones G(1995). "Evidence that cholera toxin B subunit (CTb) can be avidly taken up and transported by fibers of passage". Brain research, 674, 107-11.
- Chen W, Zhang G & Marvizón JCG(2010). "NMDA receptors in primary afferents require phosphorylation by Src family kinases to induce substance P release in the rat spinal cord". Neuroscience, 166, 924-934.
- Cheron G, Gall D, Servais L, Dan B, Maex R & Schiffmann SN(2004). "Inactivation of calcium-binding protein genes induces 160 Hz oscillations in the cerebellar cortex of alert mice". J Neurosci, 24, 434-41.
- Ciriello J & Calaresu FR(1977). "Lateral reticular nucleus: a site of somatic and cardiovascular integration in the cat". Am J Physiol, 233, R100-9.
- Clarke RW & Harris J(2004). "The organization of motor responses to noxious stimuli". Brain research. Brain research reviews, 46, 163-172.

- Clendenin M, Ekerot CF & Oscarsson O(1974 c). "The lateral reticular nucleus in the cat. III. Organization of component activated from ipsilateral forelimb tract". Experimental brain research. Experimentelle Hirnforschung. Experimentation cerebrale, 21, 501-13.
- Clendenin M, Ekerot CF & Oscarsson O(1975). "The lateral reticular nucleus in the cat. IV. Activation from dorsal funiculus and trigeminal afferents". Experimental brain research. Experimentelle Hirnforschung. Experimentation cerebrale, 24, 131-44.
- Clendenin M, Ekerot CF, Oscarsson O & Rosen I(1974 a). "The lateral reticular nucleus in the cat. I. Mossy fibre distribution in cerebellar cortex". Experimental brain research. Experimentelle Hirnforschung. Experimentation cerebrale, 21, 473-86.
- Clendenin M, Ekerot CF, Oscarsson O & Rosen I(1974 b). "The lateral reticular nucleus in the cat. II. Organization of component activated from bilateral ventral flexor reflex tract (bVFRT)". Experimental brain research. Experimentelle Hirnforschung. Experimentation cerebrale, 21, 487-500.
- Clowry GJ, Fallah Z & Arnott G(1997). "Developmental expression of parvalbumin by rat lower cervical spinal cord neurones and the effect of early lesions to the motor cortex". Brain Res Dev Brain Res, 102, 197-208.
- Cobos A, Lima D, Almeida A & Tavares I(2003). "Brain afferents to the lateral caudal ventrolateral medulla: a retrograde and anterograde tracing study in the rat". Neuroscience, 120, 485-498.
- Corvaja N, Grofova I, Pompeiano O & Walberg F(1977a). "The lateral reticular nucleus in the cat --I. An experimental anatomical study of its spinal and supraspinal afferent connections". Neuroscience, 2, 537-553.
- Corvaja N, Grofová I, Pompeiano O & Walberg F(1977b). "The lateral reticular nucleus in the cat—II. Effects of lateral reticular lesions on posture and reflex movements". Neuroscience, 2, 929-943.
- Cowley KC & Schmidt BJ(1994). "A comparison of motor patterns induced by N-methyl-D-aspartate, acetylcholine and serotonin in the in vitro neonatal rat spinal cord". Neurosci Lett, 171, 147-50.
- Craig AD, Zhang ET & Blomqvist A(2002). "Association of spinothalamic lamina I neurons and their ascending axons with calbindin-immunoreactivity in monkey and human". Pain, 97, 105-15.
- Dai Y, Iwata K, Fukuoka T, Kondo E, Tokunaga A, Yamanaka H, Tachibana T, Liu Y & Noguchi K(2002). "Phosphorylation of extracellular signal-regulated kinase in primary afferent neurons by noxious stimuli and its involvement in peripheral sensitization". J Neurosci, 22, 7737-45.
- De Biasi S & Rustioni A(1988). "Glutamate and substance P coexist in primary afferent terminals in the superficial laminae of spinal cord". Proceedings of the National Academy of Sciences, 85, 7820-7824.
- De Broucker T, Cesaro P, Willer JC & Le Bars D(1990). "Diffuse noxious inhibitory controls in man. Involvement of the spinothalamic tract". Brain : a journal of neurology, 113 ( Pt 4), 1223-34.
- De Leon RD, Hodgson JA, Roy RR & Edgerton VR(1998). "Locomotor capacity attributable to step training versus spontaneous recovery after spinalization in adult cats". J Neurophysiol, 79, 1329-40.
- Degtyarenko AM & Kaufman MP(2002). "Spinoreticular neurons that receive group III input are inhibited by MLR stimulation". Journal of applied physiology (Bethesda, Md. : 1985), 93, 92-98.
- Di Meglio T, Nguyen-Ba-Charvet KT, Tessier-Lavigne M, Sotelo C & Chédotal A(2008). "Molecular mechanisms controlling midline crossing by

- precerebellar neurons". The Journal of neuroscience : the official journal of the Society for Neuroscience, *28*, 6285-94.
- Du Beau A, Shakya Shrestha S, Bannatyne BA, Jality SM, Linnen S & Maxwell DJ(2012). "Neurotransmitter phenotypes of descending systems in the rat lumbar spinal cord". Neuroscience, *227*, 67-79.
- Duggan AW & Hendry IA(1986). "Laminar localization of the sites of release of immunoreactive substance P in the dorsal horn with antibody-coated microelectrodes". Neurosci Lett, *68*, 134-40.
- Dundee JW(1960). "Alterations in response to somatic pain associated with anaesthesia. II. The effect of thiopentone and pentobarbitone". Br J Anaesth, *32*, 407-14.
- Eccles JC(1959a). "Excitatory and inhibitory synaptic action". Annals of the New York Academy of Sciences, *81*, 247-264.
- Eccles JC, Kozak W & Magni F(1961). "Dorsal root reflexes of muscle group I afferent fibres". J Physiol, *159*, 128-46.
- Eccles RM & Lundberg A(1959a). "Supraspinal control of interneurons mediating spinal reflexes". The Journal of physiology, *147*, 565-584.
- Ekerot CF(1990a). "The lateral reticular nucleus in the cat. VI. Excitatory and inhibitory afferent paths". Experimental brain research. Experimentelle Hirnforschung. Experimentation cerebrale, *79*, 109-19.
- Ekerot CF(1990b). "The lateral reticular nucleus in the cat. VII. Excitatory and inhibitory projection from the ipsilateral forelimb tract (iF tract)". Experimental brain research. Experimentelle Hirnforschung. Experimentation cerebrale, *79*, 120-8.
- Ekerot CF(1990c). "The lateral reticular nucleus in the cat. VIII. Excitatory and inhibitory projection from the bilateral ventral flexor reflex tract (bVFRT)". Experimental brain research. Experimentelle Hirnforschung. Experimentation cerebrale, *79*, 129-37.
- El Mestikawy S, Wallen-Mackenzie A, Fortin GM, Descarries L & Trudeau LE(2011). "From glutamate co-release to vesicular synergy: vesicular glutamate transporters". Nature reviews. Neuroscience, *12*, 204-16.
- Engberg I, Lundberg A & Ryall RW(1968). "Reticulospinal inhibition of transmission in reflex pathways". J Physiol, *194*, 201-23.
- Ericson H & Blomqvist A(1988). "Tracing of neuronal connections with cholera toxin subunit B: light and electron microscopic immunohistochemistry using monoclonal antibodies". Journal of Neuroscience Methods, *24*, 225-235.
- Ezure K & Tanaka I(1997). "Convergence of central respiratory and locomotor rhythms onto single neurons of the lateral reticular nucleus". Experimental Brain Research, *113*, 230-242.
- Fields HL & Basbaum AI(1978). "Brainstem control of spinal pain-transmission neurons". Annu Rev Physiol, *40*, 217-48.
- Fields HL, Clanton CH & Anderson SD(1977). "Somatosensory properties of spinoreticular neurons in the cat". Brain research, *120*, 49-66.
- Flumerfelt BA, Hryciyshyn AW & Kapogianis EM(1982). "Spinal projections to the lateral reticular nucleus in the rat". Anatomy and embryology, *165*, 345-59.
- Foreman RD, Blair RW & Weber RN(1984). "Viscerosomatic convergence onto T2-T4 spinoreticular, spinoreticular-spinothalamic, and spinothalamic tract neurons in the cat". Experimental neurology, *85*, 597-619.
- Freneau RT, Troyer MD, Pahner I, Nygaard GO, Tran CH, Reimer RJ, Bellocchio EE, Fortin D, Storm-Mathisen J & Edwards RH(2001). "The

- expression of vesicular glutamate transporters defines two classes of excitatory synapse". Neuron, 31, 247-60.
- Fu Y, Tvrdik P, Makki N, Paxinos G & Watson C(2011). "Precerebellar Cell Groups in the Hindbrain of the Mouse Defined by Retrograde Tracing and Correlated with Cumulative Wnt1-Cre Genetic Labeling". The Cerebellum, 10, 570-584.
- Galan A, Lopez-Garcia JA, Cervero F & Laird JM(2002). "Activation of spinal extracellular signaling-regulated kinase-1 and -2 by intraplantar carrageenan in rodents". Neurosci Lett, 322, 37-40.
- Galea MP, Hammar I, Nilsson E & Jankowska E(2010). "Bilateral postsynaptic actions of pyramidal tract and reticulospinal neurons on feline erector spinae motoneurons". J Neurosci, 30, 858-69.
- Gao YJ & Ji RR(2009). "c-Fos and pERK, which is a better marker for neuronal activation and central sensitization after noxious stimulation and tissue injury?". The open pain journal, 2, 11-17.
- García-Larrea L, Charles N, Sindou M & Mauguière F(1993). "Flexion reflexes following anterolateral cordotomy in man: dissociation between pain sensation and nociceptive reflex RIII". Pain, 55, 139-149.
- Garifoli A, Maci T, Perciavalle V & Perciavalle V(2006). "Organization of bilateral spinal projections to the lateral reticular nucleus of the rat". Archives italiennes de biologie, 144, 145-57.
- Garrett KM & Gan J(1998). "Enhancement of gamma-aminobutyric acidA receptor activity by alpha-chloralose". J Pharmacol Exp Ther, 285, 680-6.
- Ghazi H, Hrycyszyn AW & Flumerfelt BA(1987). "Double-labeling study of axonal branching within the lateral reticulocerebellar projection in the rat". The Journal of comparative neurology, 258, 378-386.
- Giaquinto S & Pompeiano O(1963). "Generalized inhibition of spinal reflexes induced by cutaneous nerve stimulation in unrestrained cats". Experientia, 19, 653-654.
- Gokin AP, Pavlasek J & Duda P(1977). "Neuronal mechanisms of spino-bulbo-spinal activity". Neuroscience, 2, 297-306.
- Grant G, Koerber HR & George P(2004). "Spinal Cord Cytoarchitecture". *The Rat Nervous System (Third Edition)*. Burlington: Academic Press.
- Grant G, Oscarsson O & Rosen I(1966). "Functional organization of the spinoreticulocerebellar path with identification of its spinal component". Experimental Brain Research, 1, 306-319.
- Grillner S, Hongo T & Lund S(1968). "The origin of descending fibres monosynaptically activating spinoreticular neurones". Brain Research, 10, 259-262.
- Grillner S, Hongo T & Lund S(1968b). "Reciprocal effects between two descending bulbo-spinal systems with monosynaptic connections to spinal motoneurons". Brain Research, 10, 477-480.
- Habaguchi T, Takakusaki K, Saitoh K, Sugimoto J & Sakamoto T(2002). "Medullary reticulospinal tract mediating the generalized motor inhibition in cats: II. Functional organization within the medullary reticular formation with respect to postsynaptic inhibition of forelimb and hindlimb motoneurons". Neuroscience, 113, 65-77.
- Haber LH, Moore BD & Willis WD(1982). "Electrophysiological response properties of spinoreticular neurons in the monkey". The Journal of comparative neurology, 207, 75-84.

- Haenggeli C-A, Pongstaporn T, Doucet JR & Ryugo DK(2005). "Projections from the spinal trigeminal nucleus to the cochlear nucleus in the rat". The Journal of Comparative Neurology, 484, 191-205.
- Hagbarth KE(1952). "Excitatory and inhibitory skin areas for flexor and extensor motoneurons". Acta Physiol Scand Suppl, 26, 1-58.
- Hall JG, Duggan AW, Morton CR & Johnson SM(1982). "The location of brainstem neurones tonically inhibiting dorsal horn neurones of the cat". Brain Research, 244, 215-222.
- Hama A & Menzaghi F(2001). "Antagonist of nicotinic acetylcholine receptors (nAChR) enhances formalin-induced nociception in rats: tonic role of nAChRs in the control of pain following injury". Brain Res, 888, 102-106.
- Hammar I, Krutki P, Drzymala-Celichowska H, Nilsson E & Jankowska E(2011). "A trans-spinal loop between neurones in the reticular formation and in the cerebellum". The Journal of physiology, 589, 653-665.
- Hardy SG, Horecky JG & Presley KG(1998). "Projections of the caudal ventrolateral medulla to the thoracic spinal cord in the rat". Anat Rec, 250, 95-102.
- Heinricher MM, Tavares I, Leith JL & Lumb BM(2009). "Descending control of nociception: Specificity, recruitment and plasticity". Brain Research Reviews, 60, 214-225.
- Helke CJ, Krause JE, Mantyh PW, Couture R & Bannon MJ(1990). "Diversity in mammalian tachykinin peptidergic neurons: multiple peptides, receptors, and regulatory mechanisms". FASEB J, 4, 1606-15.
- Hellenbrand DJ, Kaeppler KE, Hwang E, Ehlers ME, Toigo RD, Giesler JD, Vassar-Olsen ER & Hanna A(2013). "Basic techniques for long distance axon tracing in the spinal cord". Microscopy research and technique, 76, 1240-1249.
- Hermann GE, Bresnahan JC, Holmes GM, Rogers RC & Beattie MS(1998). "Descending projections from the nucleus raphe obscurus to pudendal motoneurons in the male rat". J Comp Neurol, 397, 458-74.
- Holmqvist B(1960). "Crossed reflex actions evoked by high threshold muscle afferents". Experientia, 16, 459-60.
- Holmqvist B, Lundberg A & Oscarsson O(1959). "The relationship between the flexion reflex and certain ascending spinal pathways". Cellular and Molecular Life Sciences, 15, 195-196.
- Holstege G(1991). "Descending motor pathways and the spinal motor system - Limbic and nonlimbic components". Progress in brain research, 87, 307-421.
- Holstege JC(1996a). "The ventro-medial medullary projections to spinal motoneurons: ultrastructure, transmitters and functional aspects". In: G. Holstege RB & Saper CB (eds.) *Progress in Brain Research*. Elsevier.
- Honda CN & Perl ER(1985). "Functional and morphological features of neurons in the midline region of the caudal spinal cord of the cat". Brain research, 340, 285-95.
- Hossaini M, Goos JA, Kohli SK & Holstege JC(2012). "Distribution of glycine/GABA neurons in the ventromedial medulla with descending spinal projections and evidence for an ascending glycine/GABA projection". PLoS one, 7, e35293.
- Hrycyszyn AW & Flumerfelt BA(1981a). "Cytology and synaptology of the lateral reticular nucleus of the cat". The Journal of comparative neurology, 197, 459-475.

- Hrycyshyn AW & Flumerfelt BA(1981b). "A light microscopic investigation of the afferent connections of the lateral reticular nucleus in the cat". The Journal of comparative neurology, 197, 477-502.
- Hrycyshyn AW, Flumerfelt BA & Anderson WA(1982). "A horseradish peroxidase study of the projections from the lateral reticular nucleus to the cerebellum in the rat". Anatomy and Embryology, 165, 1-18.
- Huang A, Noga BR, Carr PA, Fedirchuk B & Jordan LM(2000). "Spinal cholinergic neurons activated during locomotion: localization and electrophysiological characterization". J Neurophysiol, 83, 3537-47.
- Huang X-F & Paxinos G(1995). "Human intermediate reticular zone: A cyto and chemoarchitectonic study". The Journal of Comparative Neurology, 360, 571-588.
- Huber J, Grottel K, Mrówczyński W & Krutki P(1999). "Spinoreticular neurons in the second sacral segment of the feline spinal cord". Neuroscience research, 34, 59-65.
- Hughes DI, Polgár E, Shehab SA & Todd AJ(2004). "Peripheral axotomy induces depletion of the vesicular glutamate transporter VGLUT1 in central terminals of myelinated afferent fibres in the rat spinal cord". Brain Res, 1017, 69-76.
- Huisman AM, Kuypers HGJM & Verburgh CA(1981). "Quantitative differences in collateralization of the descending spinal pathways from red nucleus and other brain stem cell groups in rat as demonstrated with the multiple fluorescent retrograde tracer technique". Brain Research, 209, 271-286.
- Hultborn H(2006). "Spinal reflexes, mechanisms and concepts: from Eccles to Lundberg and beyond". Progress in neurobiology, 78, 215-232.
- Huma Z, Du Beau A, Brown C & Maxwell DJ(2014). "Origin and neurochemical properties of bulbospinal neurons projecting to the rat lumbar spinal cord via the medial longitudinal fasciculus and caudal ventrolateral medulla". Frontiers in neural circuits, 8, 40.
- Hunt CC & Kuffler SW(1954). "Motor innervation of skeletal muscle: multiple innervation of individual muscle fibres and motor unit function". The Journal of Physiology, 126, 293-303.
- Ichikawa H, Deguchi T, Nakago T, Jacobowitz DM & Sugimoto T(1994). "Parvalbumin, calretinin and carbonic anhydrase in the trigeminal and spinal primary neurons of the rat". Brain Res, 655, 241-5.
- Ichikawa H, Mo Z, Xiang M & Sugimoto T(2004). "Effect of Brn-3a deficiency on parvalbumin-immunoreactive primary sensory neurons in the dorsal root ganglion". Brain Res Dev Brain Res, 150, 41-5.
- Iigaya K, Kumagai H, Onimaru H, Kawai A, Oshima N, Onami T, Takimoto C, Kamayachi T, Hayashi K, Saruta T & Itoh H (2007). "Novel axonal projection from the caudal end of the ventrolateral medulla to the intermediolateral cell column".
- Illert M, Lundberg A, Padel Y & Tanaka R(1978). "Integration in descending motor pathways controlling the forelimb in the cat. 5. Properties of and monosynaptic excitatory convergence on C3--C4 propriospinal neurones.". Experimental Brain Research, 33, 101-130.
- Illert M, Lundberg A & Tanaka R(1977). "Integration in descending motor pathways controlling the forelimb in the cat. 3. Convergence on propriospinal neurones transmitting disynaptic excitation from the corticospinal tract and other descending tracts". Experimental brain research. Experimentelle Hirnforschung. Experimentation cerebrale, 29, 323-46.

- Impey S, Obrietan K & Storm DR(1999). "Making new connections: role of ERK/MAP kinase signaling in neuronal plasticity". Neuron, 23, 11-4.
- Ito J, Sasa M, Matsuoka I & Takaori S(1982). "Afferent projection from reticular nuclei, inferior olive and cerebellum to lateral vestibular nucleus of the cat as demonstrated by horseradish peroxidase". Brain research, 231, 427-432.
- Jankowska E & Edgley SA (2010a). "Functional subdivision of feline spinal interneurons in reflex pathways from group Ib and II muscle afferents; an update". Eur J Neurosci. 2010/08/21 ed.
- Jankowska E & Edgley SA(2010b). "Functional subdivision of feline spinal interneurons in reflex pathways from group Ib and II muscle afferents; an update". Eur J Neurosci, 32, 881-93.
- Jankowska E, Hammar I, Slawinska U, Maleszak K & Edgley SA(2003). "Neuronal basis of crossed actions from the reticular formation on feline hindlimb motoneurons". J Neurosci, 23, 1867-78.
- Jankowska E, Lundberg A & Stuart D(1973). "Propriospinal control of last order interneurons of spinal reflex pathways in the cat". Brain Research, 53, 227-231.
- Jankowska E & Stecina K(2007). "Uncrossed actions of feline corticospinal tract neurones on lumbar interneurons evoked via ipsilaterally descending pathways". The Journal of physiology, 580, 133-47.
- Jankowska E, Stecina K, Cabaj A, Pettersson LG & Edgley SA(2006). "Neuronal relays in double crossed pathways between feline motor cortex and ipsilateral hindlimb motoneurons". The Journal of physiology, 575, 527-41.
- Janss AJ & Gebhart GF(1988 ). "Brainstem and spinal pathways mediating descending inhibition from the medullary lateral reticular nucleus in the rat". Brain Research, 440, 109-122.
- Janss AJ & Gebhart GF(1988b). "Quantitative characterization and spinal pathway mediating inhibition of spinal nociceptive transmission from the lateral reticular nucleus in the rat". J Neurophysiol, 59, 226-47.
- Ji RR, Baba H, Brenner GJ & Woolf CJ(1999). "Nociceptive-specific activation of ERK in spinal neurons contributes to pain hypersensitivity". Nat Neurosci, 2, 1114-9.
- Ji RR, Befort K, Brenner GJ & Woolf CJ(2002). "ERK MAP kinase activation in superficial spinal cord neurons induces prodynorphin and NK-1 upregulation and contributes to persistent inflammatory pain hypersensitivity". J Neurosci, 22, 478-85.
- Jones BE & Yang TZ(1985). "The efferent projections from the reticular formation and the locus coeruleus studied by anterograde and retrograde axonal transport in the rat". The Journal of comparative neurology, 242, 56-92.
- Jones SL & Gebhart GF(1988). "Inhibition of spinal nociceptive transmission from the midbrain, pons and medulla in the rat: activation of descending inhibition by morphine, glutamate and electrical stimulation". Brain Research, 460, 281-296.
- Jordan LM, Liu J, Hedlund PB, Akay T & Pearson KG(2008). "Descending command systems for the initiation of locomotion in mammals". Brain Research Reviews, 57, 183-191.
- Julius D & Basbaum AI(2001). "Molecular mechanisms of nociception". Nature, 413, 203-10.

- Kanazawa I, Sutoo D, Oshima I & Saito S(1979). "Effect of transection on choline acetyltransferase, thyrotropin releasing hormone and substance P in the cat cervical cord". Neurosci Lett, 13, 325-30.
- Kaneko T, Itoh K, Shigemoto R & Mizuno N(1989). "Glutaminase-like immunoreactivity in the lower brainstem and cerebellum of the adult rat". Neuroscience, 32, 79-98.
- Kapogianis EM, Flumerfelt BA & Hrycyshyn AW(1982a). "A Golgi study of the lateral reticular nucleus in the rat". Anatomy and embryology, 164, 243-56.
- Kapogianis EM, Flumerfelt BA & Hrycyshyn AW(1982b). "Cytoarchitecture and cytology of the lateral reticular nucleus in the rat". Anatomy and embryology, 164, 229-42.
- Karim F, Wang CC & Gereau RWT(2001). "Metabotropic glutamate receptor subtypes 1 and 5 are activators of extracellular signal-regulated kinase signaling required for inflammatory pain in mice". J Neurosci, 21, 3771-9.
- Kawamura S, Sprague JM & Niimi K(1974). "Corticofugal projections from the visual cortices to the thalamus, pretectum and superior colliculus in the cat". The Journal of Comparative Neurology, 158, 339-362.
- Kevetter GA, Haber LH, Yeziarski RP, Chung JM, Martin RF & Willis WD(1982). "Cells of origin of the spinoreticular tract in the monkey". The Journal of comparative neurology, 207, 61-74.
- Khasar SG, Mccarter G & Levine JD(1999). "Epinephrine produces a beta-adrenergic receptor-mediated mechanical hyperalgesia and in vitro sensitization of rat nociceptors". J Neurophysiol, 81, 1104-12.
- Kitai ST, DeFrance JF, Hatada K & Kennedy DT(1974b). "Electrophysiological properties of lateral reticular nucleus cells: II. Synaptic activation". Experimental Brain Research, 21, 419-432.
- Kitai ST, Hatada K & Casey W(1972). "Intracellular analysis of antidromically and synaptically activated lateral reticular neurons". Brain Research, 43, 629-634.
- Kitai ST, Kennedy DT, DeFrance JF & Hatada K(1974a). "Electrophysiological properties of lateral reticular nucleus cells: I. Antidromic activation". Experimental Brain Research, 21, 403-418.
- Kitai ST, Kennedy DT, Morin F & Gardner E(1967). "The lateral reticular nucleus of the medulla oblongata of the cat". Experimental neurology, 17, 65-73.
- Koekkoek SK & Ruigrok TJ(1995). "Lack of a bilateral projection of individual spinal neurons to the lateral reticular nucleus in the rat: a retrograde, non-fluorescent, double labeling study". Neuroscience letters, 200, 13-16.
- Krutki P, Jankowska E & Edgley SA(2003). "Are crossed actions of reticulospinal and vestibulospinal neurons on feline motoneurons mediated by the same or separate commissural neurons?". The Journal of neuroscience : the official journal of the Society for Neuroscience, 23, 8041-50.
- Kubin L, Magherini PC, Manzoni D & Pompeiano O(1980). "Responses of lateral reticular neurons to sinusoidal stimulation of labyrinth receptors in decerebrate cat". 44, 922-936.
- Künzle H(1973). "The topographic organization of spinal afferents to the lateral reticular nucleus of the cat". The Journal of comparative neurology, 149, 103-15.
- Künzle H(1975). "Autoradiographic tracing of the cerebellar projections from the lateral reticular nucleus in the cat". Experimental Brain Research, 22, 255-266.

- Kuypers HGJM, Fleming WR & Farinoholt JW(1962). "Subcortical projections in the Rhesus monkey". The Journal of Comparative Neurology, 118, 107-137.
- Ladpli R & Brodal A(1968). "Experimental studies of commissural and reticular formation projections from the vestibular nuclei in the cat". Brain Research, 8, 65-96.
- Lanteri-Minet M, Isnardon P, De Pommery J & Menetrey D(1993). "Spinal and hindbrain structures involved in visceroreception and visceronociception as revealed by the expression of Fos, Jun and Krox-24 proteins". Neuroscience, 55, 737-53.
- Lawson SN(1995). "Neuropeptides in morphologically and functionally identified primary afferent neurons in dorsal root ganglia: substance P, CGRP and somatostatin". Prog Brain Res, 104, 161-73.
- Leah J, Menetrey D & De Pommery J(1988). "neuropeptides in long ascending spinal tract cells in the rat: evidence for parallel processing of ascending information". Neuroscience, 24, 195-207.
- Leblond H, Menard A & Gossard JP(2000). "Bulbospinal control of spinal cord pathways generating locomotor extensor activities in the cat". J Physiol, 525 Pt 1, 225-40.
- Lee HS & Mihailoff GA(1999). "Fluorescent double-label study of lateral reticular nucleus projections to the spinal cord and periaqueductal gray in the rat". The Anatomical record, 256, 91-98.
- Lefler YA, Arzi A, Reiner K, Sukhotinsky I & Devor M(2008). "Bulbospinal neurons of the rat rostromedial medulla are highly collateralized". The Journal of Comparative Neurology, 506, 960-978.
- Leite-Almeida H, Valle-Fernandes A & Almeida A(2006). "Brain projections from the medullary dorsal reticular nucleus: an anterograde and retrograde tracing study in the rat". Neuroscience, 140, 577-95.
- Leong SK, Shieh JY & Wong WC(1984). "Localizing spinal-cord-projecting neurons in adult albino rats". The Journal of Comparative Neurology, 228, 1-17.
- Liang H, Paxinos G & Watson C(2011). "Projections from the brain to the spinal cord in the mouse". Brain Structure and Function, 215, 159-186.
- Light A & Perl E(1979a). "Spinal termination of functionally identified primary afferent neurons with slowly conducting myelinated fibers". journal of comparative neurology, 186, 133-50.
- Light AR & Perl ER(1979). "Spinal termination of functionally identified primary afferent neurons with slowly conducting myelinated fibers". The Journal of comparative neurology, 186, 133-50.
- Liguz-Lecznar M & Skangiel-Kramaska J(2007). "Vesicular glutamate transporters (VGLUTs): the three musketeers of glutamatergic system". Acta neurobiologiae experimentalis, 67, 207-18.
- Lima D(1990). "A spinomedullary projection terminating in the dorsal reticular nucleus of the rat". Neuroscience, 34, 577-589.
- Lima D, Mendes-Ribeiro JA & Coimbra A(1991). "The spino-latero-reticular system of the rat: Projections from the superficial dorsal horn and structural characterization of marginal neurons involved". Neuroscience, 45, 137-152.
- Littlewood NK, Todd AJ, Spike RC, Watt C & Shehab SaS(1995). "The types of neuron in spinal dorsal horn which possess neurokinin-1 receptors". Neuroscience, 66, 597-608.

- Liu C-L, Wang Y-J, Chen J-R & Tseng G-F(2002). "Parvalbumin-containing neurons mediate the feedforward inhibition of rat rubrospinal neurons". Anatomy and Embryology, 205, 245-254.
- Liu TT, Bannatyne BA, Jankowska E & Maxwell DJ(2010b). "Properties of axon terminals contacting intermediate zone excitatory and inhibitory premotor interneurons with monosynaptic input from group I and II muscle afferents". The Journal of physiology, 588, 4217-33.
- Loewy AD & Burton H(1978). "Nuclei of the solitary tract: efferent projections to the lower brain stem and spinal cord of the cat". J Comp Neurol, 181, 421-49.
- Lundberg A & Oscarsson O(1962a). "Functional organization of the ventral spino-cerebellar tract in the cat. IV. Identification of units by antidromic activation from the cerebellar cortex". Acta physiologica Scandinavica, 54, 252-69.
- Lundberg A & Oscarsson O(1962b). "Two ascending spinal pathways in the ventral part of the cord". Acta physiologica Scandinavica, 54, 270-86.
- Lundberg A & Weight F(1971). "Functional organization of connexions to the ventral spinocerebellar tract". Exp Brain Res, 12, 295-316.
- Luppi P-H, Fort P & Jouviet M(1990). "Iontophoretic application of unconjugated cholera toxin B subunit (CTb) combined with immunohistochemistry of neurochemical substances: a method for transmitter identification of retrogradely labeled neurons". Brain Research, 534, 209-224.
- Magnuson DS, Green DM & Sengoku T(1998). "Lumbar spinoreticular neurons in the rat: part of the central pattern generator for locomotion?". Annals of the New York Academy of Sciences, 860, 436-40.
- Mantyh P, Demaster E, Malhotra A, Ghilardi, Rogers S, Mantyh C, Liu H, Basbaum A, Vigna, Maggio J & Et A(1995). "Receptor endocytosis and dendrite reshaping in spinal neurons after somatosensory stimulation". Science, 268, 1629-1632.
- Marshall GE, Shehab SaS, Spike RC & Todd AJ(1996). "Neurokinin-1 receptors on lumbar spinothalamic neurons in the rat". Neuroscience, 72, 255-263.
- Martin GF, Andrezik J, Crutcher K, Linauts M & Panneton M(1977). "The lateral reticular nucleus of the opossum (*Didelphis virginiana*). II. Connections". The Journal of comparative neurology, 174, 151-86.
- Martin GF, Cabana T & Waltzer R(1988). "The origin of projections from the medullary reticular formation to the spinal cord, the diencephalon and the cerebellum at different stages of development in the North American opossum: studies using single and double labeling techniques". Neuroscience, 25, 87-96.
- Martin GF, Humbertson AO, Laxson LC, Panneton WM & Tschismadia I(1979). "Spinal projections from the mesencephalic and pontine reticular formation in the North American Opossum: a study using axonal transport techniques". The Journal of comparative neurology, 187, 373-99.
- Martin GF, Vertes RP & Waltzer R(1985). "Spinal projections of the gigantocellular reticular formation in the rat. Evidence for projections from different areas to laminae I and II and lamina IX". Experimental brain research. Experimentelle Hirnforschung. Experimentation cerebrale, 58, 154-62.
- Masson J, Sagne C, Hamon M & El Mestikawy S(1999). "Neurotransmitter transporters in the central nervous system". Pharmacological reviews, 51, 439-64.

- Matsumoto M, Xie W, Inoue M & Ueda H(2007).** "Evidence for the tonic inhibition of spinal pain by nicotinic cholinergic transmission through primary afferents". Mol Pain, 3, 41.
- Matsuyama K, Nakajima K, Mori F, Aoki M & Mori S(2004).** "Lumbar commissural interneurons with reticulospinal inputs in the cat: morphology and discharge patterns during fictive locomotion". The Journal of comparative neurology, 474, 546-61.
- Maunz RA, Pitts NG & Peterson BW(1978).** "Cat spinoreticular neurons: locations, responses and changes in responses during repetitive stimulation". Brain research, 148, 365-379.
- Mehler WR, Feferman ME & Nauta WJH(1960).** "Ascending axon degeneration following anterolateral cordotomy. An experimental study in the monkey". Brain, 83, 718-750.
- Meller ST & Gebhart GF(1993).** "Nitric oxide (NO) and nociceptive processing in the spinal cord". Pain, 52, 127-36.
- Menetrey D & Basbaum AI(1987).** "The distribution of substance P-, enkephalin- and dynorphin-immunoreactive neurons in the medulla of the rat and their contribution to bulbospinal pathways". Neuroscience, 23, 173-87.
- Menetrey D, Chaouch A & Besson JM(1980).** "Location and properties of dorsal horn neurons at origin of spinoreticular tract in lumbar enlargement of the rat". Journal of neurophysiology, 44, 862-77.
- Menetrey D, Chaouch A, Binder D & Besson JM(1982).** "The origin of the spinomesencephalic tract in the rat: an anatomical study using the retrograde transport of horseradish peroxidase". The Journal of comparative neurology, 206, 193-207.
- Menetrey D, De Pommery J & Besson JM(1984).** "Electrophysiological characteristics of lumbar spinal cord neurons backfired from lateral reticular nucleus in the rat". J Neurophysiol, 52, 595-611.
- Menetrey D, De Pommery J, Thomasset M & Baimbridge KG(1992).** "Calbindin-D28K (CaBP28k)-like Immunoreactivity in Ascending Projections". The European journal of neuroscience, 4, 70-76.
- Menetrey D, Roudier F & Besson JM(1983).** "Spinal neurons reaching the lateral reticular nucleus as studied in the rat by retrograde transport of horseradish peroxidase". The Journal of comparative neurology, 220, 439-52.
- Mense S & Meyer H(1985).** "Different types of slowly conducting afferent units in cat skeletal muscle and tendon". The Journal of Physiology, 363, 403-417.
- Mesnage B, Gaillard S, Godin AG, Rodeau JL, Hammer M, Von Engelhardt J, Wiseman PW, De Koninck Y, Schlichter R & Cordero-Erausquin M(2011).** "Morphological and functional characterization of cholinergic interneurons in the dorsal horn of the mouse spinal cord". J Comp Neurol, 519, 3139-58.
- Miller R(1996).** "Neural assemblies and laminar interactions in the cerebral cortex". Biological cybernetics, 75, 253-61.
- Mitani A, Ito K, Mitani Y & Mccarley RW(1988).** "Descending projections from the gigantocellular tegmental field in the cat: cells of origin and their brainstem and spinal cord trajectories". J Comp Neurol, 268, 546-66.
- Mitchell K, Spike RC & Todd AJ(1993).** "An immunocytochemical study of glycine receptor and GABA in laminae I-III of rat spinal dorsal horn". J Neurosci, 13, 2371-81.

- Molander C & Grant G(1987).** "Spinal cord projections from hindlimb muscle nerves in the rat studied by transganglionic transport of horseradish peroxidase, wheat germ agglutinin conjugated horseradish peroxidase, or horseradish peroxidase with dimethylsulfoxide". The Journal of comparative neurology, 260, 246-55.
- Molander C, Xu Q & Grant G(1984).** "The cytoarchitectonic organization of the spinal cord in the rat. I. The lower thoracic and lumbosacral cord". The Journal of comparative neurology, 230, 133-141.
- Morona R, Lopez JM, Dominguez L & Gonzalez A(2007).** "Immunohistochemical and hodological characterization of calbindin-D28k-containing neurons in the spinal cord of the turtle, *Pseudemys scripta elegans*". Microsc Res Tech, 70, 101-18.
- Morona R, Moreno N, Lopez JM & Gonzalez A(2006).** "Immunohistochemical localization of calbindin-D28k and calretinin in the spinal cord of *Xenopus laevis*". The Journal of comparative neurology, 494, 763-83.
- Morton CR, Johnson SM & Duggan AW(1983).** "Lateral reticular regions and the descending control of dorsal horn neurones of the cat: selective inhibition by electrical stimulation". Brain Res, 275, 13-21.
- Nahin RL(1987).** "Immunocytochemical identification of long ascending peptidergic neurons contributing to the spinoreticular tract in the rat". Neuroscience, 23, 859-69.
- Nahin RL, Madsen AM & Giesler GJ(1983).** "Anatomical and physiological studies of the gray matter surrounding the spinal cord central canal". The Journal of comparative neurology, 220, 321-35.
- Nahin RL & Micevych PE(1986).** "A long ascending pathway of enkephalin-like immunoreactive spinoreticular neurons in the rat". Neuroscience Letters, 65, 271-6.
- Naim MM, Shehab SA & Todd AJ(1998).** "Cells in laminae III and IV of the rat spinal cord which possess the neurokinin-1 receptor receive monosynaptic input from myelinated primary afferents". The European journal of neuroscience, 10, 3012-9.
- Naumann T, Hartig W & Frotscher M(2000).** "Retrograde tracing with Fluoro-Gold: different methods of tracer detection at the ultrastructural level and neurodegenerative changes of back-filled neurons in long-term studies". J Neurosci Methods, 103, 11-21.
- Ness TJ, Follett KA, Piper J & Dirks BA(1998).** "Characterization of neurons in the area of the medullary lateral reticular nucleus responsive to noxious visceral and cutaneous stimuli". Brain Research, 802, 163-174.
- Newlands SD, Vrabec JT, Purcell IM, Stewart CM, Zimmerman BE & Perachio AA(2003).** "Central projections of the saccular and utricular nerves in macaques". The Journal of Comparative Neurology, 466, 31-47.
- Newman DB(1987).** "Physiology Distinguishing rat brainstem reticulospinal nuclei by their neuronal morphology. 1. Medullary nuclei. II. Pontine and mesencephalic nuclei : J. Hirnforsch., 26 (1985) 187-226 and 385-418". Pain, 28, 270-271.
- Newman DB & Ginsberg CY(1992).** "Brainstem reticular nuclei that project to the cerebellum in rats: a retrograde tracer study". Brain, behavior and evolution, 39, 24-68.
- Nyberg-Hansen R(1965).** "Sites and mode of termination of reticulo-spinal fibers in the cat. An experimental study with silver impregnation methods". The Journal of Comparative Neurology, 124, 71-99.

- Olave MJ, Puri N, Kerr R & Maxwell DJ(2002).** "Myelinated and unmyelinated primary afferent axons form contacts with cholinergic interneurons in the spinal dorsal horn". Exp Brain Res, 145, 448-56.
- Oliveira AL, Hydling F, Olsson E, Shi T, Edwards RH, Fujiyama F, Kaneko T, Hökfelt T, Cullheim S & Meister B(2003).** "Cellular localization of three vesicular glutamate transporter mRNAs and proteins in rat spinal cord and dorsal root ganglia". Synapse (New York, N.Y.), 50, 117-129.
- Ornung G, Ottersen OP, Cullheim S & Ulfhake B(1998).** "Distribution of glutamate-, glycine- and GABA-immunoreactive nerve terminals on dendrites in the cat spinal motor nucleus". Exp Brain Res, 118, 517-32.
- Oscarsson O & Rosén I(1966).** "Response characteristics of reticulocerebellar neurones activated from spinal afferents". Experimental Brain Research, 1, 320-328.
- Park IK, Kim MK, Tomoro I & Masato U(2003).** "A study on the spinoreticulocerebellar tract in chickens". Journal of veterinary science, 4, 1-8.
- Patestas, Gartner MA & Leslie P (2007).** "A Textbook of Neuroanatomy", Blackwell science limited.
- Pawlowski SA, Gaillard S, Ghorayeb I, Ribeiro-Da-Silva A, Schlichter R & Cordero-Erausquin M(2013).** "A novel population of cholinergic neurons in the macaque spinal dorsal horn of potential clinical relevance for pain therapy". J Neurosci, 33, 3727-37.
- Paxinos G & Watson C (1986).** "The rat brain in stereotaxic coordinates", Sydney, Academic press.
- Paxinos G & Watson C (1997).** "The rat brain in stereotaxic coordinates", San Diego, Academic Press.
- Paxinos G & Watson C (2005).** "The rat brain in stereotaxic coordinates", Amsterdam; London, Elsevier Academic Press.
- Paxinos G & Watson C (2013).** "The rat brain in stereotaxic coordinates".
- Peterson BW(1979a).** "Reticulospinal projections to spinal motor nuclei". Annual review of physiology, 41, 127-40.
- Peterson BW, Pitts NG & Fukushima K(1979b).** "Reticulospinal connections with limb and axial motoneurons". Experimental Brain Research, 36, 1-20.
- Peterson BW, Pitts NG, Fukushima K & Mackel R(1978).** "Reticulospinal excitation and inhibition of neck motoneurons". Experimental Brain Research, 32, 471-489.
- Petras JM(1967).** "Cortical, tectal and tegmental fiber connections in the spinal cord of the cat". Brain Research, 6, 275-324.
- Pezet S, Onténiente B, Grannec G & Calvino B(1999).** "Chronic Pain is Associated with Increased TrkA Immunoreactivity in Spinoreticular Neurons". The Journal of Neuroscience, 19, 5482-5492.
- Pivetta C, Esposito Maria s, Sigrist M & Arber S(2014).** "Motor-Circuit Communication Matrix from Spinal Cord to Brainstem Neurons Revealed by Developmental Origin". Cell, 156, 537-548.
- Polgár E, Al Ghamdi KS & Todd AJ(2010).** "Two populations of neurokinin 1 receptor-expressing projection neurons in lamina I of the rat spinal cord that differ in AMPA receptor subunit composition and density of excitatory synaptic input". Neuroscience, 167, 1192-204.
- Polgár E, Campbell AD, Macintyre LM, Watanabe M & Todd AJ(2007).** "Phosphorylation of ERK in neurokinin 1 receptor-expressing neurons in laminae III and IV of the rat spinal dorsal horn following noxious stimulation". Molecular pain, 3, 4.

- Poppele RE, Bosco G & Rankin AM(2002).** "Independent representations of limb axis length and orientation in spinocerebellar response components". Journal of neurophysiology, 87, 409-22.
- Prentice Sd DT(2001).** "Contributions of the Reticulospinal System to the Postural Adjustments Occurring During Voluntary Gait Modifications". J Neurophysiol, 679-698.
- Qvist H(1988).** "Afferents to the lateral reticular nucleus from the oculomotor region". Anatomy and Embryology, 177, 277-283.
- Qvist H(1989).** "The cerebellar nuclear afferent and efferent connections with the lateral reticular nucleus in the cat as studied with retrograde transport of WGA-HRP". Anatomy and Embryology, 179, 471-483.
- Qvist H, Dietrichs E & Walberg F(1984).** "An ipsilateral projection from the red nucleus to the lateral reticular nucleus in the cat". Anatomy and embryology, 170, 327-330.
- Raboisson P, Dallel R, Bernard JF, Le Bars D & Villanueva L(1996).** "Organization of efferent projections from the spinal cervical enlargement to the medullary subnucleus reticularis dorsalis and the adjacent cuneate nucleus: a PHA-L study in the rat". The Journal of comparative neurology, 367, 503-17.
- Rajakumar N, Hrycyszyn AW & Flumerfelt BA(1992).** "Afferent organization of the lateral reticular nucleus in the rat: An anterograde tracing study". Anatomy and Embryology, 185, 25-37.
- Ramón-Moliner E & Nauta WJ(1966).** "The isodendritic core of the brain stem". The Journal of comparative neurology, 126, 311-335.
- Rao GS, Breazile JE & Kitchell RL(1969).** "Distribution and termination of spinoreticular afferents in the brain stem of sheep". The Journal of comparative neurology, 137, 185-195.
- Rashid MH & Ueda H(2002).** "Neuropathy-specific analgesic action of intrathecal nicotinic agonists and its spinal GABA-mediated mechanism". Brain Res, 953, 53-62.
- Reed WR, Shum-Siu A & Magnuson DS(2008).** "Reticulospinal pathways in the ventrolateral funiculus with terminations in the cervical and lumbar enlargements of the adult rat spinal cord". Neuroscience, 151, 505-17.
- Reimer RJ, Fremeau RT, Bellocchio EE & Edwards RH(2001).** "The essence of excitation". Current opinion in cell biology, 13, 417-21.
- Ren K & Ruda MA(1994).** "A comparative study of the calcium-binding proteins calbindin-D28K, calretinin, calmodulin and parvalbumin in the rat spinal cord". Brain research. Brain research reviews, 19, 163-79.
- Rexed B(1952).** "The cytoarchitectonic organization of the spinal cord in the cat". The Journal of comparative neurology, 96, 415-495.
- Ribeiro-Da-Silva A & Cuello AC(1990).** "Choline acetyltransferase-immunoreactive profiles are presynaptic to primary sensory fibers in the rat superficial dorsal horn". J Comp Neurol, 295, 370-84.
- Riddle CN, Edgley SA & Baker SN(2009).** "Direct and indirect connections with upper limb motoneurons from the primate reticulospinal tract". J Neurosci, 29, 4993-9.
- Rong-Huan L, Jing-Shi T & Zong-Lian H(1993).** "Effect of systemic morphine on neurons in the lateral reticular nucleus area of the rat". Brain Research Bulletin, 32, 179-184.
- Rong-Huan L, Jing-Shi T, Zong-Lian H & Hong J(1990).** "Responses of reticulospinal neurons in the lateral reticular nucleus area of the rat to

- cutaneous noxious and non-noxious stimulation". Neuroscience Letters, 109, 92-96.
- Rosén I & Scheid P(1973a). "Responses to nerve stimulation in the bilateral ventral flexor reflex tract (bVFRT) of the cat". Experimental Brain Research, 18, 256-267.
- Rosén I & Scheid P(1973b). "Patterns of afferent input to the lateral reticular nucleus of the cat". Experimental brain research. Experimentelle Hirnforschung. Experimentation cerebrale, 18, 242-55.
- Rosén I & Scheid P(1973c). "Responses in the spino-reticulo-cerebellar pathway to stimulation of cutaneous mechanoreceptors". Experimental brain research. Experimentelle Hirnforschung. Experimentation cerebrale, 18, 268-78.
- Rosen LB, Ginty DD, Weber MJ & Greenberg ME(1994). "Membrane depolarization and calcium influx stimulate MEK and MAP kinase via activation of Ras". Neuron, 12, 1207-21.
- Rossi GF & Brodal A(1956). "Spinoreticular connections in the cat". Bollettino della Societa italiana di biologia sperimentale, 32, 960-1.
- Rossi GF & Brodal A(1957). "Terminal distribution of spinoreticular fibers in the cat". A. M. A. archives of neurology and psychiatry, 78, 439-53.
- Rub U, De Vos RA, Schultz C, Brunt ER, Paulson H & Braak H(2002). "Spinocerebellar ataxia type 3 (Machado-Joseph disease): severe destruction of the lateral reticular nucleus". Brain, 125, 2115-24.
- Ruigrok TJ, Cella F & Voogd J(1995a). "Connections of the lateral reticular nucleus to the lateral vestibular nucleus in the rat. An anterograde tracing study with Phaseolus vulgaris leucoagglutinin". The European journal of neuroscience, 7, 1410-1413.
- Ryugo D, Haenggeli C-A & Doucet J(2003). "Multimodal inputs to the granule cell domain of the cochlear nucleus". Experimental Brain Research, 153, 477-485.
- Sahara Y, Xie YK & Bennett GJ(1990). "Intracellular records of the effects of primary afferent input in lumbar spinoreticular tract neurons in the cat". Journal of neurophysiology, 64, 1791-800.
- Sakai ST, Davidson AG & Buford JA(2009). "Reticulospinal neurons in the pontomedullary reticular formation of the monkey (*Macaca fascicularis*)". Neuroscience, 163, 1158-70.
- Sakamoto H, Spike RC & Todd AJ(1999). "Neurons in laminae III and IV of the rat spinal cord with the neurokinin-1 receptor receive few contacts from unmyelinated primary afferents which do not contain substance P". Neuroscience, 94, 903-8.
- Sardella TC, Polgar E, Watanabe M & Todd AJ(2011). "A quantitative study of neuronal nitric oxide synthase expression in laminae I-III of the rat spinal dorsal horn". Neuroscience, 192, 708-20.
- Sato K, Zhang JH, Saika T, Sato M, Tada K & Tohyama M(1991). "Localization of glycine receptor  $\alpha 1$  subunit mRNA-containing neurons in the rat brain: An analysis using in situ hybridization histochemistry". Neuroscience, 43, 381-395.
- Schepens B & Drew T(2006). "Descending signals from the pontomedullary reticular formation are bilateral, asymmetric, and gated during reaching movements in the cat". J Neurophysiol, 96, 2229-52.
- Schmidtko A, Tegeder I & Geisslinger G(2009). "No NO, no pain? The role of nitric oxide and cGMP in spinal pain processing". Trends Neurosci, 32, 339-46.

- Schmued LC & Fallon JH(1986). "Fluoro-gold: a new fluorescent retrograde axonal tracer with numerous unique properties". Brain research, 377, 147-154.
- Scholz J & Woolf CJ(2002). "Can we conquer pain?". Nat Neurosci, 5 Suppl, 1062-7.
- Schouenborg J(2002). "Modular organisation and spinal somatosensory imprinting". Brain research. Brain research reviews, 40, 80-91.
- Shehab SA & Hughes DI(2011). "Simultaneous identification of unmyelinated and myelinated primary somatic afferents by co-injection of isolectin B4 and Cholera toxin subunit B into the sciatic nerve of the rat". J Neurosci Methods, 198, 213-21.
- Shehab SA, Spike RC & Todd AJ(2003). "Evidence against cholera toxin B subunit as a reliable tracer for sprouting of primary afferents following peripheral nerve injury". Brain Res, 964, 218-27.
- Sherriff FE, Henderson Z & Morrison JF(1991). "Further evidence for the absence of a descending cholinergic projection from the brainstem to the spinal cord in the rat". Neurosci Lett, 128, 52-6.
- Sherrington CS(1910). "Flexion-reflex of the limb, crossed extension-reflex, and reflex stepping and standing". The Journal of physiology, 40, 28-121.
- Shimamura M & Aoki M(1969). "Effects of spino-bulbo-spinal reflex volleys on flexor motoneurons of hindlimb in the cat". Brain Research, 16, 333-349.
- Shimamura M & Kogure I(1979). "Reticulospinal tracts involved in the spino-bulbo-spinal reflex in cats". Brain Research, 172, 13-21.
- Shimamura M, Kogure I & Igusa Y(1976). "Ascending spinal tracts of the spino-bulbo-spinal reflex in cats". Jpn J Physiol, 26, 577-89.
- Shimamura M, Kogure I & Wada S(1980). "Three types of reticular neurons involved in the spinobulbo-spinal reflex of cats". Brain Research, 186, 99-113.
- Shimamura M, Kogure I & Wada S(1982). "Reticular neuron activities associated with locomotion in thalamic cats". Brain research, 231, 51-62.
- Shinoda Y, Kakei S & Muto N(1996). "Morphology of single axons of tectospinal and reticulospinal neurons in the upper cervical spinal cord". Progress in brain research, 112, 71-84.
- Shokunbi MT, Hryciyshyn AW & Flumerfelt BA(1985). "Spinal projections to the lateral reticular nucleus in the rat: A retrograde labelling study using horseradish peroxidase". The Journal of Comparative Neurology, 239, 216-226.
- Shore SE(2005). "Multisensory integration in the dorsal cochlear nucleus: unit responses to acoustic and trigeminal ganglion stimulation". European Journal of Neuroscience, 21, 3334-3348.
- Shrestha SS, Bannatyne BA, Jankowska E, Hammar I, Nilsson E & Maxwell DJ(2012). "Excitatory inputs to four types of spinocerebellar tract neurons in the cat and the rat thoraco-lumbar spinal cord". The Journal of physiology, 590, 1737-55.
- Shrestha SS, Bannatyne BA, Jankowska E, Hammar I, Nilsson E & Maxwell DJ(2012a). "Inhibitory inputs to four types of spinocerebellar tract neurons in the cat spinal cord". Neuroscience, 226, 253-69.
- Snell RR (2006). "clinical neuroanatomy", baltimore, lipincott williams and wilkins.
- Soteropoulos DS, Williams ER & Baker SN(2012). "Cells in the monkey ponto-medullary reticular formation modulate their activity with slow finger movements". The Journal of Physiology, 590, 4011-4027.

- Southan GJ & Szabó C(1996).** "Selective pharmacological inhibition of distinct nitric oxide synthase isoforms". Biochemical Pharmacology, 51, 383-394.
- Sqalli-Houssaini Y, Cazalets JR & Clarac F(1993).** "Oscillatory properties of the central pattern generator for locomotion in neonatal rats". J Neurophysiol, 70, 803-13.
- Stepien AE, Tripodi M & Arber S(2010).** "Monosynaptic Rabies Virus Reveals Premotor Network Organization and Synaptic Specificity of Cholinergic Partition Cells". Neuron, 68, 456-472.
- Stocker SD, Steinbacher BC, Balaban CD & Yates BJ(1997).** "Connections of the caudal ventrolateral medullary reticular formation in the cat brainstem". Experimental brain research. Experimentelle Hirnforschung. Experimentation cerebrale, 116, 270-282.
- Strassman AM, Vos BP, Mineta Y, Naderi S, Borsook D & Burstein R(1993).** "Fos-like immunoreactivity in the superficial medullary dorsal horn induced by noxious and innocuous thermal stimulation of facial skin in the rat". J Neurophysiol, 70, 1811-21.
- Sugiura Y, Lee CL & Perl ER(1986).** "Central projections of identified, unmyelinated (C) afferent fibers innervating mammalian skin". Science, 234, 358-61.
- Takakusaki K, Kohyama J, Matsuyama K & Mori S(2001).** "Medullary reticulospinal tract mediating the generalized motor inhibition in cats: parallel inhibitory mechanisms acting on motoneurons and on interneuronal transmission in reflex pathways". Neuroscience, 103, 511-27.
- Takamori S(2006).** "VGLUTs: 'exciting' times for glutamatergic research?". Neuroscience research, 55, 343-51.
- Tavares I & Lima D(2002).** "The caudal ventrolateral medulla as an important inhibitory modulator of pain transmission in the spinal cord". The journal of pain : official journal of the American Pain Society, 3, 337-346.
- Thies R(1985).** "Activation of lumbar spinoreticular neurons by stimulation of muscle, cutaneous and sympathetic afferents". Brain Res, 333, 151-5.
- Todd AJ(2002).** "Anatomy of primary afferents and projection neurones in the rat spinal dorsal horn with particular emphasis on substance P and the neurokinin 1 receptor". Exp Physiol, 87, 245-9.
- Todd AJ(2010a).** "Neuronal circuitry for pain processing in the dorsal horn". Nature Reviews Neuroscience, 11, 823-836.
- Todd AJ(2010b).** "Neuronal circuitry for pain processing in the dorsal horn". Nat Rev Neurosci, 11, 823-36.
- Todd AJ, Hughes DI, Polgár E, Nagy GG, Mackie M, Ottersen OP & Maxwell DJ(2003).** "The expression of vesicular glutamate transporters VGLUT1 and VGLUT2 in neurochemically defined axonal populations in the rat spinal cord with emphasis on the dorsal horn". The European journal of neuroscience, 17, 13-27.
- Todd AJ, McGill MM & Shehab SA(2000).** "Neurokinin 1 receptor expression by neurons in laminae I, III and IV of the rat spinal dorsal horn that project to the brainstem". The European journal of neuroscience, 12, 689-700.
- Todd AJ, Puskar Z, Spike RC, Hughes C, Watt C & Forrest L(2002b).** "Projection neurons in lamina I of rat spinal cord with the neurokinin 1 receptor are selectively innervated by substance p-containing afferents and respond to noxious stimulation". J Neurosci, 22, 4103-13.

- Todd AJ & Spike RC(1993). "The localization of classical transmitters and neuropeptides within neurons in laminae I-III of the mammalian spinal dorsal horn". Progress in Neurobiology, 41, 609-645.
- Todd AJ, Spike RC, Chong D & Neilson M(1995). "The relationship between glycine and gephyrin in synapses of the rat spinal cord". Eur J Neurosci, 7, 1-11.
- Todd AJ, Spike RC & Polgár E(1998). "A quantitative study of neurons which express neurokinin-1 or somatostatin sst2a receptor in rat spinal dorsal horn". Neuroscience, 85, 459-73.
- Todd AJ & Sullivan AC(1990). "Light microscope study of the coexistence of GABA-like and glycine-like immunoreactivities in the spinal cord of the rat". The Journal of comparative neurology, 296, 496-505.
- Todd AJ, Watt C, Spike RC & Sieghart W(1996). "Colocalization of GABA, glycine, and their receptors at synapses in the rat spinal cord". J Neurosci, 16, 974-82.
- Tripodi M & Arber S(2012). "Regulation of motor circuit assembly by spatial and temporal mechanisms". Current opinion in neurobiology, 22, 615-623.
- Valverde F(1961a). "Reticular formation of the pons and medulla oblongata. A Golgi study". The Journal of Comparative Neurology, 116, 71-99.
- Vanderhorst VG & Ulfhake B(2006). "The organization of the brainstem and spinal cord of the mouse: relationships between monoaminergic, cholinergic, and spinal projection systems". J Chem Neuroanat, 31, 2-36.
- Varoqui H, Schafer MK, Zhu H, Weihe E & Erickson JD(2002). "Identification of the differentiation-associated Na<sup>+</sup>/PI transporter as a novel vesicular glutamate transporter expressed in a distinct set of glutamatergic synapses". The Journal of neuroscience : the official journal of the Society for Neuroscience, 22, 142-55.
- Vecellio M, Schwaller B, Meyer M, Hunziker W & Celio MR(2000). "Alterations in Purkinje cell spines of calbindin D-28 k and parvalbumin knock-out mice". Eur J Neurosci, 12, 945-54.
- Villanueva L, Bing Z & Le Bars D(1994). "Effects of heterotopic noxious stimuli on activity of neurones in subnucleus reticularis dorsalis in the rat medulla". The Journal of physiology, 475, 255-266.
- Villanueva L, Chitour D & Le Bars D(1986 b). "Involvement of the dorsolateral funiculus in the descending spinal projections responsible for diffuse noxious inhibitory controls in the rat". J Neurophysiol, 56, 1185-95.
- Villanueva L, De Pommery J, Menetrey D & Le Bars D(1991). "Spinal afferent projections to subnucleus reticularis dorsalis in the rat". Neuroscience Letters, 134, 98-102.
- Villanueva L, Peschanski M, Calvino B & Le Bars D(1986 a). "Ascending pathways in the spinal cord involved in triggering of diffuse noxious inhibitory controls in the rat". J Neurophysiol, 55, 34-55.
- Voneida TJ(1967). "The effect of pyramidal lesions on the performance of a conditioned avoidance response in cats". Experimental Neurology, 19, 483-493.
- Walberg F(1952). "The lateral reticular nucleus of the medulla oblongata in mammals; a comparative-anatomical study". The Journal of comparative neurology, 96, 283-343.
- Wang C-C, Willis WD & Westlund KN(1999). "Ascending projections from the area around the spinal cord central canal: A Phaseolus vulgaris leucoagglutinin study in rats". The Journal of Comparative Neurology, 415, 341-367.

- Wang D(2009). "Reticular formation and spinal cord injury". Spinal cord, 47, 204-212.
- Wang YJ, Liu CL & Tseng GF(1996). "Compartmentalization of calbindin and parvalbumin in different parts of rat rubrospinal neurons". Neuroscience, 74, 427-34.
- Watson C, George P & Kayalioglu G(2009a). "The Organization of the Spinal Cord". In: Watson C, Paxinos G & Kayalioglu G (eds.) *The Spinal Cord*. San Diego: Academic Press.
- Watson C & Harrison M(2012). "The Location of the Major Ascending and Descending Spinal Cord Tracts in all Spinal Cord Segments in the Mouse: Actual and Extrapolated". The Anatomical Record: Advances in Integrative Anatomy and Evolutionary Biology, 295, 1692-1697.
- Watson C & Harvey AR(2009b). "Projections from the Brain to the Spinal Cord". In: Watson C, Paxinos G & Kayalioglu G (eds.) *The spinal cord*. Academic Press.
- Willis WD(1985). "Nociceptive pathways: anatomy and physiology of nociceptive ascending pathways". Philosophical transactions of the Royal Society of London. Series B, Biological sciences, 308, 253-70.
- Wojcik SM, Katsurabayashi S, Guillemín I, Friauf E, Rosenmund C, Brose N & Rhee JS(2006). "A shared vesicular carrier allows synaptic corelease of GABA and glycine". Neuron, 50, 575-87.
- Woolf CJ(2004). "Pain: moving from symptom control toward mechanism-specific pharmacologic management". Ann Intern Med, 140, 441-51.
- Woolf NJ & Butcher LL(1989). "Cholinergic systems in the rat brain: IV. Descending projections of the pontomesencephalic tegmentum". Brain Res Bull, 23, 519-40.
- Zemlan FP, Behbehani MM & Beckstead RM(1984). "Ascending and descending projections from nucleus reticularis magnocellularis and nucleus reticularis gigantocellularis: an autoradiographic and horseradish peroxidase study in the rat". Brain Res, 292, 207-20.
- Zemlan FP, Leonard CM, Kow L-M & Pfaff DW(1978). "Ascending tracts of the lateral columns of the rat spinal cord: A study using the silver impregnation and horseradish peroxidase techniques". Experimental neurology, 62, 298-334.
- Zhan X & Ryugo DK(2007). "Projections of the lateral reticular nucleus to the cochlear nucleus in rats". The Journal of comparative neurology, 504, 583-98.
- Zhang JH, Morita Y, Hironaka T, Emson PC & Tohyama M(1990). "Ontological study of calbindin-D28k-like and parvalbumin-like immunoreactivities in rat spinal cord and dorsal root ganglia". J Comp Neurol, 302, 715-28.
- Zhuo M & Gebhart GF(1991). "Tonic cholinergic inhibition of spinal mechanical transmission". Pain, 46, 211-22.
- Zieglansberger W & Reiter C(1974). "A cholinergic mechanism in the spinal cord of cats". Neuropharmacology, 13, 519-27.

## Publication

1. “Origin and neurochemical properties of bulbospinal neurons projecting to the rat lumbar spinal cord via the medial longitudinal fasciculus and caudal ventrolateral medulla”

Huma Z, Du Beau A, Brown C & Maxwell DJ(2014). *Frontiers in neural circuits*, 8, 40.

2. “The spino-bulbar-cerebellar pathway: neurochemical properties and connections of spinal cells that project to the lateral reticular nucleus in the rat.

Zilli Huma and David J. Maxwell, under review in *Frontiers in Neural Circuits* ISSN: 1662-5110, Frontiers website link: [www.frontiersin.org](http://www.frontiersin.org)